Kent Academic Repository

Investigation of drug-adapted cancer cell lines as pre-clinical models of acquired resistance

2019

Hannah Onafuye

A thesis submitted to the University of Kent for the degree of Doctor of Philosophy (cell biology)

University of Kent

Faculty of Biosciences

Declaration

No part of this thesis has been submitted in support of an application for any degree or other qualification of the University of Kent, or any other University or Institution of learning.

Hannah Onafuye   Date 28.02.19

Acknowledgements

My greatest thanks and praise goes to God for his grace from the beginning of my search for a PhD supervisor to the successful end of my journey as a PhD student; for the determination and boldness in overcoming all challenges that I experienced throughout the course of my PhD. He has made me see today and because of him, I can face tomorrow and have continuous hope for the future.

I would like to give my greatest thanks to my supervisor Professor Martin Michaelis for his great support and belief that I would succeed and achieve my goals. I am so grateful for his guidance and patience because if he had not agreed to supervise me, I would not be able to get this far.

A massive thank you and appreciation goes to my father, Michael Adewale Onafuye who funded my PhD and gave me the confidence to believe that, as a woman, I can do all things through Christ that strengthens me. I am indebted to him and literally could not have managed without his continuous support has led me to where I am today and for that I am extremely grateful.

My wonderful, loving, caring and supportive mother, aunty and siblings who contributed towards the success as they provided me continuous emotional, physical and financial support. Without them I would have struggled more than expected. I hope that continue to be a good role model and show them that hard work and determination always pays off.

I would also like to thank Emilie Saintas who trained me for cell culture experiments, Joanna Bird for her continuous support, and so many others who supported my journey.

Finally, I dedicate my successful journey of research to my handsome and intelligent son, David, who is my reason for everything, to show him that no matter the situation, keep going and put your trust in God. Thank you for being an understanding son.

Table of contents

Contents

List of figures

List of tables

List of abbreviations

ALK	Anaplastic lymphoma kinase
2D	2-dimensional
3D	3-dimensional
ABCB1	ATP binding cassette transporter 1
Abs	Absorbance
ATP	adenosine triphosphate
Caba	Cabazitaxel
CDDP	Cisplatin
CHO	Chinese hamster ovary
DMSO	Dimethyl sulfoxide
DMF	Dimethylformamide
DNA	deoxyribonucleic acid
Doce	Docetaxel
ECM	extracellular matrix
EDTA	Ethylenediaminetraacetic acid
EGFR	Epidermal growth factor receptor
EPO-B	epothilone-B
EPR	enhanced permeability and retention effect
FBS	Foetal Bovine Serum
HCl	hydrochloric acid
HeLa	Henrietta Lacks HES human endometrial epithelial cell line
IC50	Half maximal inhibitory concentration
IMDM	Iscove's Modified Dulbecco's Media
MDR	multi-drug resistance
MQ H_2O	Milli-Q water
MDR 1	multidrug resistance protein 1
MTT	3-(4,5-dimethlythiazol-2-yl)-2,5-diphenyltetrazolium bromide
NaCl	sodium chloride

NB   neuroblastoma

p53   tumour protein p53

Pac   Paclitaxel

PBS   Phosphate Buffered Saline

P-gp   P-glycoprotein 1

RCCL   Resistant Cancer Cell Line collection

RTCA   Real Time Cell Analyser

SDS   Sodium Dodecyl Sulphate

SDS-PAGE   sodium dodecyl sulphate-polyacrylamide gel electrophoresis

STDEV   standard deviation

1 Abstract

Drug-adapted cancer cell lines have been successfully used to identify clinically relevant drug resistance mechanisms. This project focused on the further development of drug-adapted cancer cell lines as pre-clinical models of acquired drug resistance in cancer. A new cell line panel consisting of the ovarian cancer cell lines EFO-21, EFO-27, and COLO-704 and their cisplatin-adapted sublines was introduced and characterised. In addition, doxorubicin-loaded human serum albumin (HSA) nanoparticles were shown to circumvent ABCB1-mediated drug efflux. Vincristine- but not doxorubicin-adapted cells were re-sensitised to the level of the respective parental cells by HSA nanoparticle-incorporated doxorubicin. This indicates that rational strategies to overcome drug resistance in cancer depend on an intimate understanding of (the complexity of) the underlying resistance mechanisms. Finally, a standardised treatment protocol revealed differences in the potential of the microtubule-stabilising agents; docetaxel, paclitaxel, cabazitaxel, and epothilone B to induce resistance in the neuroblastoma cell line UKF-NB-3. In conclusion, this project has contributed to resistance research in cancer by introducing novel models, by providing novel insights into the prospects and limitations of strategies to overcome resistance mediated by transporter-mediated drug efflux, and by developing a novel strategy to assess the potential of anti-cancer drugs to induce resistance.

2 Introduction

2.1 Resistance in cancer

Cancer has become a global burden estimating 18.1 million new cancer cases and 9.6 million cancer deaths in 2018. The most commonly diagnosed type (and leading cause of cancer death) is lung cancer followed by breast cancer, prostate cancer and colorectal cancer (F. Bray et al., 2018).

Cancer cures are largely achieved by early diagnosis and surgical removal, possibly in combination with local irradiation and systemic therapies. For most cancer types, the focus lies on the prolongation of life and the improvement of life quality, if cancer is diagnosed at an advanced, typically metastatic, state requiring systemic (drug) therapy (Fenton et al., 2018). Systemic therapies are largely limited by the occurrence of drug resistance. Resistance can be either pre-existent (intrinsic) or develop in initially sensitive tumours over time (acquired) (Lippert et al., 2008) (Moulder, 2010) (Figure 1).
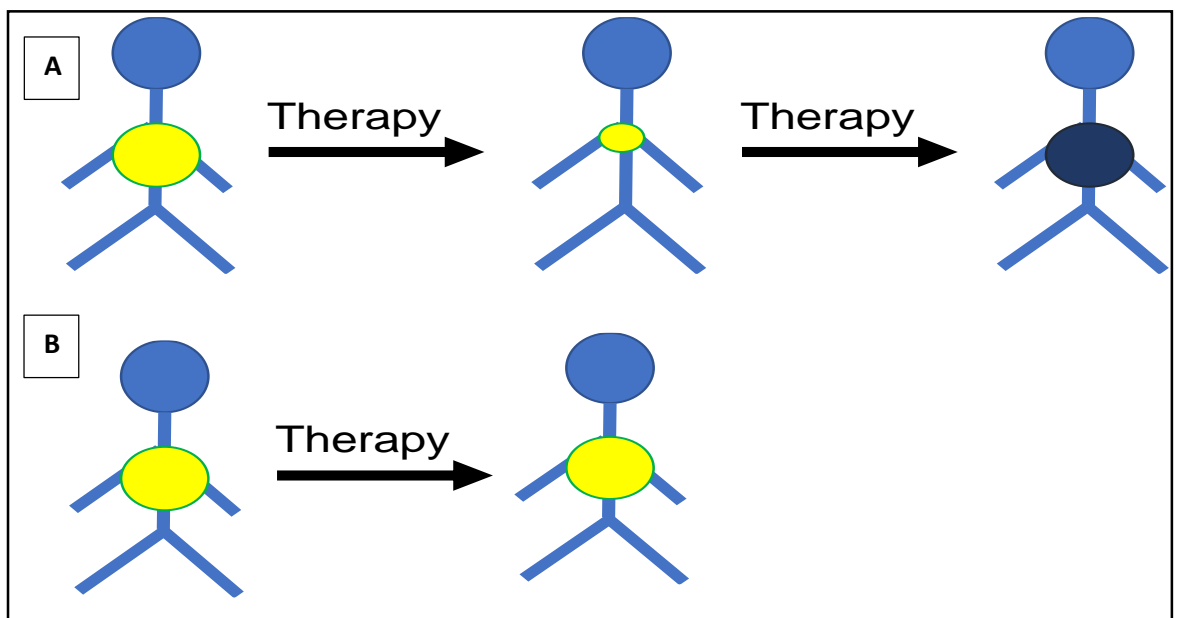
Figure 1 : **The different concepts of resistance**. A) Acquired resistance which occurs as a result of cancer cells developing adaptation characteristics, rendering the therapy ineffective and B) Intrinsic resistance mechanisms which is the pre-existing consequence of cells being insensitive to treatment.

Resistance mechanisms are manifold and complex. They may include (but may not be limited to increased drug efflux, decreased drug uptake, alterations in drug metabolism, mutations and changes of expression in the drug target, changes in pro- and anti-survival pathways, and upregulation of protective molecules (Holohan et al., 2014).

Over the course of the disease, the heterogeneity of cancer increases resulting in distinct molecular differences amongst the cells of the bulk tumour, thus causing variance levels of sensitivity to treatment. The occurrence of this heterogenic behaviour results in an uneven dissemination of the

tumour-cell subpopulations across and within the disease sites or temporary discrepancies in the molecular makeup of the cancer cells. This nature drives the resistance observed in cancer cells. (Daggo-Jack and Shaw 2018). Intra-heterogeneity and inter-heterogeneity have been well documented as the clinical determinant of patient outcomes. Intra-tumour heterogeneity includes genomic and biological variations within the primary tumour caused by tumour cell evolution under diverse microenvironment as a result of DNA damage replication whilst inter-tumour heterogeneity stands as an alteration in the genotype and phenotype of primary tumour cells and metastatic cells (Allison and Sledge 2014); (Gay et al., 2016); (McClelland, 2017); (Zardavas et al., 2014); (Melo et al., 2013) (Ogino et al., 2012); (Burrell et al., 2013); (Petrovic & Todorovic 2016).

Further complication has been identified by the tremendous immanent intra-tumour heterogeneity, which has become obvious in recent years. An increased intra-tumour heterogeneity seems to be related to therapeutic resistance and cancer progression and relapse, probably because heterogeneous populations have a higher potential to adapt to varying environmental pressures (Stanta & Bonin, 2018).

2.2 Taxanes

Researchers and clinics have developed a range of drugs with different targets. Taxane anticancer drugs work by binding to tubulin for the stabilisation of cellular microtubules (Crown and O'Leary 2000). Microtubules have dynamic structures which are composed of alpha-beta-tubulin heterodimers (Kavallaris 2010). They are structural proteins which are used for motility, secretion, cell division (mitosis), cell growth and intracellular transport (Mukhtar et al.,2014). Targeting this disruption by blocking the cell cycle progression of the spindle microtubule dynamic, has led to the development of taxanes which has been proven to be one of the most effective anticancer drugs in clinics (Mitchison 1988); (Jordan and Wilson 2004); (Abal et al., 2005).

One of the unique characteristics of the first taxol developed, paclitaxel, is its ability to stimulate the association of tubulin into microtubules and stop the separation of microtubules, inhibit the cell cycle progression, avert mitosis and prevent the growth of cancer cells (Zhu and Chen 2019). The lack of specificity in the mechanism of action of paclitaxel led to the development of its derivative, docetaxel, artificially synthesised on the basis of the paclitaxel structure (Wang and Du 2018); (Weger et al., 2014); (Herbst and Khuri 2003). Docetaxel is well known for its stronger affinity to tubulin than paclitaxel and its longer retention time in cells (Hernández-Vargas et al., 2007). However, despite the enhancement of these particular characteristics of docetaxel, (Li et al., 2019), a second generation taxane was established, cabazitaxel. Cabazitaxel is well known for its poor affinity for P-glyprotein-mediated efflux pumps exhibition, which reduces the susceptibility to pump the drug, reducing the development of resistance in tumours associated with P-glycoprotein overexpression (Galsky et al., 2010); (Paller and Antonarakis 2011); (Terada et al., 2019).

Epothilones, compounds also known to stabilise microtubules, was developed for the improvement of drug efficacy and the increase in safety profiles in comparison to taxanes (Lee and Swain 2008); (Gradishar 2009). The novel class antineoplastic agent, consisting of different subclasses, overlaps in area with the taxane-binding site on microtubules and induces microtubule polymerisation and stabilisation thus arresting the G2/M cycle and inducing apoptosis (Fumoleau et al., 2007); (Cheng et al., 2008). Vinca alkaloids are also another class of anti-mitotic agents which bind to the vinca domain on microtubules (Samadi et al., 2014). The structural differences are shown below in Table 1a.

Although treatment with anti-microtubule agents have proved successful initially, resistance development has been identified in metastatic diseases (Gómez-Miragaya et al., 2017). The mechanisms of taxane resistance include microtubule mutations, overexpression of efflux transporters, the reactivation of the androgen receptor pathway and upregulation of PI3K/AKT signalling (Bumbaca and Li 2018) which has led to the development of P-gp inhibitors to increase the efficacy of taxanes (Rechache et al., 2010); (Hendrikx et al., 2014); (Table 1b).
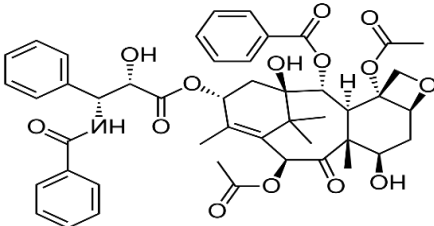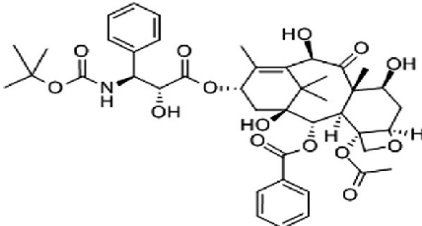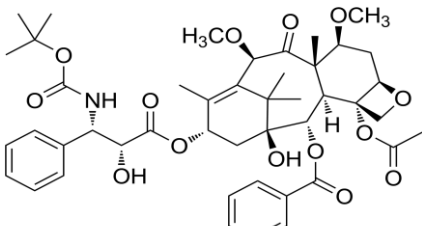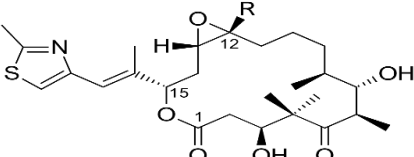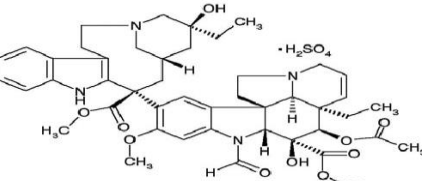
Name of drug	Target	Molecular structure
Paclitaxel	**anti-microtubule agent** -1st generation taxane -promotes assembling and stabilisation of microtubule polymers composed of repeating subunits of α and β- tubulin heterodimers	
Docetaxel	**anti-microtubule agent** -2nd generation taxane -disrupts microtubules in the cell via alteration in signal pathways involved in apoptosis e.g. Bcl-2 gene (MDR target)	
Cabazitaxel	**anti-microtubule agent** -2nd generation taxane -similar target to docetaxel -has an increased poor binding affinity for P-glycoprotein in comparison to docetaxel	
Epothilone-B	**anti-microtubule agent** -2nd generation taxane -induces microtubulue polymerisation and apoptosis	
Vincristine	**Vinca alkyloid** -disrupts tubulin and microtubule function	

Table 1a: Types of Taxane anticancer drugs with their specific targets and molecular structures.
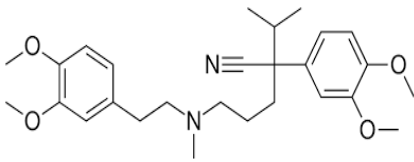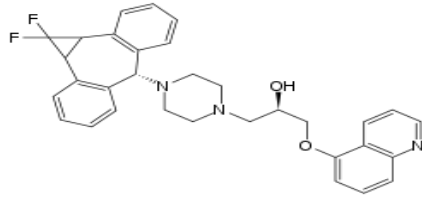
Name of drug	Target	Molecular structure
Verapamil	**1st generation multi-drug resistance inhibitor** P-glycoprotein blocker	
Zosuquidar	**3rd generation multi-drug resistance inhibitor** high affinity for P-glycoprotein	

Table 1b: **Types of P-gp inhibitors with their specific targets and molecular structures.**

2.3 DNA damaging agents

Although recent advances for the development of novel anticancer agents have led to the significant progress of efficacy in cancer patients' quality of life and survival, initial response to treatment proves favourable later leading to cancer relapse and reoccurrence due to acquired resistance (Nikolaou et al., 2018); (Meegan and O'Boyle 2019). Many anticancer drugs with different mechanisms of action, have been effective in promoting apoptosis thus reducing chemo-resistance (Senthebane et al., 2017); (Zheng 2017); (Yeldag et al., 2018); (Choi and Yu 2014).

2.3.1 Platinum based drugs

Platinum-based drugs used worldwide; cisplatin, carboplatin and oxaliplatin, have shown promising results for the palliative treatment of metastatic cancers (Hato et al., 2014; (Kelland 2007); (Dilruba and Kalayda 2016). The first discovery by Barmett Rosenberg in the 1960s began with cisplatin which proved to show anti-neoplastic activity (Rosenberg et al., 1969); (Johnstone et al., 2014). The mechanism of the platinum-based drugs differs slightly to the other compounds within the group. The Food Drug Administration (FDA) approved compound, cisplatin, which is commonly used to treat bladder, cervical, ovarian, testicular and mesothelioma, head-and-neck squamous cell carcinoma (HNSCC) and non-small cell lung cancer, is well known to induce cytotoxicity by binding to the DNA of the cell and interfere with its repair mechanism (nucleotide excision repair (NER)) (Florea and Büsselberg 2011); (Galluzzi et al 2012). Cisplatin's cytotoxicity nature is attributed to its specific interaction with DNA on the nucleophilic N7-sites of purine bases forming intra- and interstrand crosslinks (Siddik 2003); (Fuertes et al., 2012).

Carboplatin, a derivative of cisplatin, has shown increased efficacy for the treatment of ovarian and lung cancer. Despite its similarities in the mechanism of action, the toxicity and structure differs as

shown below in Table 2 (Stewart 2007); the main difference being the replacement of the chloride ligands seen on the cisplatin structure with a carboxycyclobutane moiety (Fonseca de Sousa 2014); (Townsend 2007); (Ardizzoni et al., 2007). For this reason, carboplatin exhibits a lower reactivity rate which subsequently resulting in fewer side effects and can be administered in higher doses (Dasari and Tchounwou 2014); (Johnstone et al., 2016).

Oxaliplatin, the third-generation platinum derivative used for standard chemotherapy, contains an oxalate and diaminocyclohexane (DACH) ligand in replacement of the amine group present in the chemical structure of cisplatin. This feature is responsible for the unique properties including its ability to exert its cytotoxicity intracellularly and reduced effect of cross-resistance occuring (Seetharam et al., 2009); (Alcindor and Beauger 2011); (Raymond et al., 2002); (Alian et al., 2012); (Martinez-Balibrea et al., 2015); (Arango et al., 2004).

However, despite the high response rates and increased efficacy of platinum-based drugs in comparison to other anti-cancer agents, most patients still develop acquired resistance (Ohmichi et al., 2005). Both passive and active transport have been identified as the method of intracellular and extracellular activity of platinum-based compounds and have indicated that resistance is as a result of observations in platinum-resistant tumor cells because of the decrease in drug accumulation (Campling 2006); (Holmes 2015).

Name of drug	Target	Molecular structure
Cisplatin	**Platinum based drug** -interferes with cell division and replication exerts cytotoxic effects via aquo complex -forms adducts in mitochondrial DNA on N-7 position of guanine	
Oxaliplatin	**Platinum based drug** -inhibits DNA replication and transcription -exerts cytotoxic effects via oxalate ligand -forms adducts in mitochondrial DNA on N-7 position of guanine	
Carboplatin	**Platinum based drug** -binds on DNA via CBDCA (bidentate dicarboxylate)	

Table 2: Types of platinum-based anticancer drugs with their specific targets and molecular structures.

2.3.2 Other DNA damaging agents

In the last decades, there has been an increased interest in the development of anticancer compounds that are able to react directly with DNA. The interactions include direct modification with the DNA bases via intercalation, crosslinking, alkylation or methylation on purine bases preventing DNA replication leading to cell death via apoptosis. (Cheung-Ong et al., 2013); (Sato and Itamochi 2015). A summary is shown in Table 3a and 3b.

The complexity of cancer with the different hallmarks, has led to the vast array of cytotoxic compounds (chemotherapy) and/or ionising radiation (radiation therapy). DNA damage remains a significant target by chemotherapeutic agents with different mechanisms of action (Swift and Golsteyn 2014); (Norbury and Zhivotoysky 2004); (Roos and Kaina 2013); (Table 3a and 3b).

The first class of anticancer drugs are alkylating agents. Most are monofunctional methylating agents such as temozolomide, which substitute alkyl groups for hydrogen atoms on the DNA structure forming inter-strand cross links (Kondo et al., 2010); (Khalife et al., 2015). As a result of alkylation, misreading of the genetic code occurs, inhibiting DNA, RNA and protein synthesis activating apoptosis (Drabløs et al., 2004); (Sarkaria et al., 2008).

Topoisomerase enzymes are enzymes which are associated with DNA replication, transcription, recombination and chromatin remodelling by the introduction of single- or double-strand breaks in the DNA structure (Champoux 2001); (Wang 2002).

There are two which have been discovered and the mechanisms of action have been used for the development of inhibitors (Dezhenkova et al., 2014). Clinically successful targeted anticancer drugs which arrest the DNA and form double-strand breaks are divided into two classes; topoisomerase I and topoisomerase II inhibitors (Delgado et al., 2018); (Pommier et al., 2016). The main difference between them is topoisomerase I causes single strand DNA breaks whilst topoisomerase II induces double-strand DNA breaks (Banerji and Los 2006).

Other DNA damaging agents include anticancer drugs that are able to cleave the DNA molecule. Bleomycins are well known to recruit single-stranded DNA (ssDNA) and double-stranded DNA (dsDNA) cleavage at specific sites in the DNA molecule; pyrimidines to guanine generating blunt ends (Trastoy et al., 2005); (Chankova et al., 2007). The group of antitumour antibiotics have been of interest due to their chemical properties in selectively degrading DNA (Hecht 2000).

2.3.3 Ultra-violet light C (UVC)

Ultra-violet (UV) light with short-wavelengths ranging from 200-280 nm, is another form of DNA damage specifically interacting with nucleic acids blocking the transcription process (Seltsam and Müller 2011). There are multiple pathways affected by UVC irradiation which include the introduction of bulky adducts causing single-strand and double-strand breaks blocking the ability

of the cancer cells to divide and proliferate further (Gill et al., 2015); (Baskar et al 2012); (Yoshino et al., 2019); (Oehler et al., 2007).

2.3.4 Pathway inhibitors

Tyrosine kinases are recognised for their signalling cascade and key roles in growth, differentiation, metabolism and apoptosis (Paul and Mukhopadhyay 2012) which have led to more recent efforts in designing and identifying oncogenic receptor tyrosine kinase inhibitors for the enhancement of clinical efficacy and improved survival for many advanced tumours (Chiarlie et al., 2002). The drugs used for most therapies have a narrow therapeutic index and often responses are palliative and unpredictable. Therefore, targeted therapies such as tyrosine kinases inhibitors help to improve the potency and specificity of existing therapy (Arora and Scholar 2005).

Other specific targeted therapies include epidermal growth factor inhibitors. Epidermal growth factor receptor (EGFR) is a transmembrane glycoprotein that has an intracellular tyrosine kinase domain and extracellular epidermal growth factor binding domain which are important for signalling pathways for the control of cellular growth and proliferation (da Cunha Santos et al., 2011); (Bethune et al., 2010); (Ohashi et al., 2013); (O'Kane et al., 2018). The structure of EGFR led to the pharmacologic approach to develop small-molecule inhibitors of the EGFR tyrosine kinase enzymatic activity due to the correlation between the overexpression in many human cancers (Lenz 2006); (Hao et al., 2017); (Wu et al., 2013). Erlotinib, an EGFR tyrosine kinase inhibitor, is well known to selectively and reversibly inhibit tyrosine kinase activity which has resulted in improved quality of life and tumour response rates (Schettino et al., 2008); (Wang et al., 2014); (Morgillo et al., 2016); (Table 3b).
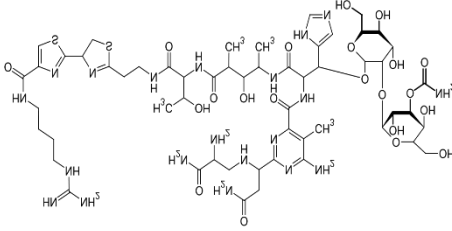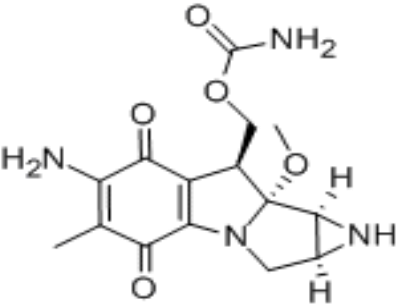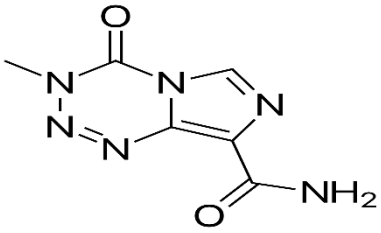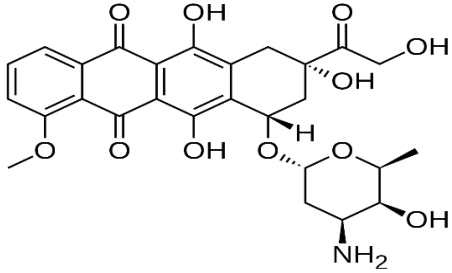
Name of drug	Target	Molecular structure
Zeocin	**anti-tumour antibiotic** causes double stranded and single stranded DNA breaks degrades DNA via inhibition of DNA synthesis with less inhibition of RNA and protein synthesis	
Mitomycin C	**anti-tumour antibiotic** alkylating agent (alkylates cellular nucleophiles) requires an enzymatic bioreduction to exert effects induces interstrand crosslinks prevents replication and RNA synthesis	
Temozolomide	**alkylating and methylating agent** causes damage to DNA and triggers apoptosis	
Doxorubicin	**anthracycline drug** interacts with DNA via intercalation leading to the disruption of DNA repair mediated by topoisomerase II prevents recombination of DNA during transcription generates free radicals resulting to DNA damage and cell death	

Table 3a: **Types of DNA damaging anticancer drugs with their specific targets and molecular structures.**
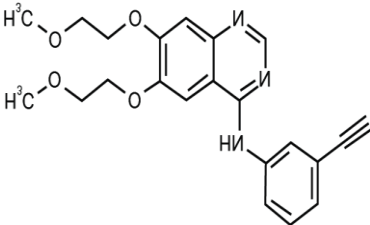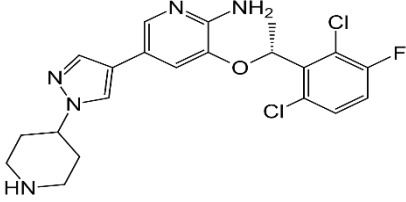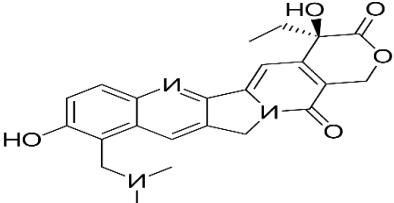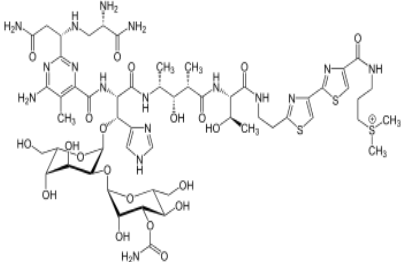
Name of drug	Target	Molecular structure
Erlotinib	**EGFR (epidermal growth factor receptor) inhibitor** Prevents cell division	
Crizotinib	**ALK (anaplastic lymphoma kinase) and MET inhibitor** -suppresses c-MET gene responsible for tumor growth and survival -prevents activation of signals e.g. P13K, RAS, JAK -inhibits phosphorylation of c-MET dependent oncogenic phenotypes	
Topotecan	**Topoisomerase II inhibitor** -cuts both strands of DNA simultaneously using ATP -inhibits the second step of DNA re-ligation	
Bleomycin	**glycopeptide anti-tumour antibiotic** binds to G-C rich portions of DNA uses free radicals to break single strand DNA	

Table 3b: Types of DNA damaging anticancer drugs with their specific targets and molecular structures.

2.4 Pre-clinical models

The existing evidence for tumour heterogeneity has provided insights for cancer therapeutics and biomarker discovery, predominantly targeted therapy, via extensive research. Accurate assessment has permitted the development of current approaches used to understand heterogeneity and the consequences. As a result, exploration for more-effective personalised therapies have been developed with the use of pre-clinical models to depict the variations in different cancer types (Fisher et al., 2013).

Pre-clinical model systems are needed to study cancer. They enable functional studies, systems level investigations, the testing of non-standard therapies, and the direct comparison of different therapies, which cannot be performed in the clinics and with the use of clinical samples alone (Dhandapani & Goldman, 2017).

In vitro and *in vivo* tumour models have been used to identify the cellular, genetic and epigenetic composition of different types of cancers. By using these models, extensive research can be carried out to highlight the complexity and diversity of cancer types. A range of preclinical tumour models have been widely used which ranges from spontaneous or induced tumours in genetically engineered or wild-type organisms to primary human tour grafts, each with differences in strengths and limitations (Galuschka et al., 2017); (Ogilvie et al., 2017); (Jackson and Thomas 2017).

2.4.1 In-vivo tumour models

Animal tumour models play a significant role in drug target and biomarker discovery for improved care for the cancer patients. The development of therapeutics has been assisted significantly by the use of many mouse tumour models which include cell line-derived xenografts (CDXs), patient derived-xenografts (PDXs), genetically engineered mouse models (GEMMs), cell lines- or primary tumour-derived homographs in syngeneic mice etc (Guo et al., 2019).

The use of clinical trials using mouse models have been known to provide more rational and flexible analysis of cancer research and drug development (Day et al., 2015); (Khaled and Liu 2014); (Li et al., 2017). Clinical trial successes include 71-91% of full remission of patients with acute promyelocytic leukaemia (APL) treated with retinoic acid (RA) in comparison with standard chemotherapy using transgenic murine models since the late 1990s (Gargiulo 2019).

Several studies have suggested the combination of *in vivo/in vitro* techniques are more reliable than the use of each on its own (Rosa et al., 2014); (HogenEsch and Nikitin 2012). Clinical research conducted by *Lorger et al., 2011,* discovered that using *in vivo* and *in vitro* brain microvascular endothelial cells of five different metastatic breast cancer cell lines, indicated that *in vitro* assays alone provide lesser reflection in the ability of breast cancer cells to colonise the brain suggesting

a more thorough investigation using animal model for definitive and clinical relevance (Lorger et al., 2011).

One of the major advantages of *in vivo* models is the close comparison with the human disease. As all models, murine models in particular, still require the need for improvement in the relevance which is one of the limitations, despite being the most accessible animal model. Recent advances have led to the development of cell lines being incorporated into xenografts where the tumour cells are injected into immunocompromised mice. However, the usefulness still remains uncertain (Cook at al., 2012).

Nevertheless, the comparison of pharcokinetics and pharmacodynamics of a drug in a rodent in comparison to a human remains as one of the major limitation of *in vivo* models. Although traditional cell-line-derived xenografts have been effective in measuring the efficacy of drugs during clinical trial and have led to the approval of anti-cancer drugs, differences between the species include the differences in target cell sensitivity and drug metabolism. Therefore, the cytotoxicity of experimental drugs and standard drugs in a human cancer cell, may reveal differences in drug responses (Lopez-Lazaro 2015); (Koga and Ochiai 2019).

Despite the ability to conduct large-scale screening techniques for the detection of drug biomarkers, cancer cell lines have been limited to its validation of clinical heterogeneity, genetic disarray and their adaptation to their artificial environment, which makes it difficult to capture the true perception of the primary tumours (Borrell 2010). Recently, the use of patient-derived xenografts has been introduced to demonstrate the heterogeneity response of cancer. A controlled trial using patient-derived xenografts of head and neck squamous cell carcinoma (HNSCCs) was conducted to demonstrate the efficacy of inhibiting PI3Kα signalling pathway, a biomarker for tumour growth. It was revealed that using both an HNSCC specific, cell line panel alongside, patient-derived xenografts were much closely correlated with patient outcomes; emphasizing the potential of personalised therapy for HNSCC patients (Ruicci et al., 2019); (Zhang et al., 2018). Another major advantage is, unlike *in vitro* models, limitations such as cross-contamination, misauthentication and mycoplasma contamination do not affect *in vivo* models (Wilding et al., 2014).

2.3.2 In-vitro tumour models

Extensive research has been conducted using large-scale drug screens of cell line panels to detect mechanisms of growth inhibition and tumour-cell death. The use of these *in vitro* models have enabled the examination of chemotherapeutics and targeted therapeutic potential (Pauli et al., 2017); (Cook et al.,2012).

Cancer cell lines have a been a leading model system for the investigation of cancer, because they are easy to handle and manipulate (S. V. Sharma et al., 2010); (Gradinaru et al., 2007). Also, cancer cell lines as preclinical models enable comparisons of experimental results which are widely used

to study molecular mechanisms of tumour cell biology at a low cost. However, one of the major setbacks of the model is the inability to replicate the three dimensional tumour structure, the absence of the tumour microenvironment and the presence of growth factors and cytokines in cell culture media (Katt et al., 2016).

The characterisation of cancer cell lines has proved, that they are useful tools for the study of the biological mechanisms involved in cancer (Van staveren et al., 2009). The reproducibility of results produced from experiments conducted with the cell lines has increased the validity of the results produced. Nevertheless, all models have their limitations; one of which includes the genomic instability of the original tumour and the respective cell line as a result of routine culturing which has caused phenotypic changes by the appearance of subpopulations selected from competitive clones (Ferreira et al 2013); (Niu and Wang 2015).

The development of multidrug resistance (MDR) to chemotherapy remains as the greatest challenge to date (Gillet and Gottesman 2010) and to overcome this, drug-adapted cancer cell lines, which mimic the intrinsic resistance of metastatic cancers, have been developed and have been successful in screening for the identification of anticancer compounds performed under normal conditions such as oxygen pressure and pH in comparison to solid tumours which are limited to nutrients, reduced oxygen supply and acidosis (Pellegrini et al., 2018); (Wong et al 2017); (Szakács et al., 2006); (Housman et al 2014); (Filipits 2004).

2.5 ABC drug transporters

Drug-adapted cancer cell lines have been used to discover many important resistance mechanisms. This includes drug effluxion caused by the superfamily of ATP-binding cassette (ABC) transmembrane transporters which convert the energy gained from ATP hydrolysis into transportation of their substrates into the cytoplasm (import) or out of the cytoplasm (export) (Locher 2009). It is well documented that these transporters significantly decrease the intracellular concentration of certain anti-cancer drugs by effluxion of substrate drugs out of cancer cells disrupting the efficacy (Liu et al., 2013); Yang et al., 2015); (Ji et al., 2015).

Evidence suggests that resistance to cytotoxic and targeted chemotherapy is a result of the expression of ABC transporters, especially ABCB1 which is encoded by the subfamily B member 1, commonly known as the multidrug resistance protein 1 (MDR1, P-glycoprotein or P-gp) (Robey et al., 2018). Other well researched transporters include multidrug resistance-associated proteins ABCC1 and breast cancer resistance protein ABCG2 (Xiong et al., 2015).

2.5.1 ABCB1 (MDR1/P-gp)

The first ABC transporter, ABCB1 (P-glycoprotein (P-gp) or MDR1), was identified in colchicine-adapted Chinese hamster ovarian (CHO) cells (Juliano & Ling, 1976). The discovery has provided the understanding that this transporter recognises and effluxes a large number of structurally and

biochemically related substrates of different molecular weights and has led to pharmaceuticals developing compounds such as inhibitors which may modulate P-gp activity thus resulting in a competitive relationship amongst substrates (Hodges et al., 2011); (Chang et al., 2006).

The use of cancer cell lines has enabled the development of targeted therapy to overcome multi-drug resistance caused by the overexpression of P-gp (McIntosh et al., 2016). More specifically, the transmembrane domains of ABCB1 are responsible for the characteristic determination of the anti-cancer substrates for their effective transportation. These include vinca alkyloids, anthracyclines and taxanes.

2.5.2 ABCC1 (MRP1)

ABCC1 (MRP1), another major ABC transporter involved in anti-cancer drug resistance, was identified in doxorubicin-adapted H69 lung cancer (Cole et al., 1992). These transporters are promiscuous drug efflux pumps that transport a wide range of structurally different anti-cancer drug classes out of cancer cells (Szakács et al., 2006);(Robey et al., 2018). In addition, many further clinically relevant resistance mechanisms have been discovered in drug-adapted cancer cell lines (S. V. Sharma et al., 2010); (Nazarian et al., 2010); (Korpal et al., 2013); (Schneider et al., 2017); (Joseph et al., 2013); (Jung et al., 2016); (M. Michaelis et al., 2011); (M. Michaelis et al., 2012).

These pumps are known to extrude both hydrophobic, uncharged molecules and water soluble anionic compounds making the substrate selectivity broad. These include anthracyclines, vinca alkyloids, epipodo-phyllotoxins, camptothecins and methotrexate, but not to taxanes which is a significant component of P-gp profile (Yuan et al., 2016); (Silva et al., 2014).

2.5.3 ABCG2 (BCRP)

ABCG2 (ATP Binding cassette subfamily G member 2) often referred to as the breast cancer resistance protein (BCRP) is a protein for the protection of many tissues from xenobiotic molecules. The overexpression is well known in breast cancer cell lines and is recognised to inhibit the pharmacokinetic properties of commonly used drugs by limiting the delivery of therapeutics into the tumour cells consequently contributing to multidrug resistance (Taylor et al., 2017); (Mo and Zhang 2012).

The efflux pump, located on the apical membranes, is known to exhibit a broad spectrum of endogenous and exogenous substrates. More specifically, observations of significant ABCG2-mediated resistant cancer cell lines have demonstrated resistance to anthracyclines, mitoxantrone and several tyrosin kinase inhibitiors (Toyoda et al., 2019); (Vähäkangas et al., 2011); (Mao 2008); (Wu et al., 2015).

This project, drug-adapted cancer cell were further investigated as pre-clinical model systems.

2.6 Project aims

This project investigated the use of cancer cell lines as pre-clinical model systems of acquired resistance mechanisms in different contexts.

1) A new set of cisplatin-adapted ovarian cancer cell lines was introduced and characterised.
2) Drug-adapted neuroblastoma cell lines were used to investigate the potential of doxorubicin-loaded nanoparticles to circumvent transporter-mediated drug resistance.
3) A standardised drug adaptation protocol was developed to compare the relative potential of drugs to induce resistance.

3 Materials

The materials, reagents and equipment used and where they were obtained, as used for the research in this thesis is as shown below in Table 4-7.

3.1 Reagents

Name of reagent	Source
Iscove's Modified Dulbecco's Medium (IMDM)	Gibco™ (Life Technologies), Paisely, UK
100mg/ml streptomycin	Gibco™ (Life Technologies), Paisely, UK
Dimethyl-2-thiazolyl)-2,5-diphenyl-2H-tetrazolium-bromide	Universal biologicals (Cambridge), Cambridgeshire, UK
Foetal Bovine Serum (FBS)	Sigma Aldrich®, Dorset, UK
Trypsin – 0.02% (w/v) EDTA solution	Sigma Aldrich®, Dorset, UK
DMSO	Sigma Aldrich®, Dorset, UK
0.01% poly-l-lysine solution (MW 150, 000-300,000)	Sigma Aldrich®, Dorset, UK
Paraformaldehyde powder, 95%	Sigma Aldrich®, Dorset, UK
Trition™X-100 solution	Sigma Aldrich®, Dorset, UK
Bovine Serum Albumin	Sigma Aldrich®, Dorset, UK
Tween-20 solution	Sigma Aldrich®, Dorset, UK
cOmplete mini EDTA-free protease inhibitor cocktail tablets	Sigma Aldrich®, Dorset, UK
BCA assay (bicinchoninic acid kit)	Sigma Aldrich®, Dorset, UK
PVDF membrane	Sigma Aldrich®, Dorset, UK
gentian violet dilution	Sigma Aldrich®, Dorset, UK
Oxoid- ®phosphate buffered saline tablets	Thermo Fisher scientific, Ashford, UK
Sodium chloride	Thermo Fisher scientific, Ashford, UK
D-Glucose, anhydrous	Thermo Fisher scientific, Ashford, UK
N, N-dimethylformamide solution	Thermo Fisher scientific, Ashford, UK
sodium dodeylsulfate (SDS) powder	Thermo Fisher scientific, Ashford, UK
Marvel milk powder	Thermo Fisher scientific, Ashford, UK
DTT (Dithiothreitol) solution	Thermo Fisher scientific, Ashford, UK
Sodium fluoride (NaF)	Thermo Fisher scientific, Ashford, UK
β-Glycerophosphate disodium salt hydrate	Thermo Fisher scientific, Ashford, UK
Sodium Orthovanadate ≥90% (titration)	Thermo Fisher scientific, Ashford, UK
HEPES (N-2-hydroxyethylpiperazine-N-2-ethane sulfonic acid)	Thermo Fisher scientific, Ashford, UK
Glycerol	Thermo Fisher scientific, Ashford, UK
Tris hydrochloride powder (Tris-HCl)	Thermo Fisher scientific, Ashford, UK
β-mercaptoethanol ≥99.0%	Thermo Fisher scientific, Ashford, UK
Bromophenol blue	Thermo Fisher scientific, Ashford, UK
APS (ammonium persulfate)	Thermo Fisher scientific, Ashford, UK
Glycine	Thermo Fisher scientific, Ashford, UK
PageRuler Plus Prestained Protein Ladder	Thermo Fisher scientific, Ashford, UK
Methanol ≥99.9%	Thermo Fisher scientific, Ashford, UK
Pierce™ ECL western blotting substrate	Thermo Fisher scientific, Ashford, UK
primary antibody Anti-P Glycoprotein mAb [EPR10364-57]	Abcam, Cambridge, UK
Donkey ani-rabbit Alexa Fluor™ 488 secondary antibody	Life technologies (Thermo scientific), Paisley, UK
ProLong™ Diamond Anti-fade Mountant with DAPI	Life technologies (Thermo scientific), Paisley, UK
TEMED	BioRad, USA
30% (v/v) acrylamide/bis solution 37:5:1 ratio	BioRad, USA
Whatman filter paper	GE healthcare, USA
Amersham hyperfilm ECL film	GE healthcare, USA
Anti-Rabbit IgG HRP-linked	Cell signalling technology, Danvers, USA
Anti-tubulin antibody	Bio-Rad, Kidlington, UK

Table 4: Reagents. **List of the reagents used and the source of purchase.**

3.2 Chemotherapeutic drugs

Name of chemotherapeutic drug	Source
Cisplatin	Accord Healthcare Ltd, Middlesex, UK
Oxaliplatin	TEVA Pharmaceutical Industries Ltd, Eastbourne, UK
Carboplatin	Sun pharmaceutical industries, Hayes, UK
Temozolomide	Cayman chemical company, Michigan, USA
Etoposide	Cayman chemical company, Michigan, USA
Erlotinib	Cayman chemical company, Michigan, USA
Topotecan (hydrochloride)	Cayman chemical company, Michigan, USA
Paclitaxel	(Cambridge Biosciences, Cambridge, UK)
Docetaxel	(Cambridge Biosciences, Cambridge, UK)
Epothilone-b	(Cambridge Biosciences, Cambridge, UK)
Vincristine	(Cambridge Biosciences, Cambridge, UK)
Doxorubicin (hydrochloride)	(Cambridge Biosciences, Cambridge, UK)
Cabazitaxel	(Cambridge Biosciences, Cambridge, UK)
Mitomycin C	(Cambridge Biosciences, Cambridge, UK)
Bleomycin (sulphate)	(Cambridge Biosciences, Cambridge, UK)
Zeocin	Life Technologies (Thermo scientific), Paisley, UK
Crizotinib	SYNkinase, Parkvile, Australia

Table 5: Chemotherapeutic drugs. **List of the chemotherapeutic drugs used and the source of purchase.**

3.3 Plastics

Name of plastic	Source
T25cm^2 sterile flask	Sarstedt ®, Leicester, UK
cryotube vial in 1.8 mL volumes	Nunc, Thermo Fisher Scientific, Loughborough, Leicestershire, UK
Sterile circular coverslips and glass slides	
cryovial freezing container	Nalgene, Thermo Fisher Scientific, Loughborough, Leicestershire, UK
Sterile 96-well plates	Greiner bio-one cellstar Ltd, Gloucestershire, UK
Sterile 24-well plates	
Sterile 6-well plates	
deep well drug block	VWR, Leicestershire, UK
BMG Labtech FLuostar Omega plate reader	BMG Labtech, Aylesbury, UK
E-plate VIEW 16 PET	ACEA Biosciences Inc. San Diego, CA, U.S.A
Invitrogen^{TM} Novex^{TM} empty gel cassettes	Thermo Fisher scientific, Ashford, UK

Table 6: Plastics. **List of plastics used and the source of purchase.**

3.4 Equipment

Name of equipment	Source
Eppendorf Centrifuge 5702	Eppendorf, Hamburg, Germany
Eppendorf 5702 benchtop centrifuge	Eppendorf, Stevenage, Hertfordshire, UK
xCELLigence Real-Time Cell Analyser (RTCA)	Cambridge Biosciences, Cambridge, United Kingdom
Olympus CKX53 light microscope with GXCAM-U3-5 industrial camera	Olympus, Southend-on-Sea, UK
Zeiss LSM 880 Elyra confocal microscope with airyscan and PALM/STORM super resolution	Stockholm, Sweden
Hoefer^{TM} TE22 Mini Tank Blotting unit	Thermo Fisher scientific, Ashford, UK
UV chamber and Spectroline model ENF-240 C/FE Ultraviolet Inspection lamp machine	Che Scientific, Kwai Chung, Hong Kong

Table 7: Equipment. List of equipment used and the source of purchase.

4 methods

4.1 Cell lines used

The MYCN-amplified neuroblastoma cell line, UKF-NB-3, was derived from a stage 4 patient (Kotchetkov et al 2005). Drug-resistant sublines were established by continuous exposure to step-wise increase drug concentrations as previously described (Kotchetkov et al., 2005; M. Michaelis et al., 2011) and derived from the Resistant Cancer Cell Line (RCCL) collection (https://research.kent.ac.uk/ibc/the-resistant-cancer-cell-line-rccl-collection/). UKF-NB-3-^{r}DOX[20] was adapted to grow in the presence of 20 ng/ml of doxorubicin and UKF-NB-3-^{r}VCR[1] was adapted to grow in the presence of 1ng/mL of vincristine.

The ovarian cancer cell lines EFO-27, EFO-21 and COLO-704 were obtained from DSMZ (Braunschweig, Germany). The cisplatin-resistant cell lines cultivated in the presence of cisplatin were derived from the Resistant Cancer Cell Line (RCCL) collection (www.kent.ac.uk/stms/cmp/RCCL/RCCLabout.html). These cell lines were grown in the presence of 2μg/ml of cisplatin (EFO-27^{r}CDDP[2000] and EFO-21^{r}CDDP[2000)]), whilst COLO-704^{r}CDDP[1000] was grown in the presence of 1μg/ml of cisplatin; cisplatin was added immediately after re-suspension.

Cisplatin exposure was discontinued for EFO-27^{r}CDDP[2000 (-)], EFO-21^{r}CDDP[2000 (-)] and COLO-704^{r}CDDP[1000 (-)] cell lines by myself in order to generate a cisplatin drug released cell line. These cell lines were derivatives of the originally cisplatin resistant cell lines from the RCCL collection.

4.2 Cell culture

All cell lines were cultivated in Iscove's Modified Dulbecco's Medium (IMDM) supplemented with 50 mL (v/v) (10%) of Foetal Bovine Serum (FBS) and 5 mL (v/v) (1%) of 100 IU/ml penicillin and 100mg/ml streptomycin and were incubated in a 37°C /5% CO_2 incubator. The medium of the drug-adapted UKF-NB-3 sublines was supplemented with the indicated drug concentrations.

When adherent cells reached the confluence between 70-80% (determined by visualising under the light microscope), medium was aspirated and cells were washed with 2 mL of sterilised phosphate buffered saline solution (w/v 1mg/ml). Adherent cells were detached using 2ml of 0.25% (w/v) Trypsin – 0.02% (w/v) EDTA solution and was incubated at 5% CO_2/37°C for 2-3 minutes. The cells were then re-suspended into 8 mL of supplemented IMDM and cultured into a new T25cm^2 flask. All cell lines were routinely tested for mycoplasma contamination.

When the suspension cell line, once 70-80% confluence was achieved (determined by visualising under the microscope), the cells were aspirated into a 15 ml sterile falcon tube and spun down to

a pellet using Eppendorf centrifuge 5702 at 10500 rpm (x 8000 g) for 3 minutes. The cell pellet was re-suspended into 2 ml of sterile PBS solution and spun down again at the same speed and duration. The PBS solution was aspirated and the cells were re-suspended into 1 ml of 0.25% (w/v) Trypsin – 0.02% (w/v) EDTA solution and left for 2-3 minutes before re-suspending into supplemented IMDM.

4.3 Cryopreservation

1×10^6 cells from a T75 cm^2 flask that had reached about 70-80% confluence, were trypsinised, re-suspended in 8 ml cell culture medium and centrifuged for 3 min at x 8000 g at room temperature using Eppendorf 5702 benchtop centrifuge. Then, the supernatant was removed and cells were re-suspended into cryoprotectant medium (34.5 mL IMDM supplemented with 5 mL DMSO, 10 mL FBS and 0.5 mL of 100 IU/mL penicillin and 100 µg/mL streptomycin) and passed into a cryotube vial in 1.8 mL volumes. The vials were then transferred into a cryovial freezing container and was stored at -80°C overnight and then transferred to liquid nitrogen for long-term storage. Cryopreserved cells were resuscitated by thawing at 37°C and resuspension using cell culture medium.

4.4 Viability test

Cell viability was determined by Dimethyl-2-thiazolyl)-2,5-diphenyl-2H-tetrazolium-bromide (MTT) assay modified after (Mosmann, 1983) and previously described by (M Michaelis et al., 2015). The yellow MTT reagent is reduced into an insoluble purple formazan in the mitochondria of viable cells indicating oxidative phosphorylation (Riss, Moravec, Niles, Duellman, & Benink, 2013).

4.5 Experiment method
7,000 cells were seeded into 96-well plates according to figure 2A-C.

An 8-point serial drug dilution was pre-made in a deep well drug block. The drug dilution was added to the 96-well plate in triplicates; enabling two drugs per plate to be tested (figure 8C). After incubation for 120 hours at 5% CO_2/37°C, 25 µL of MTT reagent (2mg/mL Dimethyl-2-thiazolyl)-2,5-diphenyl-2H-tetrazolium-bromide (w/v) in PBS) was added to each well followed by a further 4-hour incubation period. After this, 100 µL of 20% (w/v) sodium dodeylsulfate (SDS) solution in 50% (v/v) N, N-dimethylformamide and 50% purified water adjusted to pH-4 was added and incubated overnight at CO_2/37°C to lyse cells and solubilise the formazan salt.

Absorbance was then determined using BMG Labtech FLuostar Omega plate reader read at 600nm; the background absorbance was subtracted and the absorbance relative to untreated control wells was determined using the formula:

Relative absorbance = (Absorbance of sample – average absorbance of minimum wells)/ (Average absorbance of maximum wells – Average absorbance of minimum wells).

Drug concentrations that reduce the cell viability by 50% relative to untreated control (IC50) was determined using CalcuSyn (Biosoft, Cambridge, UK). CalcuSyn software was used to analyse the drug dose-effect for single and multiple drugs on the cells' viability to quantify the efficacy of the drug using the absorbance data.

A. Addition of medium

	1	2	3	4	5	6	7	8	9	10	11	12
A	50µl	50µl	50µl	50µl	50µl	50µl	50µl	50µl	50µl	50µl	50µl	50µl
B	50µl	50µl									100µl	50µl
C	50µl	50µl									100µl	50µl
D	50µl	50µl									100µl	50µl
E	50µl	50µl									100µl	50µl
F	50µl	50µl									100µl	50µl
G	50µl	50µl									100µl	50µl
H	50µl	50µl	50µl	50µl	50µl	50µl	50µl	50µl	50µl	50µl	50µl	50µl

B. Addition of cells

	1	2	3	4	5	6	7	8	9	10	11	12
A												
B		50µl	50µl	50µl	50µl	50µl	50µl	50µl	50µl	50µl		
C		50µl	50µl	50µl	50µl	50µl	50µl	50µl	50µl	50µl		
D		50µl	50µl	50µl	50µl	50µl	50µl	50µl	50µl	50µl		
E		50µl	50µl	50µl	50µl	50µl	50µl	50µl	50µl	50µl		
F		50µl	50µl	50µl	50µl	50µl	50µl	50µl	50µl	50µl		
G		50µl	50µl	50µl	50µl	50µl	50µl	50µl	50µl	50µl		
H												

C. Addition of 8-serial point dilutions

	1	2 Max	3	4	5	6	7	8	9	10	11 Min	12
A												
B			1	2	3	4	5	6	7	8		
C			1	2	3	4	5	6	7	8		
D			1	2	3	4	5	6	7	8		
E			1	2	3	4	5	6	7	8		
F			1	2	3	4	5	6	7	8		
G			1	2	3	4	5	6	7	8		
H												

Figure 2 : Schematic layout for the viability test. A. Plate preparation with volume of IMDM for wells covered in red. Volume of IMDM to prevent evapouration in pink. B. Volume of suspended cells at 7000 cells per well in green. C. Wells B1-G1 = maximum wells highlighted in red (cells and medium alone) and B11-G11 = minimum wells highlighted in green (medium alone). C. Addition of the 8-serial point dilutions at 50 µL per well. Purple and orange represent two different chemotherapeutic agents.

4.6 Chemotherapeutic drugs

All drugs used were stored and diluted according to the manufacturer's guidelines.

Cisplatin aliquots of 1mg/ml (w/v) in 0.9% NaCl solution were kept at room temperature away from light due to the sensitivity. Oxaliplatin and Carboplatin aliquots of 1mg/ml (w/v) in 5% sterile-filtered glucose solution, were stored at -20˚C.

Temozolomide aliquots of 10mg/ml (w/v) in 1ml DMSO, Etoposide aliquots of 25mg/ml (w/v) in 1 ml of DMSO, Erlotinib aliquots of 250mg/ml (w/v) in 1ml of DMSO, Topotecan (hydrochloride) aliquots of 5mg/ml (w/v) in 1 ml of DMSO and paclitaxel, docetaxel, epothilone-b, vincristine, doxorubicin (hydrochloride) and cabazitaxel aliquots of 1mg/ml (w/v) in 1 ml DMSO, were all stored at -20°C.

Mitomycin C and Bleomycin (sulphate) aliquots of 10mg/ml (w/v) in 1 ml of DMSO, Zeocin aliquots of 100mg/ml (w/v) in 1 ml of DMSO and Crizotinib aliquots of 2.3mg/ml (w/v) in 1 ml of DMSO.

4.7 xCELLigence Real-Time Cell Analyser (RTCA)

The growth kinetics were determined using the xCELLigence Real-Time Cell Analyser (RTCA) following the manufacturer's instructions; the set up was inside a 37°C/5% CO_2 incubator. Cells were seeded at 3,000 per well and performed in triplicates on an E-plate VIEW 16 PET. The cell index was taken every thirty minutes for six days or until the plateau of the growth curve; from this the exponential phase of the growth curve was used to generate the doubling times.

4.8 Growth kinetics using cell viability (MTT) assay

To determine the growth kinetics of the cells, a 120 hour MTT assay was performed. The assay was composed of a separate assay every 24 hours to assess the cells' viability. The cells were seeded at 3,000 cells per well of each cell line and sub-line in triplicate as with the drug sensitivity assay. Here, no treatment was given to the cells.

The doubling time was determined at the log phase where the growth became constant using the exponential curve. Using excel an equation was generated; y = Ae^{Bx} where A and B were numbers. T_d or doubling time was then calculated by dividing ln2 (0.693) by B (derived from y = Ae^{Bx}). This was repeated for each biological repeat (n=3) and the average was calculated. An example is shown below in Figure 3.
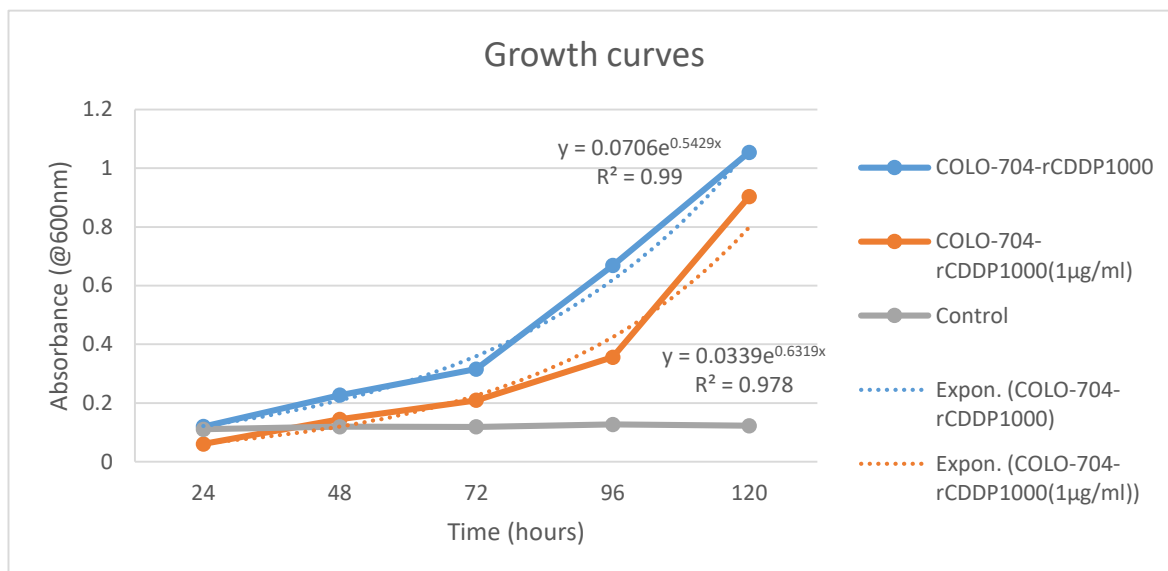
Figure 3 : **Doubling time determined using an exponential curve**. COLO-704-rCDDP[1000(-)] and COLO-704-rCDDP[1000] results determined using the equation y = Ae^{Bx}. Td = 0.693 divided by B. All values presented in the graph are of one biological repeat.

4.9 Morphological analysis

The morphology of each cell line and subline was determined using an Olympus CKX53 light microscope with GXCAM-U3-5 industrial camera using different magnifications using a x 10 and x 20 objective.

4.10 Immunostaining protocol

Circular coverslips were placed into 2 wells of a 24-well plate using pre-autoclaved tweezers; two wells represented a positive and negative control. One 24-well plate was used for each sub-line and the cell line for the comparison. The coverslips were treated with 0.5ml of 0.01% poly-l-lysine solution (MW 150, 000-300,000) and left for 5 minutes. The poly-l-lysine solution was aspirated and left to dry for 2 hours under sterile conditions. The cells were seeded at 1 x 10^5 cells per well into a total volume of 1 ml per well. The plates were then incubated at 5% CO_2/37°C.

Following a 48-hour incubation period, the plates were removed and the confluence of the cells were determined using a light microscope to ensure the confluence was at 30-40%. The IMDM was aspirated and washed with sterile PBS solution thrice. The coverslips were then fixed with 500 µl of 4% w/v MW 30.03 paraformaldehyde solution in PBS for 15-20 minutes at room temperature. After aspiration, the wells were washed with 1 ml of PBS thrice. Cells were then permeabilised using 500 µl of Trition™X-100 solution (0.1% w/v) in 3% BSA (Bovine Serum Albumin) in PBS for 20 minutes at room temperature. After aspiration, wells were washed with 1 ml of PBS thrice. The cells were then blocked using 200 µl of BSA solution (3% w/v in PBS) for 1 hour. After aspiration, the cells were washed twice. The coverslips were then transferred from the 24 well plate and inverted on to parafilm inside a humidity chamber containing the primary antibody Anti-P Glycoprotein mAb

45

[EPR10364-57] (1:250 dilutions in a BSA solution (3% w/v in PBS). A positive and negative control was used at this stage; positive control whereby the coverslip was inverted on to 25 µl of the primary antibody dilution and the negative control with 25 µl of BSA (3% w/v in PBS). The coverslips were incubated overnight at 4°C.

The coverslips were then removed from the fridge and wash four times with Tween-20 solution (0.1% v/v in PBS). The excess liquid was removed by lightly tapping onto tissue and being transferred onto 100 µl of the wash solution. This process was repeated four times.

The positive and negative control coverslips were then incubated with Donkey Anti-Rabbit IgG (H+L) highly cross-absorbed, Alexa Fluor™ 488 secondary antibody dilution (3% BSA v/v in PBS) of 1:500 for 1 hour 30 minutes at 4°C. This stage was performed in the dark and incubated in the dark.

After incubation, the coverslips were washed again four times in the Tween-20 solution (0.1% v/v in PBS). The coverslips were then inverted onto a glass slide containing 5 µL of ProLong™ Diamond Anti-fade Mountant with DAPI. The slides were then left in a dark box to dry at room temperature for 24 hours before taking images using Zeiss LSM 880 Elyra confocal microscope with airyscan and PALM/STORM super resolution.

4.11 Western blot analysis

The antibody used was as mentioned above for the immunofluorescence protocol. The dilution used was 1:500 and blocking agent was Marvel Milk (5% w/v in 1% v/v Tween-20 solution).

4.11.1 Protein extraction

Cells were plated into a polystyrene cell culture dish 100 x 20 mm and incubated at 37°C/5% CO_2 in an incubator. After a monolayer formation, the media was aspirated and cells were washed with PBS. The cells were lysed for 30 minutes on ice using 100µl of lysis buffer (50mM HEPES (pH 7.4) 250mM NaCl, 0.1% v/v NP40, one tablet of cOmplete mini EDTA-free protease inhibitor cocktail tablet, 1mM DTT, 1mM NAF, 10Mm β-Glycerophosphate and 0.1mM Sodium Orthovanadate). The lysates were centrifuged at 14,000 rpm for 10 minutes at 4°C. The supernatants were then used to determine the protein concentration using a BCA assay (bicinchoninic acid kit). The assay involved the preparation of BSA protein standards made from a stock solution (w/v 1 mg/mL in distilled water) of 0.1 mg/mL, 0.2 mg/mL, 0.4 mg/mL, 0.6 mg/mL, 0.8 mg/mL and 1.0 mg/mL. Both sample and standards were loaded into a 96-well plate and after the addition of the BCA dye, the absorbance was measured at 560 nm. The protein concentration of the samples was then determined using a standard curve in Excel 2013.

Samples were normalised to the desired concentration (typically 30-50µg per lane) using lysis buffer and 5 x sample buffer (50% v/v glycerol, 0.3 M Tris-HCl pH 6.8, 10% (w/v) SDS, 20% β-

mercaptoethanol and 0.05% (w/v) bromophenol blue. The diluted samples were then vortexed, heated to 95 °C and loaded into the 1.0 mm thick 8% acrylamide gels.

4.11.2 SDS-PAGE gel preparation

The sodium dodecyl sulphate polyacrylamide gels (SDS-PAGE) were made according to the recipe in table 1. 10% (w/v in distilled water) APS (ammonium persulfate) was made on the day of use likewise the stacking gel. 10 mL of resolving gel and 5 mL of stacking gel was enough to make two gels.

Components	Stacking gel	Resolving gel
30% acrylamide/bis	2 mL	4 mL
Stacking buffer (0.5 M Tris-HCl and 0.4 % (w/v) SDS, pH 6.8	3.75 mL	~
Resolving buffer (1.5 M Tris-HCl and 0.4% (w/v) SDS, pH 6.8	~	3.75 mL
Distilled water	9 mL	7.25 mL
10% APS	75 µL	75 µL
TEMED	15 µL	7.5 µL

Table 8: Composition of the SDS-PAGE polyacrylamide gels. Volumes made was enough for 2 gels. Recipe is as recommended by Fisher Scientific.

The resolving gel was poured into Invitrogen™ Novex™ empty gel cassettes which were pre-sealed to prevent leakage and left to polymerise for 45 minutes – 1 hour. After 24 hours, the overlayer of distilled water was removed and the stacking gel was added. Immediately after pouring, a 12-lane comb was inserted and after 45 minutes of polymerisation, the comb was removed and placed into the electrophoresis tank filled with 1L of running buffer (0.192 M glycine, 0.025 Tris-HCl and 0.1% w/v SDS in distilled water. Each sample was loaded in each lane including a lane for the DNA ladder (PageRuler Plus Prestained Protein Ladder) and the gel was ran at 80V for 30 min and then 120V until the desired migration was visual.

The SDS-PAGE gel was then transferred at 100V for 90 minutes to activated PVDF membranes using 2 sheets of Whatman filter paper sandwiched between the transfer cassettes with provided 0.13 inches' thick foam sponges and placed into the Hoefer™ TE22 Mini Tank Blotting unit containing 1L of transfer buffer (0.025 M Tris-HCl, 0.192M glycine and 10% (v/v) methanol in distilled water. The schematic layout used is shown in figure 4.
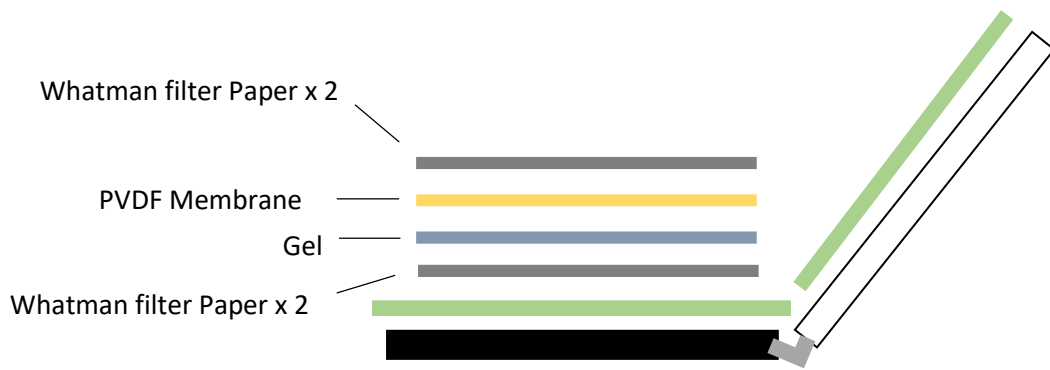
Figure 4: Schematic layout for the transfer sandwich. Representation of the sandwich used to transfer the proteins from the polyacrylamide gel onto the PVDF membrane. The stack is prepared in the cassette and placed in the transfer tank.

The membranes were then re-activated in methanol for 30 seconds before staining with ponceau to identify the transferring on the protein. After washing with distilled water, the membrane was cut to appropriate sizes of interest, re-activated and washed with TBST buffer x 2 (150 mM NaCl, 25 Mm Tris-HCl in 0.1% (v/v) Tween-20 in 1L of distilled water). The membrane was then blocked in 5% (w/v) milk in TBS-T buffer to avoid non-specific interactions. The blots were then incubated overnight at 4°C with primary antibody rabbit mAb Anti-P Glycoprotein [EPR10364-57] in 5% milk (w/v in TBS-T) and and washed 3 times for 5 minutes in TBS-T and incubated for 30 minutes at room temperature with secondary antibody; Anti-Rabbit IgG HRP-linked 1:10000 dilution using 5% milk in TBS-T.

The blots were then washed and developed using Pierce™ ECL western blotting substrate and Amersham hyperfilm ECL film. Anti-tubulin antibody was used as a protein loading control at dilution of 1:500.

4.12 Determining the effect of UVC on the cells' viability

Cells were passaged and seeded into a 6-well plate and incubated at 5% CO_2/37°C for 48 hours. Without disturbing the monolayer of adhered cells, the cultured media was aspirated and the cells were washed with 1 ml of PBS solution (1mg/ml w/v in sterile water). Before being trypsinised, the EFO-21 and EFO-27 cell lines were irradiated with dosages of shortwave ultraviolet 254nm UVC, ranging from 0-32 J/m^2 using a pre-made UV chamber and Spectroline model ENF-240 C/FE Ultraviolet Inspection lamp machine. The non-adherent COLO-704 cell lines were irradiated immediately after 48 hours without removing the cultured media.

After exposition was completed, the cells were trypsinised, counted and seeded into a 96-well plate to determine the cells' viability at different exposures using the MTT assay.

4.13 Colony formation assay

The ability of the adherent cells; EFO-27 and EFO-21 with their respective sub-lines (cultivated in the presence and absence of drug), to form colonies was tested. Different treatments were given to the cells for the determination of the effect on their viability. These included irradiation doses at 32, 16, 8 and 4 J/m^2, 2 µg/ml of cisplatin and a control which no prior treatment was applied. The cells were seeded in triplicates at 500 cells per well in a 6-well plate and were incubated at 5% CO_2/37°C. After 11 days of incubation, the cells were washed with 1 ml of PBS solution (1mg/ml w/v in sterile water) and fixed with 1 ml (80% v/v) methanol in distilled water for 5 minutes. Once fixed, they were then left to dry overnight and then stained with (50% v/v in distilled water) gentian violet dilution for 5 minutes before being washed with distilled water 4 times to remove excess gentian violet solution. The plates were then left again overnight to dry and images were taken using an Olympus light microscope. The number of colonies forms / number of cultured cells were plotted.

4.14 Nanoparticles efficacy

All nanoparticles used for this part of the study were prepared by our collaborators (Sebastian Pieper, Dennis Mulac, Klaus Langer) at the Institute of Pharmaceutical Technology and Biopharmacy, University of Münster, Corrensstr. 48, D-48149 Münster, Germany. All nanoparticle efficacy in cell culture were tested using the cell viability test as described in 3.4 performed by myself.

4.15 Statistical analysis

The statistical method called one-way ANOVA (analysis of variance) was used to analyse the variation amongst the means of the three independent (unrelated) groups (the resistant sub-lines to the respective parental cell line). To define the means as statistically significant, the p-values (denoted as α or alpha of 0.05) were assessed according to the null hypothesis which states that the population means are equal. A p-value less than 0.05 specified that there was statistical significance between the means and when the p-value was greater than 0.05, it indicated that there was no statistical significance between the means. The value was determined using the data analysis in excel 2016.

5 Cisplatin-adapted Ovarian cancer cell lines

5.1 Introduction

Ovarian cancer cells differ from other metastasising tumours due to its rapid circulation and invasive nature which compresses visceral organs. The deadly gynaecological neoplastic cancer is a result of the temporary chemosensitive nature of the cancer cells which has led to a low cure rate of 30% (Lengyel, 2010); (Barber, 1984).

Cisplatin has improved the therapy outcome of ovarian cancer. It is assumed to exert its anti-cancer effects primarily through the damage in the nuclear DNA (but also, probably to a lesser extent, in the mitochondrial DNA). Cisplatin becomes intracellularly activated into an aqua complex, which interacts with nucleophilic N7-sites of purine bases in the DNA producing inter- and intra-strand crosslinks (Shaloam & Tchounwou, 2014); (Towne & Murray, 2014). (Dasari et al., 2014); (Galluzzi et al., 2012).

Adjuvant chemotherapy using platinum-based drugs as a monotherapy, has shown good response rates for patients with ovarian cancer especially those at an earlier stage or poorer performance status (Ai et al., 2016); (Adams et al., 2010). However, the metastatic nature remains problematic and can result in relapse due to resistance formation (Sharma et al., 2017);(Mansoori et al., 2017). In addition, the increased toxicity of cisplatin has led to platinum-based combinational therapies with taxanes (Eckstein, 2011).

The mechanisms underlying acquired cisplatin resistance are complex and may include changes to drug efflux and uptake, changes in the DNA repair mechanisms, increased drug inactivation, and altered expression of pro-survival and/ or anti-survival proteins (Siddik, 2003); (Amable, 2016); (Dilruba & Kalayda, 2016); (Damia & Broggini, 2019). Thus, the use of cell line investigations at molecular biology levels provide insight on the mechanisms of adaptation to chemotherapeutic drugs (Di Nicolantonio et al., 2005); (Saintas et al., 2017).

In this chapter, we assess the mechanism of acquired resistance in cisplatin-adapted sublines of the ovarian cancer cell lines EFO-21, EFO-27, and COLO-704 are introduced and characterised.

5.2 Results

In this project part, the ovarian cancer cell lines EFO-21, EFO-27, and COLO-704 and their cisplatin-adapted sublines EFO-21-rCDDP^{2000}, EFO-27-rCDDP^{2000}, and COLO-704-rCDDP^{1000} were characterised. The cisplatin-adapted sublines were continuously cultivated in the presence of the indicated cisplatin concentrations. In addition, we cultivated the cisplatin-adapted sublines in the absence of cisplatin to investigate the effects on the phenotype including the resistance status. The respective sublines were designated as EFO-21-rCDDP$^{2000(-)}$, EFO-27-rCDDP$^{2000(-)}$, and COLO-704-rCDDP$^{1000(-)}$.

5.2.1 Cell doubling times

The differences and similarities of the doubling times amongst the group of cell lines and their respective resistant sublines varied. EFO-21 and its sublines as well as EFO-27 cell line and its sublines displayed similar doubling times. In contrast, COLO-704 and COLO-704-rCDDP$^{1000(-)}$ displayed reduced doubling times in comparison to COLO-704-rCDDP^{1000} (Figure 5-7; Table 9-11) which was of statistical significance.
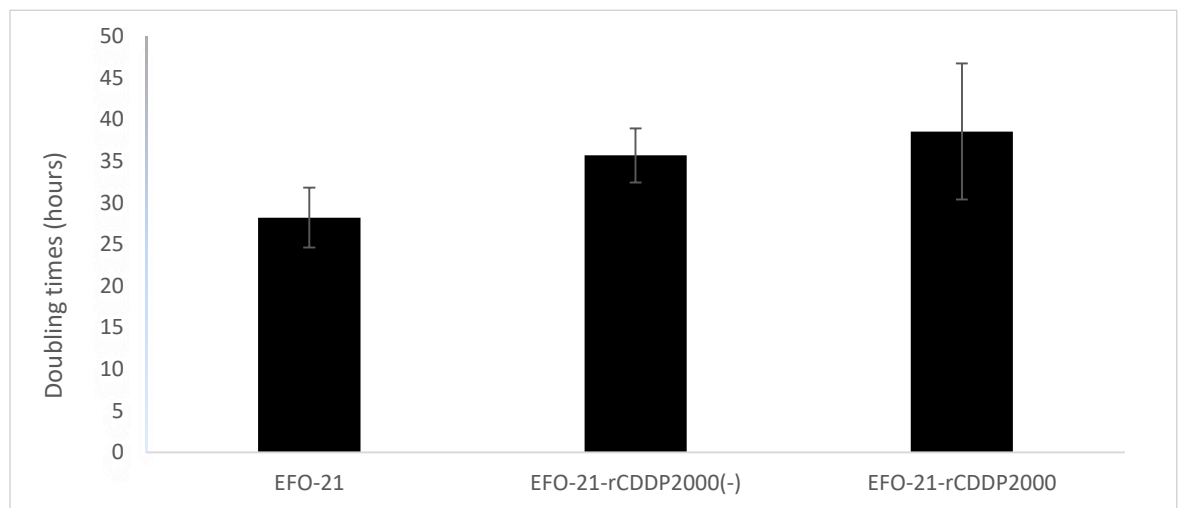
Figure 5: Doubling times for EFO-21 cancer cell lines. Data expressed as a mean ± SD, n=3.

Name of cell line	Doubling time (hours)
EFO-21	28.21 ± 3.61
EFO-21-rCDDP$^{2000(-)}$	35.68 ± 3.24
EFO-21-rCDDP^{2000}	38.56 ± 8.18

Table 9: Doubling times of EFO-21 cell lines generated from growth curves. Data is expressed as a mean ± SD, n=3. Statistical difference: p=0.135.
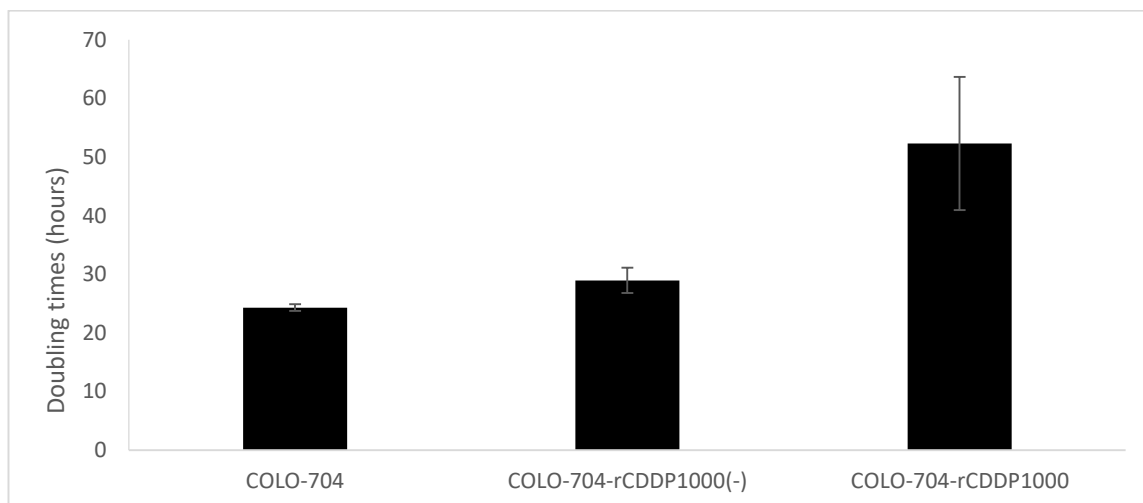
Figure 6 : Doubling times for COLO-704 cancer cell lines. Data expressed as a mean ± SD, n=3.

Name of cell line	Doubling time (hours)
COLO-704	24.32 ± 0.55
COLO-704-rCDDP$^{1000(-)}$	28.96 ± 2.15
COLO-704-rCDDP^{1000}	52.32 ± 11.34

Table 10: Results showing the doubling times of EFO-21 cell lines. Data is expressed as a mean ± SD, n=3. Statistical difference: p=0.004.
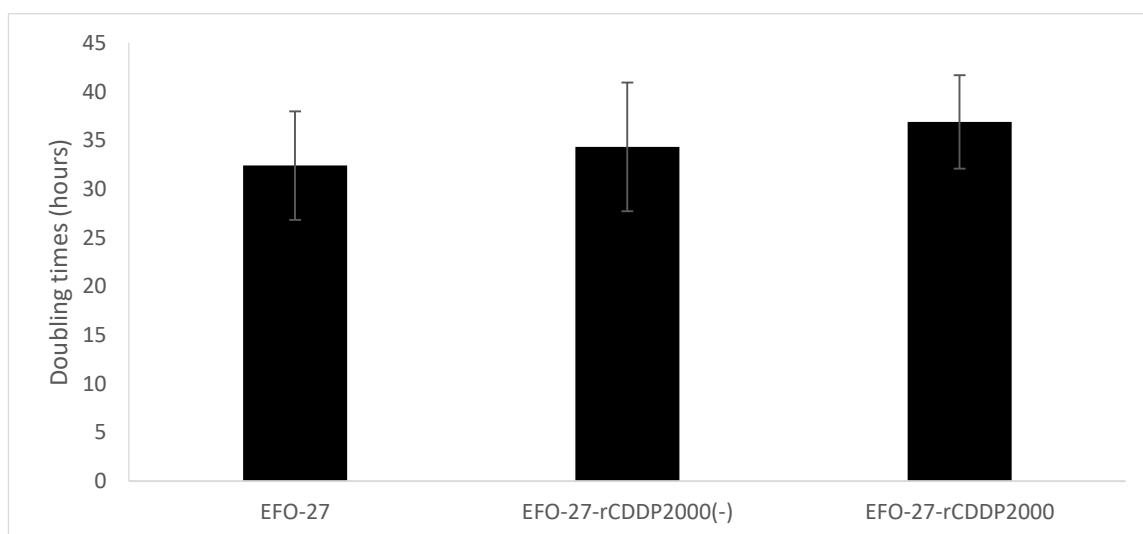
Figure 7 : Doubling times for EFO-27 cancer cell lines. Data expressed as a mean ± SD, n=3.

Name of cell line	Doubling time (hours)
EFO-27	32.4 ± 5.58
EFO-27-rCDDP$^{2000(-)}$	34.32 ± 6.60
EFO-27-rCDDP^{2000}	36.88 ± 4.80

Table 11: Results showing the doubling times of EFO-21 cell lines. Data is expressed as a mean ± SD, n=3. Statistical significance: p=0.649.

5.2.2 Cell line morphology

EFO-27 and EFO-21 adherent cell lines displayed an epithelial-like cell structure which grew as a monolayer. The cells appeared to have a polygonal shape with regular dimensions (Figure 8A-8B, 8A-8B). Adaptation of these two cell lines was associated with morphological changes that were not reversible upon drug removal. The cells appeared smaller in size with large nuclei. The cisplatin-resistant sublines (EFO-21-rCDDP$^{2000\ (-)}$, EFO-27-rCDDP$^{2000\ (-)}$, EFO-21-rCDDP^{2000} and EFO-27-rCDDP^{2000}) displayed a more spindle-shaped morphology with pronounced cytoplasmic elongations (figure 8C-8D, 9C-D).

The cell line COLO-704 grew in clusters. Adaptation to cisplatin was not associated with major morphological changes (Figure 10A-F).
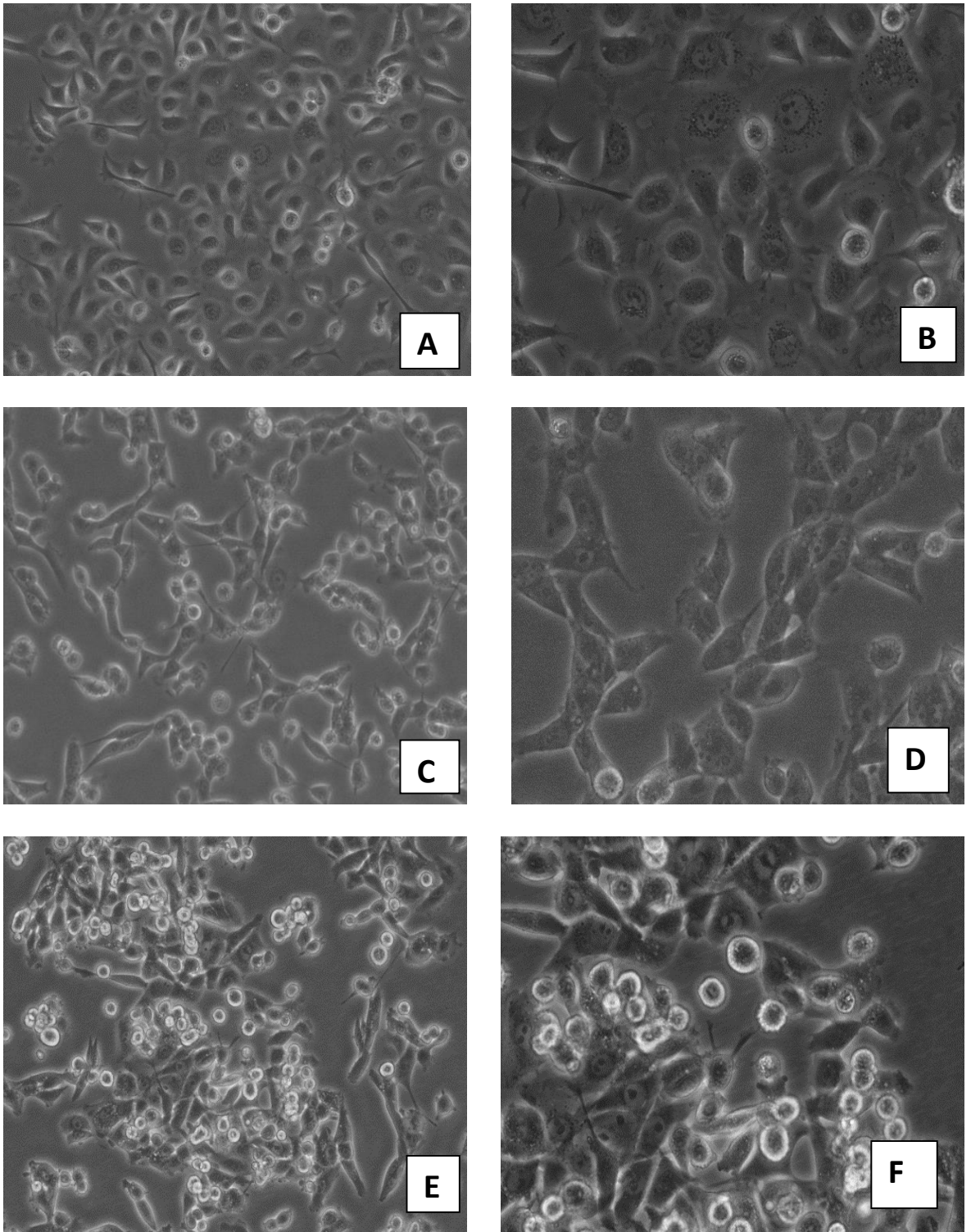
Figure 8 : **Microscopic images of ovarian cancer cell lines. (A) EFO-21 at 1000 X magnification, (B) EFO-21 at 2000 X magnification, (C) EFO-21-rCDDP$^{2000(-)}$ at 1000 X magnification, (D) EFO-21-rCDDP$^{2000(-)}$ at 2000 X magnification, (E) EFO-21-rCDDP^{2000} at 1000 X magnification and EFO-21-rCDDP^{2000} at 2000 X magnification.**
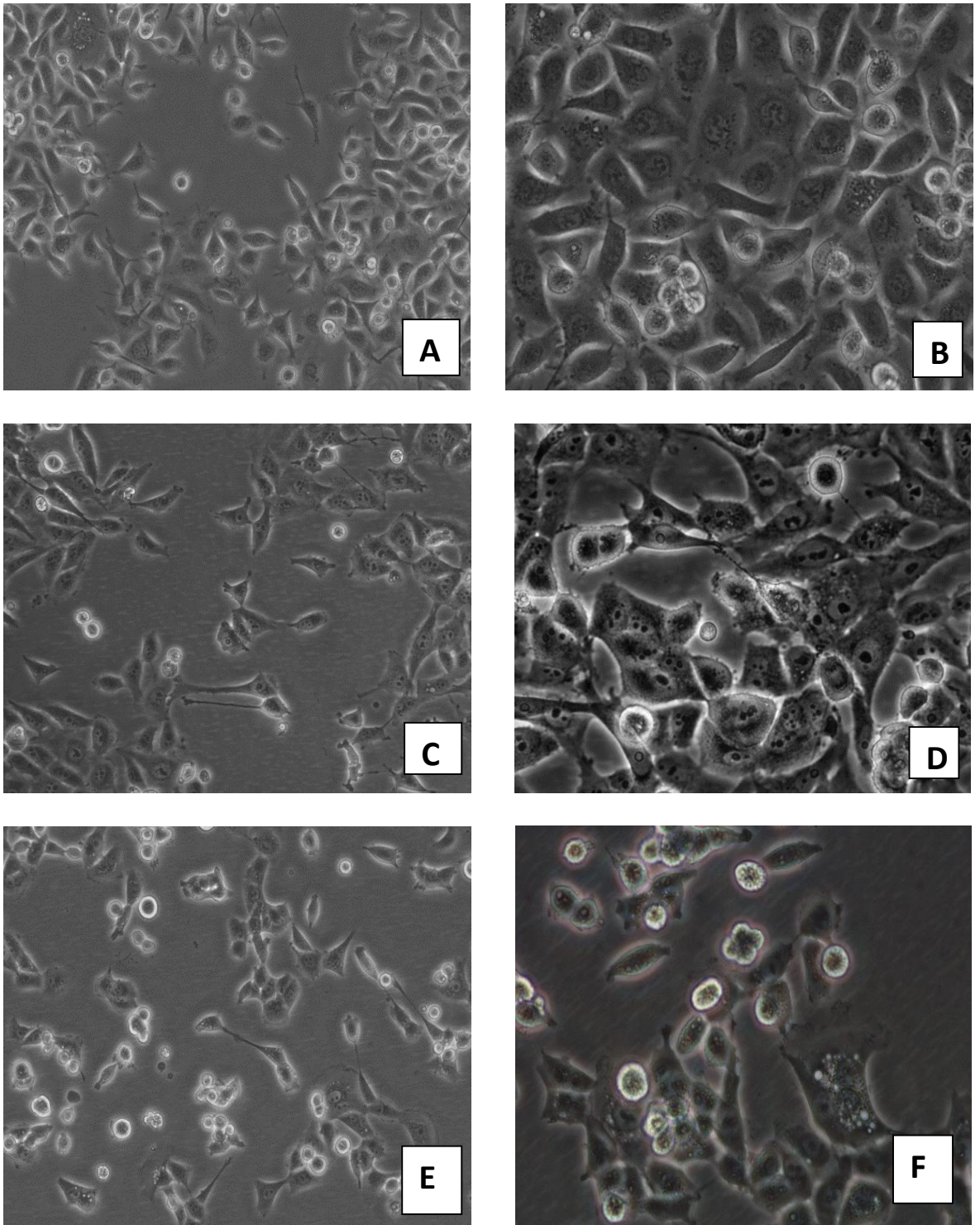
Figure 9 : Microscopic images of ovarian cancer cell lines. (A) EFO-27 at 1000 X magnification, **(B)** EFO-27 at 2000 X magnification, **(C)** EFO-27-rCDDP$^{2000(-)}$ at 1000 X magnification, **(D)** EFO-27-rCDDP$^{2000(-)}$ at 2000 X magnification, **(E)** EFO-27-rCDDP^{2000} at 1000 X magnification and EFO-27-rCDDP^{2000} at 2000 X magnification.
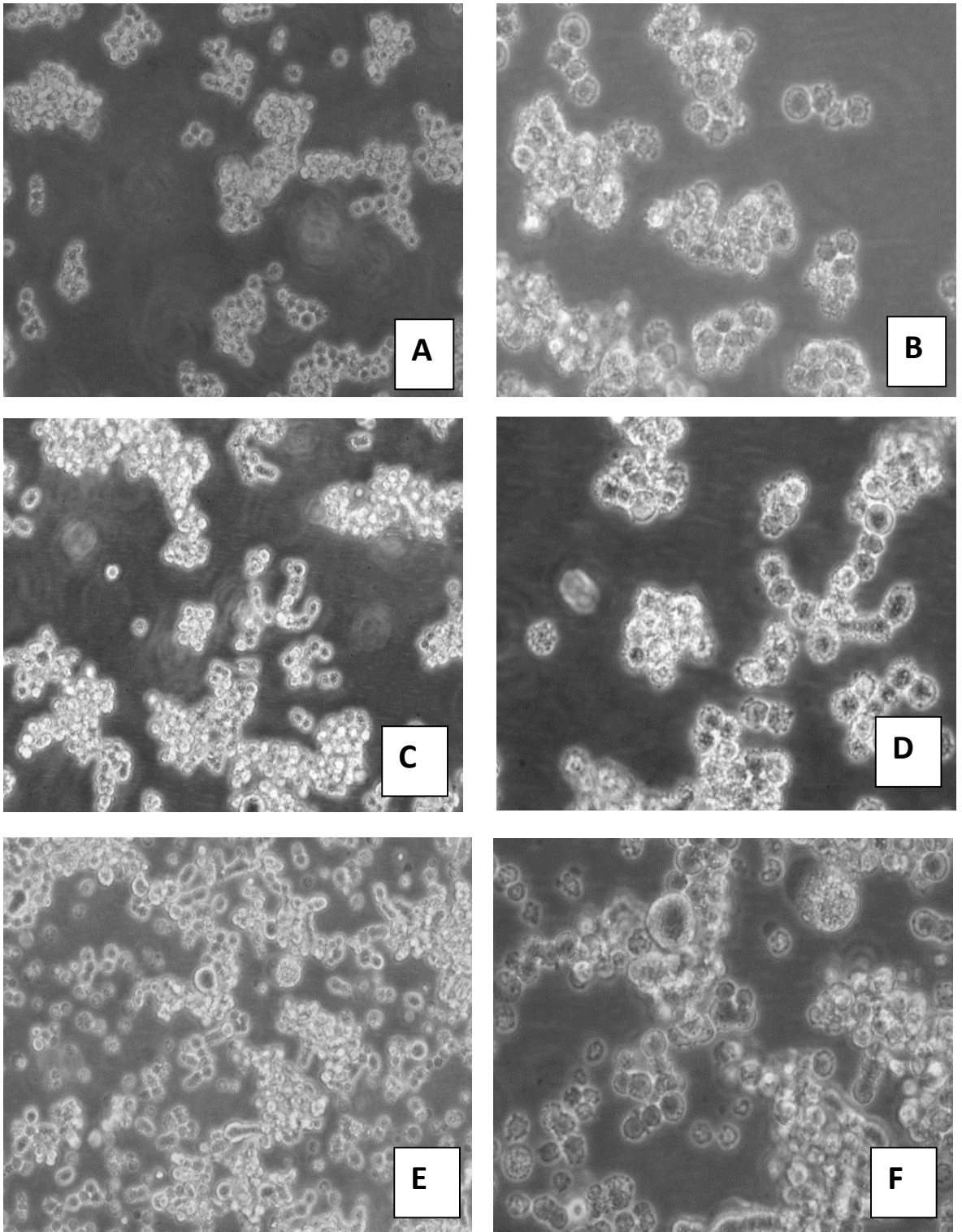
Figure 10 : Microscopic images of ovarian cancer cell lines. (A) COLO-704 at 1000 X magnification, (B) COLO-704 at 2000 X magnification, (C) COLO-704-rCDDP$^{1000(-)}$ at 1000 X magnification, (D) COLO-704-rCDDP$^{1000(-)}$ at 2000 X magnification, (E) COLO-704-rCDDP^{1000} at 1000 X magnification and COLO-704-rCDDP^{1000} at 2000 X magnification.

5.2.3 Resistance phenotype over time

Cisplatin resistance was monitored over the course of the study by performing monthly MTT assays to determine the concentration at which each of the cell lines' viability was reduced BY 50% (IC_{50}). COLO-704-rCDDP[1000] cells displayed a consistent resistance phenotype over the project duration. In contrast, the IC_{50} values of EFO-21-rCDDP[2000] and EFO-27-rCDDP[2000] appeared to increase during the course of the project (Figure 11-13, Table 12-14). This may indicate a re-adaptation period after resuscitation and/ or a continued adaptation to the presence of cisplatin (Figure 11-13, Table 12-14). EFO-21-rCDDP[2000(-)] seemed to gradually loose cisplatin resistance over time (Figure 11, Table 12). EFO-27-rCDDP[2000(-)] displayed similar cisplatin sensitivity like EFO-27 after about 7 months (Figure 13, Table 14), while COLO-704-rCDDP[1000(-)] cells seemed to immediately loose cisplatin resistance upon cisplatin removal (Figure 12, Table 11).
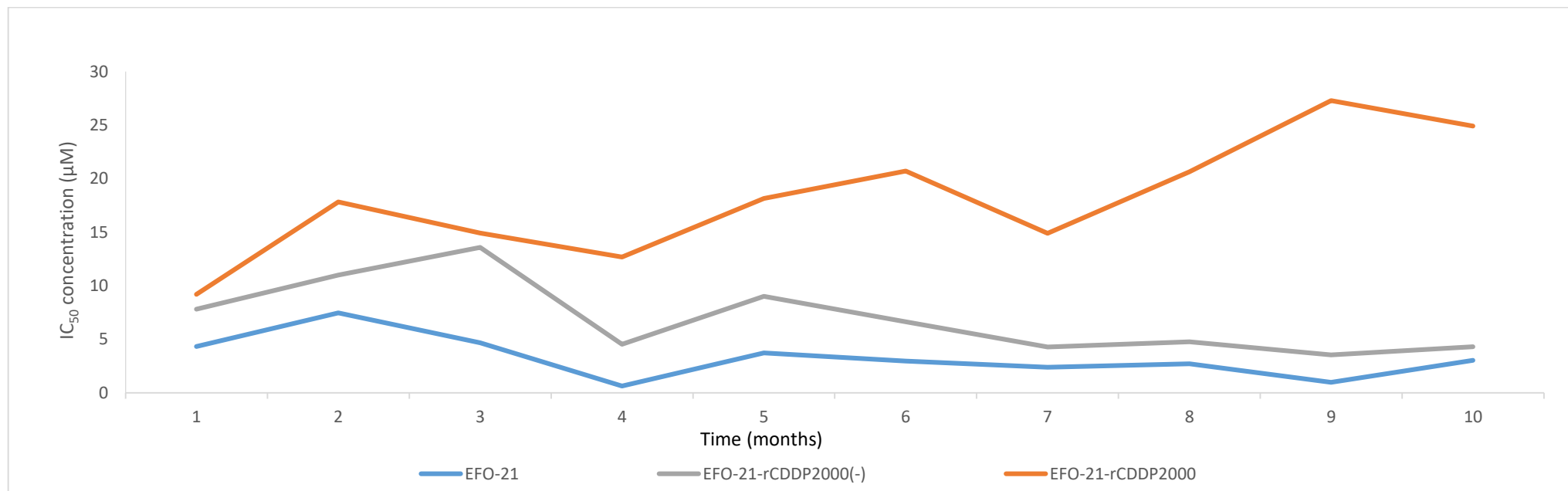
Figure 11 : **IC$_{50}$ concentration of cisplatin over a two year period for the cancer cell lines' characterisation. Results showing the characterisation of EFO-21 cell lines.**

	Time (months)									
Name of cell line	1	2	3	4	5	6	7	8	9	10
EFO-21	4.33	7.47	4.68	0.64	3.74	2.96	2.39	2.72	0.98	3.04
EFO-21-rCDDP$^{2000(-)}$	7.82	11.00	13.58	4.53	9.02	6.64	4.28	4.76	3.55	4.31
EFO-21-rCDDP^{2000}	9.21	17.84	14.91	12.68	18.16	20.72	14.91	20.66	27.29	24.91

Table 12: Results showing the IC$_{50}$ concentration values over 2 years to determine the resistance/sensitivity profiles of the EFO-21 cell lines. Each data is a representative of one biological repeat (n=1).
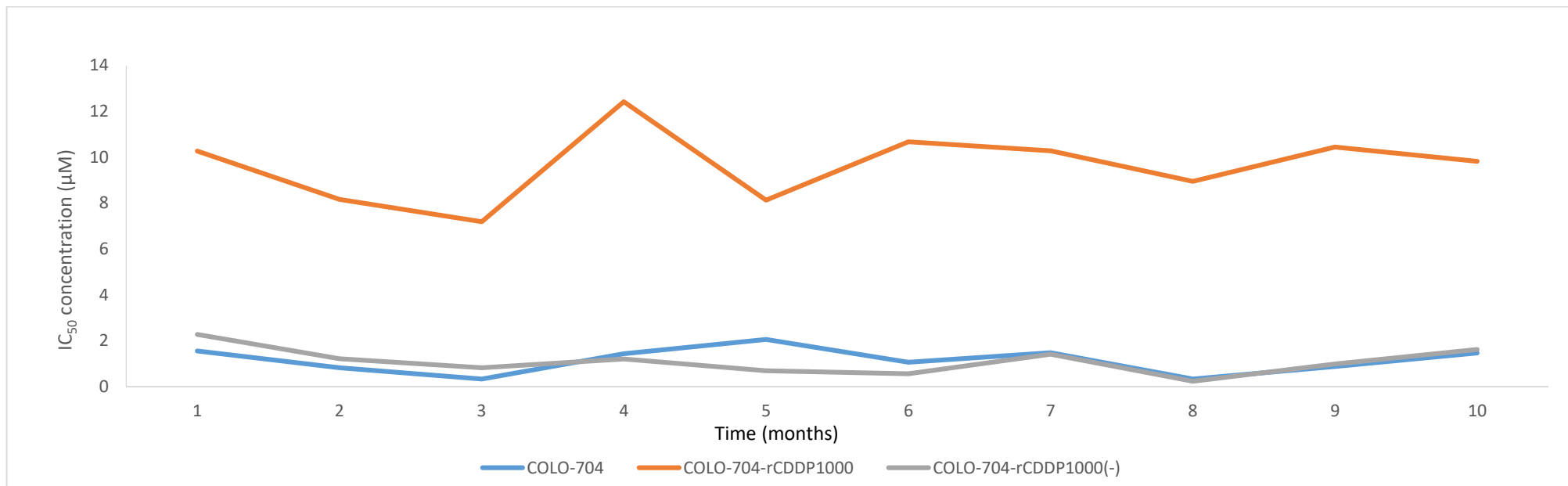
Figure 12 : IC$_{50}$ concentration of cisplatin over a two-year period for the cancer cell lines' characterisation. **Results showing the characterisation of COLO-704 cell lines.**

	Time (months)									
Name of cell line	1	2	3	4	5	6	7	8	9	10
COLO-704	1.55	0.82	0.33	1.43	2.06	1.06	1.47	0.32	0.870	1.47
COLO-704-rCDDP^{1000}	10.27	8.16	7.19	12.42	8.12	10.67	10.28	8.94	10.44	9.82
COLO-704-rCDDP$^{1000(-)}$	2.28	1.21	0.82	1.20	0.69	0.56	1.41	0.23	0.98	1.62

Table 13: Results showing the IC$_{50}$ concentration values over 2 years to determine the resistance/sensitivity profiles of the COLO-704 cell lines. Each data is a representative of one biological repeat (n=1).
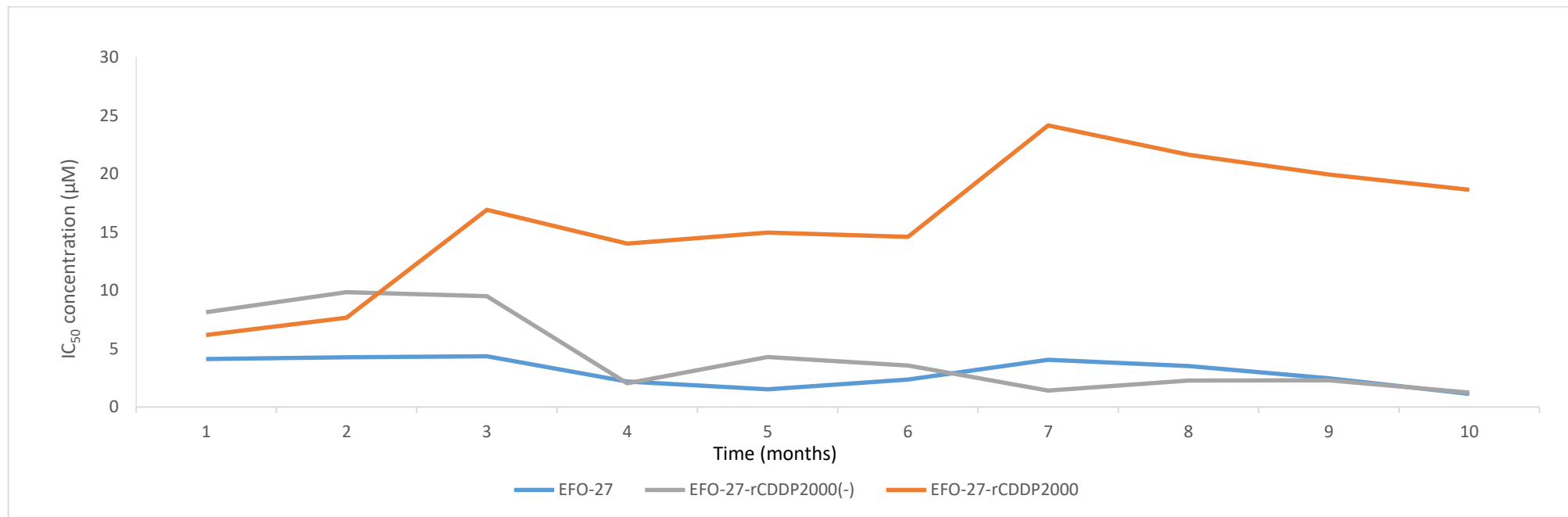
Figure 13: IC$_{50}$ concentration of cisplatin over a two-year period for the cancer cell lines' characterisation. Results showing the characterisation of EFO-27 cell lines. Each data is a representative of one biological repeat (n=1) in each month.

Name of cell line	Time (months)									
	1	2	3	4	5	6	7	8	9	10
EFO-27	4.13	4.26	4.35	2.18	1.52	2.36	4.05	3.53	2.46	1.13
EFO-27-rCDDP$^{2000(-)}$	8.13	9.86	9.50	2.02	4.30	3.56	1.41	2.27	2.30	1.23
EFO-27-rCDDP^{2000}	6.18	7.67	16.93	14.02	14.97	14.61	24.15	21.63	19.93	18.63

Table 14: Results showing the IC$_{50}$ concentration values over 2 years to determine the resistance/sensitivity profiles of the EFO-27 cell lines. Each data is a representative of one biological repeat (n=1).

5.2.4 Cross-resistance drug profiles

5.2.4.1 Platinum based drugs

Cisplatin, carboplatin and oxaliplatin resistance profiles were determined between July and September 2018, where the sublines that were cultivated in the absence of drug had largely (EFO-21-rCDDP$^{2000\,(-)}$) or completely (EFO-27-rCDDP$^{2000\,(-)}$, COLO-704-rCDDP$^{1000\,(-)}$) lost their cisplatin resistance phenotype (Table 12-14).

The arbitrary cut off point for cross-resistance determination was identified by a 2-fold difference in the IC$_{50}$ concentration of the resistant in comparison to the parental cell line. EFO-21-rCDDP^{2000} and EFO-27-rCDDP^{2000} displayed cross resistance to oxaliplatin and carboplatin. Cross-resistance to oxaliplatin was less pronounced than cross-resistance to carboplatin (Figure 14-19). COLO-704-rCDDP^{1000} also showed cross-resistance to carboplatin but not to oxaliplatin (Figure 20-22). Notably, EFO-27-rCDDP$^{2000(-)}$ cells displayed increased sensitivity to cisplatin and oxaliplatin (but not to carboplatin) when compared to parental EFO-27 cells (Figure 17-19, Table 15). In contrast, COLO-704-rCDDP$^{1000(-)}$ cells were more sensitive than parental COLO-704 cells to oxaliplatin and carboplatin (but not to cisplatin) (Figure 20-22, Table 17). This indicates that the adaptation of different ovarian cancer cell lines to cisplatin resulted in different phenotypic outcomes. Cultivation the cisplatin-adapted EFO-27 and COLO-704 sublines in the absence of drug even resulted in increased vulnerability to certain platinum-based drugs.

Cell line	Cisplatin (µM)	Oxaliplatin (µM)	Carboplatin (µM)
EFO-27	4.25 ± 0.11	1.87 ± 0.69	17.81 ± 3.91
EFO-27-rCDDP$^{2000(-)}$	2.08 ± 0.17	0.84 ± 0.13	12.57 ± 1.86
EFO-27-rCDDP^{2000}	14.53 ± 0.48	4.46 ± 0.41	80 ± 2.91

Table 15: The cross-resistance profiles for EFO-27 cells. IC50 concentrations of platinum-based drugs were determined using MTT assays. Results are expressed as an average of three biological repeats. (n=3 ± SD). Statistical significance comparison of resistant sublines to parental sublines: Carboplatin p=≤0.05; Oxaliplatin p=≤0.05; Cisplatin p=≤0.05.

Cell line	Cisplatin (µM)	Oxaliplatin (µM)	Carboplatin (µM)
EFO 21 PTL	2.69 ± 0.29	0.31 ± 0.09	16.18 ± 4.48
EFO-21-rCDDP$^{2000(-)}$	4.53 ± 0.24	0.43 ± 0.11	19.69 ± 4.03
EFO-21-rCDDP^{2000}	18.91 ± 1.58	0.98 ± 0.20	73.55 ± 5.46

Table 16: The cross-resistance profiles for EFO-21 cells. IC50 concentrations of platinum-based drugs were determined using MTT assays. Results are expressed as an average of three biological repeats. (n=3 ± SD). Statistical significance comparison of resistant sublines to parental sublines: Carboplatin p=≤0.05; Oxaliplatin p=≤0.05; Cisplatin p=≤0.05.

Cell line	Cisplatin (µM)	Oxaliplatin (µM)	Carboplatin (µM)
COLO-704	1.27 ± 0.39	2.59 ± 0.37	17.71 ± 0.81
COLO-704-rCDDP$^{1000(-)}$	1.08 ± 0.22	1.11 ± 0.19	7.36 ± 2.44
COLO-704-rCDDP^{1000}	7.82 ± 0.55	1.45 ± 0.33	34.79 ± 2.82

Table 17: **The cross-resistance profiles for COLO-704 cells.** IC50 concentrations of platinum-based drugs were determined using MTT assays. Results are expressed as an average of three biological repeats. (n=3 ± SD). Statistical significance comparison of resistant sublines to parental sublines: Carboplatin p=≤0.05; Oxaliplatin p=≤0.05; Cisplatin p=≤0.05.
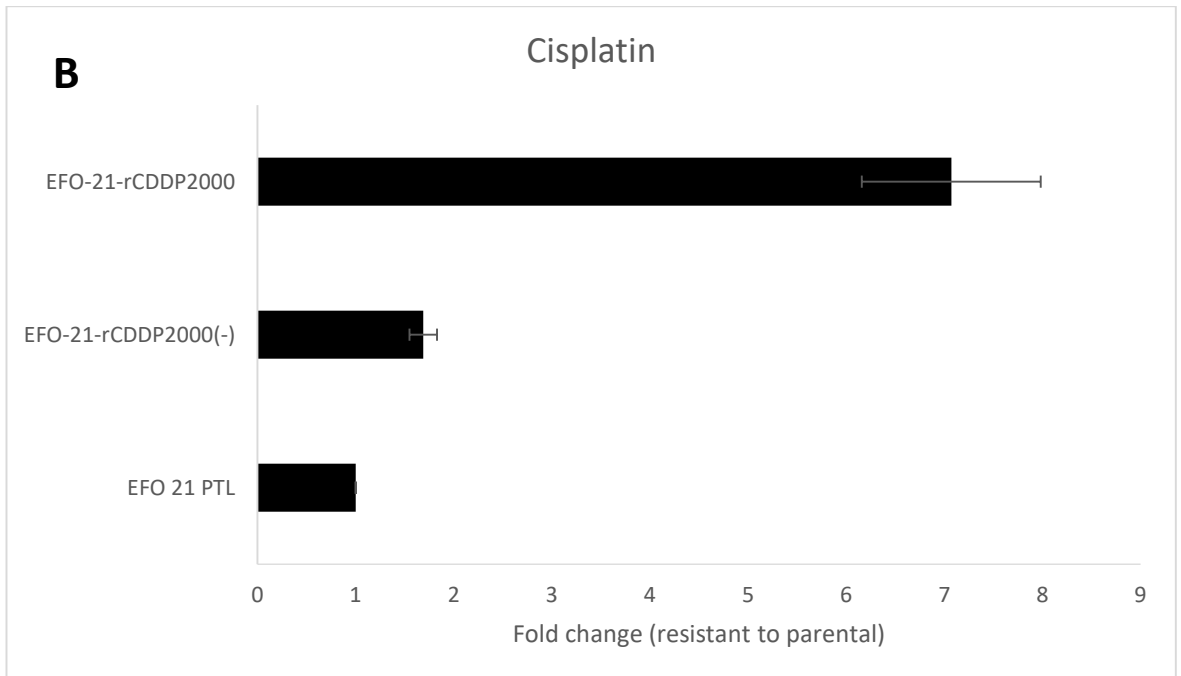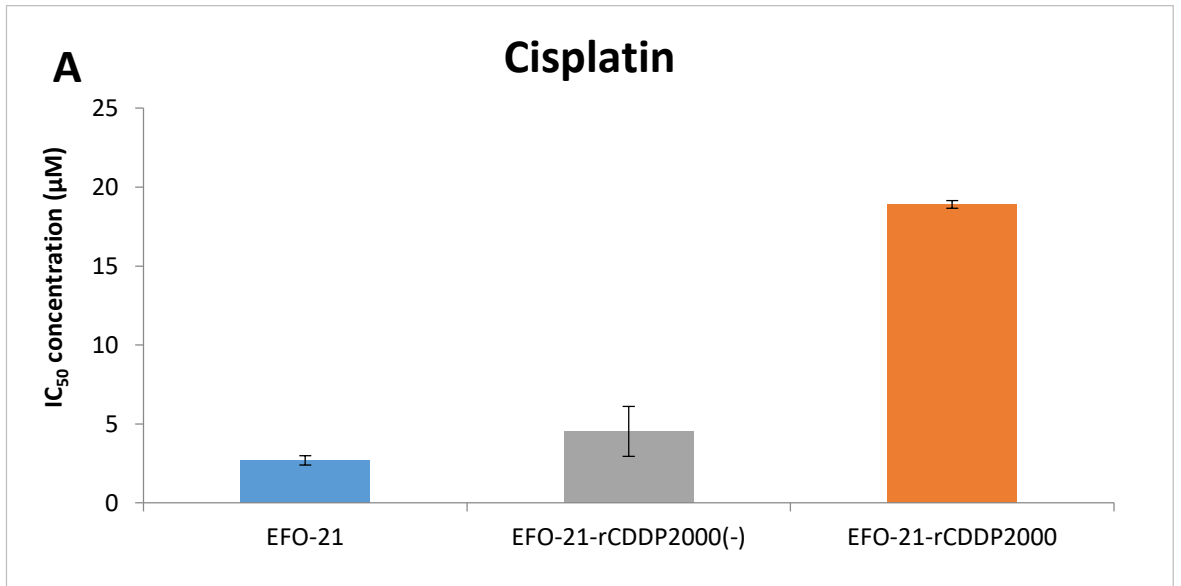
Figure 14: (A) IC$_{50}$ concentration of cisplatin and (B) fold change (resistant to sensitive) for the EFO-21 cell lines. Each data expressed is expressed as a mean ± SD, n=3.
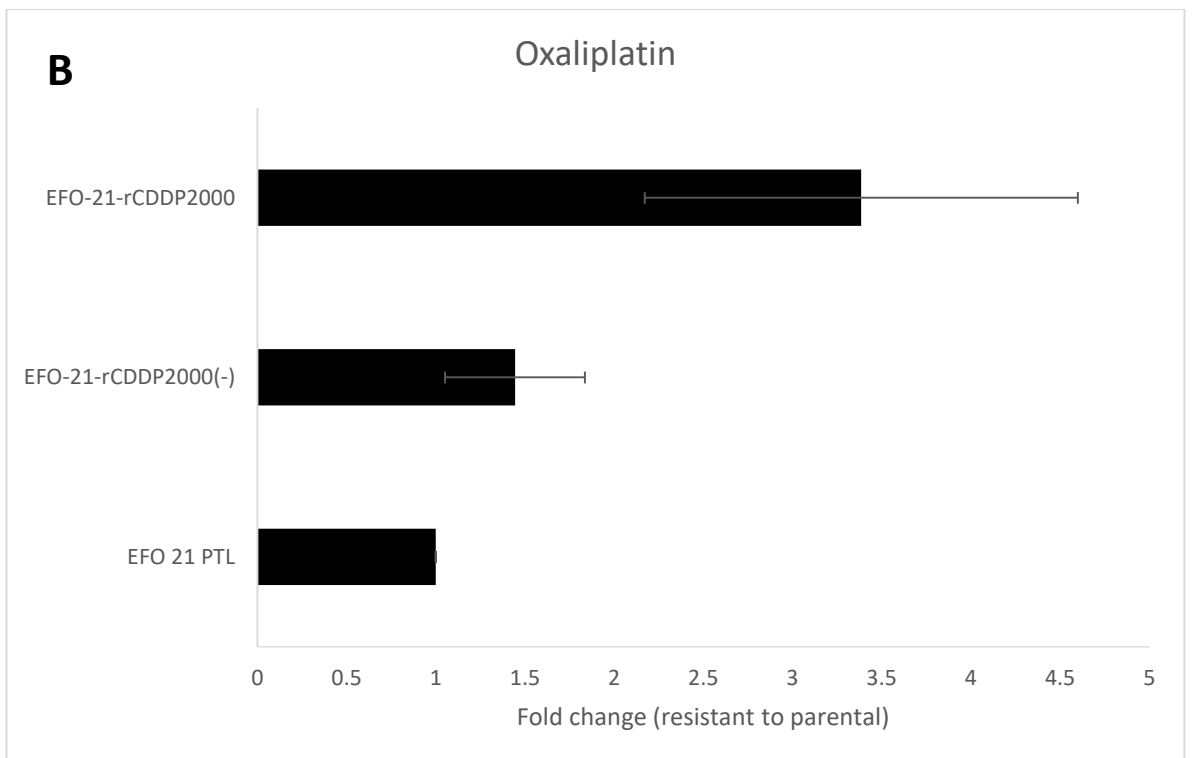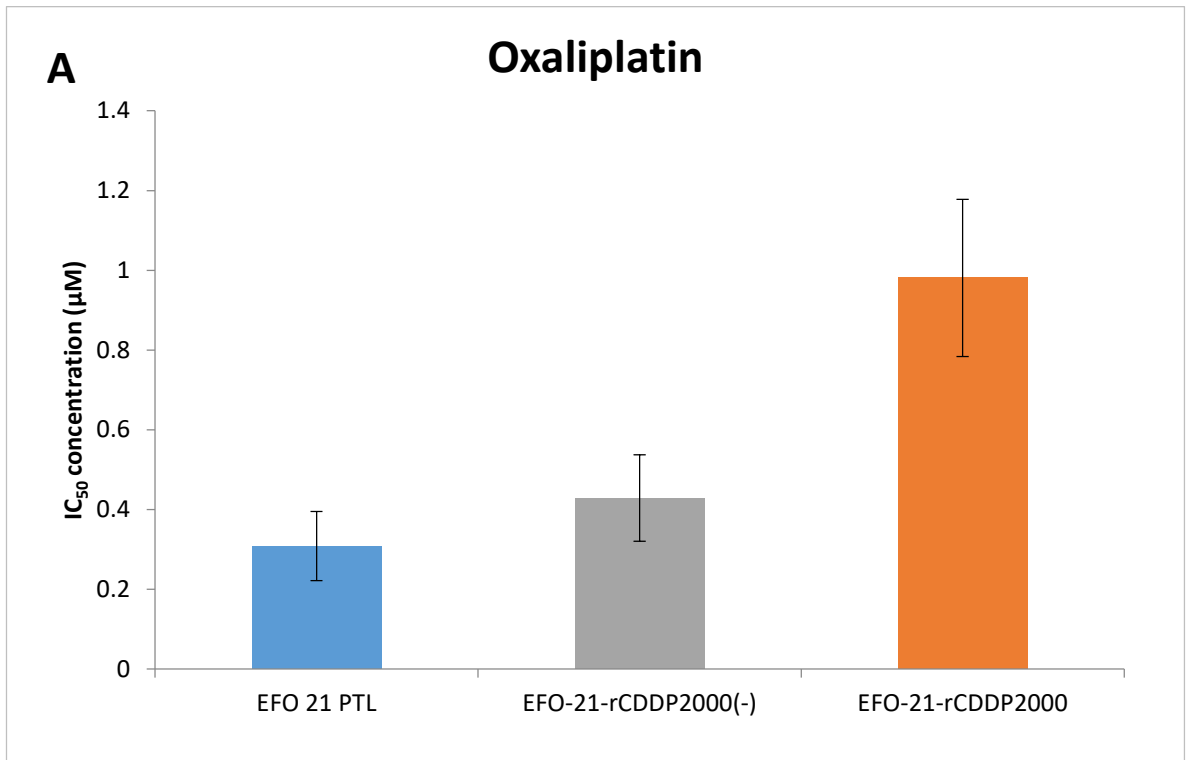
Figure 15: (A) IC$_{50}$ concentration of oxaliplatin and (B) fold change (resistant to sensitive) for the EFO-21 cell lines. Each data expressed is expressed as a mean ± SD, n=3.
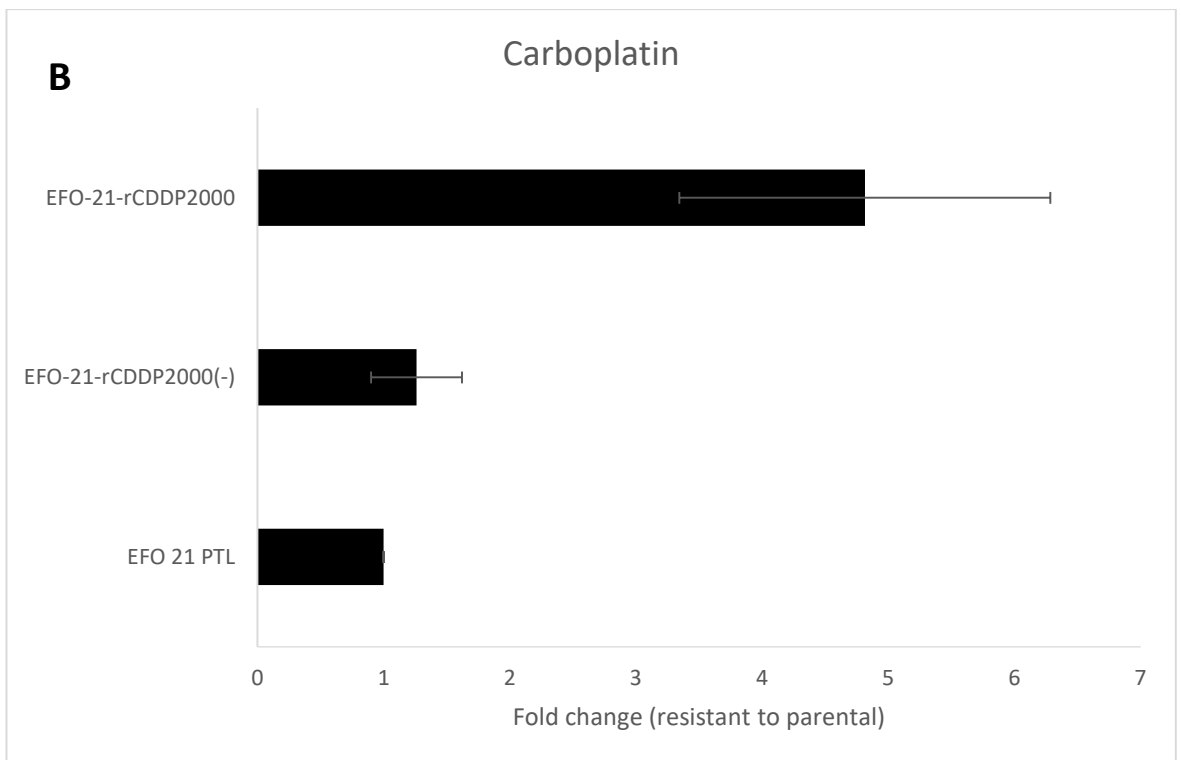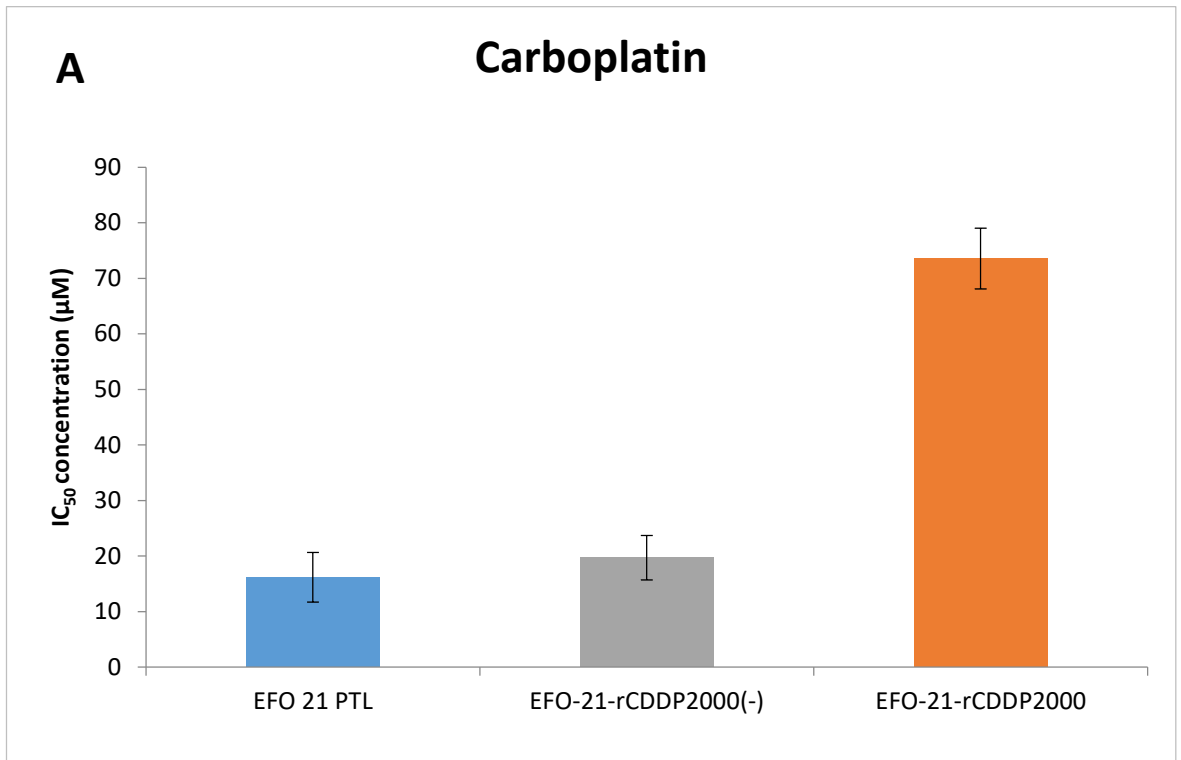
Figure 16: (A) IC$_{50}$ concentration of carboplatin and (B) fold change (resistant to sensitive) for the EFO-21 cell lines. Each data expressed is expressed as a mean ± SD, n=3.
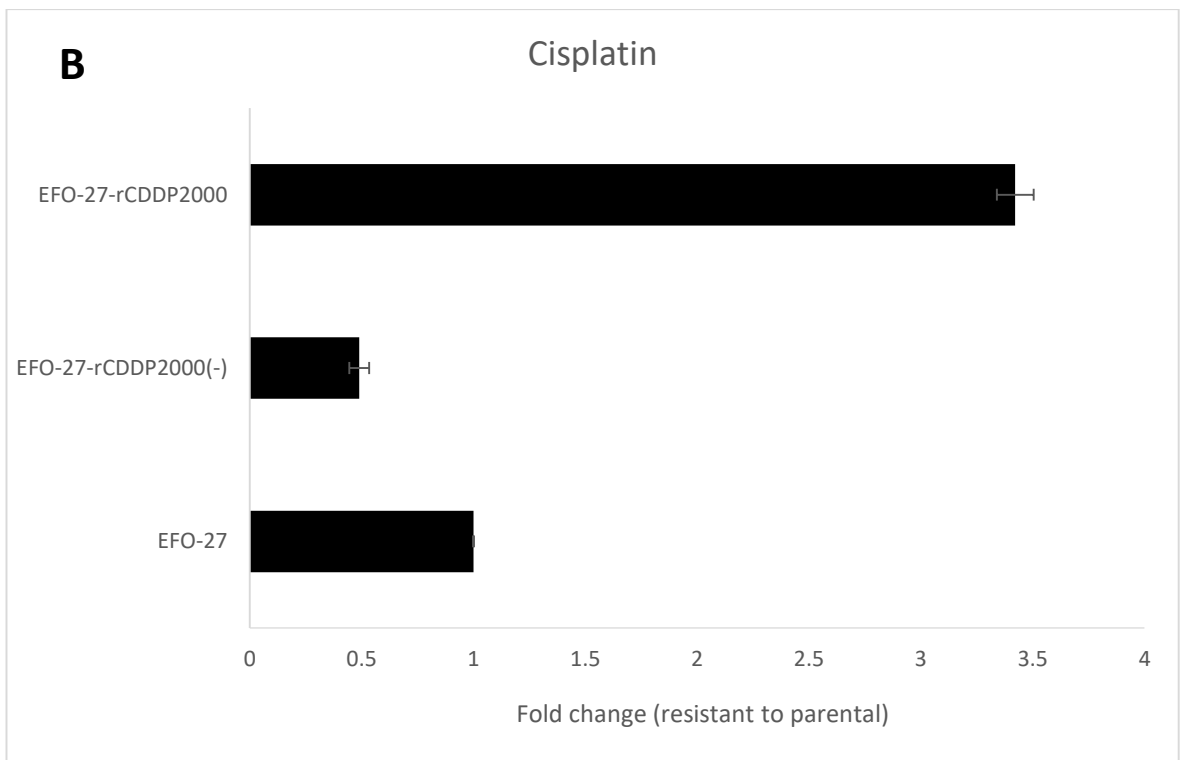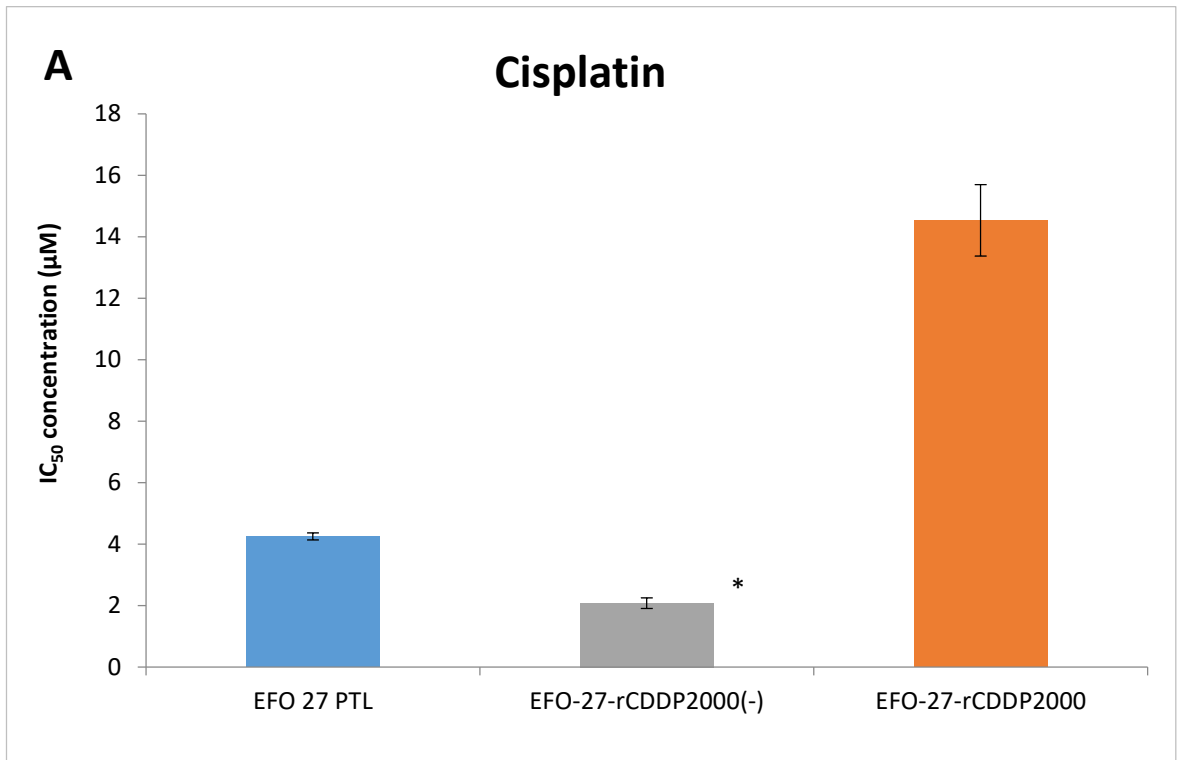
Figure 17: (A) IC$_{50}$ concentration of cisplatin and (B) fold change (resistant to sensitive) for the EFO-27 cell lines. Each data expressed is expressed as a mean ± SD, n=3.
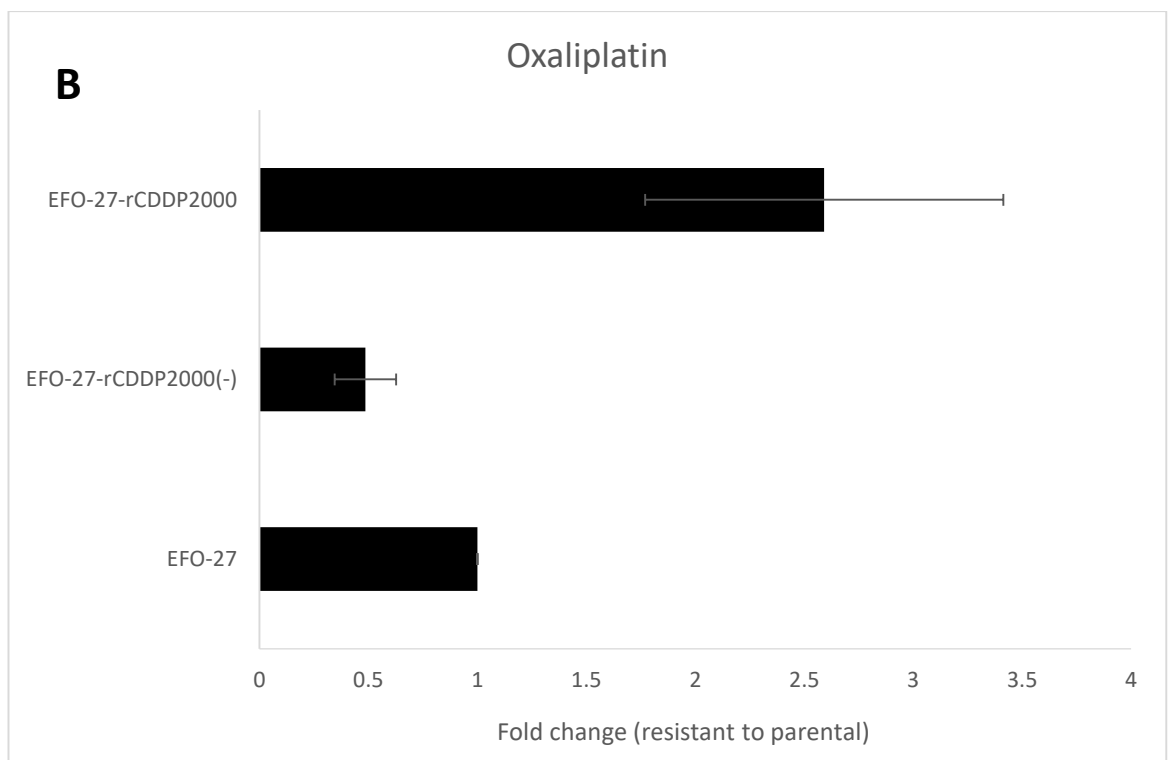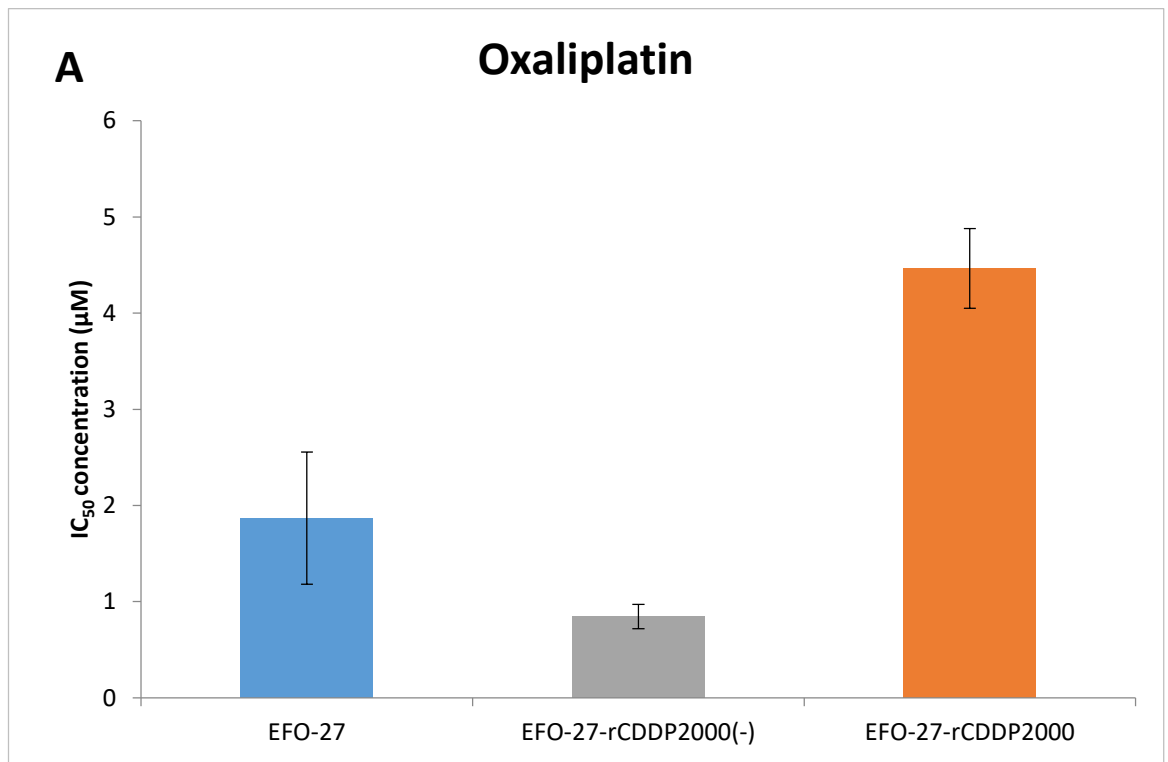
Figure 18: (A) IC$_{50}$ concentration of oxaliplatin and (B) fold change (resistant to sensitive) for the EFO-27 cell lines. Each data expressed is expressed as a mean ± SD, n=3.
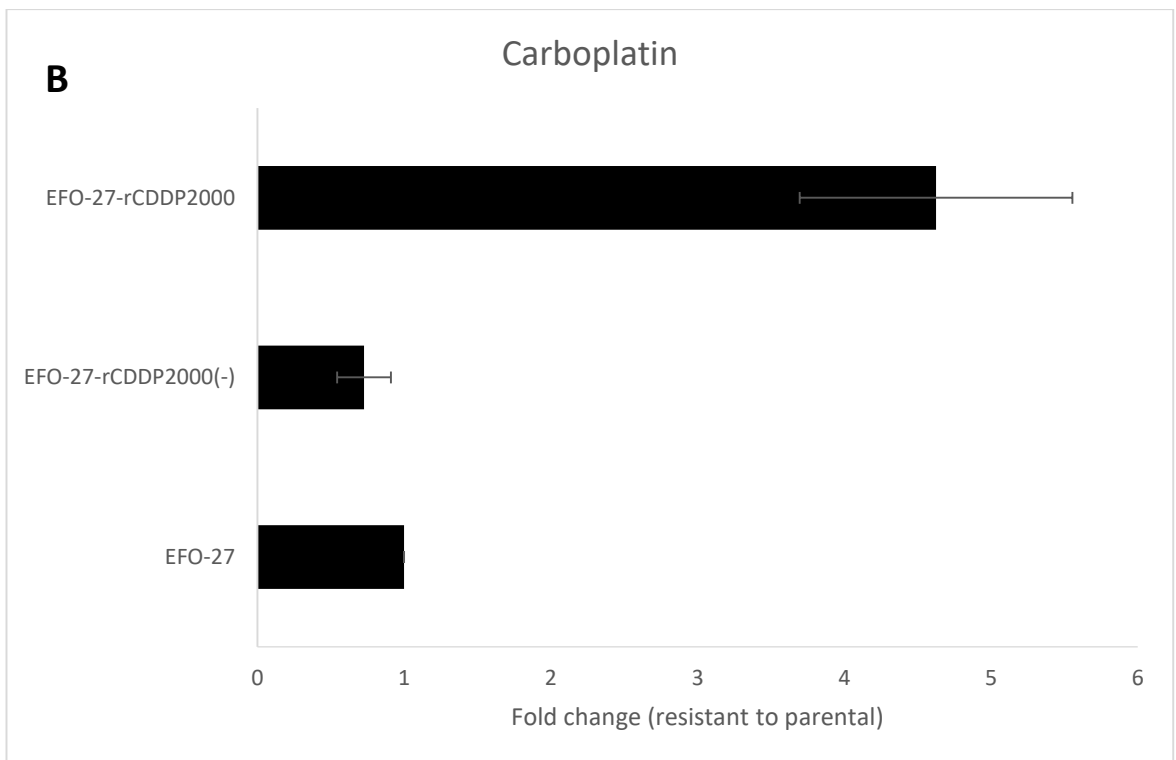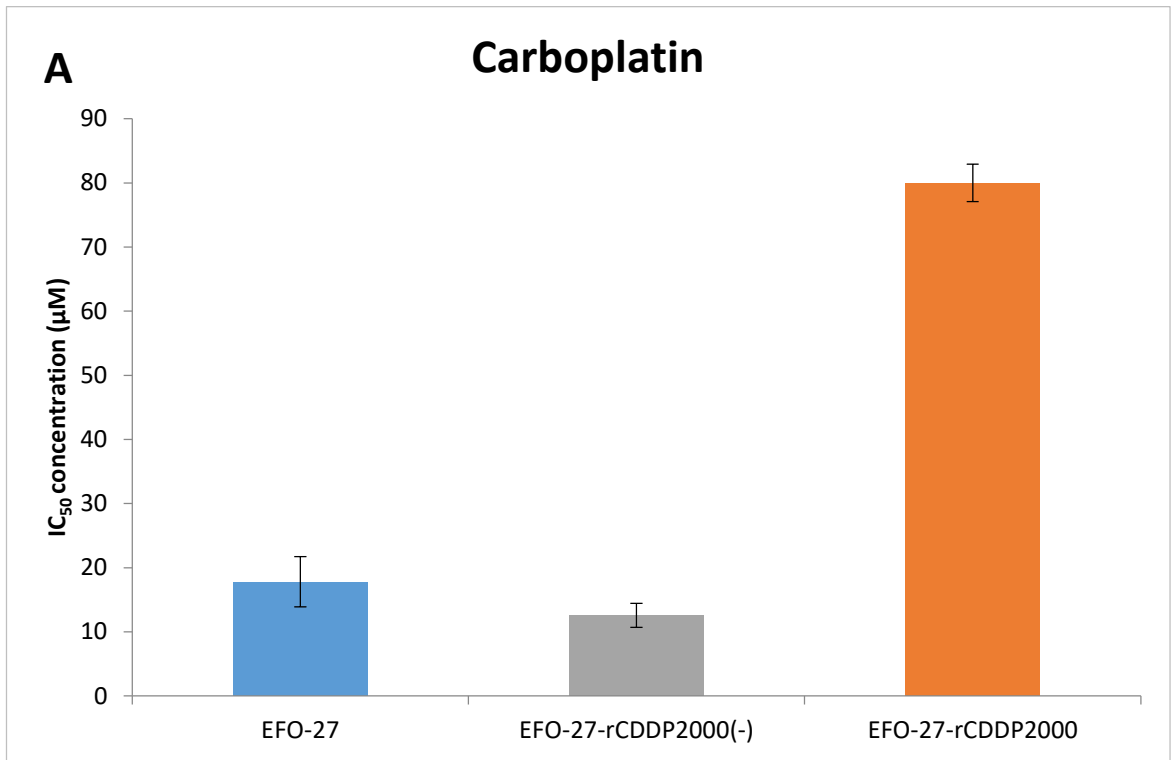
Figure 19: (A) IC$_{50}$ concentration of carboplatin and (B) fold change (resistant to sensitive) for the EFO-27 cell lines. Each data expressed is expressed as a mean ± SD, n=3.
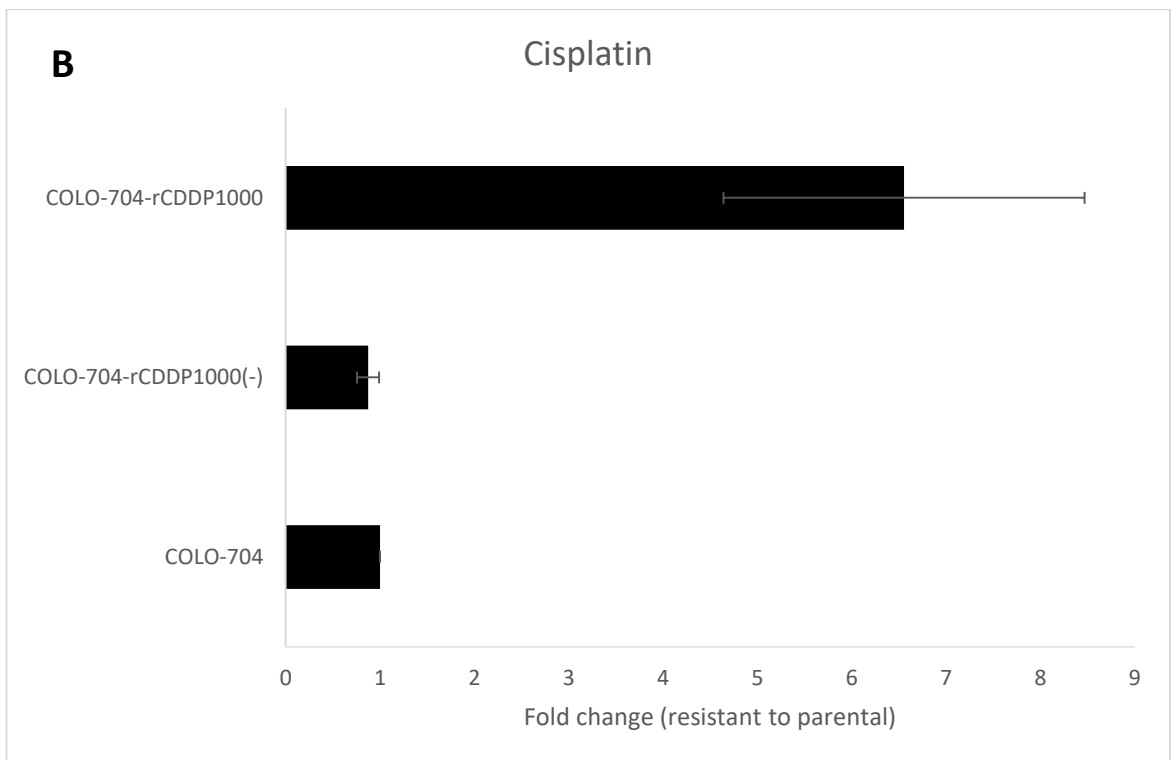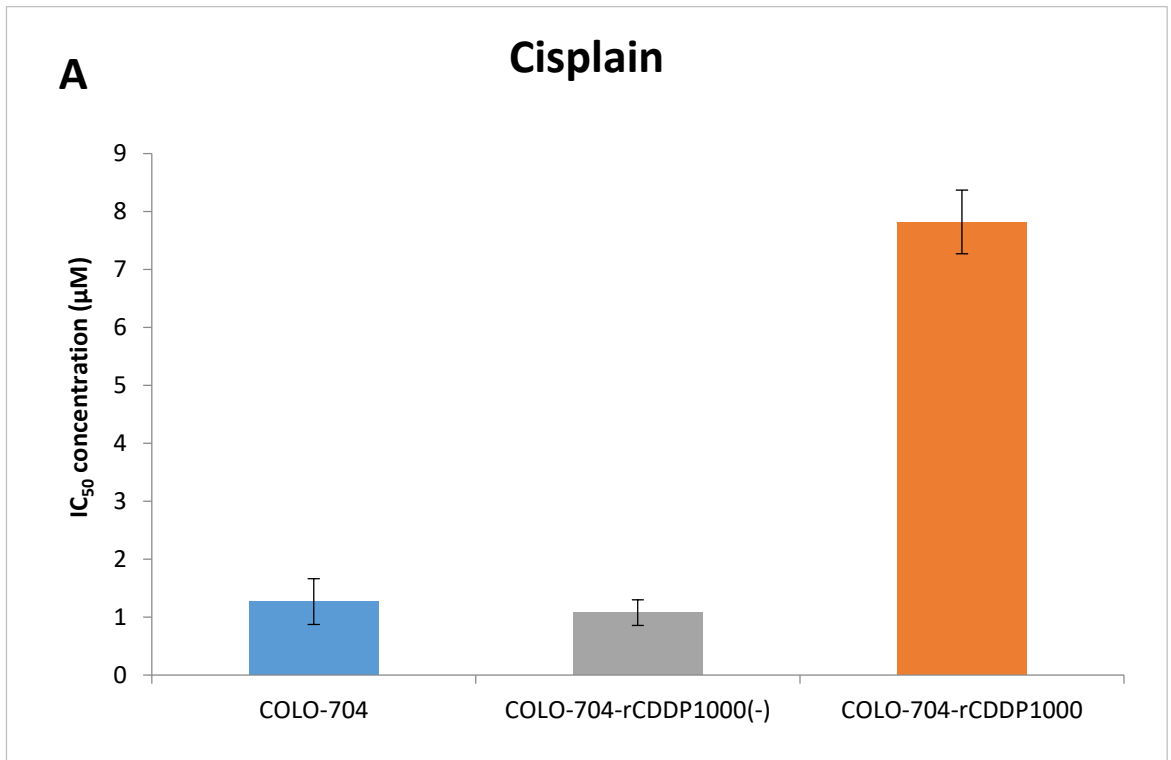
Figure 20: (A) IC$_{50}$ concentration of cisplatin and (B) fold change (resistant to sensitive) for the COLO-704 cell lines. Each data expressed is expressed as a mean ± SD, n=3.
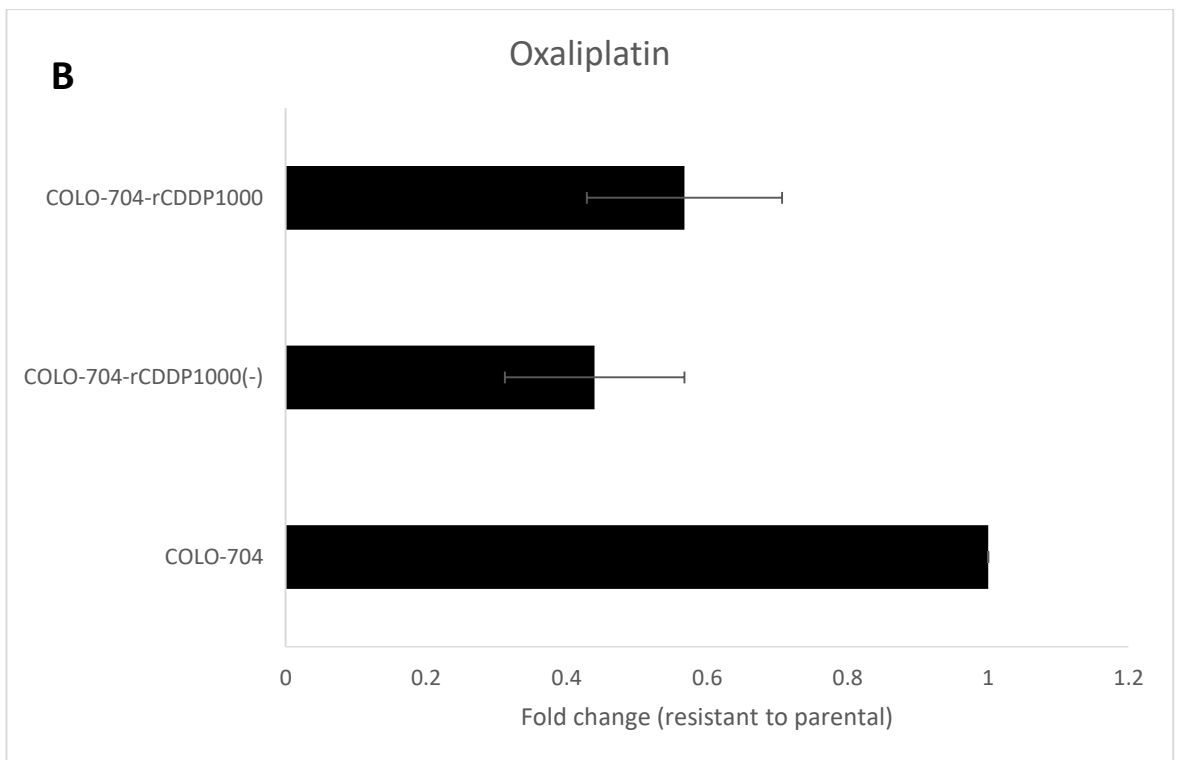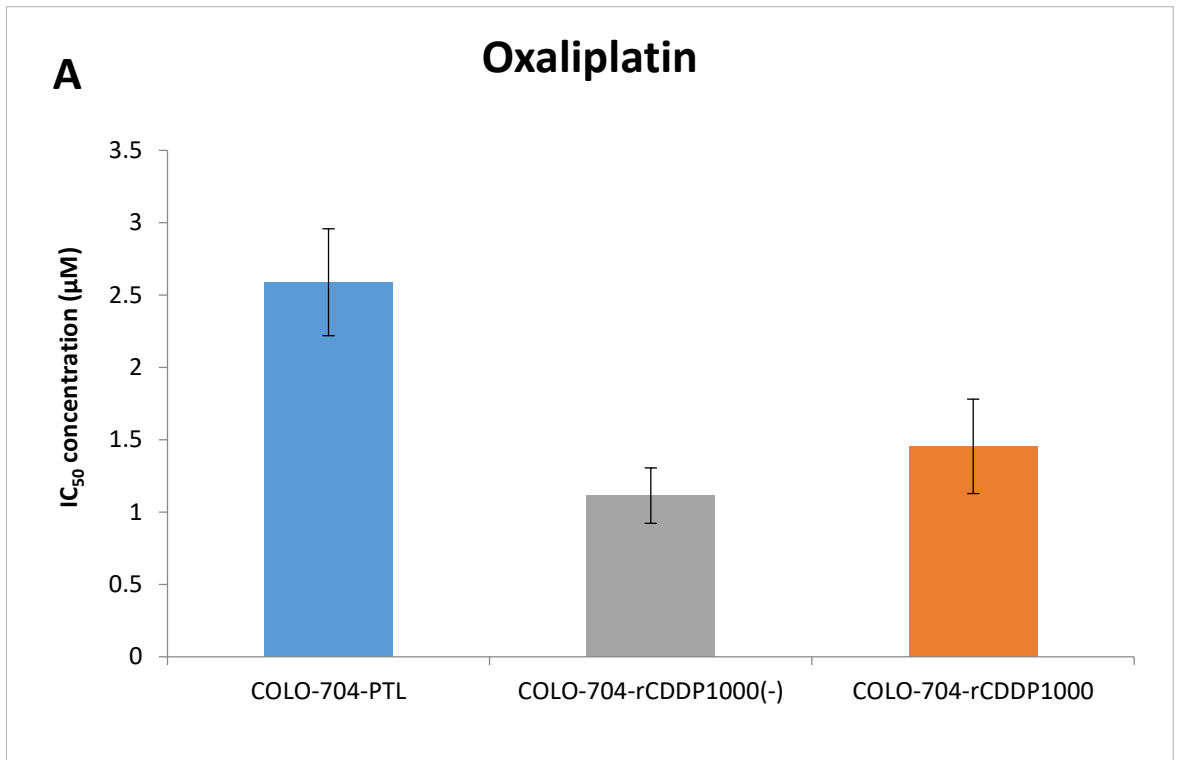
Figure 21: (A) IC$_{50}$ concentration of oxaliplatin and (B) fold change (resistant to sensitive) for the COLO-704 cell lines. Each data expressed is expressed as a mean ± SD, n=3.
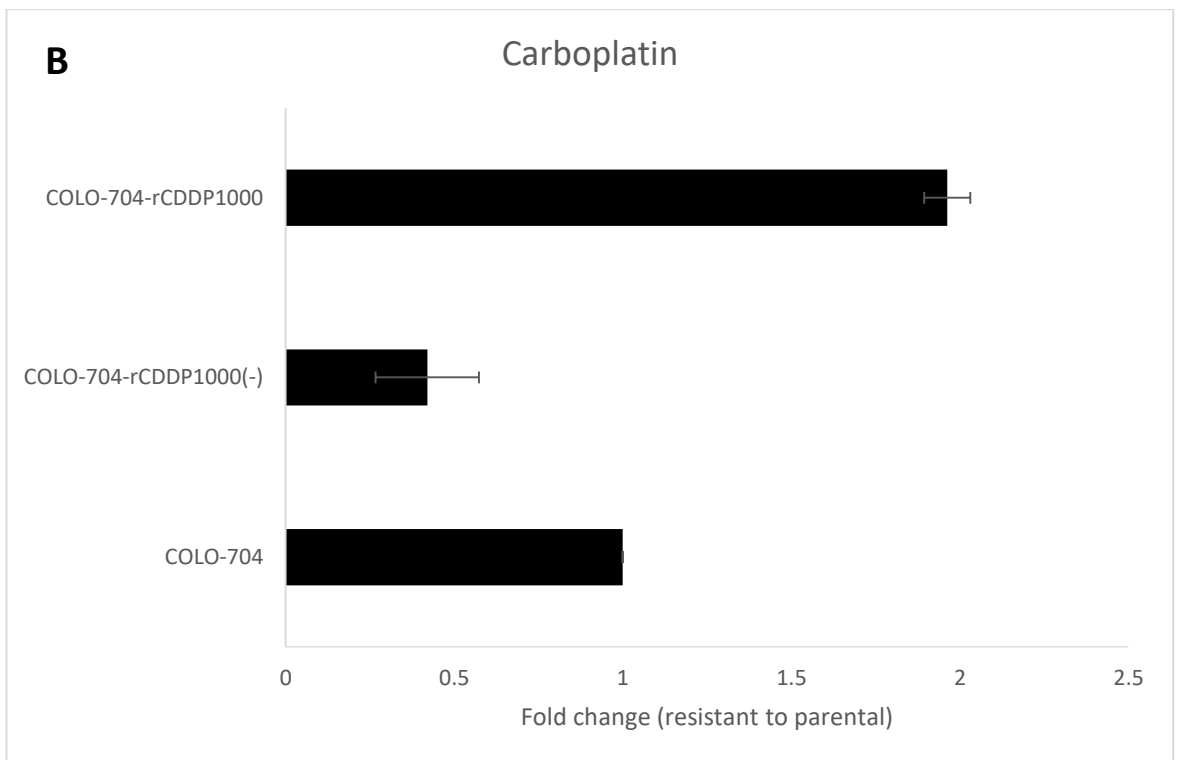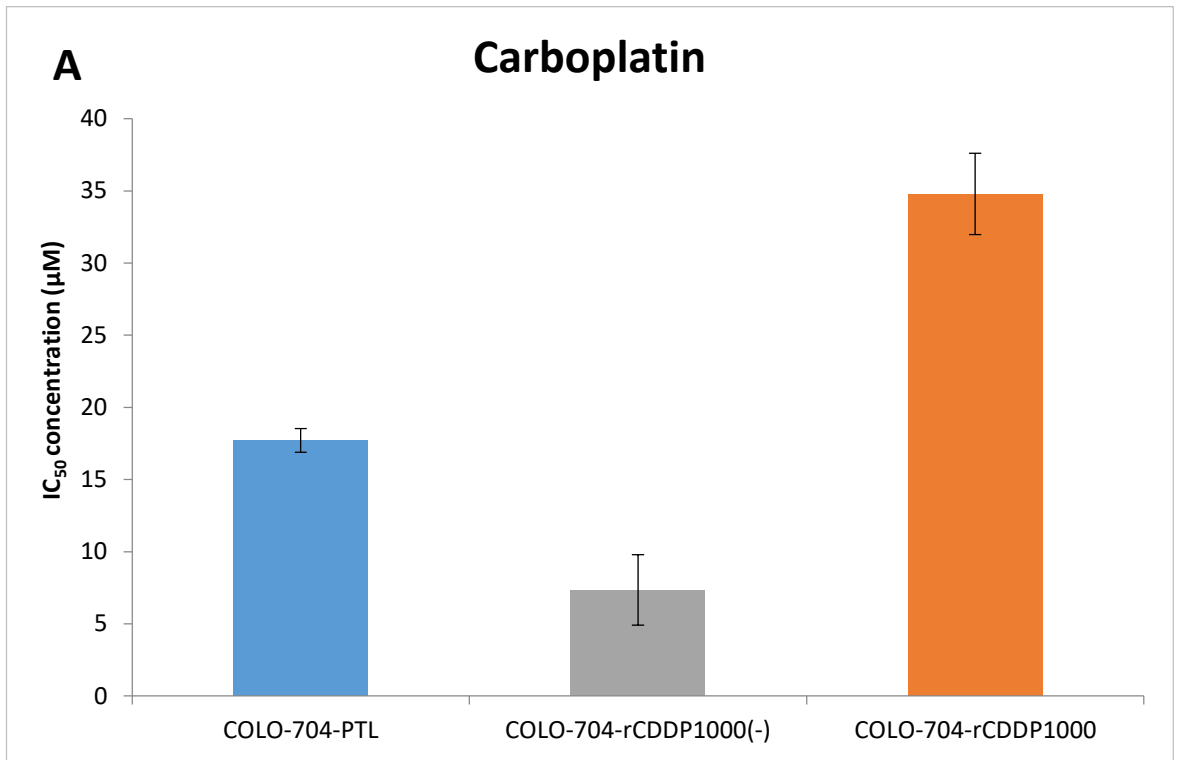
Figure 22: (A) IC$_{50}$ concentration of carboplatin and (B) fold change (resistant to sensitive) for the COLO-704 cell lines. Each data expressed is expressed as a mean ± SD, n=3.

5.2.4.2 Other anti-cancer drugs

To determine the cross-resistance patterns in the EFO-27, EFO-21 and COLO-704 cell lines as well as the respective sub-lines, several chemotherapeutic agents were examined.

The project cell line panel was further investigated for sensitivity to the EGFR tyrosine kinase inhibitor erlotinib, the Alk and Met inhibitor crizotinib, and the DNA damaging agents topotecan (topoisomerase I inhibitor), etoposide (topoisomerase II inhibitor), zeocin (intercalator that induces DNA double strand breaks), bleomycin (induces free radicals that induce DNA double strand breaks), temozolomide (alkylating agent), and mitomycin C (DNA crosslinker) (Table 18a-c; Table 19a-c, Figure 23-46).

Cell lline	Etoposide	Crizotinib	Erlotinib	Zeocin
EFO-21	0.74 ± 0.04	0.39 ± 0.02	0.002 ± 0.00	1.27 ± 0.30
EFO-21-rCDDP$^{2000(-)}$	0.23 ± 0.06	0.51 ± 0.08	0.13 ± 0.06	2.21 ± 0.58
EFO-21-rCDDP^{2000}	0.71 ± 0.15	0.62 ± 0.06	0.52 ± 0.03	2.97 ± 0.26

Table 18a: Cross-resistance profiles for EFO-21 cell line and the respective resistant sublines. IC50 concentrations were determined using MTT assays. Results are averages of three biological repeats (n=3 ± SD). Statistical significance comparison of resistant sublines to parental sublines: etoposide p=≤0.05, crizotinib p=≤0.05, erlotinib p=≤0.05 and zeocin p=≤0.05.

Cell lline	Etoposide	Crizotinib	Erlotinib	Zeocin
EFO-27	0.80 ± 0.04	0.52 ± 0.01	0.08 ± 0.02	3.00 ± 0.38
EFO-27-rCDDP$^{2000(-)}$	0.25 ± 0.02	0.49 ± 0.11	0.48 ± 0.09	1.06 ± 0.05
EFO-27-rCDDP^{2000}	0.52 ± 0.04	0.48 ± 0.13	0.15 ± 0.03	2.17 ± 0.29

Table 18b: Cross-resistance profiles for EFO-27 cell line and the respective resistant sublines. IC50 concentrations were determined using MTT assays. Results are averages of three biological repeats (n=3 ± SD). Statistical significance comparison of resistant sublines to parental sublines: etoposide p=≤0.05, crizotinib p=≥0.05, erlotinib p=≤0.05 and zeocin p=≤0.05.

Cell lline	Etoposide	Crizotinib	Erlotinib	Zeocin
COLO-704	0.56 ± 0.11	0.54 ± 0.09	0.43 ± 0.06	5.12 ± 1.21
COLO-704-rCDDP$^{1000(-)}$	0.29 ± 0.02	0.50 ± 0.03	0.48 ± 0.13	5.97 ± 0.46
COLO-704-rCDDP^{1000}	0.65 ± 0.06	0.43 ± 0.05	0.72 ± 0.07	10.16 ± 0.59

Table 18c: Cross-resistance profiles for COLO-704 cell line and the respective resistant sublines. IC50 concentrations were determined using MTT assays. Results are averages of three biological repeats (n=3 ± SD). Statistical significance comparison of resistant sublines to parental sublines: etoposide p=≤0.05, crizotinib p=≥0.05, erlotinib p=≤0.05 and zeocin p=≤0.05.

Cell lline	Bleomycin	Temozolomide	Topotecan	Mitomycin C
EFO-21	0.09 ± 0.00	0.15 ± 0.02	0.03 ± 0.00	0.07 ± 0.01
EFO-21-rCDDP$^{2000(-)}$	0.14 ± 0.01	0.50 ± 0.01	0.03 ± 0.00	0.13 ± 0.02
EFO-21-rCDDP^{2000}	0.23 ± 0.05	0.59 ± 0.03	0.05 ± 0.00	0.08 ± 0.02

Table 19a: **Cross-resistance profiles for EFO-21 cell line and the respective resistant sublines.** IC50 concentrations were determined using MTT assays. Results are averages of three biological repeats (n=3 ± SD). Statistical significance comparison of resistant sublines to parental sublines: bleomycin p=≤0.05, temozolomide p=≤0.05, topotecan p=≤0.05 and mitomycin C p=≤0.05.

Cell lline	Bleomycin	Temozolomide	Topotecan	Mitomycin C
EFO-27	0.14 ± 0.13	0.14 ± 0.01	0.03 ± 0.00	0.05 ± 0.00
EFO-27-rCDDP$^{2000(-)}$	0.18 ± 0.02	0.30 ± 0.04	0.03 ± 0.00	0.02 ± 0.01
EFO-27-rCDDP^{2000}	0.32 ± 0.10	0.58 ± 0.02	0.03 ± 0.00	0.07 ± 0.02

Table 19b: **Cross-resistance profiles for EFO-27 cell line and the respective resistant sublines**. IC50 concentrations were determined using MTT assays. Results are averages of three biological repeats (n=3 ± SD). Statistical significance comparison of resistant sublines to parental sublines: bleomycin p=≤0.05, temozolomide p=≤0.05, topotecan p=≥0.05 and mitomycin C p=≤0.05.

Cell lline	Bleomycin	Temozolomide	Topotecan	Mitomycin C
COLO-704	0.23 ± 0.09	0.27 ± 0.05	0.01 ± 0.00	0.01 ± 0.00
COLO-704-rCDDP$^{1000(-)}$	0.42 ± 0.08	0.50 ± 0.02	0.01 ± 0.00	0.02 ± 0.00
COLO-704-rCDDP^{1000}	0.96 ± 0.16	1.13 ± 0.10	0.02 ± 0.00	0.13 ± 0.02

Table 19c: **Cross-resistance profiles for COLO-704 cell line and the respective resistant sublines**. IC50 concentrations were determined using MTT assays. Results are averages of three biological repeats (n=3 ± SD). Statistical significance comparison of resistant sublines to parental sublines: bleomycin p=≤0.05, temozolomide p=≤0.05, topotecan p=≤0.05 and mitomycin C p=≤0.05.
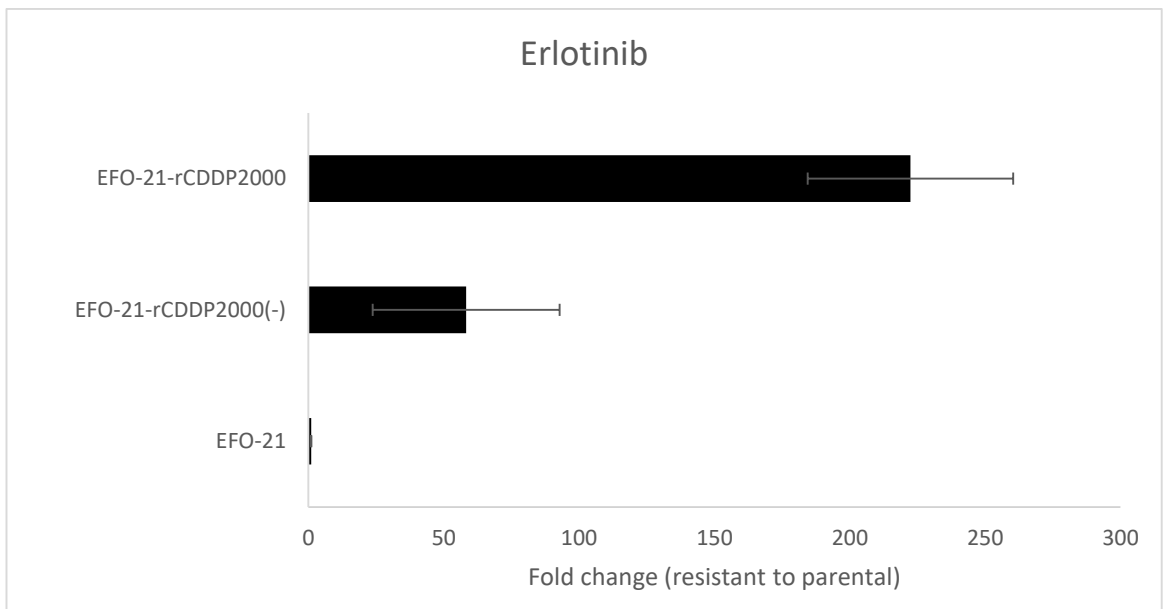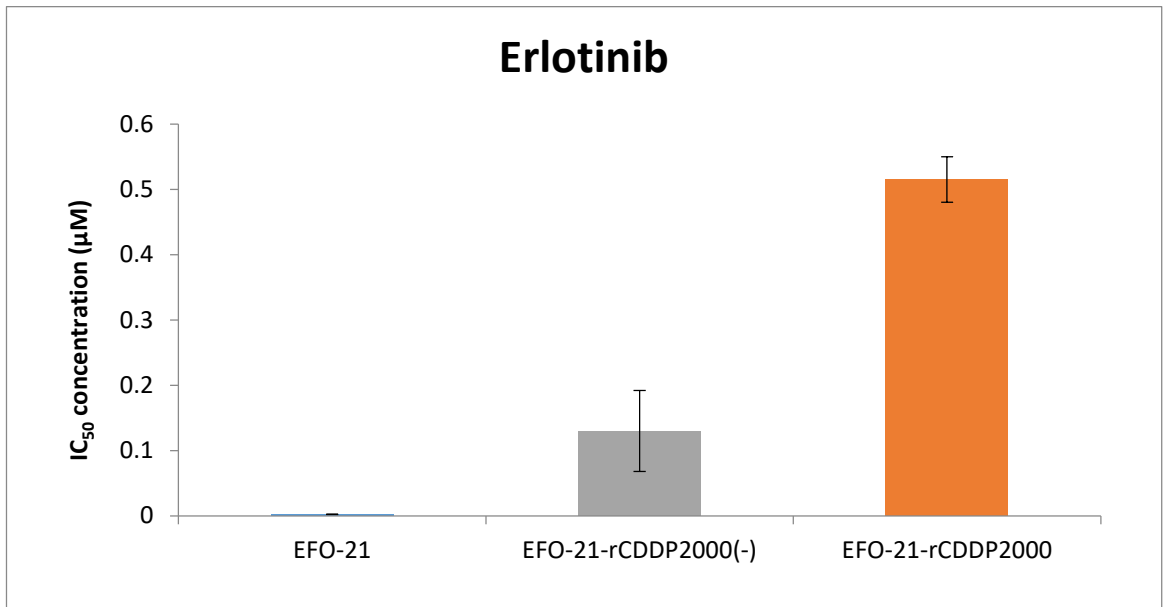
Figure 23: (A) IC$_{50}$ concentration of Erlotinib and (B) fold change (resistant to sensitive) for the EFO-21 cell lines. Each data expressed is expressed as a mean ± SD, n=3.
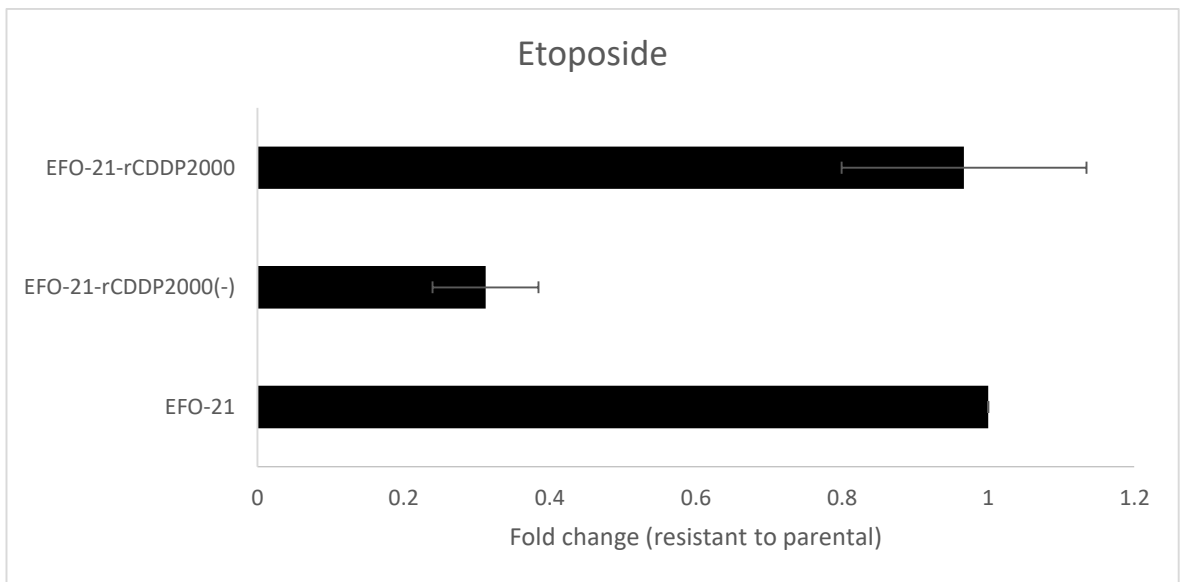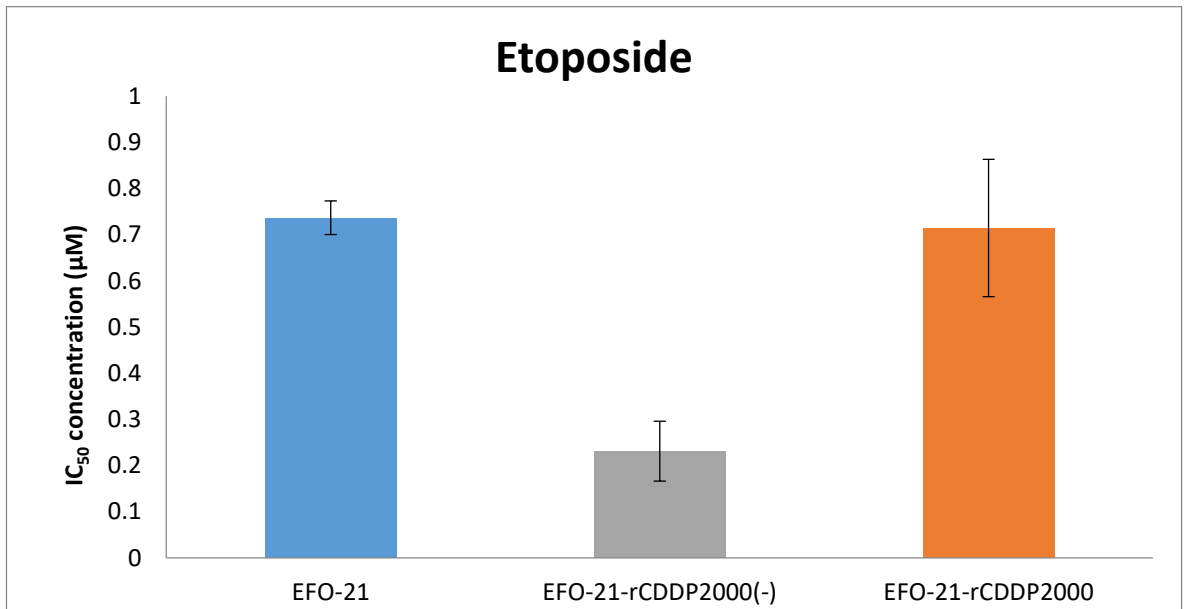
Figure 24: (A) IC$_{50}$ concentration of Etoposide and (B) fold change (resistant to sensitive) for the EFO-21 cell lines. Each data expressed is expressed as a mean ± SD, n=3.
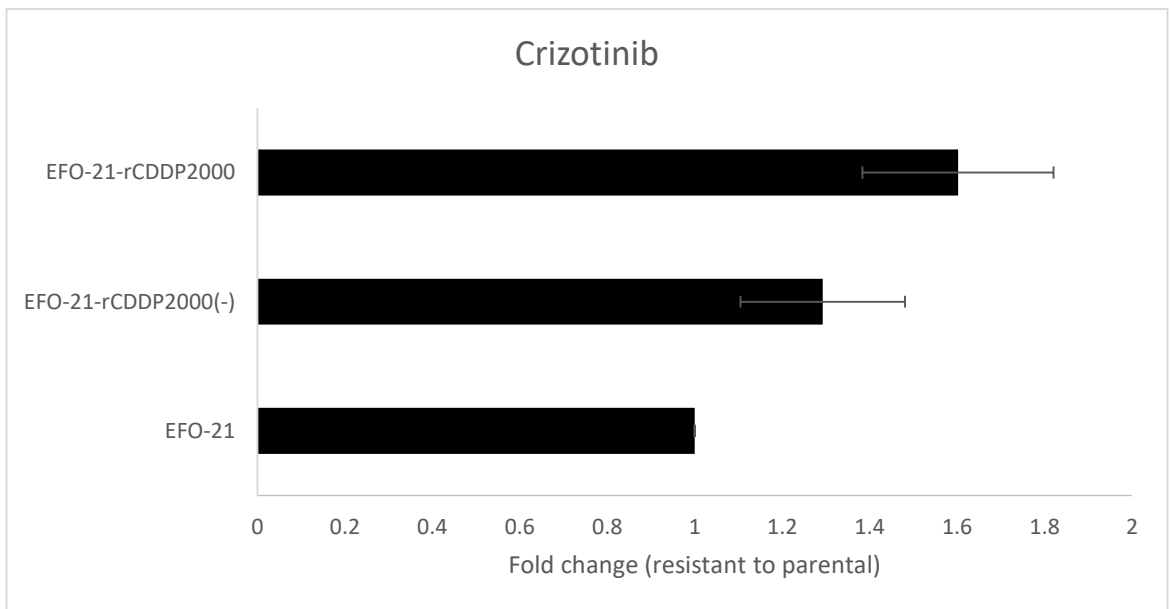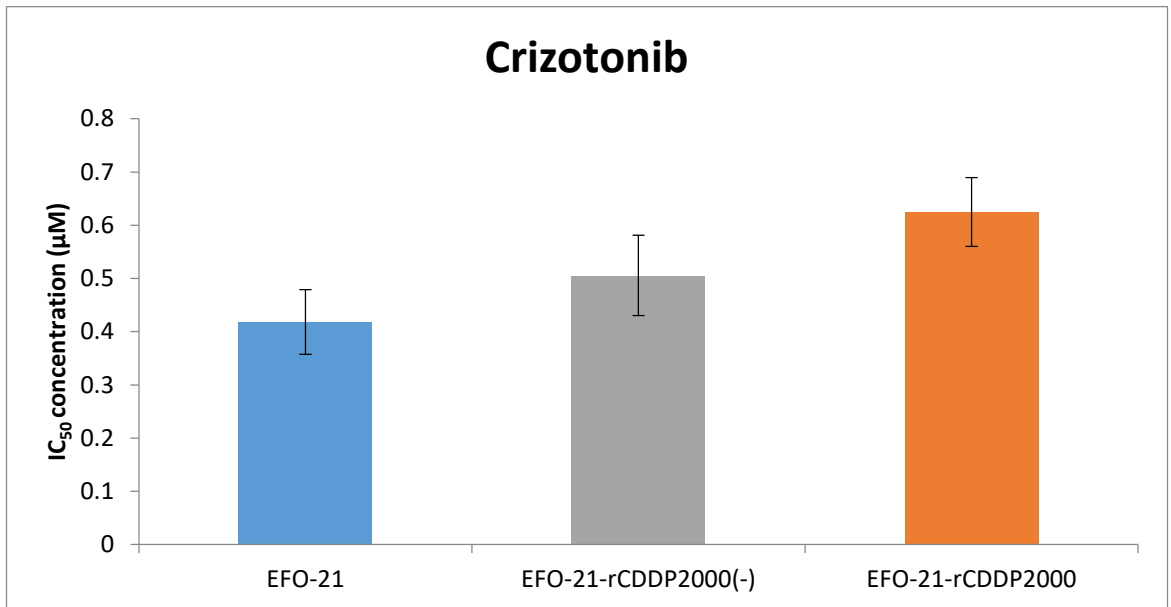
Figure 25: (A) IC$_{50}$ concentration of Crizotinb and (B) fold change (resistant to sensitive) for the EFO-21 cell lines. Each data expressed is expressed as a mean ± SD, n=3.
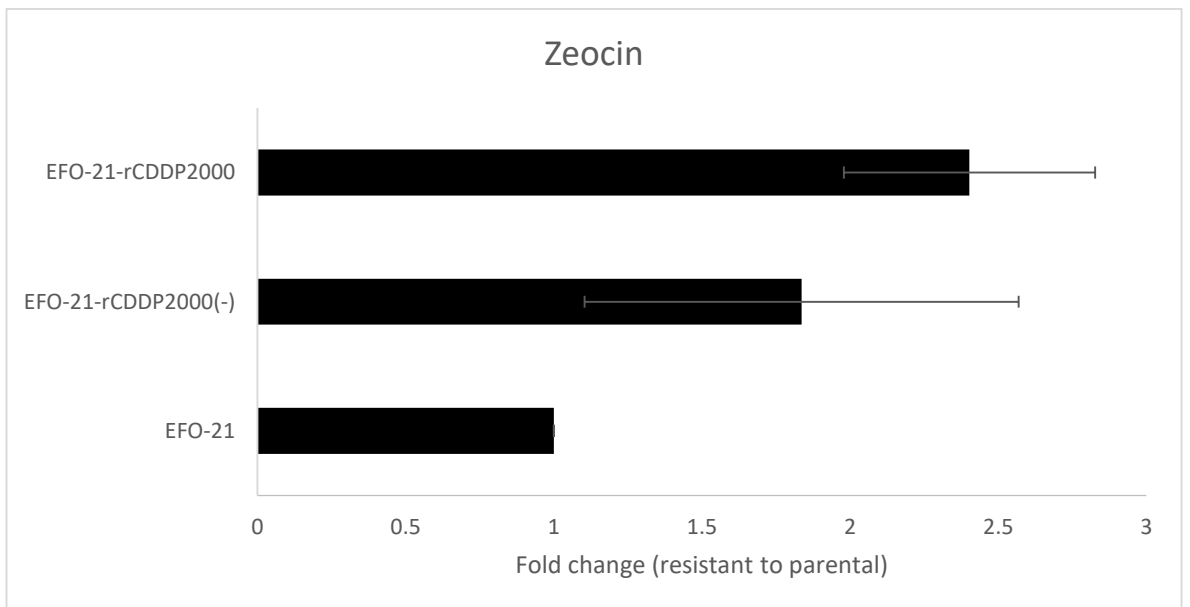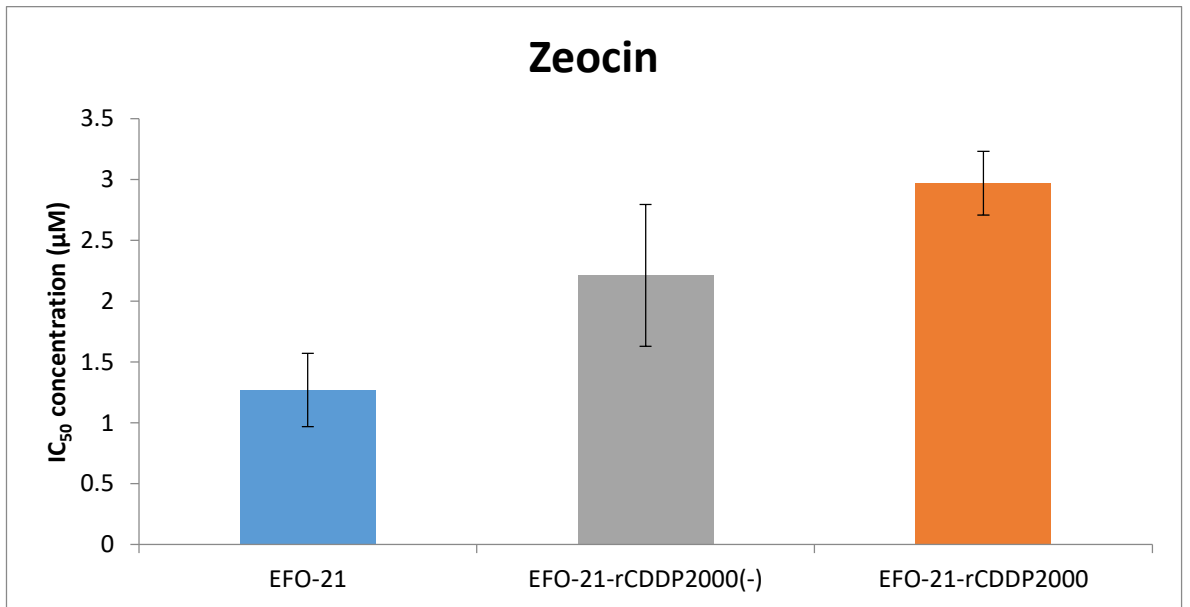
Figure 26: (A) IC$_{50}$ concentration of Zeocin and **(B)** fold change (resistant to sensitive) for the EFO-21 cell lines. Each data expressed is expressed as a mean ± SD, n=3.
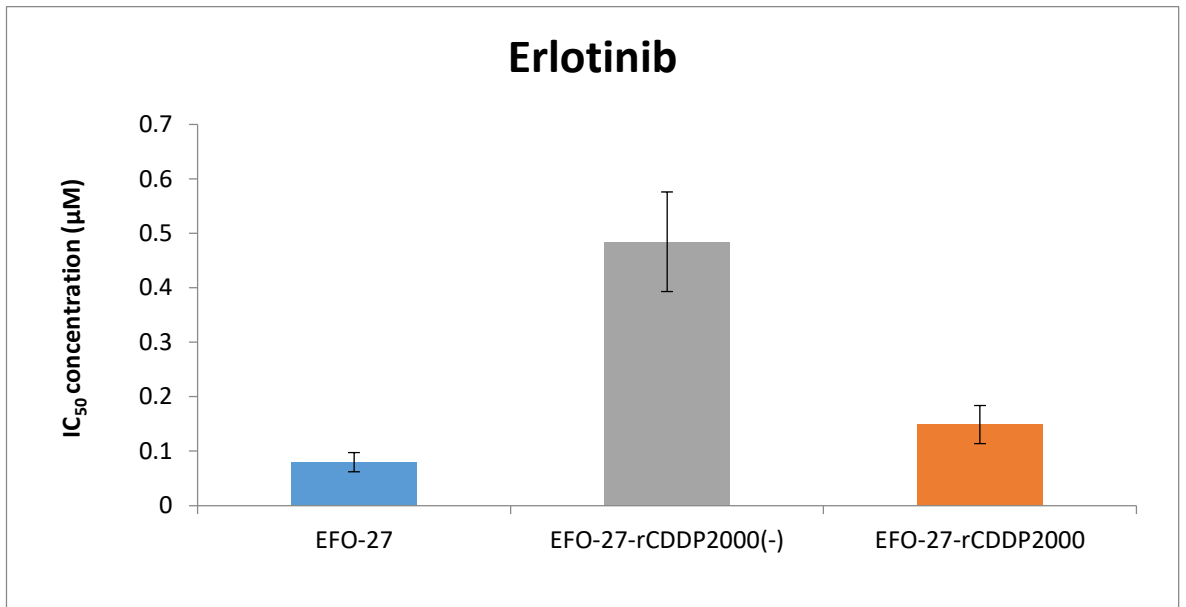
Figure 27: (A) IC$_{50}$ concentration of Erlotinib and (B) fold change (resistant to sensitive) for the EFO-27 cell lines. Each data expressed is expressed as a mean ± SD, n=3.
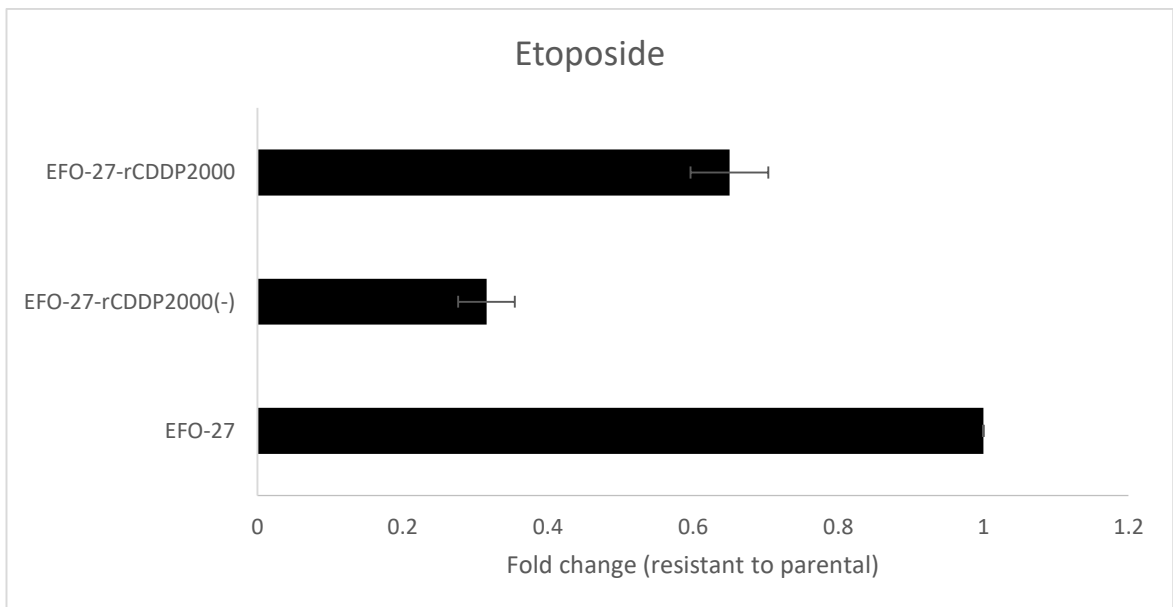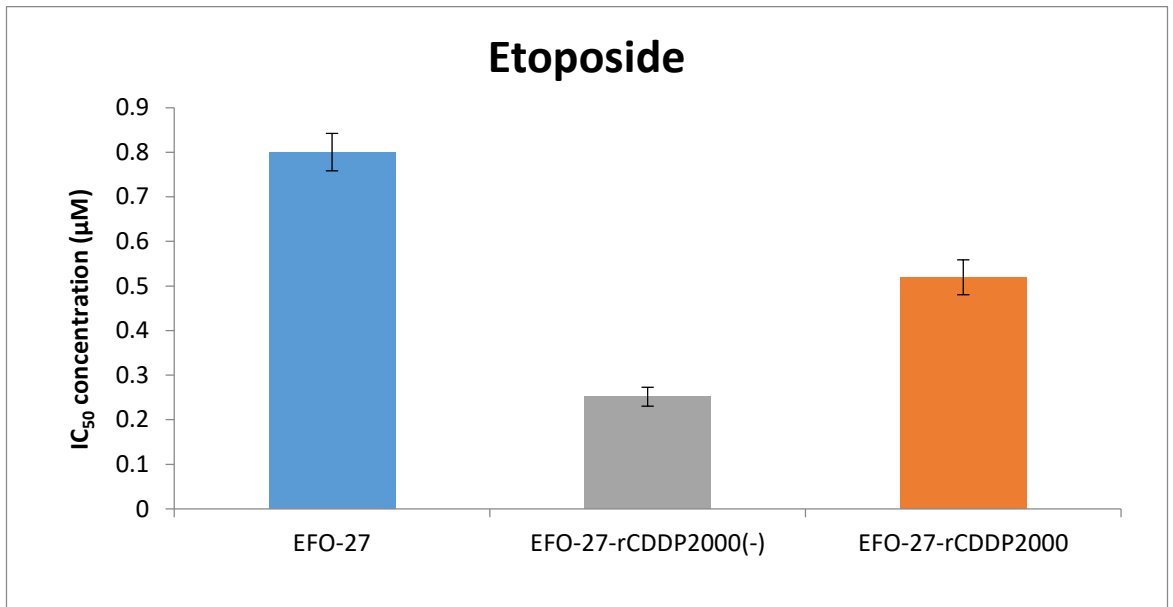
Figure 28: (A) IC$_{50}$ concentration of Etoposide and (B) fold change (resistant to sensitive) for the EFO-27 cell lines. Each data expressed is expressed as a mean ± SD, n=3.
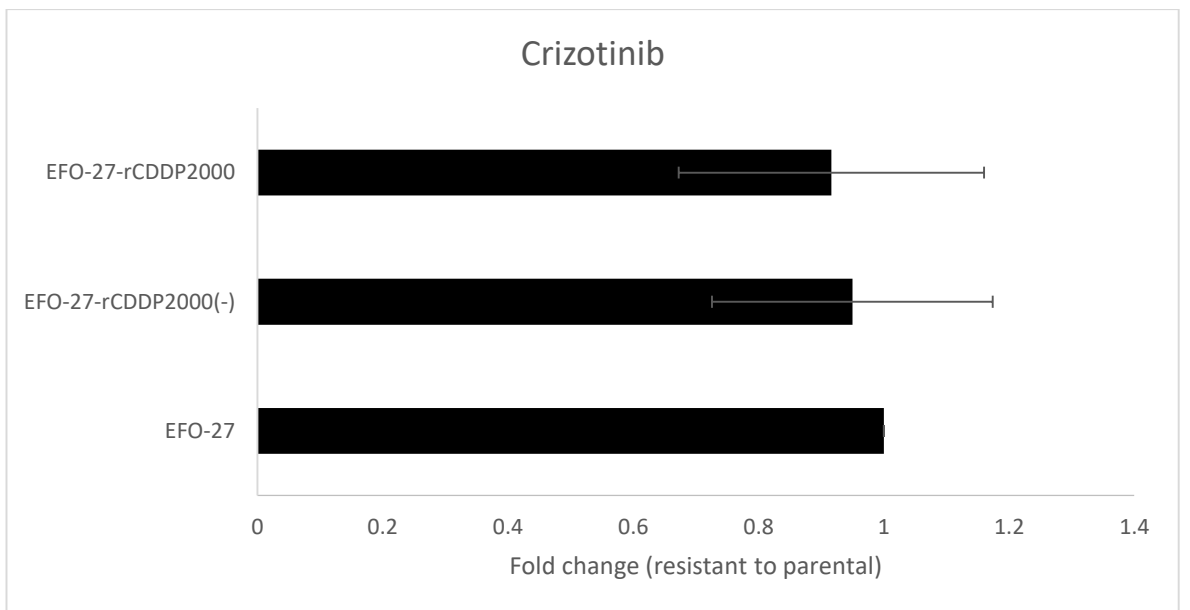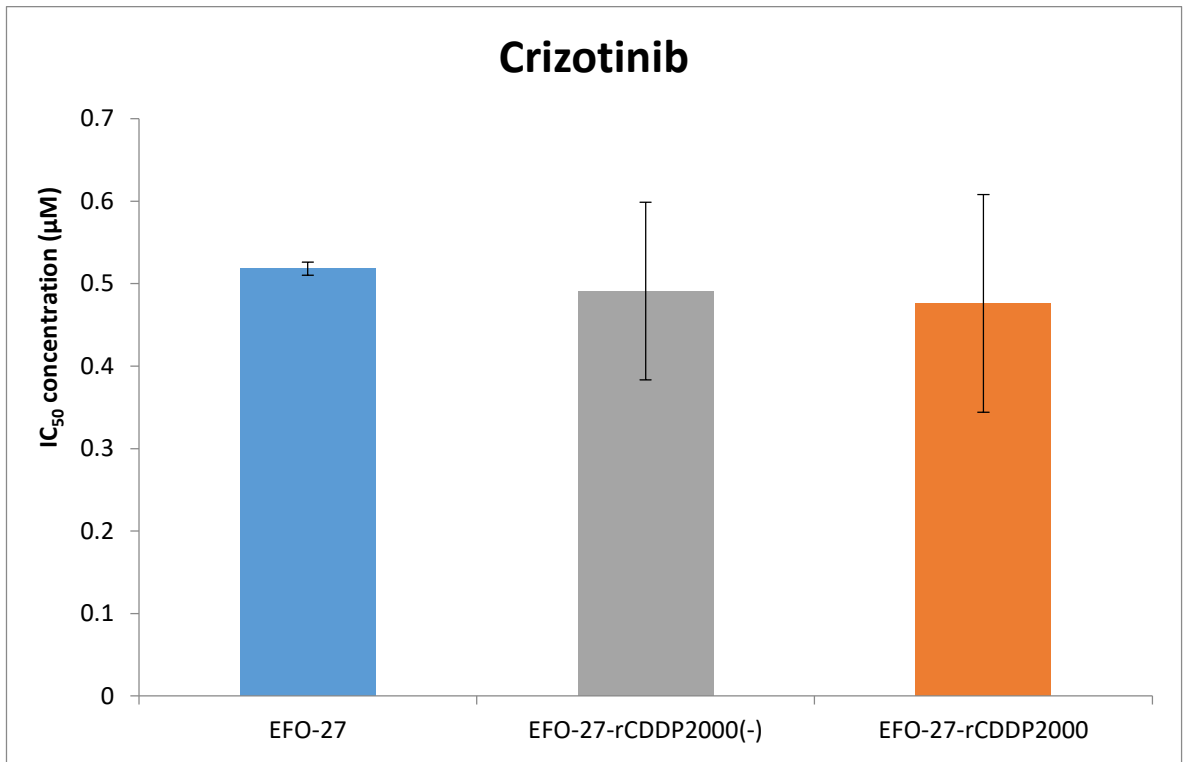
Figure 29: (A) IC$_{50}$ concentration of crizotinib and (B) fold change (resistant to sensitive) for the EFO-27 cell lines. Each data expressed is expressed as a mean ± SD, n=3.
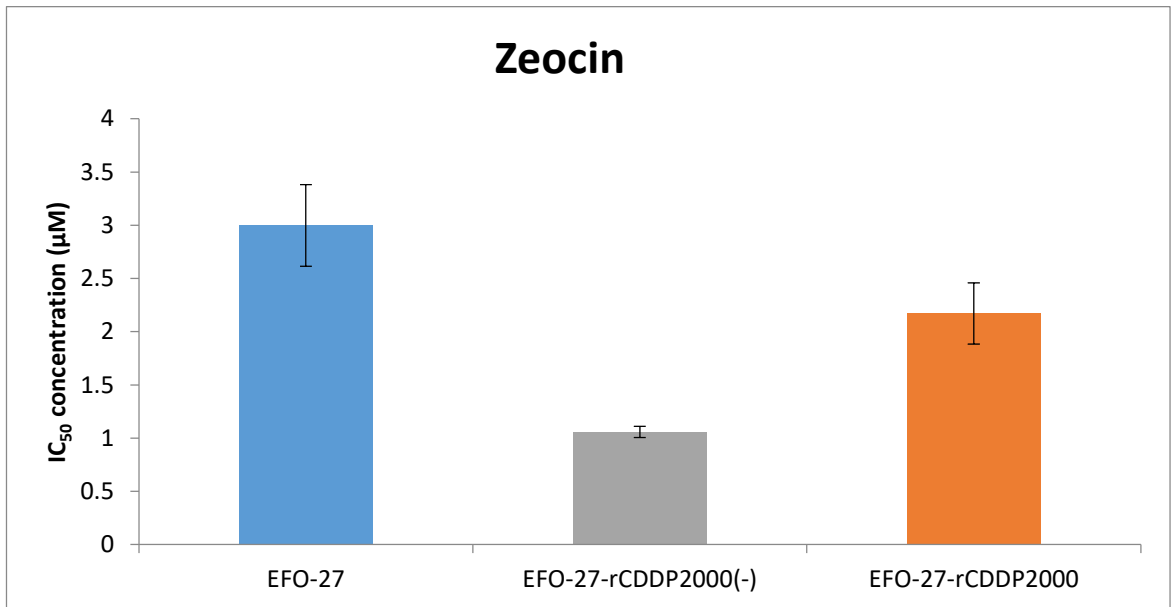
Figure 30: (A) IC$_{50}$ concentration of Zeocin and (B) fold change (resistant to sensitive) for the EFO-27 cell lines. Each data expressed is expressed as a mean ± SD, n=3.
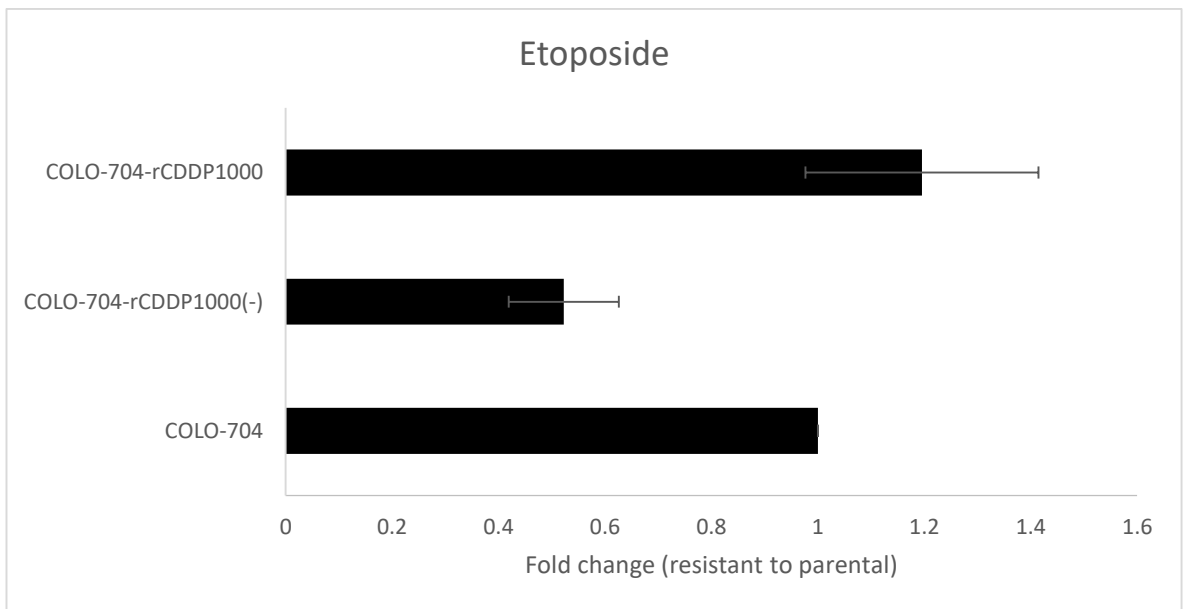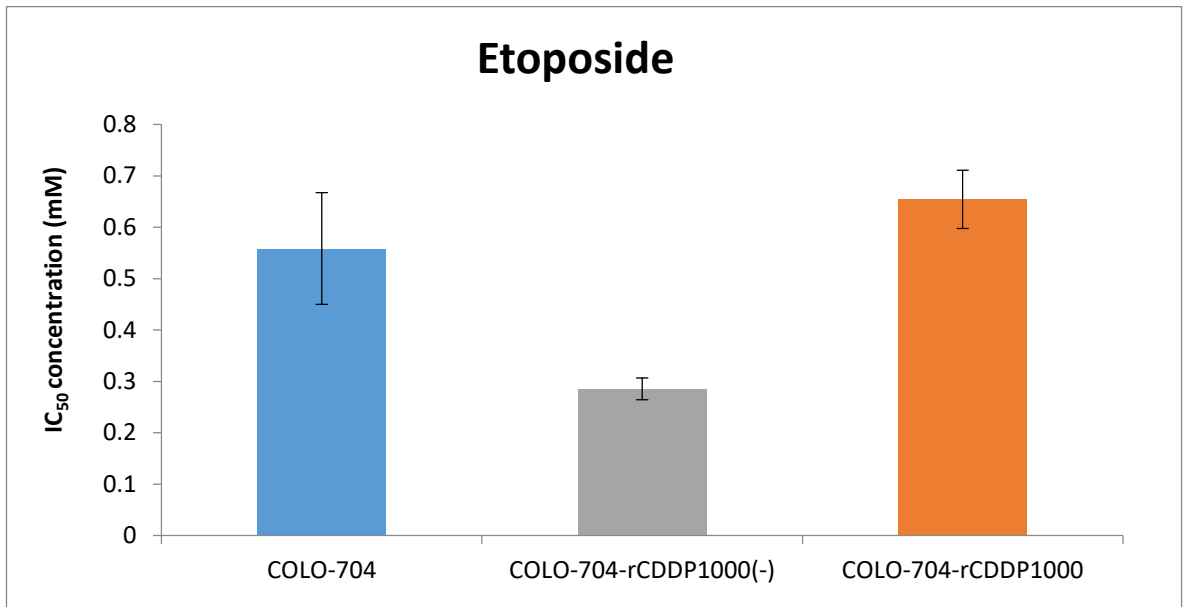
Figure 31: (A) IC$_{50}$ concentration of Etoposide and (B) fold change (resistant to sensitive) for the COLO-704 cell lines. Each data expressed is expressed as a mean ± SD, n=3.
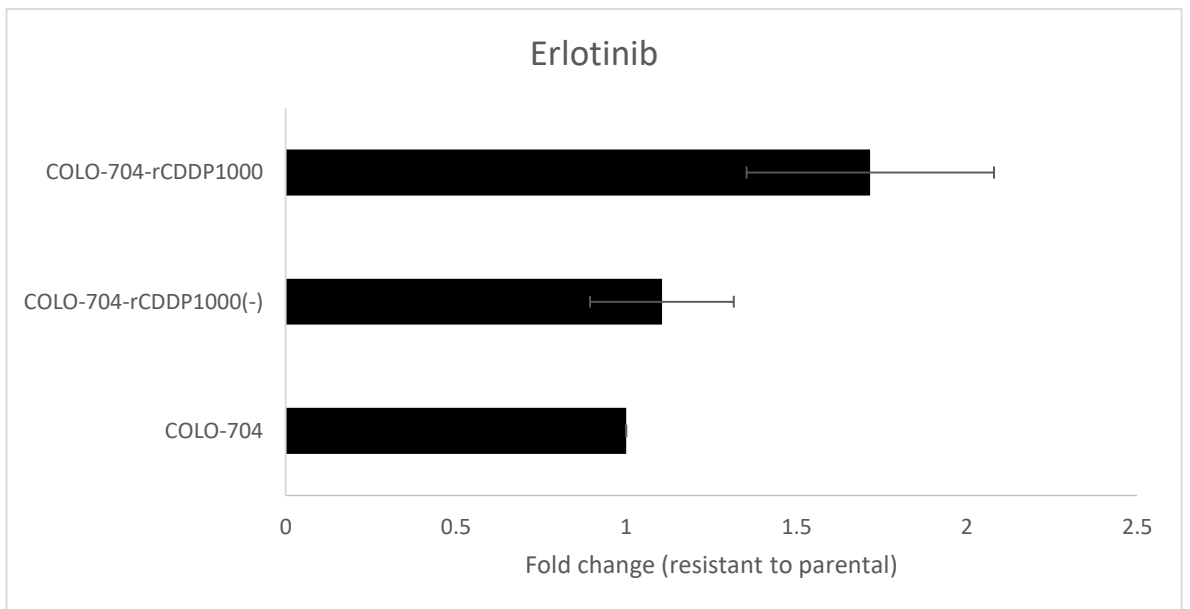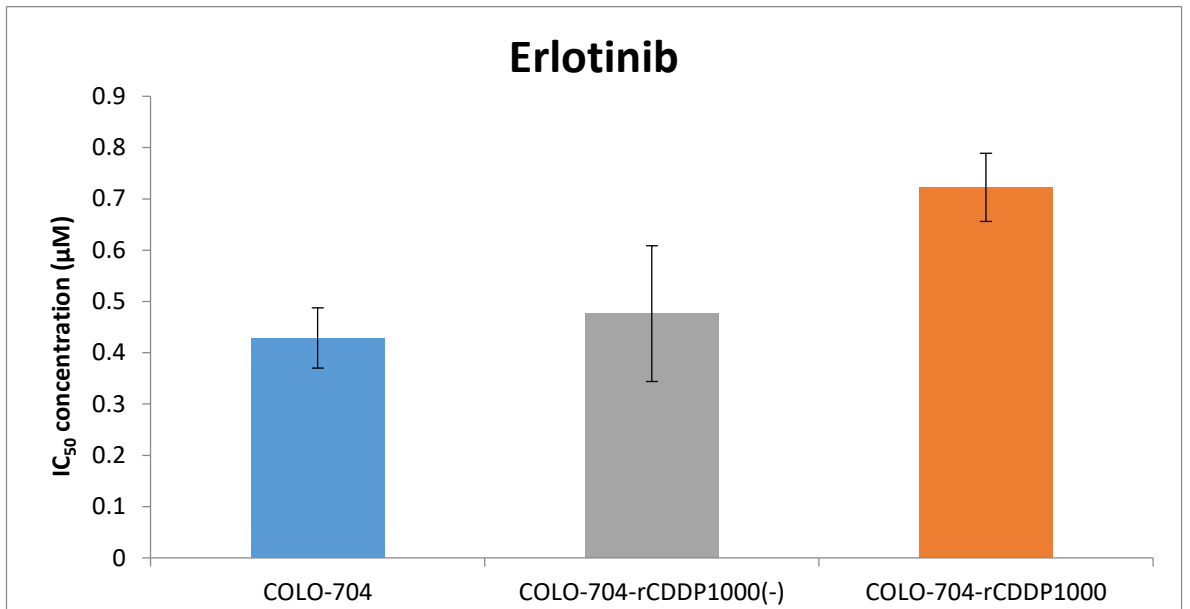
Figure 32: (A) IC$_{50}$ concentration of Erlotinib and (B) fold change (resistant to sensitive) for the COLO-704 cell lines. Each data expressed is expressed as a mean ± SD, n=3.
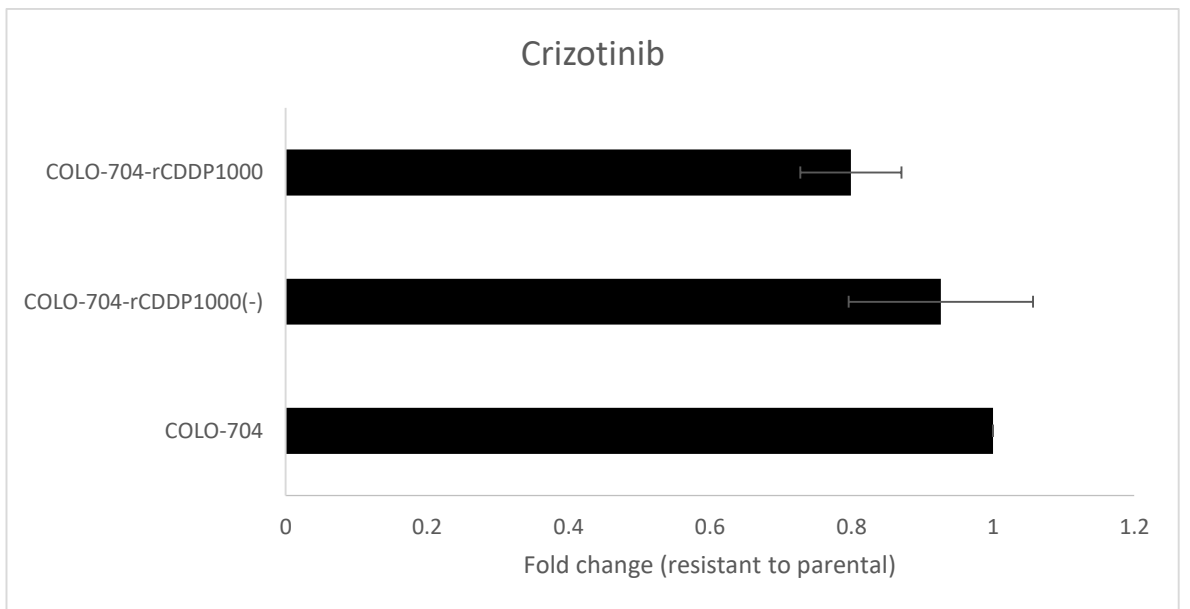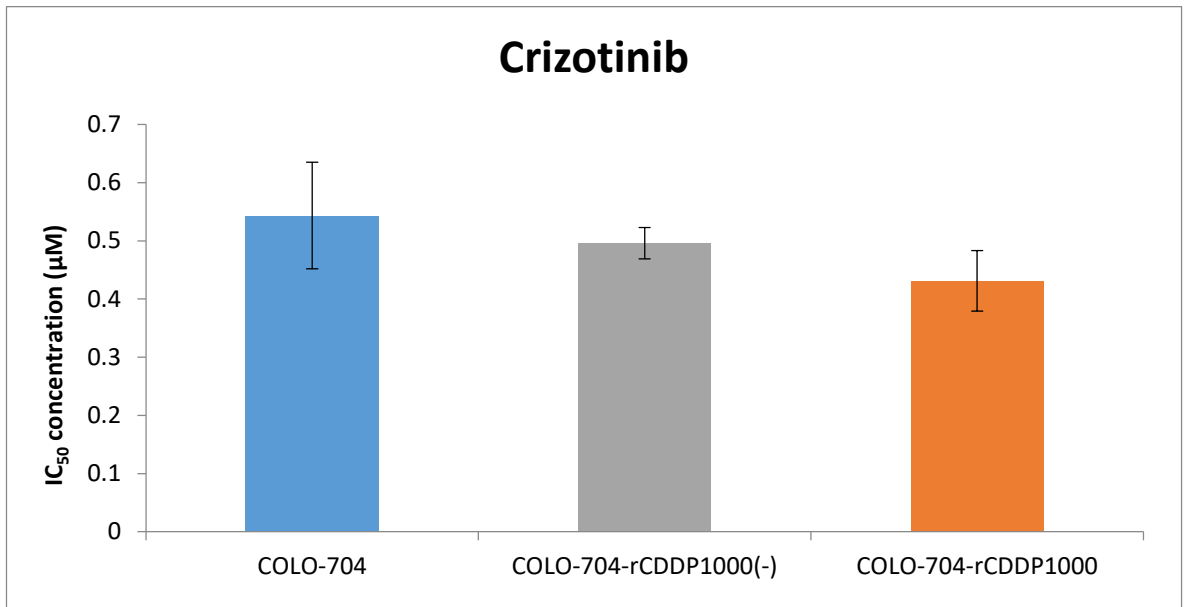
Figure 33: (A) IC$_{50}$ concentration of crizotinib and (B) fold change (resistant to sensitive) for the COLO-704 cell lines. Each data expressed is expressed as a mean ± SD, n=3.
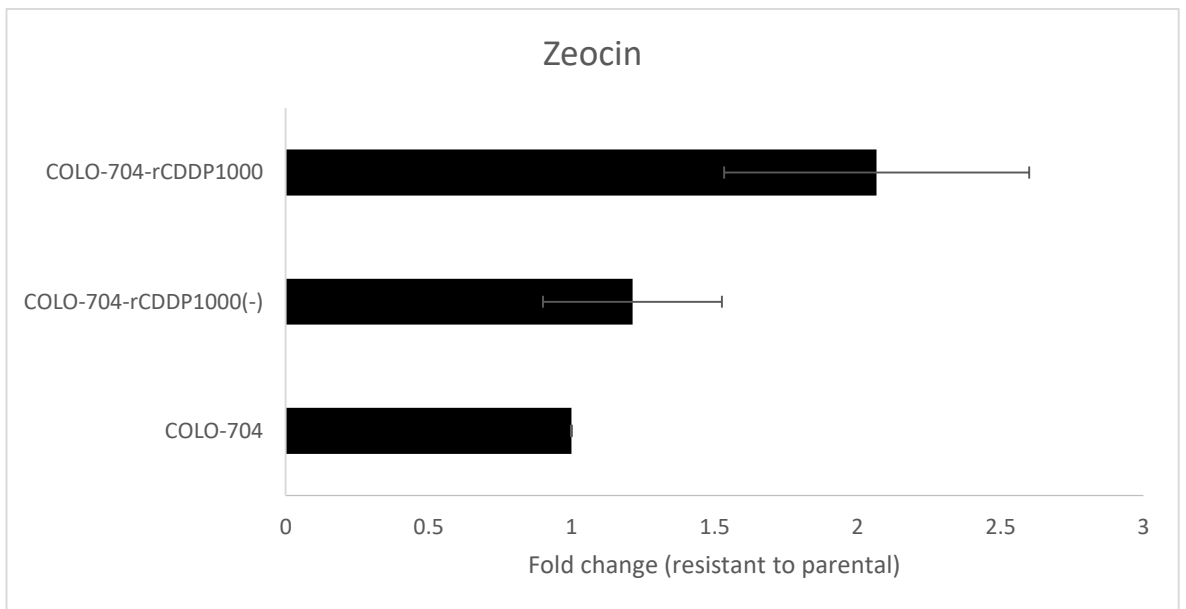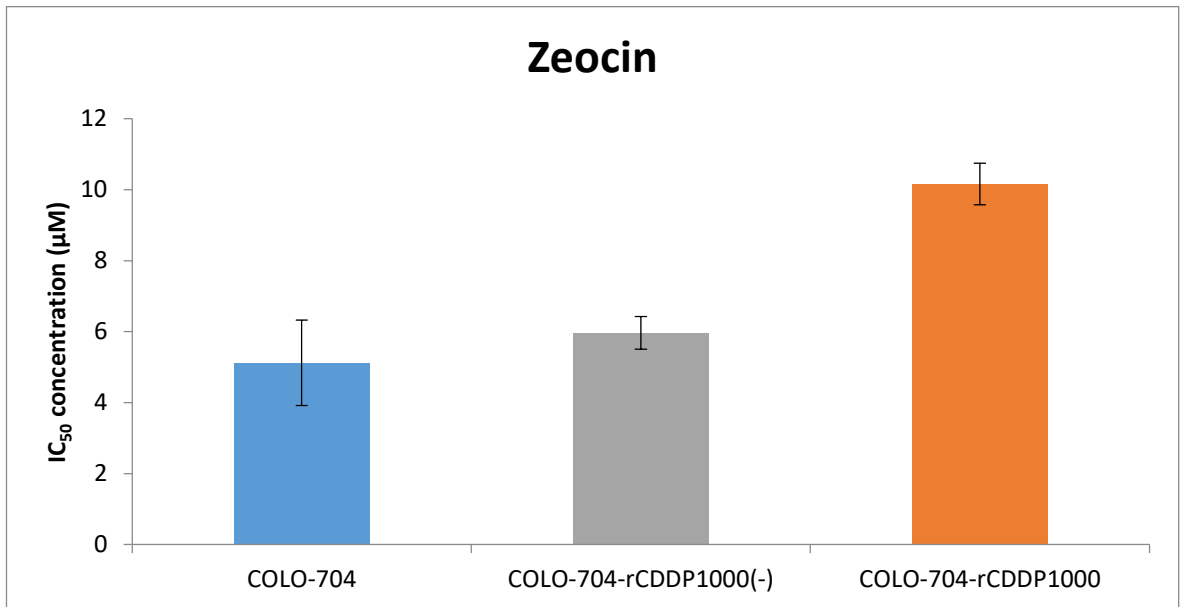
Figure 34: (A) IC$_{50}$ concentration of Zeocin and **(B)** fold change (resistant to sensitive) for the COLO-704 cell lines. Each data expressed is expressed as a mean ± SD, n=3.
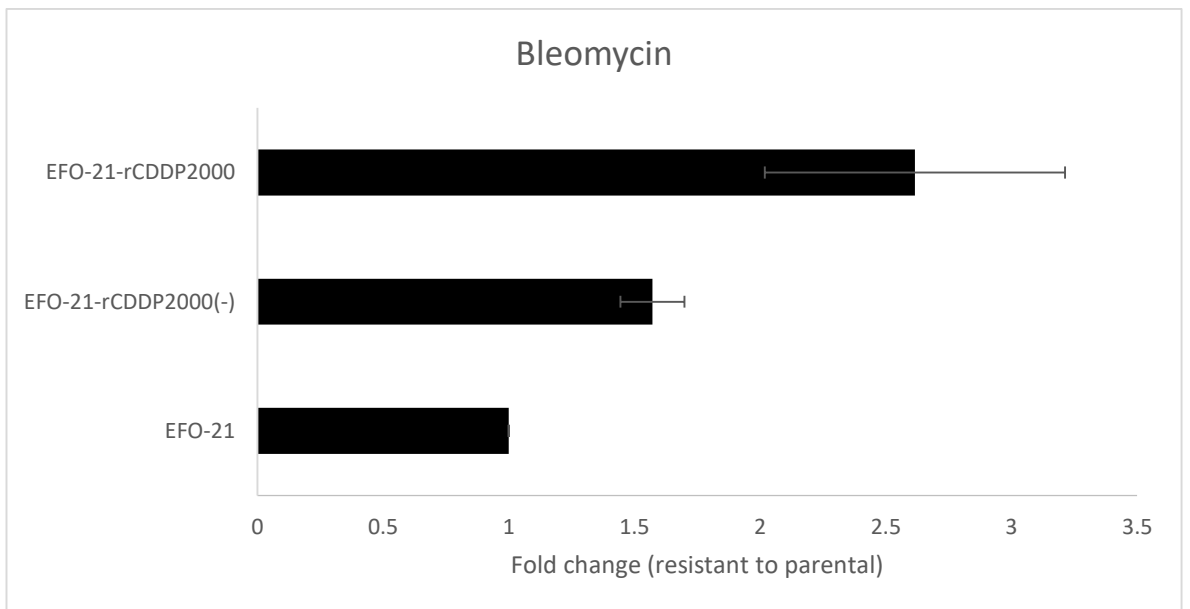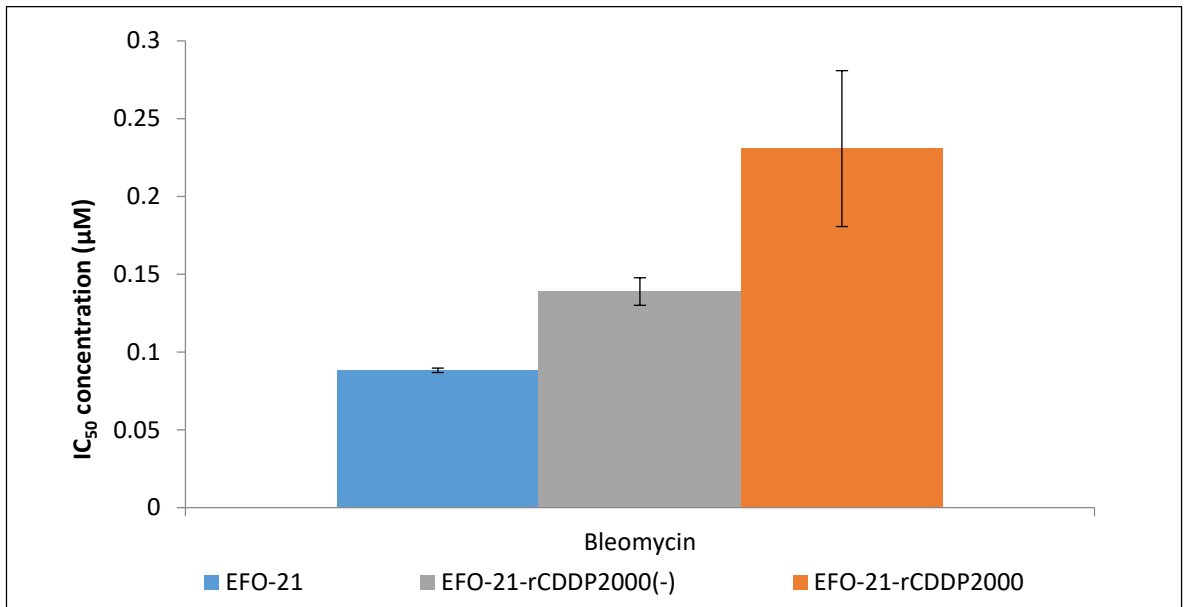
Figure 35: (A) IC$_{50}$ concentration of Bleomycin and (B) fold change (resistant to sensitive) for the EFO-21 cell lines. Each data expressed is expressed as a mean ± SD, n=3.
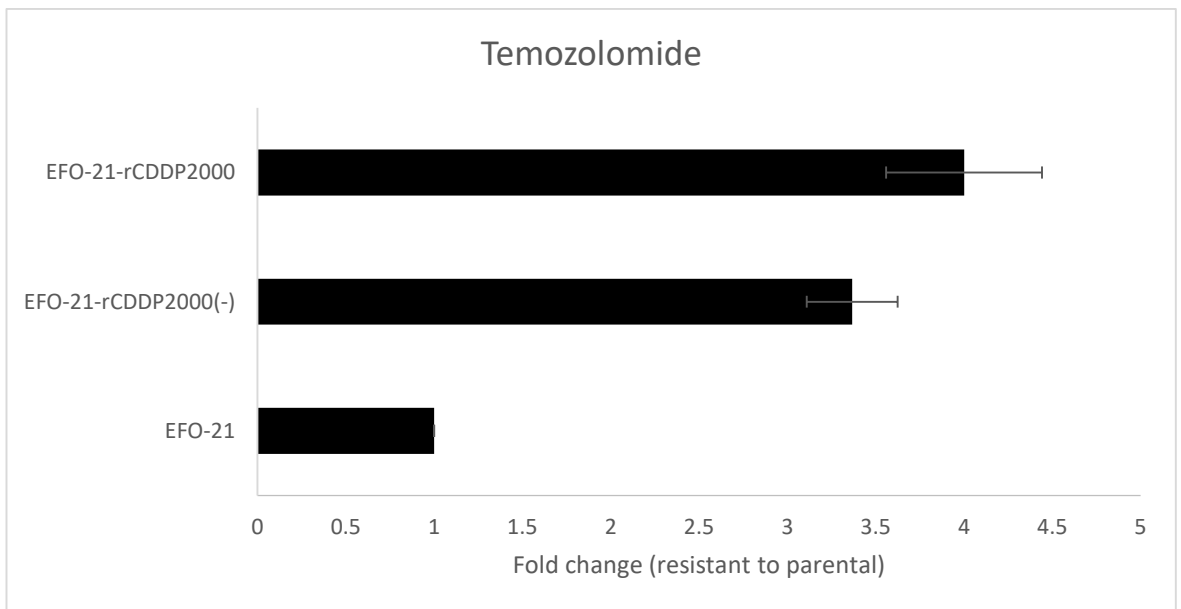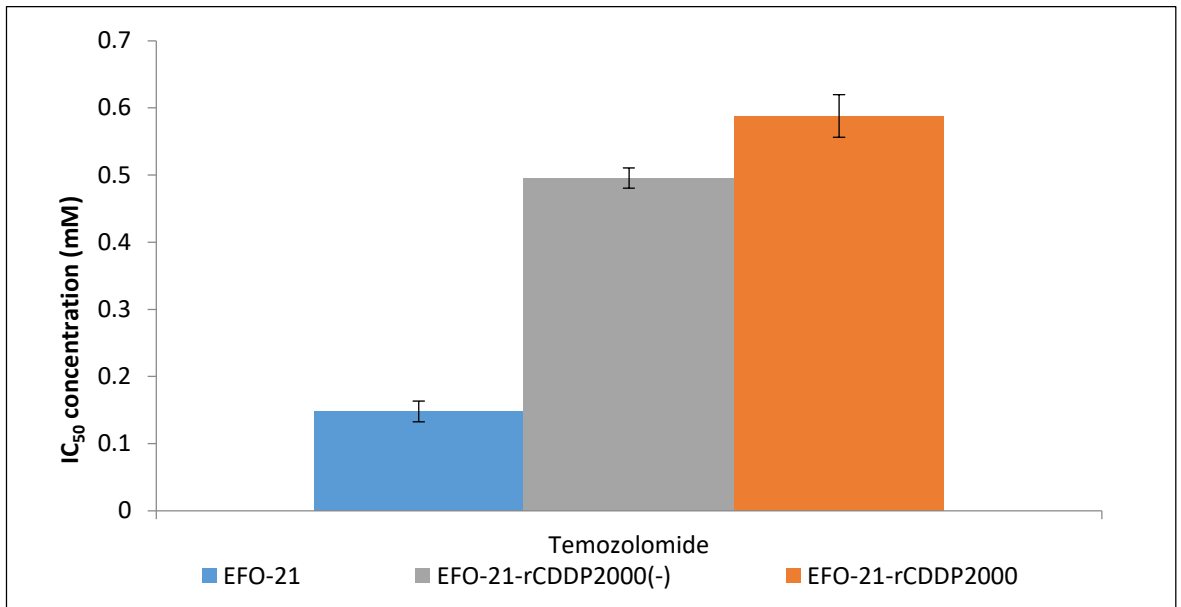
Figure 36: (A) IC$_{50}$ concentration of Temozolomide and (B) fold change (resistant to sensitive) for the EFO-21 cell lines. Each data expressed is expressed as a mean ± SD, n=3.
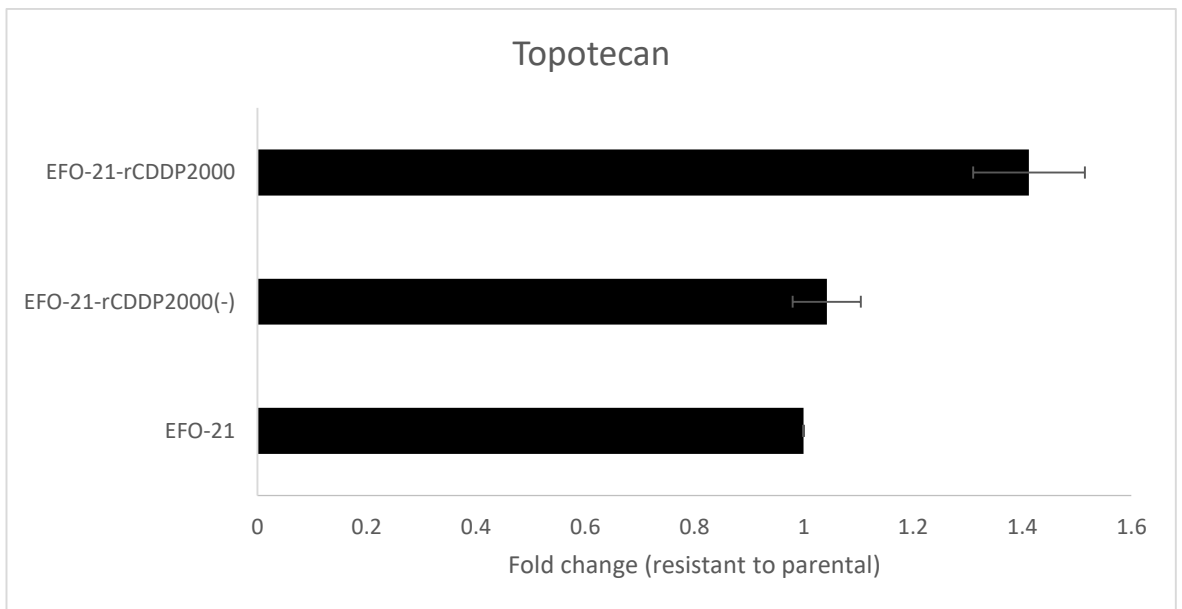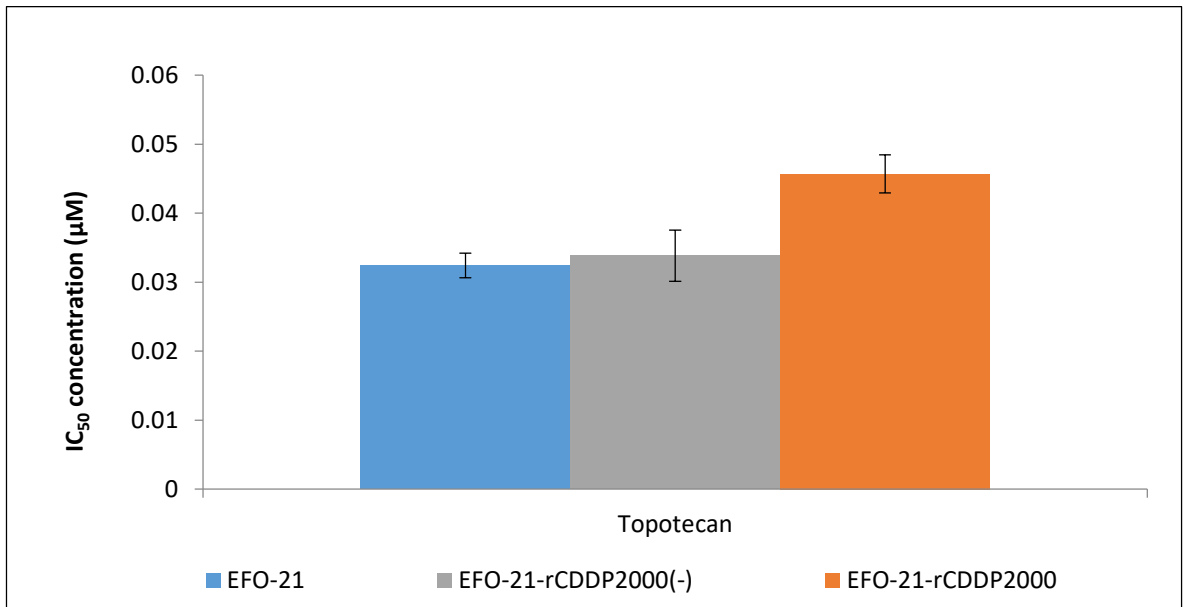
Figure 37: (A) IC$_{50}$ concentration of Topotecan and (B) fold change (resistant to sensitive) for the EFO-21 cell lines. Each data expressed is expressed as a mean ± SD, n=3.
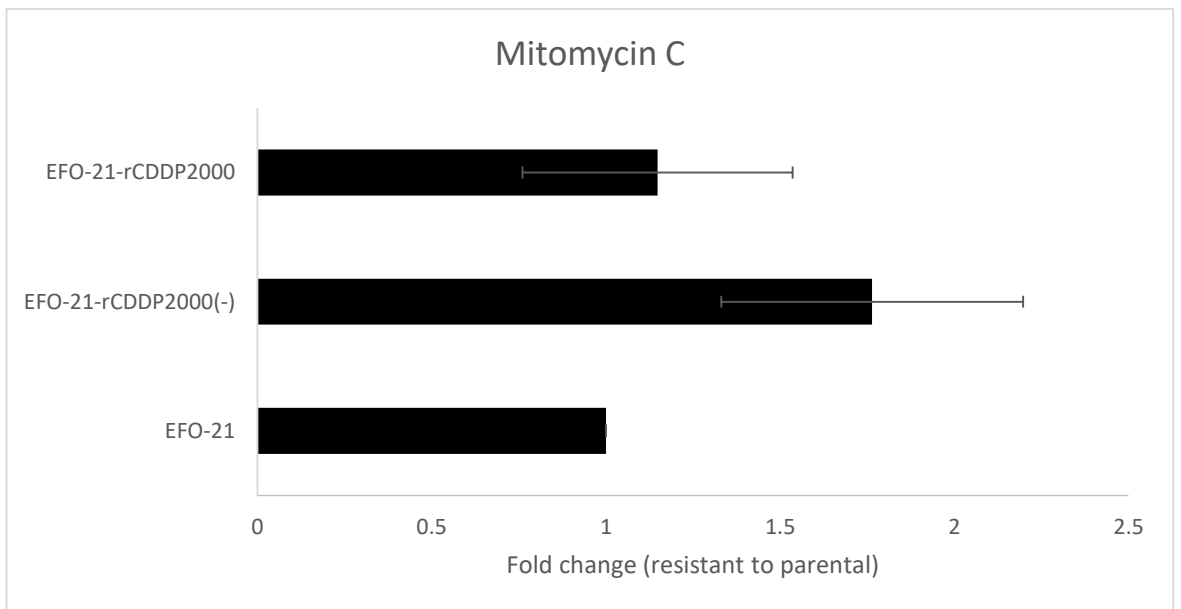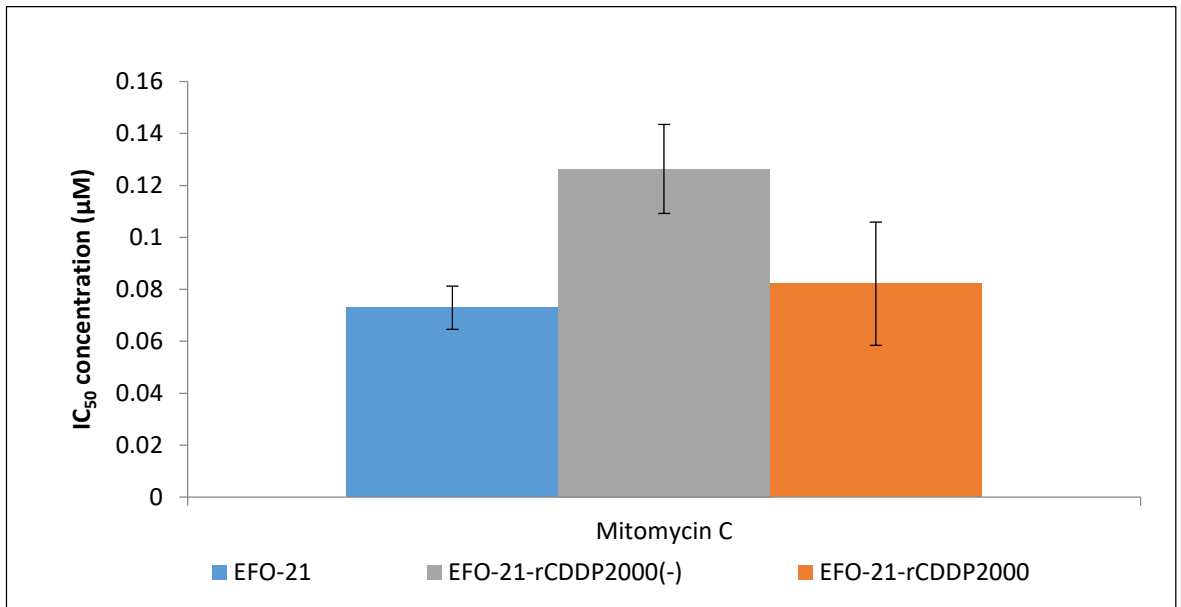
Figure 38: (A) IC$_{50}$ concentration of Mitomycin C and (B) fold change (resistant to sensitive) for the EFO-21 cell lines. Each data expressed is expressed as a mean ± SD, n=3.
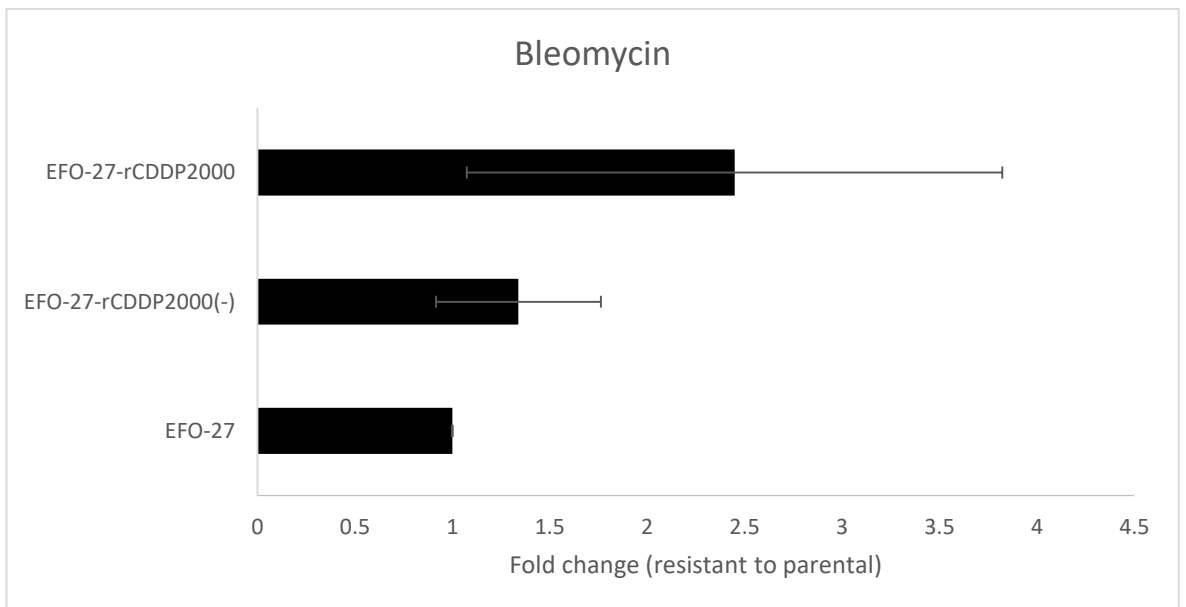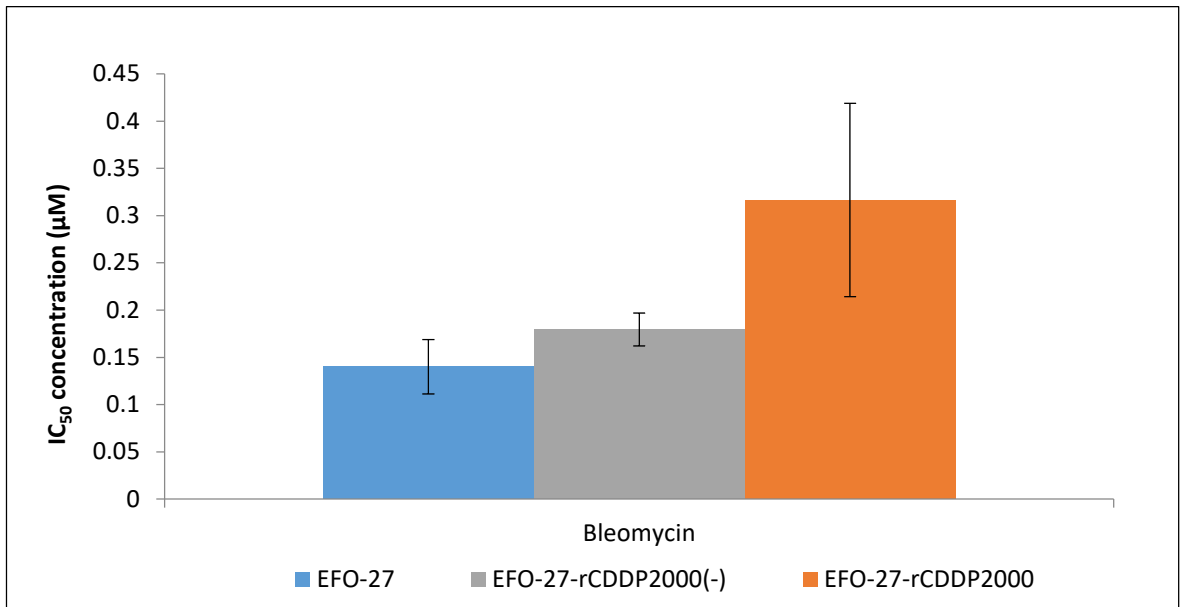
Figure 39: (A) IC$_{50}$ concentration of Bleomycin and (B) fold change (resistant to sensitive) for the EFO-27 cell lines. Each data expressed is expressed as a mean ± SD, n=3.
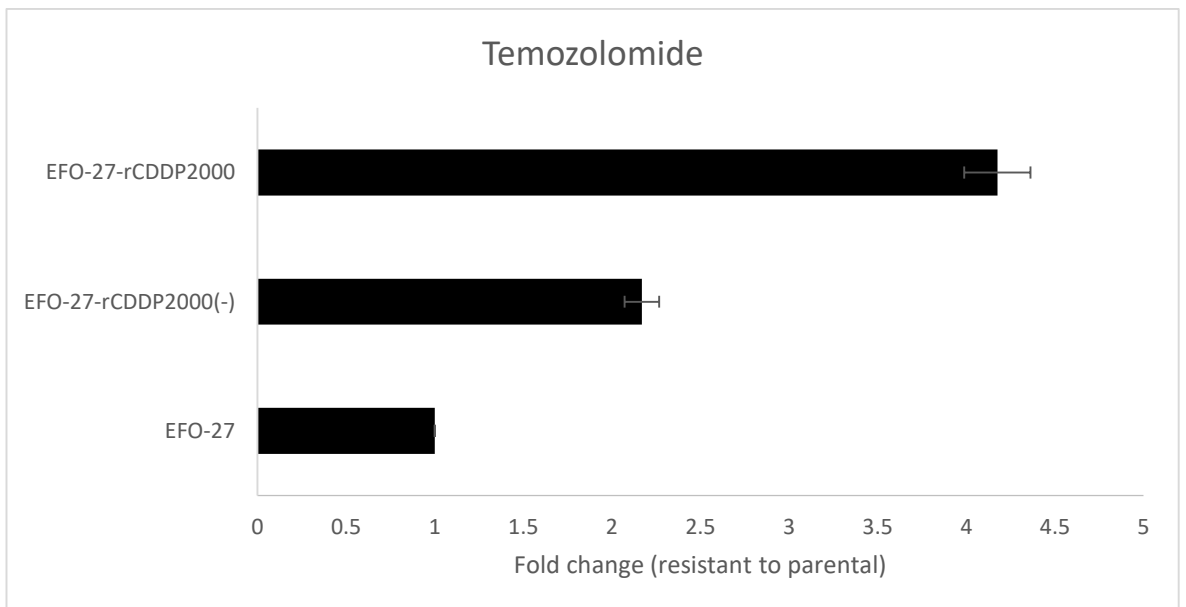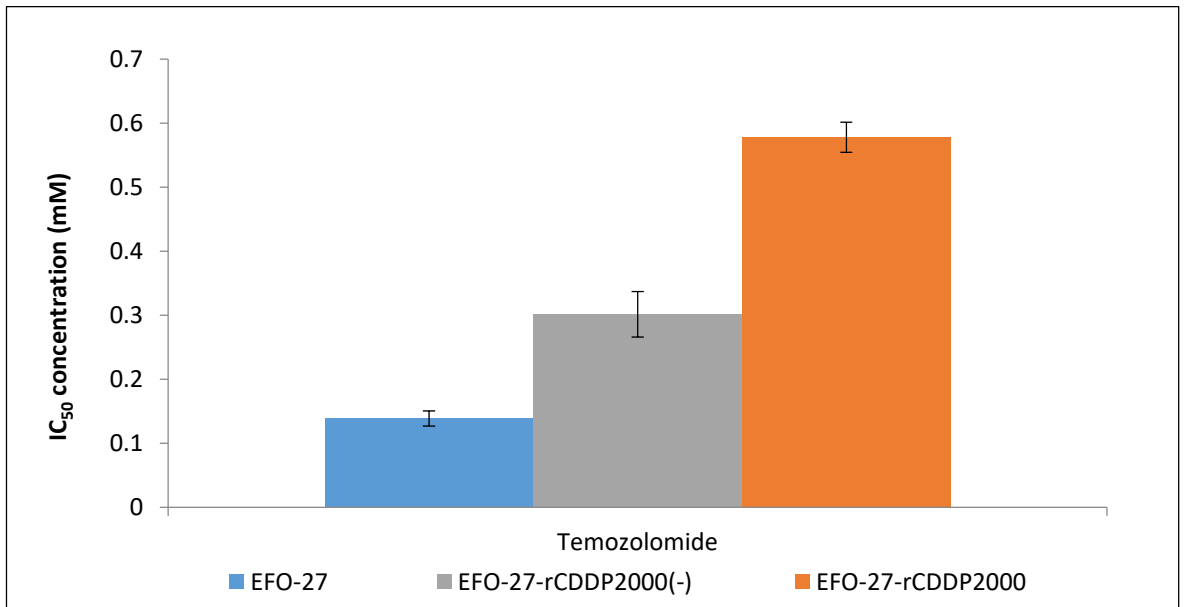
Figure 40: (A) IC$_{50}$ concentration of Temozolomide and (B) fold change (resistant to sensitive) for the EFO-27 cell lines. Each data expressed is expressed as a mean ± SD, n=3.
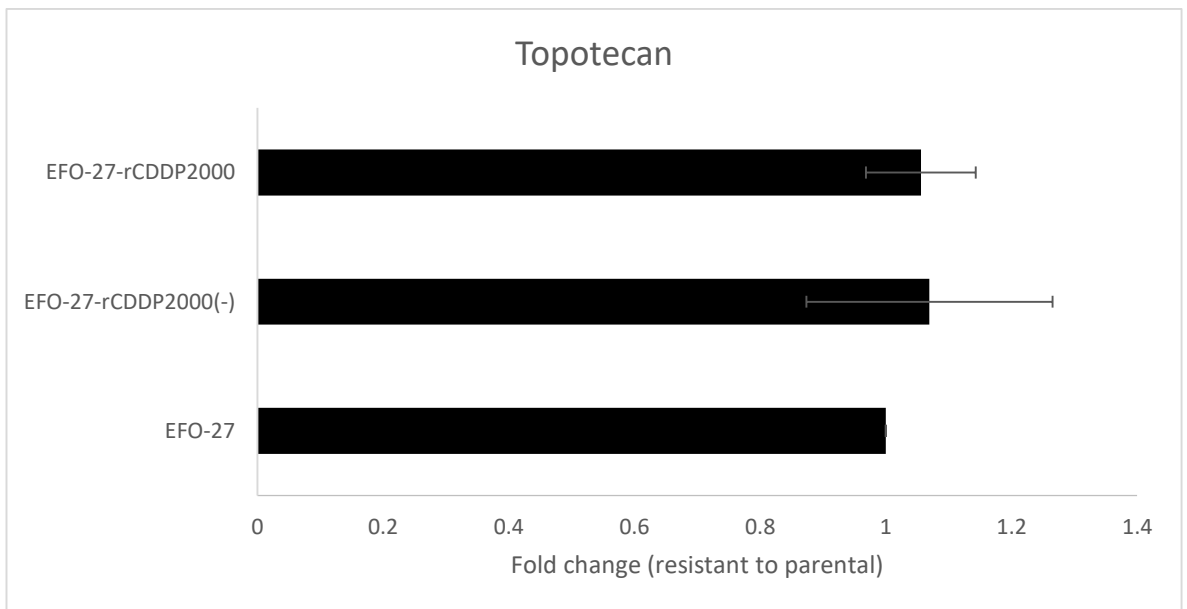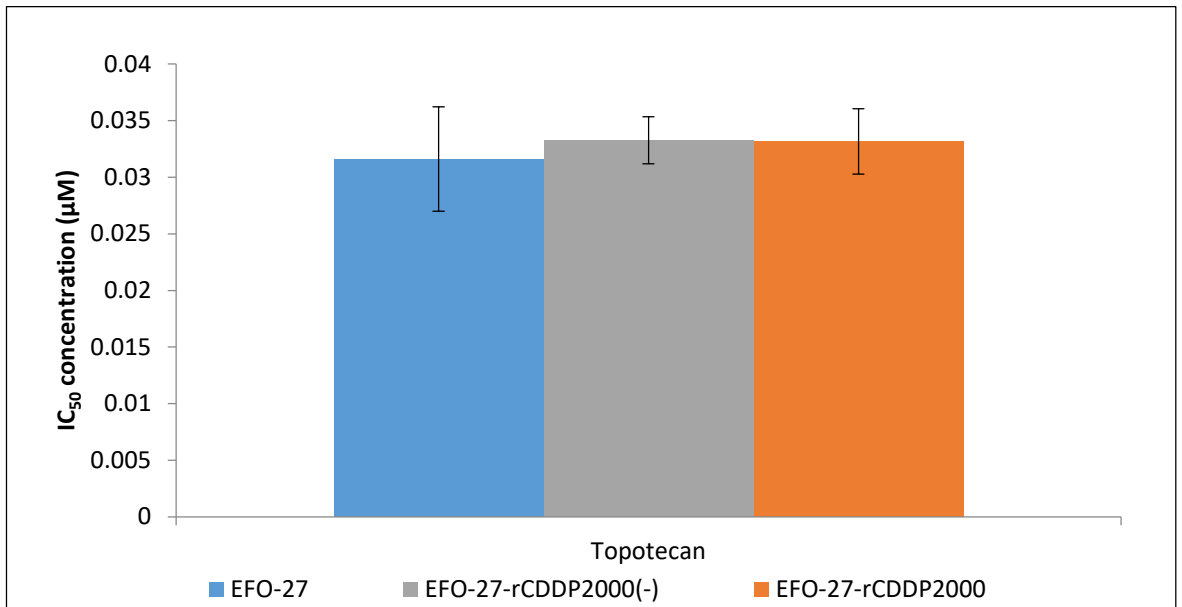
Figure 41: (A) IC$_{50}$ concentration of Topotecan and (B) fold change (resistant to sensitive) for the EFO-27 cell lines. Each data expressed is expressed as a mean ± SD, n=3.
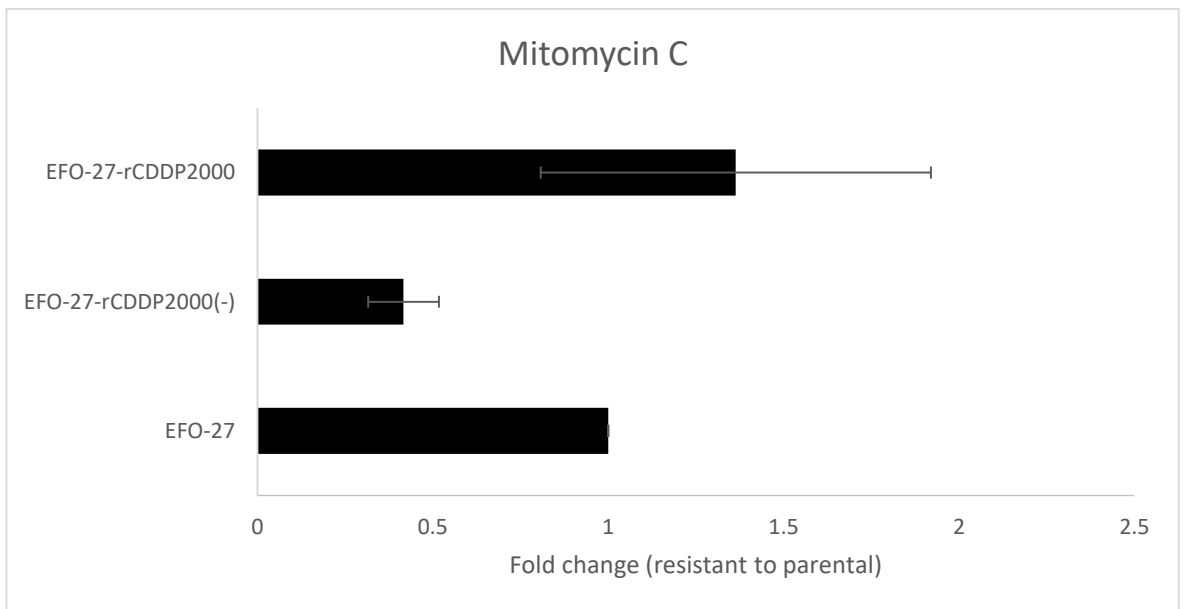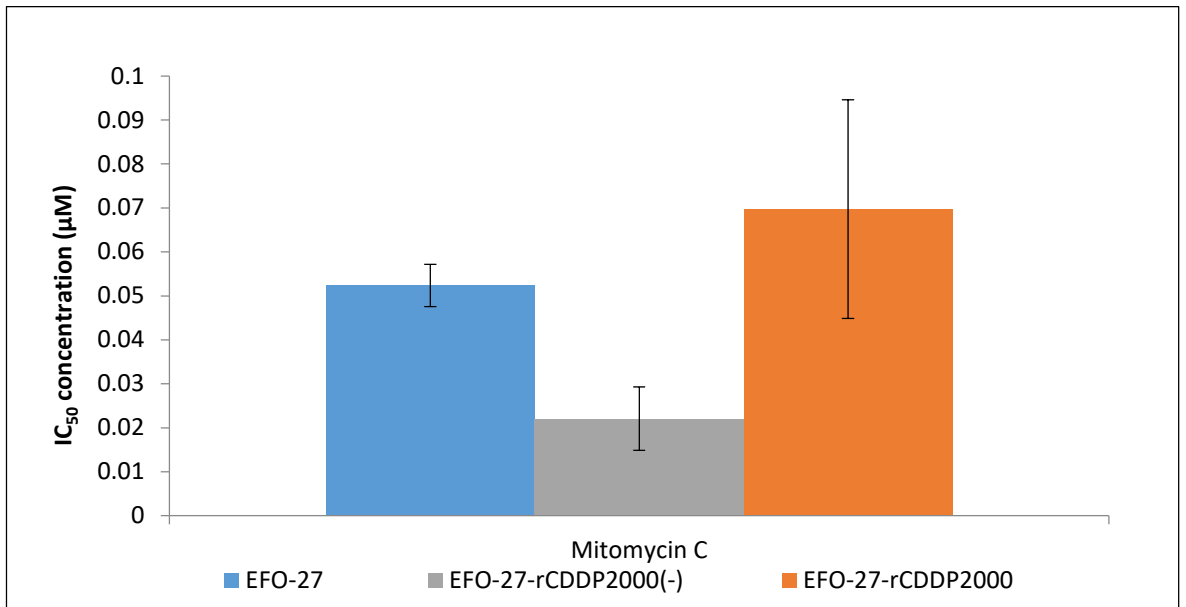
Figure 42: (A) IC$_{50}$ concentration of Mitomycin C and (B) fold change (resistant to sensitive) for the EFO-27 cell lines. Each data expressed is expressed as a mean ± SD, n=3.
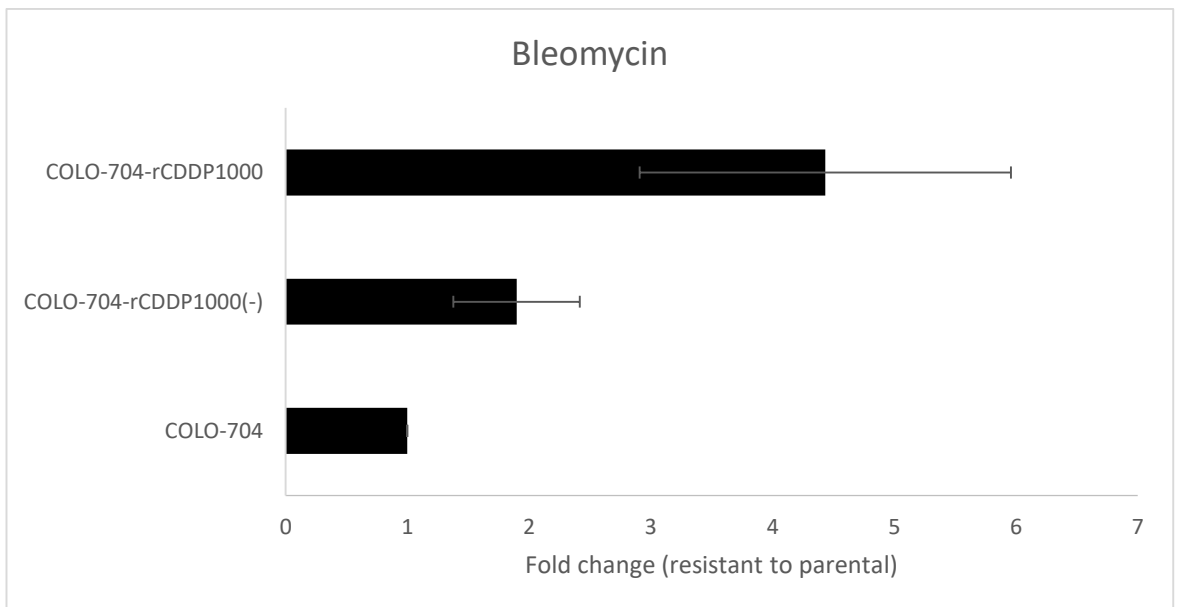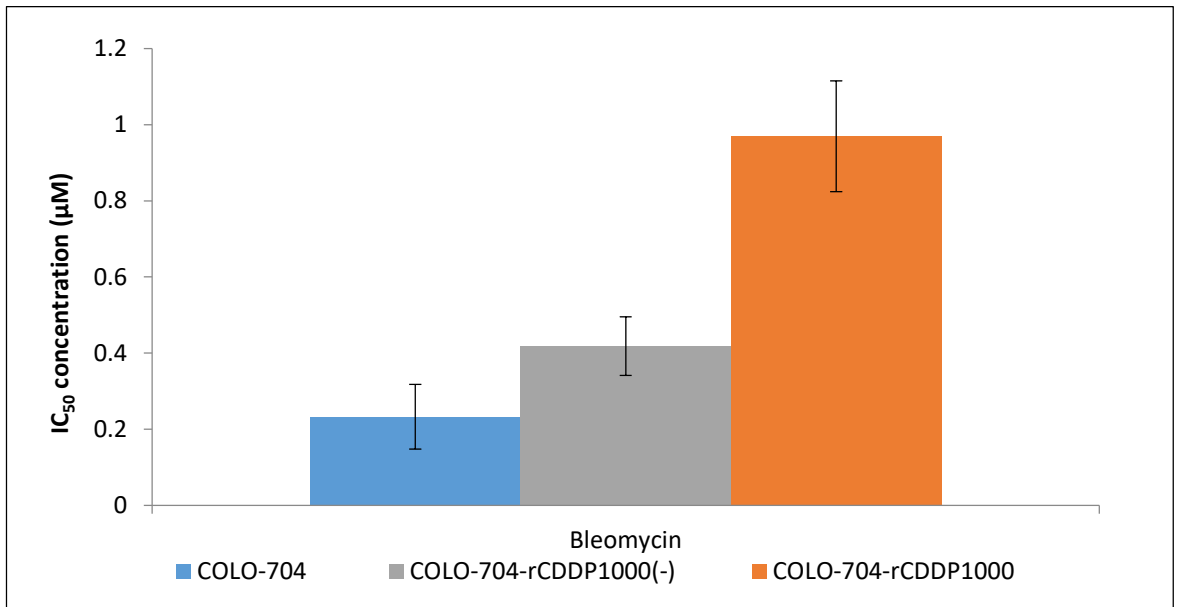
Figure 43: (A) IC$_{50}$ concentration of Bleomycin and (B) fold change (resistant to sensitive) for the COLO-704 cell lines. Each data expressed is expressed as a mean ± SD, n=3.
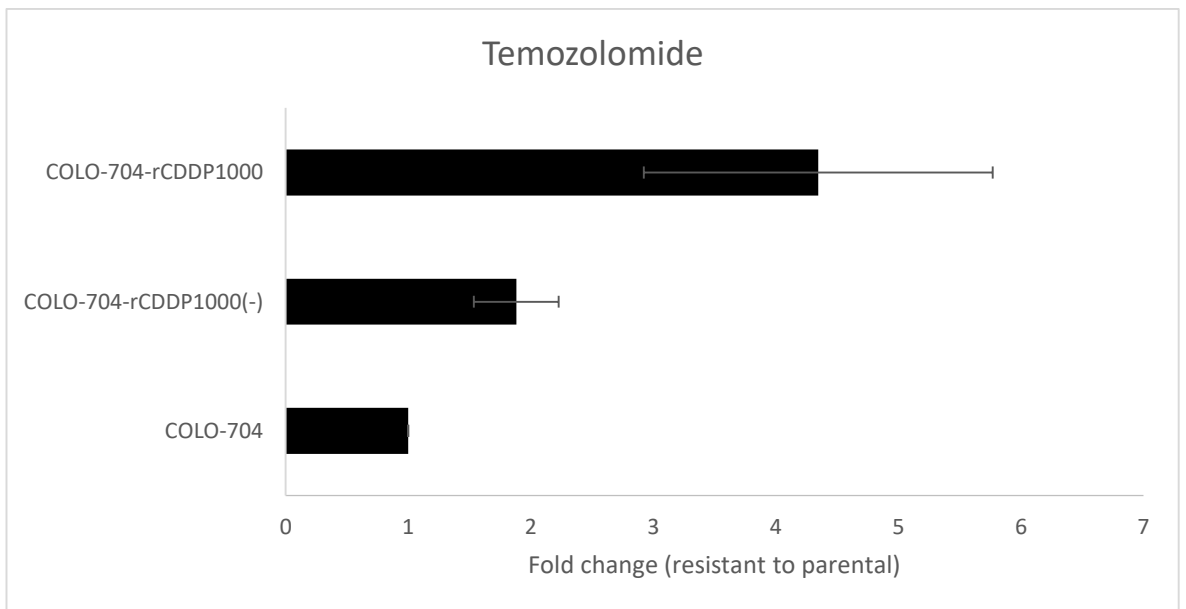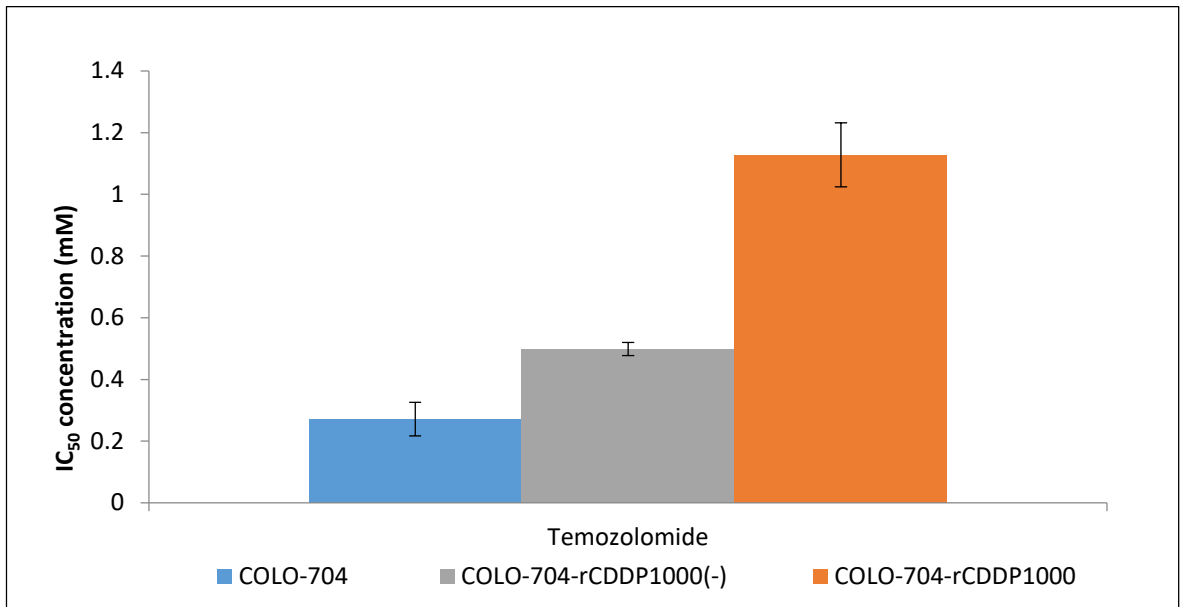
Figure 44: (A) IC$_{50}$ concentration of Temozolomide and (B) fold change (resistant to sensitive) for the COLO-704 cell lines. Each data expressed is expressed as a mean ± SD, n=3.
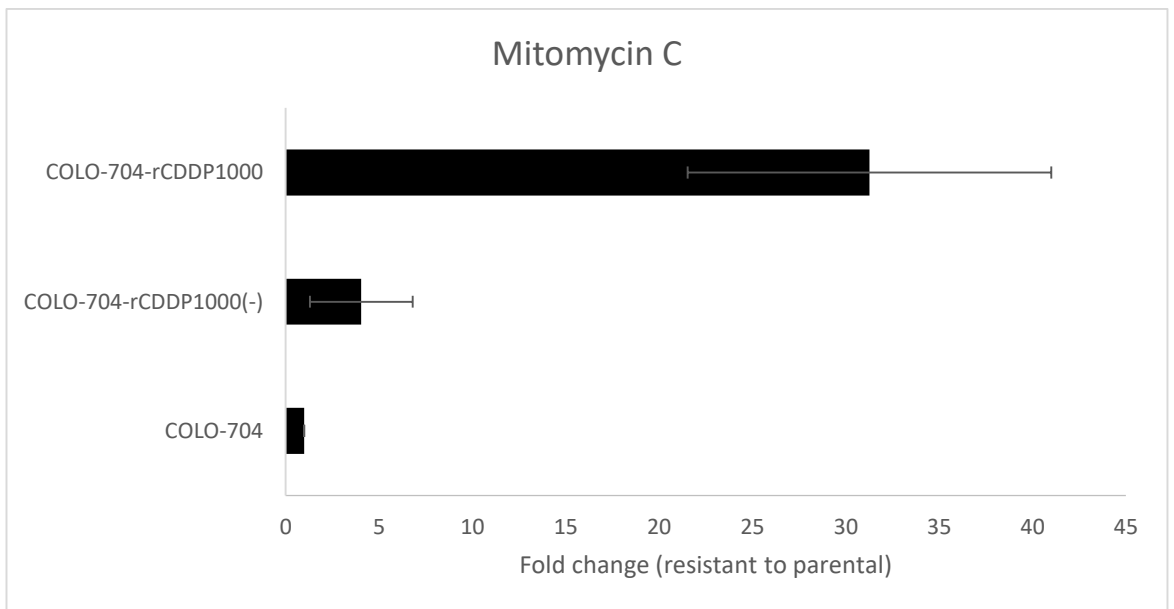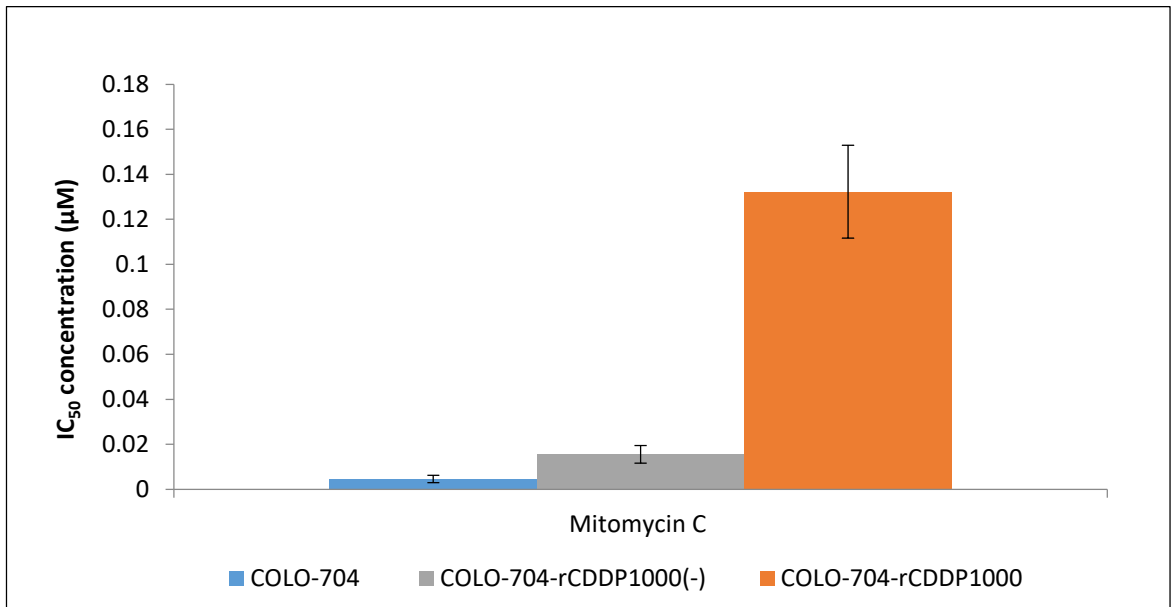
Figure 45: (A) IC$_{50}$ concentration of Mitomycin C and (B) fold change (resistant to sensitive) for the COLO-704 cell lines. Each data expressed is expressed as a mean ± SD, n=3.
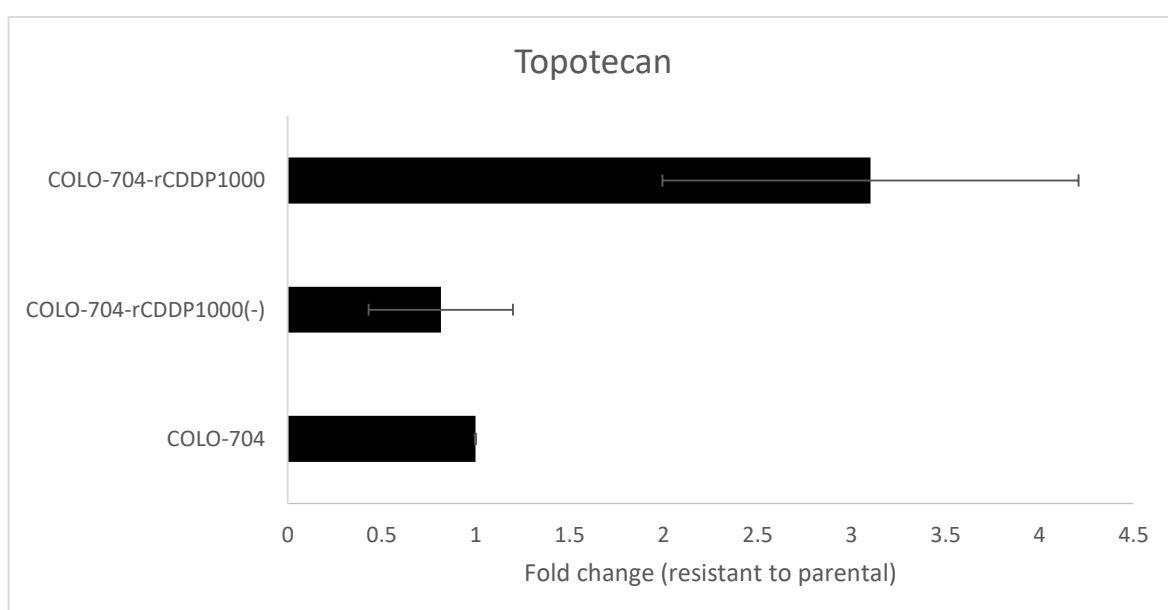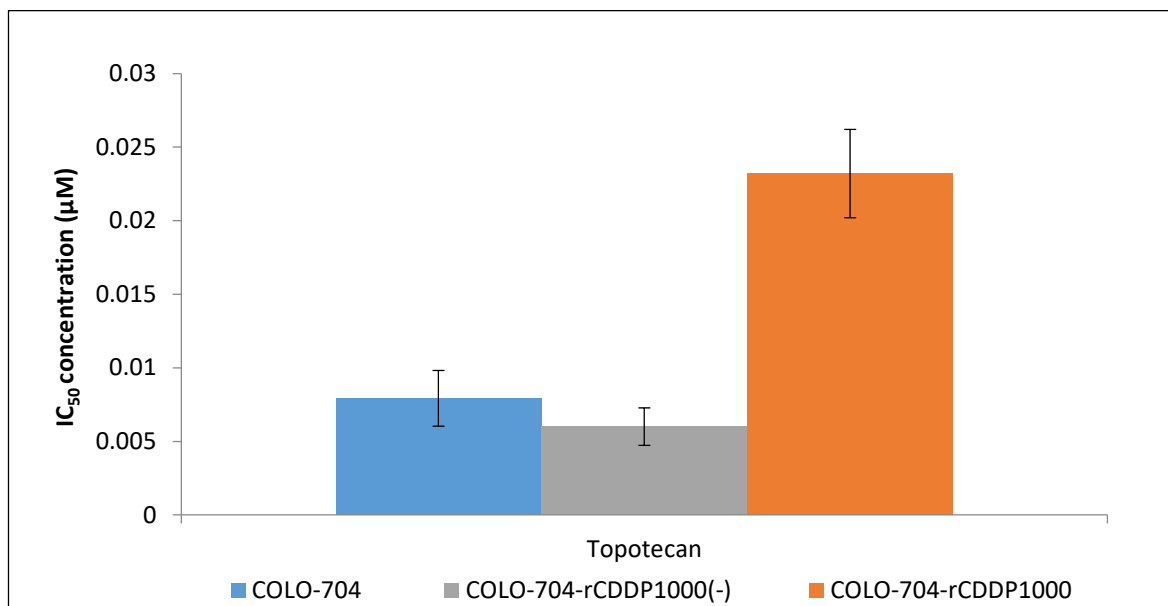
Figure 46: (A) IC$_{50}$ concentration of Topotecan and (B) fold change (resistant to sensitive) for the COLO-704 cell lines. Each data expressed is expressed as a mean ± SD, n=3.

The results are summarised in a heatmap (Figure 47). A >2-fold increase in the drug IC$_{50}$ was defined as increased resistance. A >2-fold decrease in the drug IC$_{50}$ was defined as increased sensitivity. A number of cisplatin-adapted sublines displayed increased resistance to different anti-cancer drugs. None of the cisplatin-adapted sub-lines displayed increased sensitivity to any of the investigated drugs. Typically, the cross-resistance resistance phenotype was similar or more pronounced in the cisplatin-adapted sublines compared to the cisplatin-adapted sublines that had been continuously cultivated in the absence of drug. The only exception was the erlotinib cross-resistance in EFO-27^{r}CDDP^{2000} and EFO-27^{r}CDDP$^{2000(-)}$ cells, where EFO-27^{r}CDDP$^{2000(-)}$ cells displayed erlotinib cross-resistance, whereas EFO-27^{r}CDDP^{2000} cells were similar sensitive to erlotinib as parental EFO-27 cells. EFO-21^{r}CDDP$^{2000(-)}$ cells were more sensitive to etoposide than parental EFO-21 cells. EFO-

27^{r}CDDP$^{2000(-)}$ cells were more sensitive to etoposide, zeocin, and mitomycin C than parental EFO-27 cells. There was no consistent resistance pattern across all three cisplatin-adapted ovarian cancer cell lines apart from all three sublines displaying cross-resistance to bleomycin and telozolomide (Figure 35-44, heatmap)

5.2.5 Determination of cell sensitization to Ultraviolet C (UVC)-induced DNA damage

The effect of UVC on the cells' viability was analysed using cell viability MTT assays (Figure 48-50) after 18 months, when the sublines that had been cultivated in the absence of cisplatin, had lost their resistance phenotype and was maintained (EFO-27-rCDDP$^{2000(-)}$, COLO-704-rCDDP$^{1000(-)}$ and EFO-21-rCDDP$^{2000(-)}$).

Resistance was defined as a fold change >2. EFO-21-rCDDP$^{2000(-)}$ and EFO-27-rCDDP$^{2000(-)}$ showed increased sensitivity to UVC irradiation in comparison to the respective parental cell lines (Figure 47-48) when exposed to the higher doses between 32 J/m^2-8 J/m^2. EFO-21-rCDDP^{2000} and EFO-27-rCDDP^{2000} cells displayed similar UVC irradiation sensitivity as the respective parental cell lines (Figure 47-48). UVC irradiation at the highest dose of 32 J/m^2 did not affect the viability of COLO-704 and COLO-704-rCDDP$^{1000(-)}$. However, only COLO-704-rCDDP^{1000} cells showed a reduced viability (66% relative to COLO-704) (Figure 50). Results at each dose showed no statistical significance for EFO-21 and EFO-27 cell lines in comparison to their respective resistant sublines (p=≥0.05) except for COLO-704 cell line and the respective resistant sublines at the highest dose of 32 J/m^2 (p= ≤0.01).

A

Cell lines	Drugs							
	Erlotinib	Crizotinib	Topotecan	Etoposide	Zeocin	Bleomycin	Temozolomide	Mitomycin C
EFO-21-rCDDP$^{2000(-)}$								
EFO-21-rCDDP^{2000}								
EFO-27-rCDDP$^{2000(-)}$								
EFO-27-rCDDP^{2000}								
COLO-704-rCDDP$^{1000(-)}$								
COLO-704-rCDDP^{1000}								

- more sensitive than parental cell line
- similarly sensitive as parental cell line
- more resistant than parental cell line

B

Cell lines	Drugs							
	Erlotinib	Crizotinib	Topotecan	Etoposide	Zeocin	Bleomycin	Temozolomide	Mitomycin C
EFO-21-rCDDP$^{2000(-)}$								
EFO-27-rCDDP$^{2000(-)}$								
COLO-704-rCDDP$^{1000(-)}$								

- more sensitive than cisplatin-adapted cell line
- similarly sensitive as parental cell line
- more resistant than parental cell line

Figure 47: Heatmap of cross-resistance profiles of the ovarian cancer cell lines. **Heatmap image of comparative drug-resistance to the different anti-cancer drugs of the parental cell lines and their respective cisplatin-adapted sublines cultivated in the presence and absence of drug. A) The comparison of each subline against the parental level of resistance B) The comparison of the cisplatin-adapted sublines cultivated in the absence of drug in comparison to the cisplatin-adapted cell line cultivated in the presence of drug and the parental cell line**
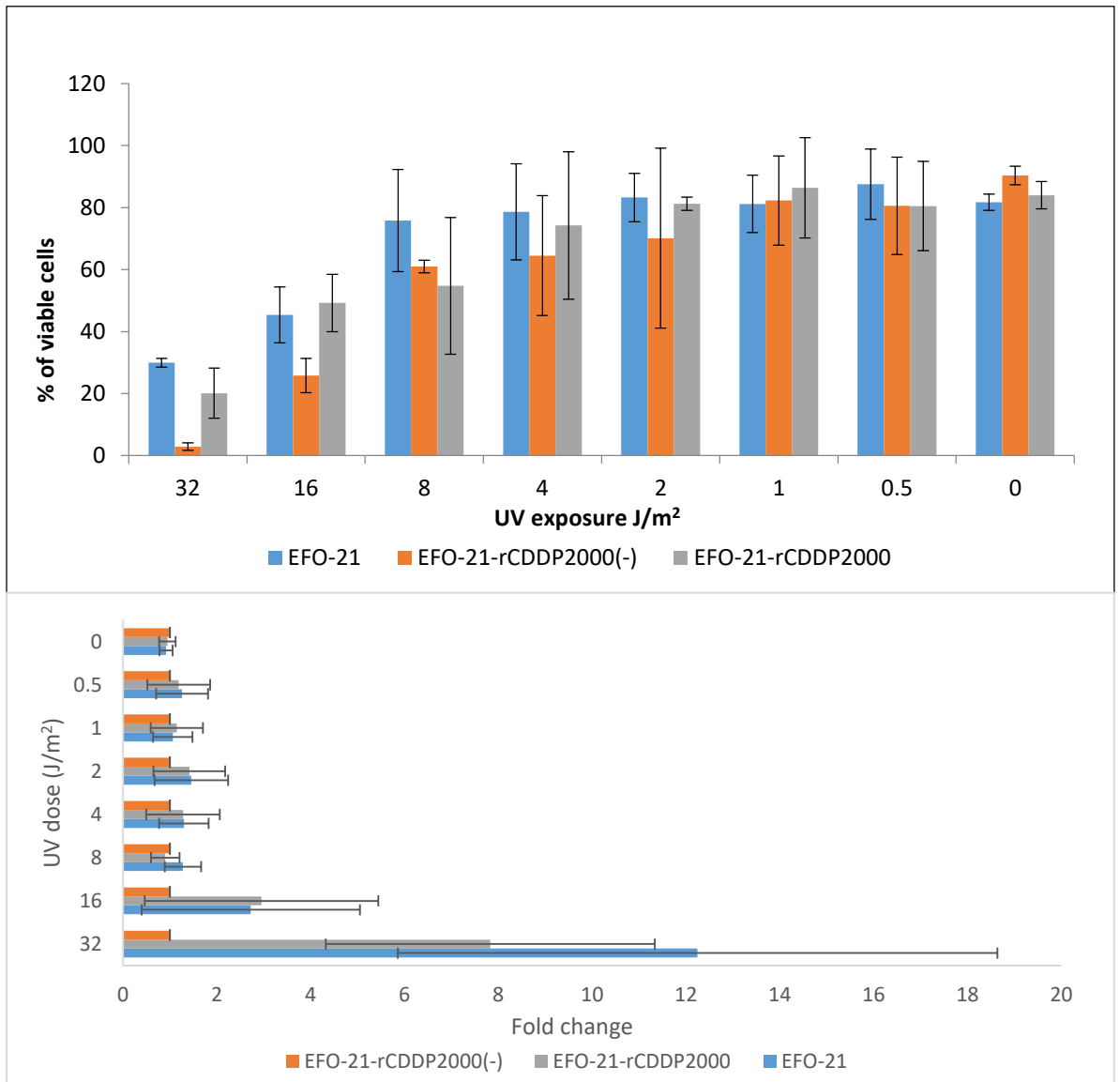
Figure 48: (A) cell viability percentage of EFO-21 cell lines exposed to different doses of UVC and (B) Fold change relative to CDDP(-) which showed greater levels of sensitivity. Each data is expressed as a mean (n=4 ± SD). Statisical significance: 32 J/m^2 -0 J/m^2 p=≥0.05).
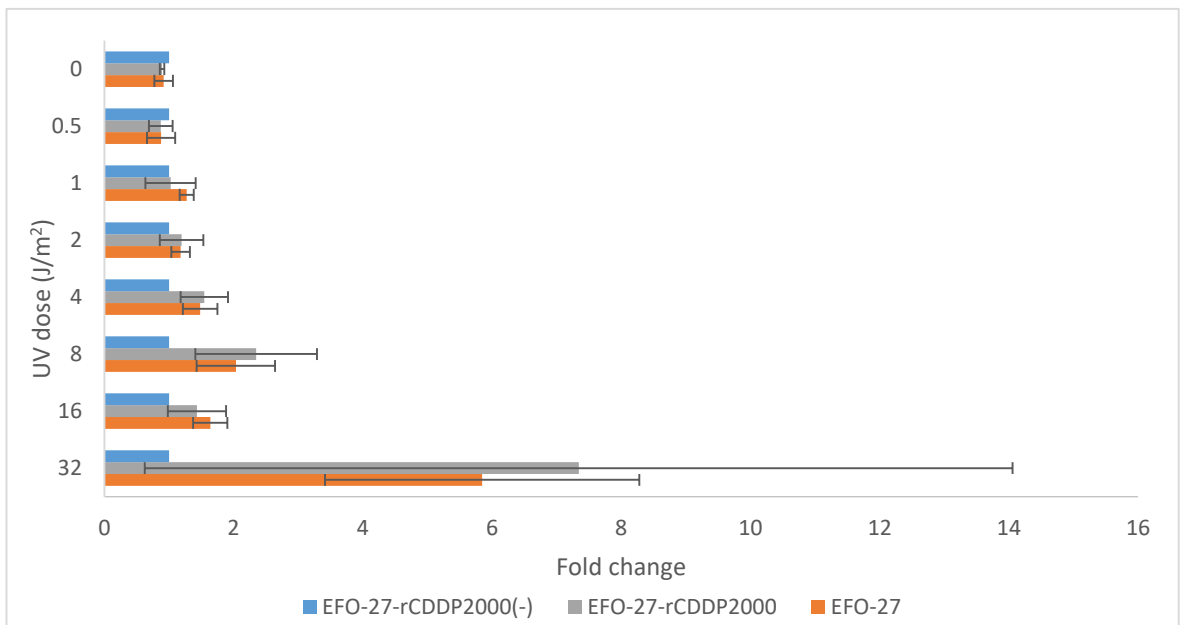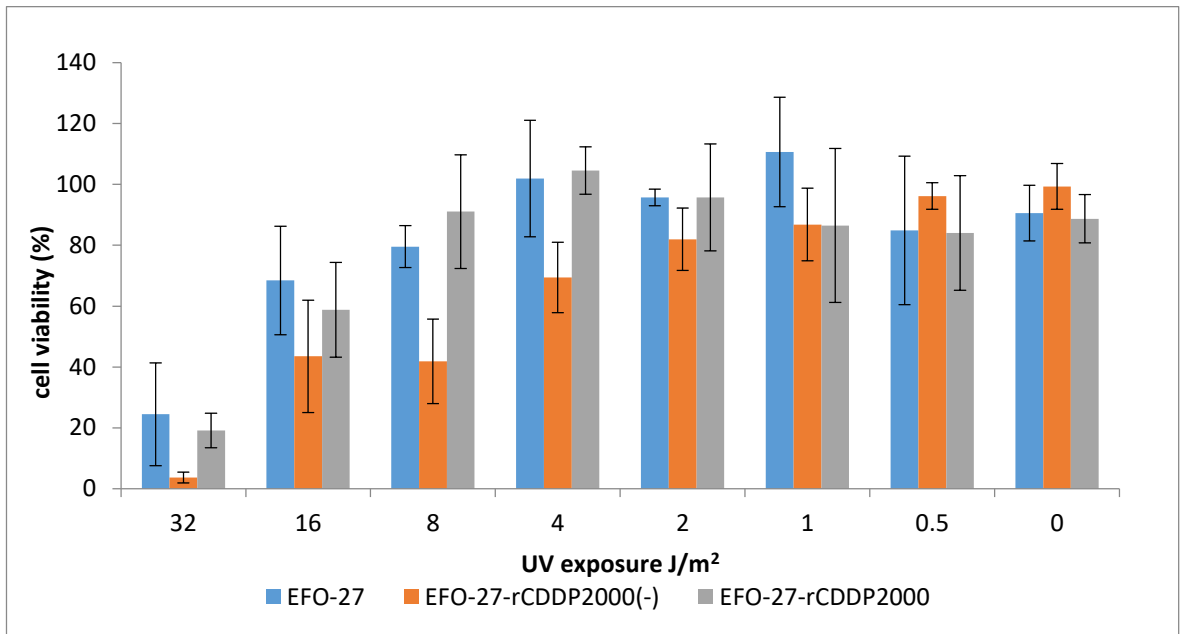
Figure 49: (A) cell viability percentage of EFO-27 cell lines exposed to different doses of UVC and (B) Fold change relative to CDDP(-) which showed greater levels of sensitivity. Each data is expressed as a mean ± SD, n=4. Statisical significance: 32 J/m^2 -0 J/m^2 p=≥0.05).
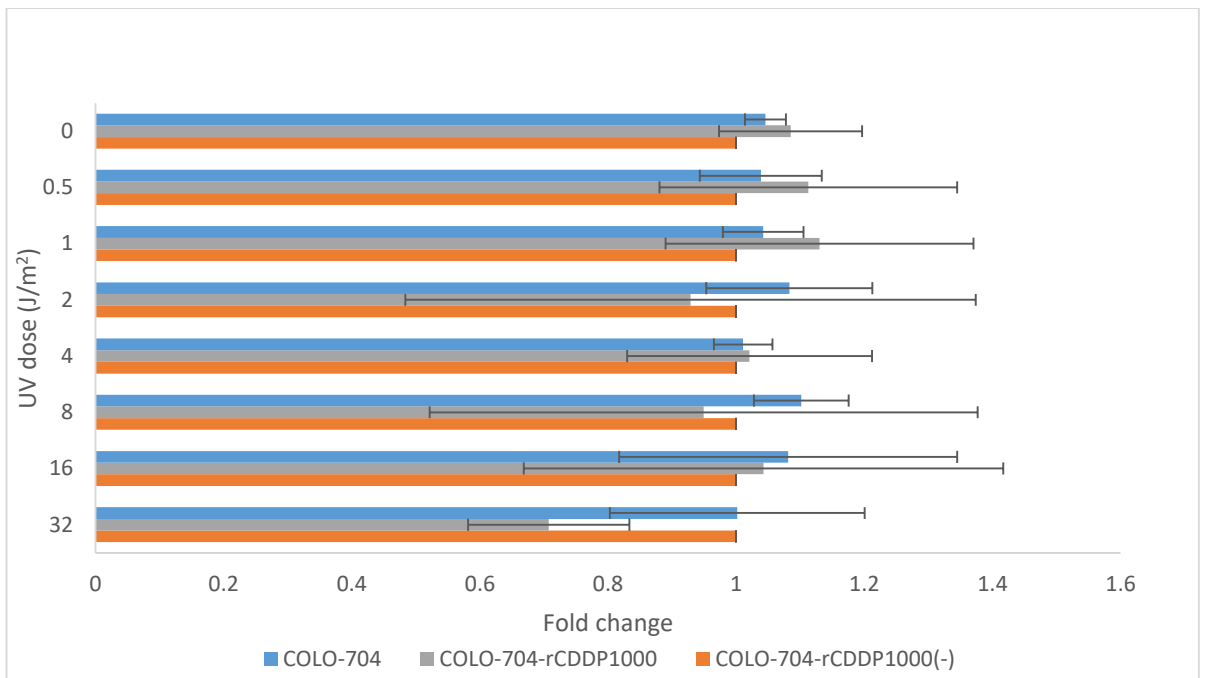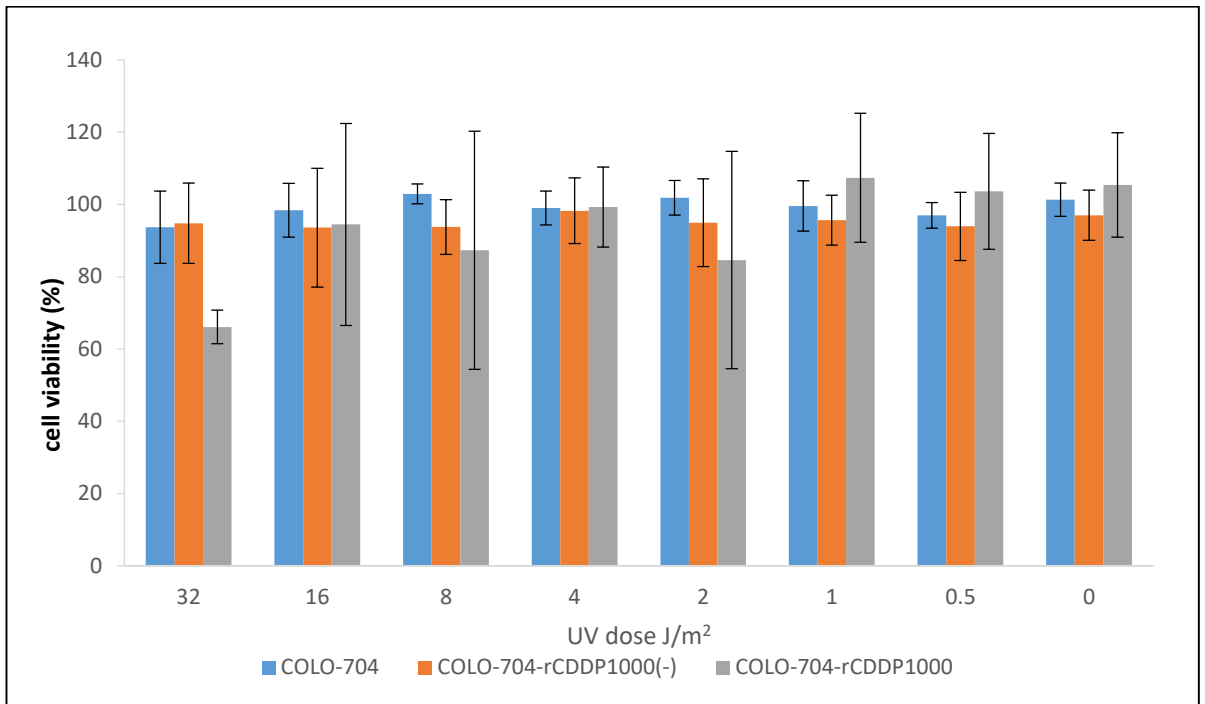
Figure 50: (A) cell viability percentage of COLO-704 cell lines exposed to different doses of UVC and (B) Fold change relative to CDDP(-) which showed greater levels of sensitivity. Each data is expressed as a mean ± SD, n=4. Statisical significance: 32 J/m² p=≤0.05; 16 J/m² -0 J/m² p=≥0.05).

5.2.6 Measurement of adherent cell survival using colony formation assay

The colony formation assay as used as a long term assay to identify the proliferative potential (cell death or loss of function) of cells which is not always identified using cell viability assays. It indicates the population of cells which may be determined dead by trypan blue staining during the counting of cells for a cell viability assay but still has the ability to proliferate.

EFO-21-rCDDP^{2000} and EFO-21-rCDDP$^{2000(-)}$ cells displayed similar colony formation capacity as EFO-21 (p=≤0.05) as shown in Figure 51a. In contrast, EFO-27-rCDDP^{2000} and EFO-27-rCDDP$^{2000(-)}$ showed a significant reduction in the colony formation capacity compared to EFO-27 (p=≤0.05) as shown as figure 51b. Cisplatin treatment confirmed the cisplatin sensitivity/ resistance status of the investigated cell lines with their respective sublines. The results confirmed that cisplatin can be used as a sensitizer with lose dose irradiation for resistant cells as shown for EFO-21-rCDDP^{2000} (figure 51a). However, a difference was identified in the EFO-27 cell line and its respective cisplatin resistant sublines. Notably, the investigated cell lines showed more complex UVC irradiation sensitivity patterns in the colony formation patterns in comparison to the cell viability assay (Figure 52-57). Hence further research is required to come to a definitive conclusion on the UVC irradiation sensitivity of the cell lines.
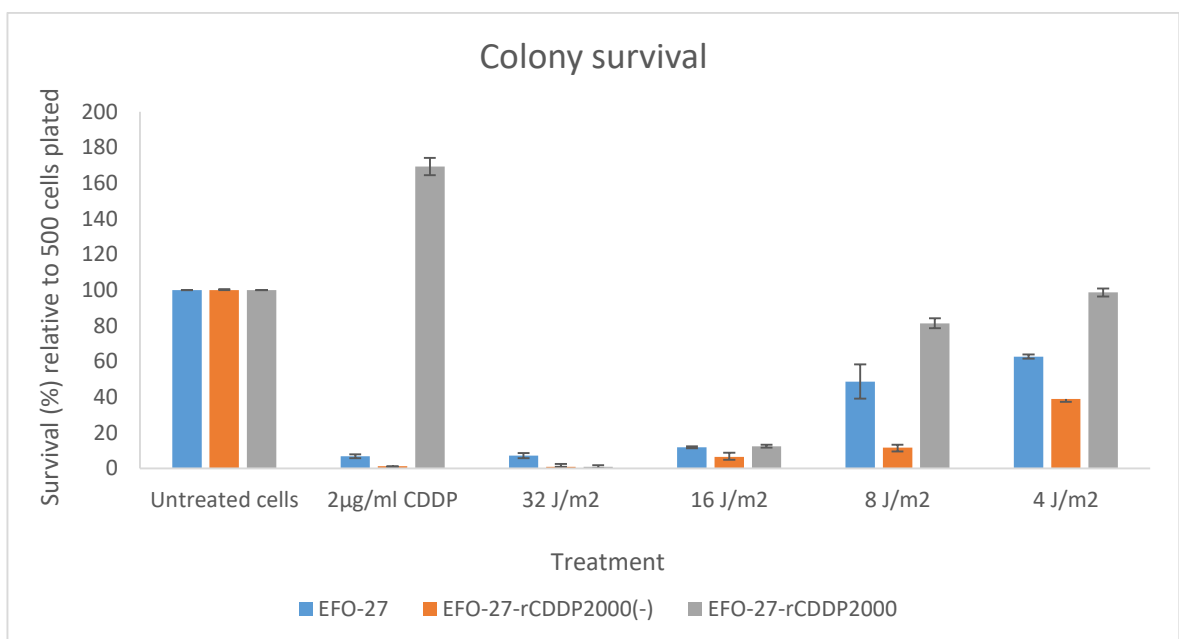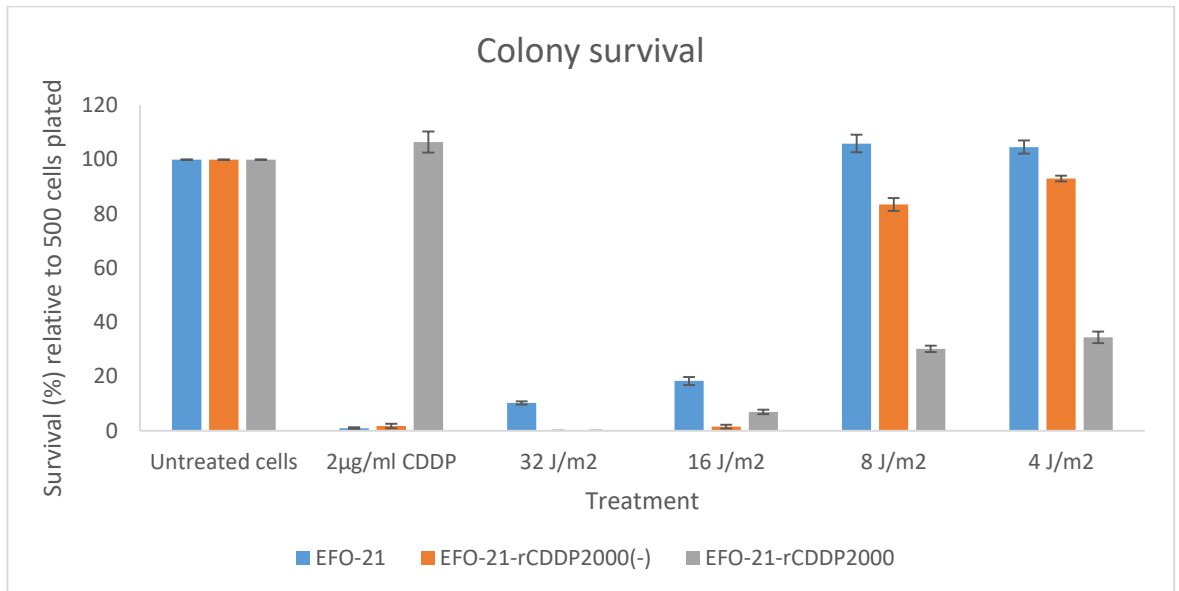
Figure 51: **Number of colonies formed with different treatment conditions in colony formation assay for (a) EFO-21 and (b) EFO-27 cell lines with their respecitive sub-lines.** The total number of colonies quantified indicated reduced ability in treatment conditions 2 μg/ml, 32 and 16 J/m^2. All values are mean ± SD, n=3. Statistical significance for EFO-21 and the respective sublines; Untreated cells p=≤0.05, 2 μg/ml CDDP P= p=≤0.05, 32-4 J/m^2 p=≤0.05.   Statistical significance for EFO-27 and the respective sublines; Untreated cells p=≤0.05, 2 μg/ml CDDP P= p=≤0.05, 32-4 J/m^2 p=≤0.05.
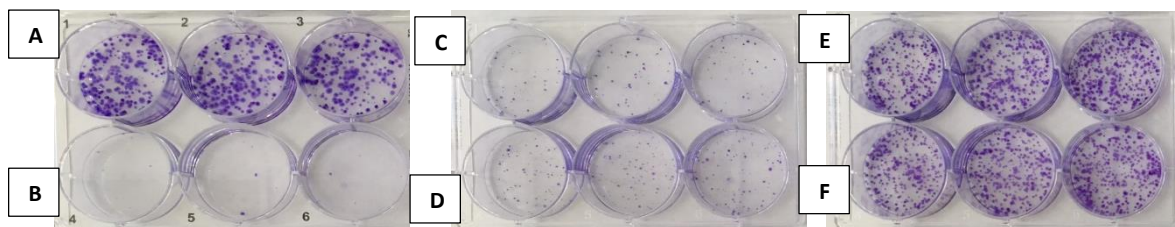
Figure 52: **Colony formation assay.** Images of EFO-21 cells stained with crystal violet to demonstrate the visual differences in colony formation with treatment conditions; (a) untreated, (b) 2 µg/ml of CDDP, (c) 32 J/m^2, (d) 16 J/m^2, (e) 8 J/m^2 and (f) 4 J/m^2.
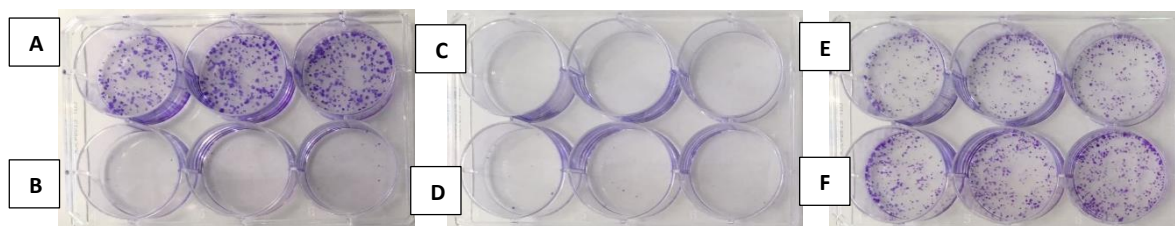
Figure 53: **Colony formation assay.** Images of EFO-21-rCDDP^{2000} cells stained with crystal violet to demonstrate the visual differences in colony formation with treatment conditions; (a) untreated, (b) 2 µg/ml of CDDP, (c) 32 J/m^2, (d) 16 J/m^2, (e) 8 J/m^2 and (f) 4 J/m^2.
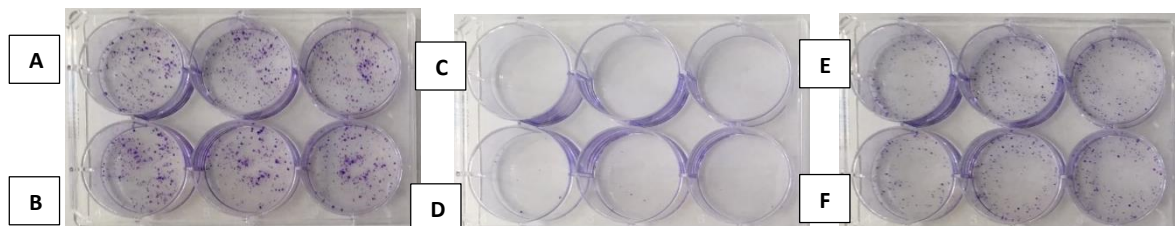
Figure 54: Colony formation assay. Images of EFO-21-rCDDP$^{2000(-)}$ cells stained with crystal violet to demonstrate the visual differences in colony formation with treatment conditions; (a) untreated, (b) 2 µg/ml of CDDP, (c) 32 J/m^2, (d) 16 J/m^2, (e) 8 J/m^2 and (f) 4 J/m^2.
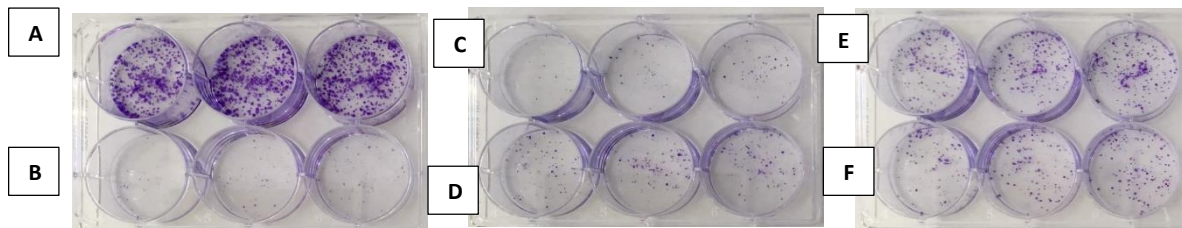
Figure 55: **Colony formation assay**. Images of EFO-27 cells stained with crystal violet to demonstrate the visual differences in colony formation with treatment conditions; (a) untreated, (b) 2 µg/ml of CDDP, (c) 32 J/m^2, (d) 16 J/m^2, (e) 8 J/m^2 and (f) 4 J/m^2.
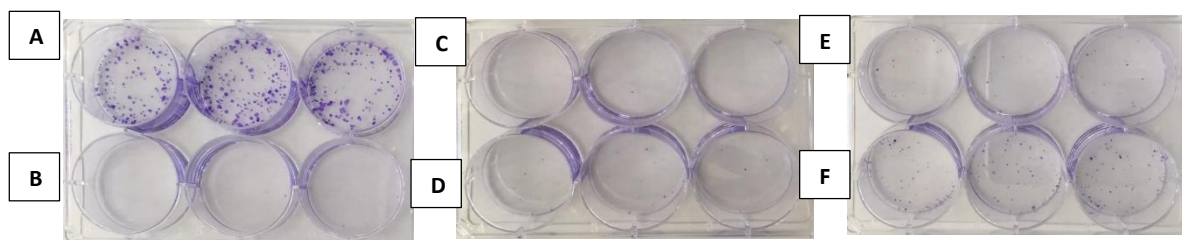
Figure 56: **Colony formation assay.** Images of EFO-27-rCDDP$^{2000(-)}$ cells stained with crystal violet to demonstrate the visual differences in colony formation with treatment conditions; (a) untreated, (b) 2 µg/ml of CDDP, (c) 32 J/m^2, (d) 16 J/m^2, (e) 8 J/m^2 and (f) 4 J/m^2.
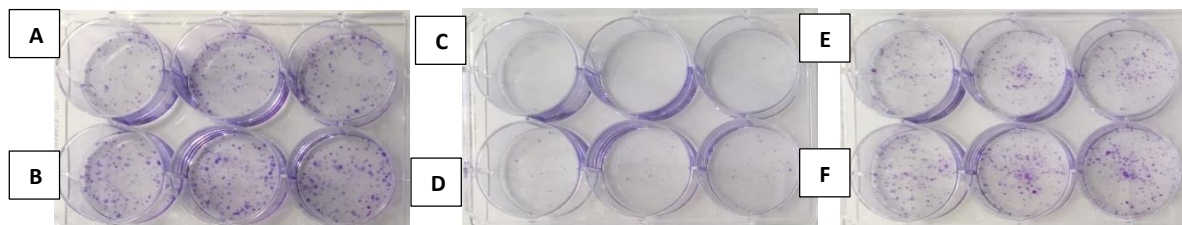
Figure 57: **Colony formation assay.** Images of EFO-27-rCDDP^{2000} cells stained with crystal violet to demonstrate the visual differences in colony formation with treatment conditions; (a) untreated, (b) 2 µg/ml of CDDP, (c) 32 J/m^2, (d) 16 J/m^2, (e) 8 J/m^2 and (f) 4 J/m^2

5.3 Discussion

5.3.1 morphological changes

The adaptation of EFO-21 and EFO-27 sublines adapted to cisplatin displayed no differences in the morphology compared to the sublines cultivated in the absence of drug; the morphology was maintained despite the release of drug. This is in agreement with other studies that indicated that the adaptation of cancer cell lines to anti-cancer drugs is associated with morphological changes (Domura et al., 2017), (Pasqualato et al., 2012); (Kotchetkov et al., 2005).

5.3.2 cell doubling times

The similarities observed in the morphology was reflected in the doubling times where the parental cell lines, EFO-21 and the respective sublines (p=0.35) and EFO-27 and the respective sublines (p=0.649) showed no statistical significance. However, changes were indicated in COLO-704^{r}CDDP^{1000} cells where adaptation to cisplatin had resulted in a significant increase in the cell doubling time compared to COLO-704^{r}CDDP$^{1000(-)}$ and COLO-704 (p=0.04). In a previous study, it had been shown that resistance formation to cisplatin can be associated with an increased doubling time (Prabhakaran et al., 2013).

5.3.3 resistant phenotype over time

All three cisplatin-adapted ovarian cancer cell lines partially or completely lost their cisplatin resistance phenotype in the absence of cisplatin relatively quickly. The reversible enrichment of a drug-resistant subpopulations has been described as resistance mechanisms to drugs including cisplatin. Cell lines rapidly acquired resistance to drugs and returned to the original phenotype after the removal of drug (Levina et al., 2008). However, EFO-21^{r}CDDP$^{2000(-)}$, EFO-27^{r}CDDP$^{2000(-)}$, and COLO-704^{r}CDDP$^{1000(-)}$ cells differed in their drug resistance profiles from the respective parental cell lines. This suggests that cisplatin adaptation is associated with adaptation processes that changes cellular properties and not the sole consequence of the enrichment of pre-existing cell fractions.

5.3.4 cross-resistance phenotype to platinum based drugs

All three cisplatin-adapted ovarian cancer cell lines displayed statistically significant cross-resistance to carboplatin (p=≤0.05). EFO-21^{r}CDDP^{2000} and EFO-27^{r}CDDP^{2000} also displayed statistically significant cross-resistance to oxaliplatin (p=≤0.05). In contrast, the resistant subline COLO-704^{r}CDDP^{1000} were more sensitive to oxaliplatin than parental COLO-704 cells (p=≤0.05). This is in agreement with the perception that cisplatin and carboplatin are more closely related to each other in their mechanisms of action than to oxaliplatin but oxaliplatin should not be considered broaded active in all cisplatin-resistant cancers despite its favourable increased toxicity (Stordal., et al 2007); (Montagnani et al., 2011).

The level of cross-resistance identified in cisplatin-resistant cells to carboplatin can be explained as a result of their structural similarities as described in chapter 2.3.1. Oxaliplatin as a single agent

demonstrates minimal cross-resistance, but not complete sensitivity in all cisplatin-resistant cancers, indicating the difference in the mechanism of action (Stordal et al., 2005); (Matsuo et al., 2010). Cisplatin resistance occurs via acquired resistance in most ovarian cancer cases (Eckstein 2011). When placed in a low concentration of chloride ions, cisplatin binds to mitochondrial and nuclear DNA causing intra- and inter-strand breaks in the DNA molecule, due to the replacement of water molecules with the *cis* chlorine groups (Galluzzi et al., 2014). Many studies have validated that cisplatin uses the high-affinity copper transporter 1 (Ctr1), copper transporter 2 (Ctr2) and the P-type copper-transporting ATPases, ATP7A and ATP7B for the transportation of drug across the cancer cell membrane and that the resistance is a result of P-glycoprotein (MDR1) expression which causes reduced intracellular concentrations in the cell (Chen and Kuo 2013); (Borst et al., 2008). The expression of the two copper exporters ATP7A and ATP7B, have been detected in ovarian cancer patients and have been associated with lower survival rates (Tapia and Diaz-Padill 2013); (Rabik and Dolan 2007). Oxaliplatin resistance is caused by the over-expression of the ATP-binding cassette (ABC) drug transporter ABCG2 which differs from that of cisplatin and carboplatin (Hsu et al., 2018).

5.3.5 cross-resistance to other anti-cancer drugs

The determination of drug sensitivity profiles against selected kinase inhibitors and DNA damaging agents resulted in complex patterns. EGFR tyrosine kinase inhibitors including erlotinib had been suggested as therapy candidates for the treatment of cisplatin-resistant ovarian cancer but their value has not been confirmed in clinical trials yet (Murphy & Stordal, 2011); (Vergote et al., 2014). In contrast, erlotinib displayed a statistical significance in activity against cisplatin-adapted ovarian cancer cells relative to the respective parental cell lines (p=≤0.05). In addition, the MET and ALK inhibitor crizotinib did not display promising effects, although MET has been described to be a potential therapeutic target in ovarian cancer (Kim et al., 2016). There was no significant difference found in the levels of resistance between the parental and resistant sublines for COLO-704 and EFO-27 (P=≥0.05). On the other hand, the EFO-21 cell line showed significant sensitivity in comparison to the resistant sublines (p=≤0.05).

Cisplatin resistance was not generally associated with cross-resistance to other DNA damaging agents. All cisplatin-adapted ovarian cancer cell lines were similar or less sensitive to the investigated DNA damaging agents as the respective parental cell lines. The cisplatin-resistant sublines differed considerably in their drug sensitivity profiles. This suggests that they individually had developed differing (combinations of) cisplatin resistance mechanisms. These discrepancies may not be too surprising since cisplatin resistance mechanisms are known to be complex and multifactorial (Dilruba & Kalayda, 2016); (Damia & Broggini, 2019); (Amable, 2016). Consistent cross-resistance was only observed against temozolomide. Notably, high glutathione levels are known to be cisplatin resistance mechanism and were shown to mediate resistance to both cisplatin

and temozolomide (Amable, 2016); (Rocha, Kajitani, Quinet, Fortunato, & Menck, 2016); (Zhu et al., 2018). GSH is a highly abundant, low molecular weight peptide that maintains the cellular oxidative balance of cells, providing protection against toxic agents (Chen at al., 2008). The transporters recognised as responsible for drug efflux, require GSH for transportation of the substrate and may serve as a substrate for conjugation reaction with cisplatin before (multidrug resistance proteins) MRP-mediated transport (Kuo and Chen 2010); (Rabik and Dolan 2007). However, further research is needed to elucidate the underlying mechanisms of the temozolomide resistance observed in cisplatin-adapted ovarian cancer cell lines in more detail.

5.3.6 Ultraviolet C (UVC)-induced DNA damage

Varied responses were observed across the cell lines and their respective sublines. The effect of inducing DNA damage was determined using two methods; cell viability assay and colony formation assay. Results indicated differences in the ovarian cancer cell lines. At doses between 16-0 J/m^2 which were determined, no statistical significance in resistance/sensitivity was observed between the COLO-704 cell line and its respective sublines (p=≥0.05) and therefore the colony formation assay was not conducted; only COLO-704-rCDDP^{1000} displayed increased sensitivity to UVC at the highest dosage of 32 J/m^2 (p=≤0.05). Nevertheless, EFO-21 and EFO-21-rCDDP$^{2000(-)}$ showed significant sensitivity to UVC at higher doses in comparison to EFO-21-rCDDP^{2000}. In a previous study, it had been shown that low dose cisplatin with low dose UVC, had exerted synergistic effects in cancer cells by down regulating EGFR tyrosine kinase responsible for proliferation (Kawaguchi,et al., 2012).

In correlation, EFO-21-rCDDP^{2000}, cultivated in cisplatin, showed significant effects 8 J/m^2 and 4 J/m^2 (P=≤0.05) showing cisplatin sensitises cells to UVC at lower dosages. EFO-27-rCDDP$^{2000(-)}$ displayed an increased sensitivity to UVC dosages and cisplatin treatment in comparison to the parental and resistant subline cultivated in the presence of drug. This therefore indicates that there remains complexity in the understanding of resistance to ultraviolet C irradiation in ovarian cancer cells.

Taken together, we have introduced three novel cisplatin-adapted ovarian cancer cell lines. Cisplatin resistance was reversible upon cultivation of the cisplatin-resistant sublines in the absence of cisplatin. However, resistance did not seem to be caused by the reversible selection of a pre-existing resistant subpopulation. The cisplatin-resistant sublines displayed varying drug sensitivity profiles, which suggests differences in the individual resistance mechanisms.

6 Nanoparticles

6.1 Introduction

There has been a rapid increase in cancer incidence and mortality rates within the UK and the risk factors for cancer has resulted in the estimation of up to 18.1 million new cases and 9.6 million cancer deaths in 2018 (F. Bray et al., 2018).

Drug delivery systems such as nanoparticles, can be made of different materials. Doxorubicin, the anthracycline chemotherapeutic agent, may be absorbed onto the particle surface or through particle preparation, incorporated into the particle matrix and has demonstrated promising effects in reducing high cardiotoxicity and increasing the efficacy of antineoplastic drugs (Dreis et al., 2007); (McGowan et al., 2017).

Treatment failure due to drug resistance remains as the main cause of increased mortality rates of cancer patients. P-glycoprotein (P-gp) which belongs to the family of ATP-binding cassette (ABC) transporter proteins are known to contribute to drug resistance as they cause the chemotherapeutic agents to be effluxed resulting in reduced toxicity and increased drug metabolism (Leonard, 2003).

More specifically, characterisation of multidrug resistance (MDR) is the over-expression of transporters responsible for drug effluxion by ABCB1 (also known as P-glycoprotein (P-gp or MDR1) display has been acknowledged as the paramount cause of reduced sensitivity to anti-cancer drugs (Callaghan et al., 2014; Yuan et al., 2016).

The drug transporter, P-glycoprotein, part of the ABC protein superfamily, is encoded by ABCB1 known to mediate chemotherapeutic multidrug resistance. Tumour cells which express P-gp, have low concentrations of anti-cancer drugs that are transported by ABCB1 in comparison to tumour cells that do not express P-gp. As Doxorubicin and vincristine are both ABCB1 substrates, it is assumed that the resistance mechanism of UKF-NB-3[r]DOX[20] and UKF-NB-3[r]VCR[1], is as a result of P-gp expression (Mealey & Fidel, 2015).

As a result, target strategies such as drug-loaded nanoparticles have illustrated success in protecting and transporting the drug to the target cell by overruling defence mechanisms and side effects thus increasing the efficacy of the chemotherapeutic drug (Casals et al., 2017); (Park et al., 2016).

The use of liposomes as potential drug carrier systems has been effective in treatment for cancer due to its biocompatible and biodegradable property enabling the encapsulation of hydrophobic and hydrophilic compounds. Successes of the small sized spherical vesicles made from cholesterol and phospholipids, include doxorubicin (Doxil/Caelyx) monotherapy for HIV-associated Kaposi's sarcoma and ovarian cancer which work by increasing drug delivery to the tumour by reducing the

toxicity (Zabielska-Koczywąs & Lechowski, 2017). The most significant FDA-approved nanodrugs include loaded with doxorubicin or danuorubicin, include Doxil® and DaunoXome®(Li et al., 2016); (Rizvi & Saleh, 2018).

Albumin-bound paclitaxel (Abraxane; nab ®- Paclitaxel) has remained as a prosperous chemotherapy for the treatment of metastatic breast cancer (MBC), ovarian cancer and advanced non-small cell lung cancer (NSCLC) (Yardley, 2013). It has illustrated pharmacokinetic advantages over solvent-based taxanes due to its higher maximum concentrations (C_{max}) and increased volume distribution for faster clearance (Al-Batran et al 2014).

In addition, drug-loaded nanoparticles as well as liposomes enable the increase of drug concentration intake in the cancer cells by averting cytotoxic effects to the normal cells and are predominantly constructed on the "enhanced permeability and retention (EPR) effect via the accumulation in the tumour tissue more than normal tissues (figure 58). The successful mechanism of action involves the enveloped structure by endosomes through receptor-mediated endocytosis entering into the tumor cells circumventing the P-glycoprotein recognition site responsible for drug resistance (Xin et al., 2017);(Baetke et al., 2015); (Deshpande et al., 2013); (Baetke et al., 2015).

PEGylation coating of the nanoparticles surface with polyethylene glycol (PEG) has been successful in improving drug efficiency and delivery to target cells and tissues; it protects the surface from opsonisation, aggregation, pahgocytosis and increases the circulation time of the nanoparticles (Suk et al., 2016).
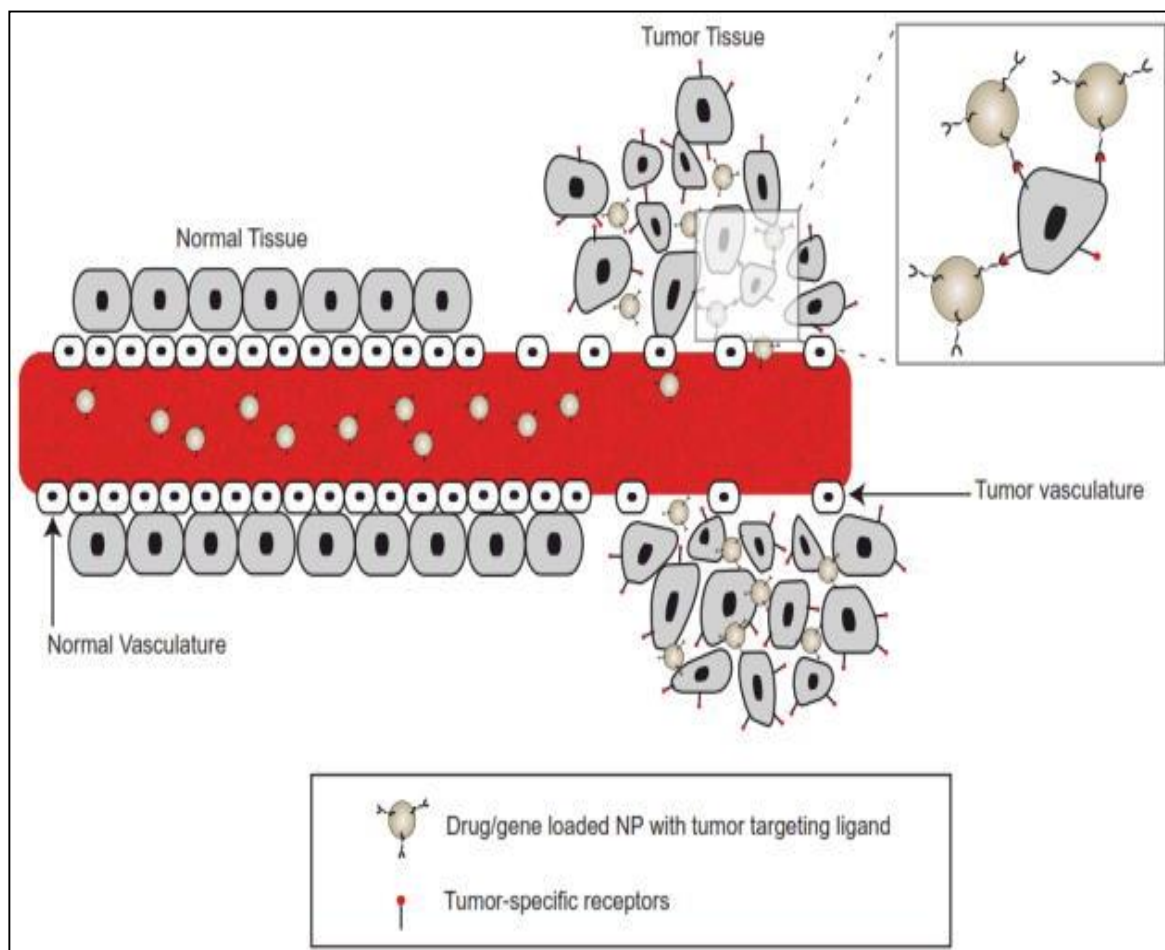
Figure 58: **Drug-loaded nanoparticles targeting tumour cells showing passive (EPR) effect and active targeting with tumour targeting ligands (Zhang & Marksaltzman, 2013).**

Nanoparticles can be prepared from a wide range of natural and synthetic polymers (Zhang & Marksaltzman, 2013). FDA- and EMA-approved Poly (D, L-lactic-co-glycolic acid) (PLGA), Poly-lactic acid (PLA) and human serum albumin (HSA) biodegradable and biocompatible polymers can be used to produce nanoparticles that display high drug encapsulation efficiency and modifiable drug release properties (Ansary. R, Awang. M, Rahman. M 2014); (Luz et al., 2017).

HSA nanoparticles may be internalised into cells through interaction with the glycoprotein60 (gp60) cell surface receptor originating on the surface of cancer cells without triggering an immune response (Lomis et al., 2016).

Here, we investigated different doxorubicin-loaded PLGA, PLA, and HSA preparations for their effects on ABCB1-expressing neuroblastoma cells.

6.2 Results

6.2.1 Nanoparticle characterisation

The nanoparticles tested were prepared and characterised by our collaborators in Germany. The optimisation preparation methods varied according to the type of preparation (solvent displacement (SD) and emulsion diffusion (ED)), type of polymer, particle size, polydispersity value, drug load and drug release of the nanoparticles as shown in summary in table 2 and appendix 1. PLA nanoparticles prepared by solvent displacement were selected based upon their smaller size and higher drug load efficiency. The IC$_{50}$ concentration of the nanoparticles were determined as described in chapter 3.4 using the cell viability assay experiment.

Nanoparticle	Type of polymer	Drug load (µg dox/mg np)	Diameter (nm)	Polydispersity
PLGA-PEG-NP-SD	*Poly(lactic-co-glycolic acid)-PEGylation*	4.1	72.6	<1
PLGA-PEG-NP-ED	*Poly(lactic-co-glycolic acid)-PEGylation*	3	>200	<1
PLGA-NPpH7	*Poly(lactic-co-glycolic acid)-PEGylation*	6.7	174.1	0.057
PLGA-NP	*Poly(lactic-co-glycolic acid)*	5.1	179.4	<1
PLA-NP	*Polylactic acid*	2.6	246.2	<1
Dox HSA (200%) NP	*Human Serum Albumin*	164.8	463.4	0.153
Dox HSA (100%) NP	*Human Serum Albumin*	190.5	496.4	0.213
Dox HSA (40%) NP	*Human Serum Albumin*	151.9	485.8	0.189
Dox HSA (0%) NP	*Human Serum Albumin*	370.9	848.7	0.500

Table 20: **Summary profiles of doxorubicin loaded nanoparticles.** PLA nanoparticles prepared by solvent displacement, PLGA nanoparticles prepared by solvent displacement at pH 7 and unmodified pH and PLGA-PEG nanoparticles prepared by emulsion diffusion and solvent displacement and HSA nanoparticles crosslinkined with glutaraldehyde at different percentages (0%, 40%, 100%, 200%). Statistical significance for all: p=≤0.05.

6.2.2. Polymer nanoparticle efficacy in cell culture

The neuroblastoma cell line UKF-NB-3, its doxorubicin-resistant sub-line UKF-NB-3[r]DOX[20], and its vincristine-resistant sub-line UKF-NB-3[r]VCR[1] were used to determine the effect of doxorubicin-loaded nanoparticles.

A reduced efficacy was shown in the three cell lines when tested against PLA nanoparticles, PLGA nanoparticles prepared by solvent displacement at uncontrolled pH and PLGA-PEG nanoparticles prepared by emulsion diffusion when compared to doxorubicin solution (Figure 59). However, PLGA nanoparticles prepared by solvent displacement at pH 7 and PLGA-PEG nanoparticles prepared by solvent displacement displayed similar activity like doxorubicin solution (Figure 59). The corresponding empty nanoparticles showed no effect on the cell viability in the tested concentrations.

The distinctive difference between the doxorubicin-loaded PLGA-PEG nanoparticles by solvent displacement preparation compared to others was the size which was smaller than 100 nm (72.6 ± 3.3 nm, appendix 1). Hence, smaller sized may display increased cellular uptake compared to larger sized nanoparticles. PLGA nanoparticles prepared by solvent displacement at pH 7 showed the highest drug load. Thus increased effectiveness may be the consequence of an increased drug transport per nanoparticle into the cells.

The parental UKF-NB-3 cell line does not display ABCB1 activity (Kotchetkov et al., 2005). Doxorubicin and vincristine are both ABCB1 substrates and doxorubicin- and vincristine- adapted cancer cell lines including UKF-NB-3[r]DOX[20], have been shown to typically show an ABCB1-associated resistance phenotype (Kotchetkov et al., 2005); (Hui et al., 2008); (Szakács et al., 2006); (Löschmann et al., 2013); (Martin Michaelis et al., 2009); (M Michaelis et al., 2015); (Voges et al., 2016). In agreement, UKF-NB-3[r]VCR[1] cells were sensitised to the ABCB1 substrate, doxorubicin by the specific ABCB1 inhibitor zosuquidar (figure 60). However, the tested doxorubicin-loaded PLGA-, PLGA-PEG-, and PLA-based nanoparticles did not display superior activity relative to doxorubicin solution in UKF-NB-3[r]DOX[20] and UKF-NB-3[r]VCR[1] cells. Hence, these drug carrier systems do not seem to bypass effectively ABCB1-mediated drug efflux (figure 59).
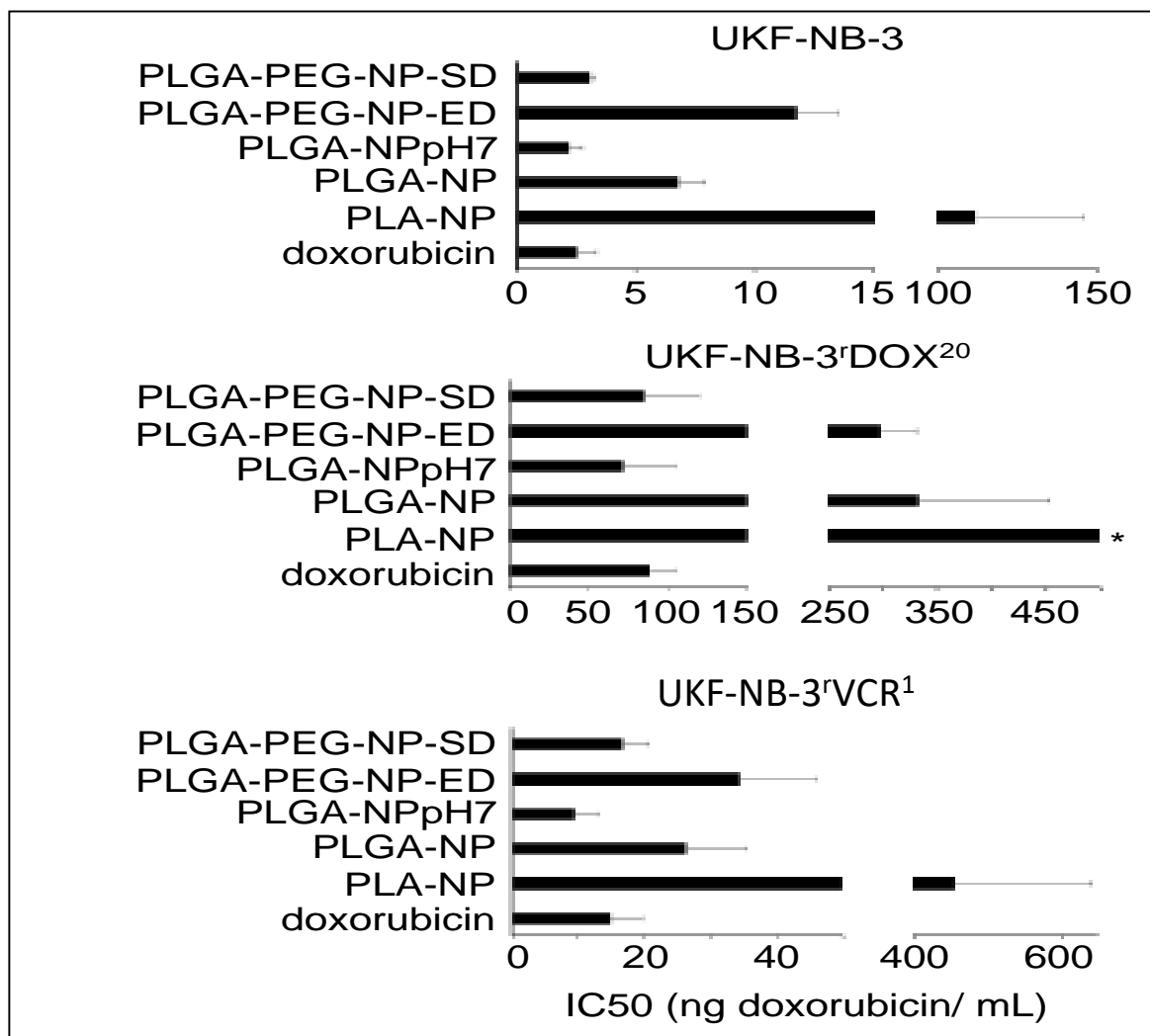
Figure 59: **Doxorubicin concentrations that reduce neuroblastoma cell viability by 50% (IC50) when administered encapsulated into different nanoparticle preparations (PLA-NP, PLA nanoparticles prepared by solvent displacement; PLGA-NP, PLGA nanoparticles prepared by solvent displacement at non-adjusted pH; PLGA-NPpH7, PLGA nanoparticles prepared by solvent displacement at pH7; PLGA-PEG-ED, PLGA-PEG nanoparticles prepared by emulsion diffusion; PLGA-PEG-SD, PLGA-PEG nanoparticles prepared by solvent displacement) compared to doxorubicin solution (doxorubicin). Unloaded nanoparticles did not affect cell viability in the tested concentration range. * IC50 > 500 ng/mL..**
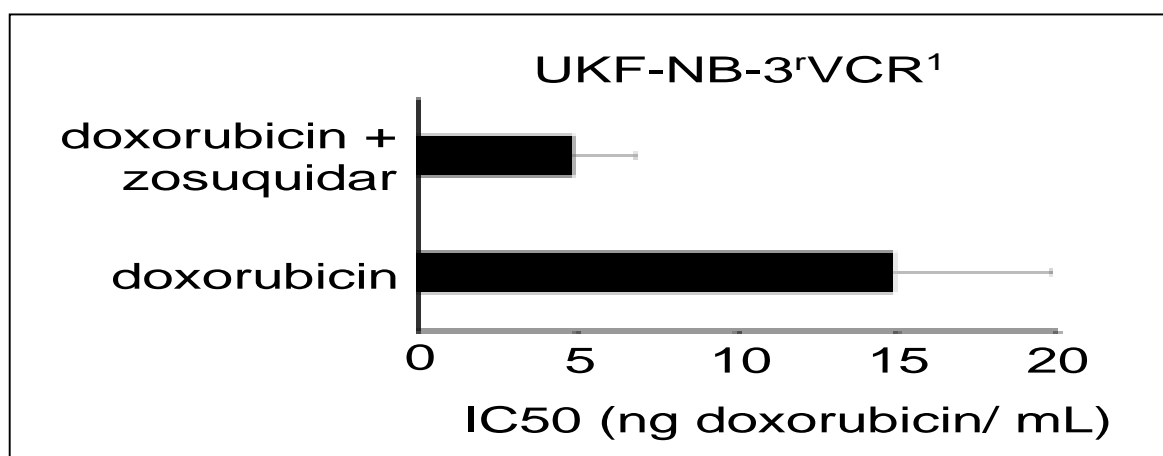
Figure 60: Doxorubicin concentrations that reduce UKF-NB-3[r]VCR[1] viability by 50% (IC50) in the absence or presence of the ABCB1 inhibitor zosuquidar (1µM). Zosuquidar did not affect cell viability when administered alone.

6.2.3 Human serum albumin (HSA) nanoparticle

6.2.3.1 Doxorubicin sensitivity of investigated neuroblastoma cell lines

ABCB1-expressing UKF-NB-3 sublines (UKF-NB-3[r]DOX[20] and UKF-NB-3[r]VCR[1]) displayed reduced doxorubicin sensitivity than parental UKF-NB-3 cells (figure 61 and table 21).
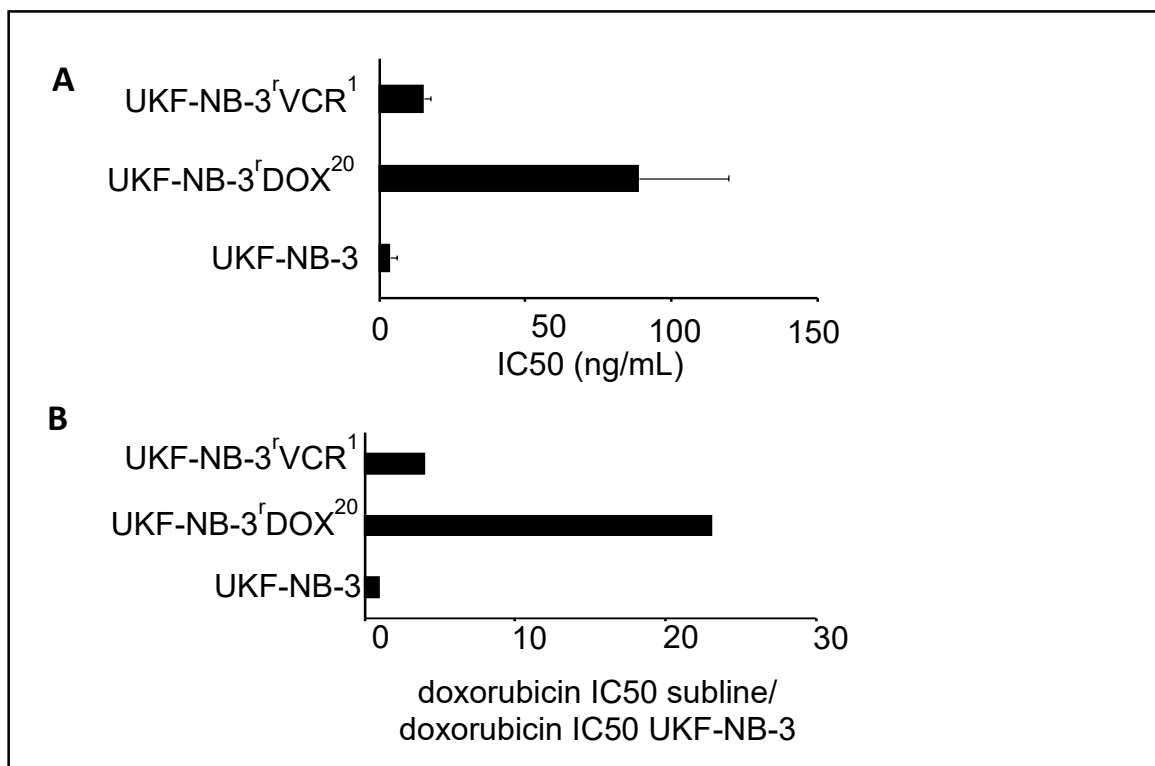
Figure 61: (A) **Doxorubicin drug effect on cell viability of neuroblastoma cell lines; UKF-NB-3[r]VCR[1] and UKF-NB-3[r]DOX[20].** Statistical significance: p=≤0.05) (B) **Fold change difference of the drug adapted cell lines in comparison to the sensitive cell line, UKF-NB-3.**

6.2.3.2 Efficacy of doxorubicin-loaded nanoparticles on neuroblastoma cell viability

The IC50 values of doxorubicin encapsulated into HSA nanoparticles did not significantly differ from those of doxorubicin solution in UKF-NB-3 cells, although there seemed to be a non-significant trend towards increased efficacy for the doxorubicin-loaded HSA (40%), HSA (100%) and HSA (200%) nanoparticles (figures 62 and 63, Table 21). Similar results were observed in UKF-NB-3[r]DOX[20] cells, although the difference between doxorubicin solution and doxorubicin-loaded HSA (200%) nanoparticles reached statistical significance (figures 62 and 63, Table 21). Notably, HSA nanoparticle encapsulation did not reduce UKF-NB-3[r]DOX[20] cell sensitivity to the level of UKF-NB-3 cells. In contrast, doxorubicin-loaded HSA (40%), HSA (100%) and HSA (200%) were significantly more active than doxorubicin solution in UKF-NB-3[r]VCR[1] cells and reduced the doxorubicin sensitivity to the level of parental UKF-NB-3 cells (figures 62 and 63, Table 21). Empty control nanoparticles did not affect cell viability at the investigated concentrations.
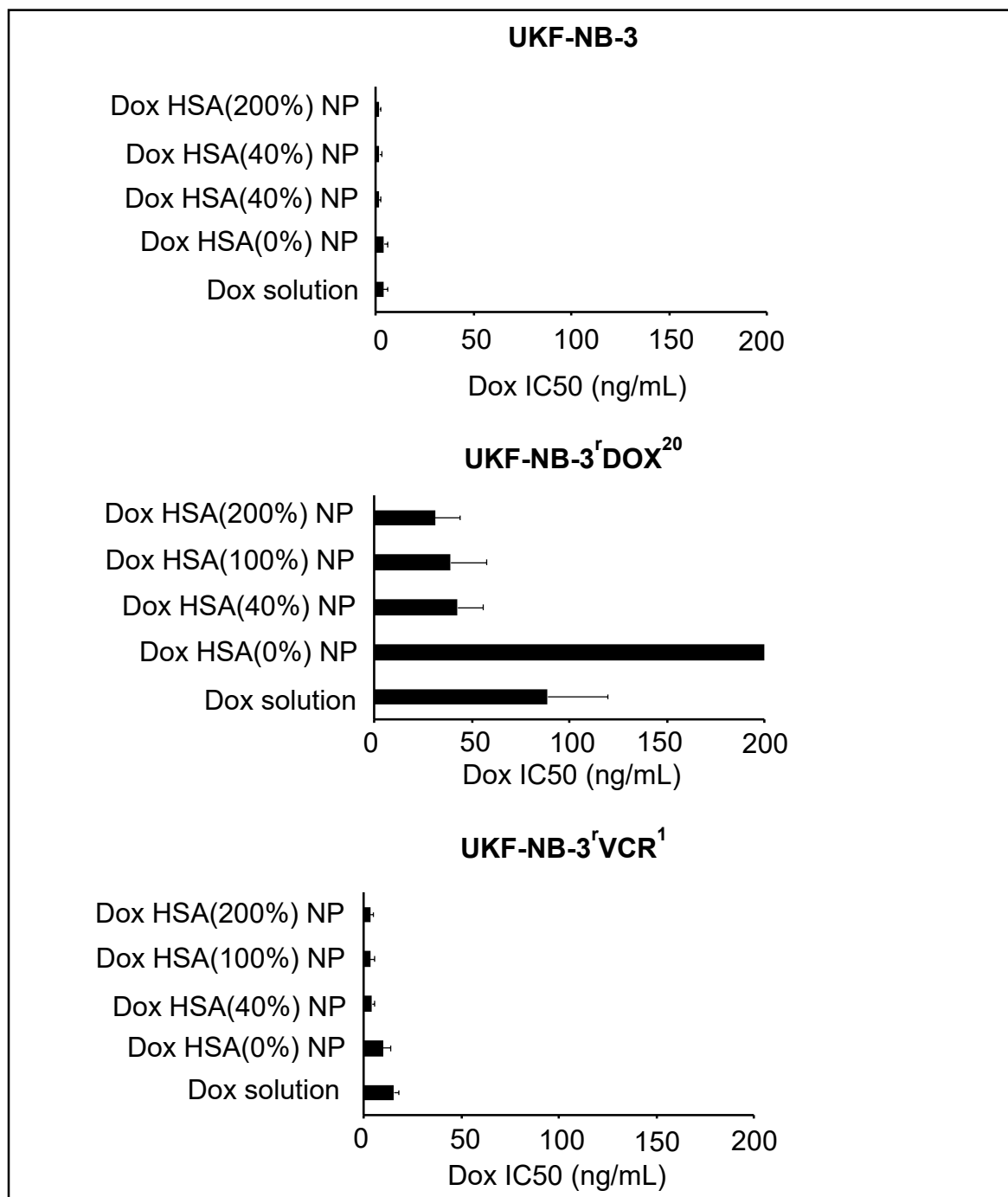
Figure 62: IC$_{50}$ concentrations of Doxorubicin-loaded human serum albumin nanoparticles (HSA) of different cross-linking percentages and Doxorubicin solution efficacy against UKF-NB-3, UKF-NB-3[r]DOX[20] and UKF-NB-3[r]VCR[1]. **Data is expressed as an average of three biological repeats (n=3 ± SD). Statistical significance: Dox solution p=≤0.05; Dox HSA (0%) p=≤0.05, Dox HSA (40%) p=≥0.05, Dox HSA (100%) p=≥0.05, Dox HSA (200%) p=≥0.05.**

	IC50 doxorubicin (ng/mL)		
	UKF-NB-3	UKF-NB-3[r]DOX[20]	UKF-NB-3[r]VCR[1]
Dox solution	3.85 ± 2.46	89.0 ± 30.8 (23.1)[1]	15.5 ± 2.3 (4.03)[1]
DoxHSA(0%)	4.20 ± 1.72 (1.09)[2]	>200[3] (>2.25)[2]	9.88 ± 3.78 (0.64)[2]
DoxHSA(40%)	1.55 ± 1.00 (0.40)[2]	42.8 ± 13.3 (0.48)[2]	4.25 ± 1.35 (0.27)[2]
DoxHSA(100%)	1.98 ± 1.03 (0.51)[2]	39.1 ± 18.6 (0.44)[2]	3.52 ± 2.00 (0.23)[2]
DoxHSA(200%)	1.78 ± 1.04 (0.46)[2]	31.2 ± 12.9 (0.35)[2]	3.51 ± 1.66 (0.23)[2]

Table 21 : **The doxorubicin loaded Human Serum Albumin (HSA).** The nanoparticles cross-linking percentages corresponded with the amount of glutaraldehyde used for the stability. Doxorubicin solution and Dox-HSA (0%) were both used as the control. [1] fold change in doxorubicin sensitivity relative to UKF-NB-3, [2] fold change in doxorubicin sensitivity relative to doxorubicin solution and [3] cell viability in the presence of doxorubicin 200 ng/mL applied as non-stabilised HSA preparation: 81.9 ± 12.9% relative to untreated control. Values are derived from the MTT assay and results are expressed as an IC_{50} concentration (concentration that reduced cell viability by 50%).
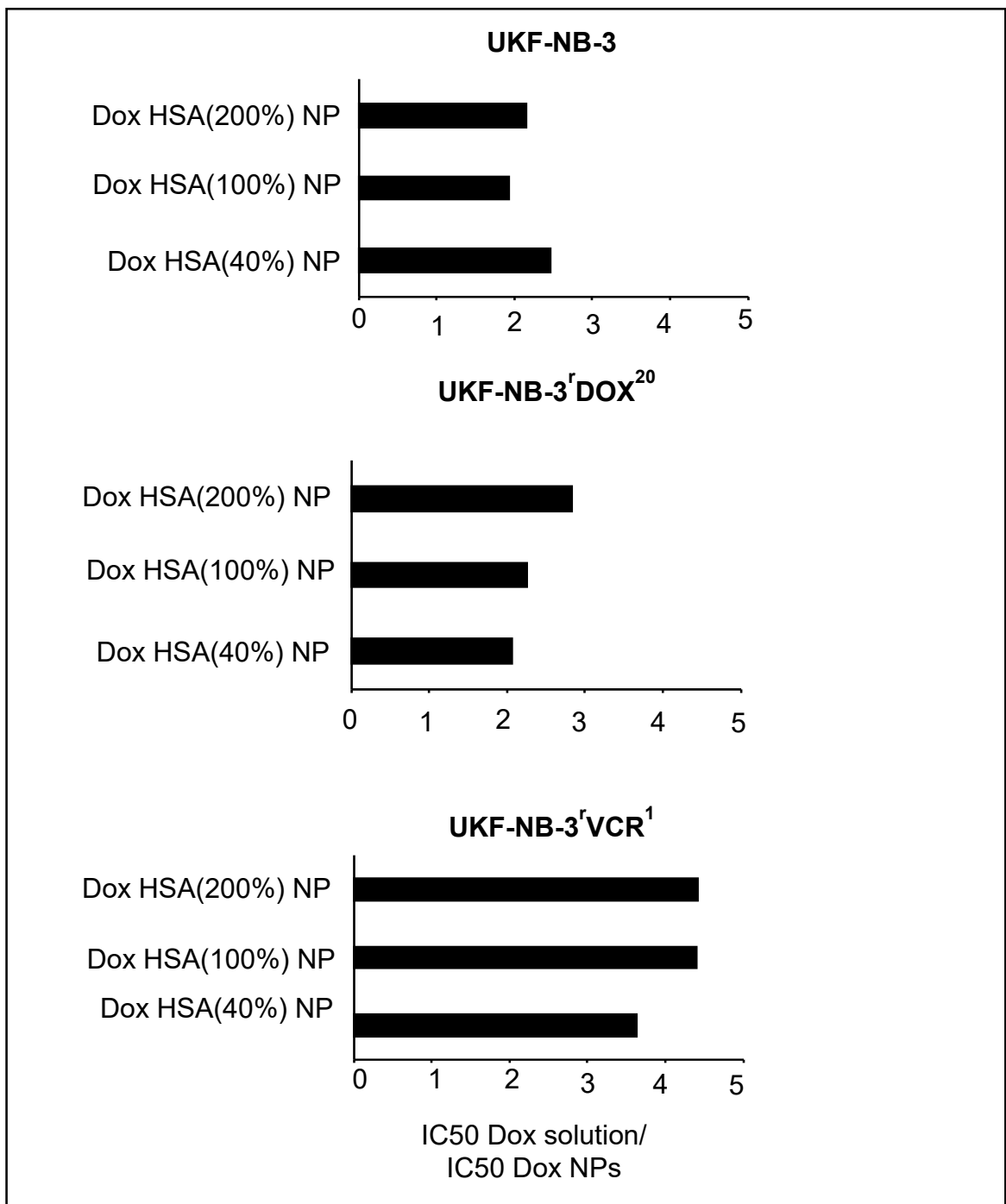
Figure 63: Fold change IC_{50} concentrations of Doxorubicin-loaded human serum albumin nanoparticles (HSA) of different cross-linking percentages relative to Doxorubicin solution efficacy against UKF-NB-3, UKF-NB-3[r]DOX[20] and UKF-NB-3'VCR[1].

6.2.3.3 The ABCB1 inhibitor Zosuquidar does not increase the effects of HSA nanoparticle-bound doxorubicin in UKF-NB-3rDOX20 cells

The ABCB1 inhibitor, zosuquidar increased UKF-NB-3[r]DOX[20] cell sensitivity to doxorubicin solution but not to HSA nanoparticle-incorporated doxorubicin. In addition, zosuquidar did not affect the sensitivity of UKF-NB-3 cells to free or HSA nanoparticle-bound doxorubicin (Figure 64, Table 22). However, UKF-NB-3[r]DOX[20] cells were not sensitised to doxorubicin to the level of parental UKF-NB-3 cells.
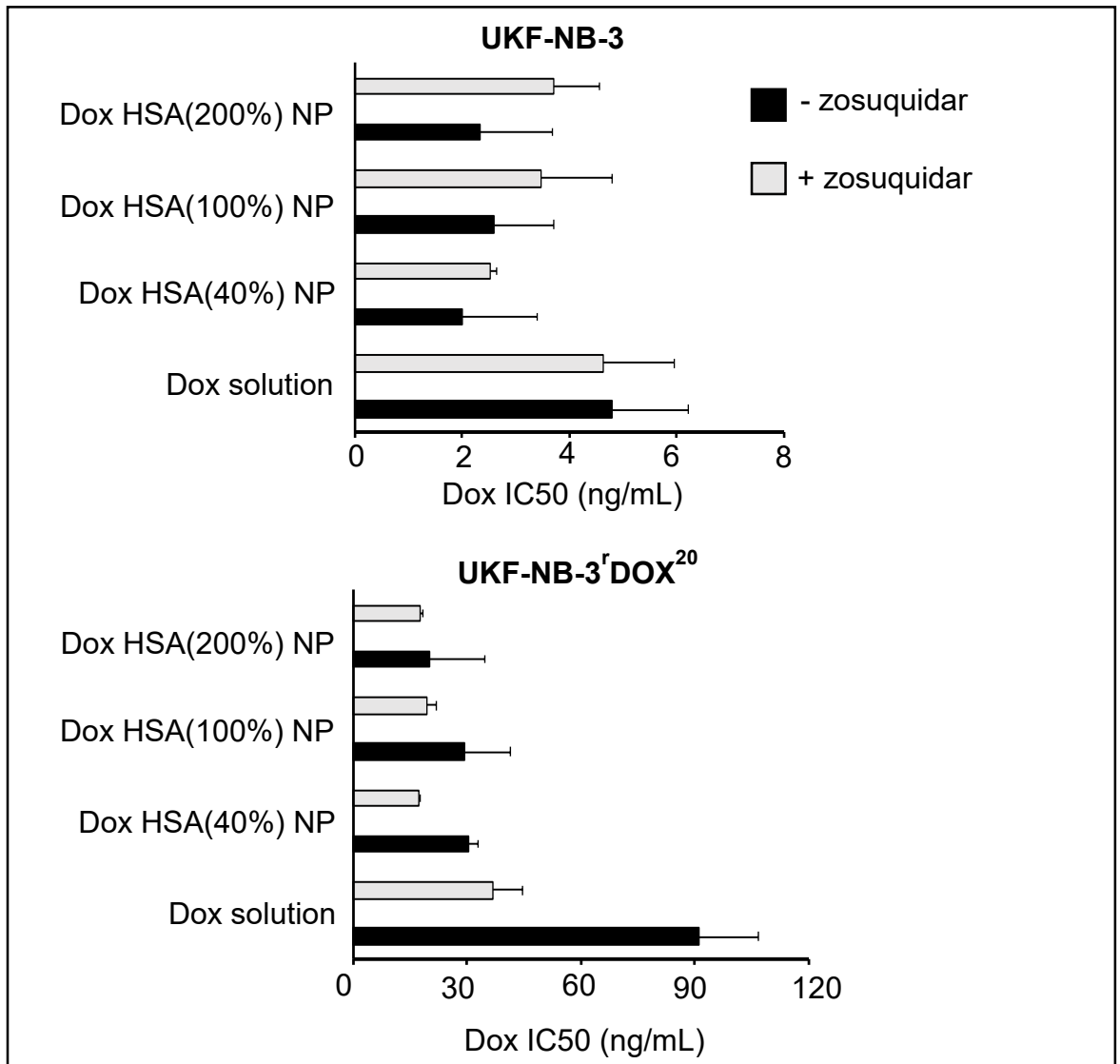
Figure 64: **The effect of Zosuquidar on the cells' viability in the presence of the doxorubicin-loaded human serum albumin nanoparticles (HSA) of different cross-linking and doxorubicin solution. Results of the IC$_{50}$ concentrations were expressed as an average of three biological repeats (n=3 ± SD).** Statistical significance: in the presence of zosuquidar: Dox solution p=≤0.05, Dox HSA (40%) p=≤0.05, Dox HSA (100%) p=≤0.05, Dox HSA (200%) p=≤0.05 and in the absence of zosuquidar: Dox solution p=≤0.05, Dox HSA (40%) p=≤0.05, Dox HSA (100%) p=≤0.05, Dox HSA (200%) p=≥0.05.

UKF-NB-3		+ Zosuquidar (1µM)		
	Doxorubicin IC50 (ng/mL)	Zosuquidar alone[1]	Doxorubicin IC50 (ng/mL)	Fold change[2]
Doxorubicin	4.80 ± 1.41	107 ± 24	4.64 ± 1.33	1.04
Dox HSA (40%) NP	2.01 ± 1.40	107 ± 24	2.52 ± 0.11	0.80
DOX HSA (100%) NP	2.61 ± 1.11	107 ± 24	3.48 ± 1.31	0.75
DOX HSA (200%) NP	2.34 ± 1.35	107 ± 24	3.70 ± 0.86	0.63

UKF-NB-3[r]DOX[20]		+ Zosuquidar (1µM)		
	Doxorubicin IC50 (ng/mL)	Zosuquidar alone[1]	Doxorubicin IC50 (ng/mL)	Fold change[2]
Doxorubicin	91.0 ± 15.9	112 ± 17	36.9 ± 7.7	2.47
Dox HSA (40%) NP	30.5 ± 2.4	112 ± 17	17.4 ± 0.3	1.75
DOX HSA (100%) NP	29.3 ± 12.2	112 ± 17	19.3 ± 2.5	1.52
DOX HSA (200%) NP	20.1 ± 14.4	112 ± 17	17.7 ± 0.6	1.14

Table 22 : **Effects of doxorubicin (Dox) applied as solution or incorporated into human serum albumin (HSA) nanoparticles on neuroblastoma cell viability in the absence or presence of zosuquidar (1µM).** The investigated nanoparticles differed in the amount of the crosslinker glutaraldehyde that was used for nanoparticle stabilisation. The glutaraldehyde amount corresponded to 40% (Dox HSA (40%) NP), 100% (Dox HSA (100%) NP), or 200% (Dox HSA (200%) NP) of the theoretical amount of available amino groups present on HSA. Values are expressed as concentrations that reduce cell viability by 50% (IC50) as determined by MTT assay after 120h of incubation.[1] cell viability in the presence of Zosuquidar (1µM) expressed as % untreated control. [2] doxorubicin IC50/ Doxorubicin IC50 in the presence of zosuquidar.

In contrast to previous experiments, the differences in efficacy between doxorubicin solution and doxorubicin-loaded HSA nanoparticles reached statistical significance in these experiments, indicating in combination with the previously observed trend that HSA nanoparticle-bound doxorubicin does indeed display increased efficacy in UKF-NB-3[r]DOX[20] cells relative to doxorubicin solution. Since zosuquidar did not further increase the effects of nanoparticle-bound doxorubicin and no differences were observed between the UKF-NB-3 sensitivity to free and nanoparticle-bound doxorubicin, the HSA nanoparticle-induced effects seem to be caused by circumvention of ABCB1-mediated drug efflux.

In addition, UKF-NB-3[r]VCR[1] cells were sensitised by zosuquidar to doxorubicin to the same level as UKF-NB-3 cells (Figure 77) in a similar way as by encapsulation into HSA nanoparticles and therefore testing the efficacy of the nanoparticles in the presence of zosuquidar was not required. This further suggests that the increased activity of HSA nanoparticles-incorporated doxorubicin relative to doxorubicin solution is primarily caused by the circumvention of ABCB1-mediated doxorubicin efflux.
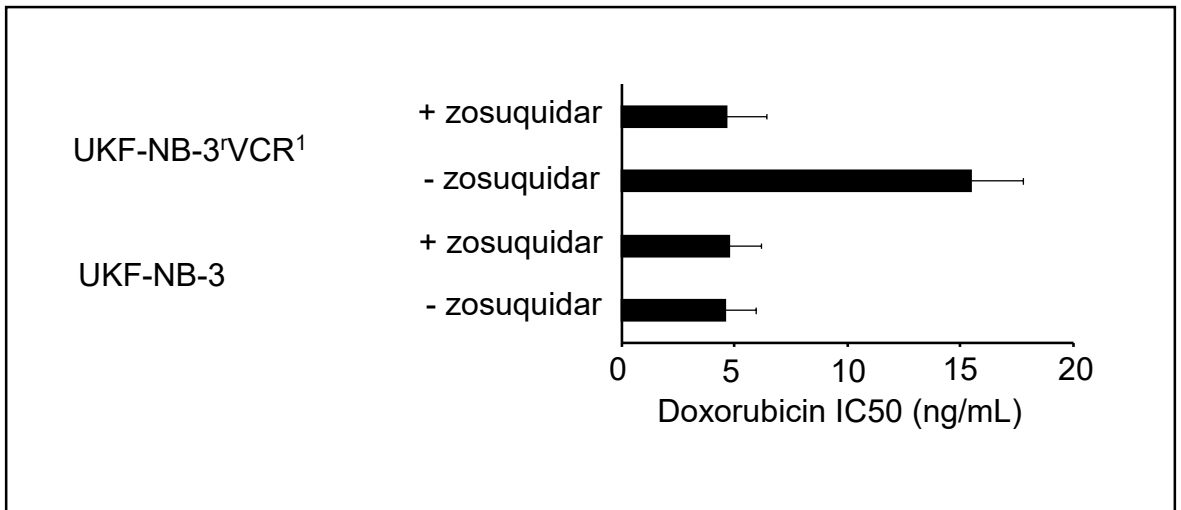
Figure 65: **Doxorubicin concentrations that reduce neuroblastoma cell viability by 50% (IC50) in the absence or presence of the ABCB1 inhibitor zosuquidar (1µM).**

6.3 Discussion
6.3.1 PLGA, PLA, PLGA-PEG nanoparticles
In the last decades, the particle size of PLGA has played a significant role in its therapeutic efficacy; the smaller the size the better cellular uptake (Huang and Zhang 2018). In addition to this, PEGylation which is known to reduce interparticle attractive forces that contribute to acidic conditions, works by PEG conjugates using the mechanism of enhanced permeation and retention (EPR) effect which the tumours implement and accumulates in the microenvironment of the tumour vessels through leaky vasculature and poor lymphatic drainage (Mishra et al., 2016); (Hadjesfandiari & Parambath, 2018). Previous studies have also indicated that PEGylation enhances the stability of the nanoparticles for better drug transportation (Ameller et al., 2003); (Zhou et al.,2015); (Singh & Lillard, 2009); (Danhier et al., 2012).

The determination of Poly (lactic-*co*-glycolic) acid (PLGA) and Poly-lactic acid (PLA) doxorubicin-loaded nanoparticles enhancing the efficacy of doxorubicin was successfully demonstrated. Here, we observe that the use of these polymers enabled the chemotherapeutic drug to exert enhanced cytotoxic effects in comparison to the unbound-nanoparticles and the doxorubicin solution (Rodrigues de Azevedo et al., 2017); (Corrigan & Li, 2009) .

Our results demonstrated that PEGylation enabled the production of smaller particle diameters (≤100) of the doxorubicin-loaded PLGA-PEG nanoparticles, which appeared to be more effective in sensitising the cells thus confirming that aggregation of the particles were controlled to allow effective drug release of the bound- compared to the unbound- nanoparticles (Danaei et al., 2018); (Chen, Mohanraj, & Parkin, 2003). Our findings is also in accordance with (Ruan & Feng, 2003) as it was described that PEGylated polymers validate an increased release of drug due to the porous particle structure illustrated as a result of the aqueous channels created by PEG chains. In addition, strategies using saline buffer and poly-vinyl alcohol (PVA) film to increase the yield of doxorubicin in encapsulation efficacy was demonstrated by our findings (Shah et al., 2017); (Johnstone & Lippard, 2013).

The preparation at pH 7 of the doxorubicin-loaded nanoparticles contributed to the enhanced lipophilicity effect, cellular uptake and retention resulting in the sustained anti-cancer activity compared to the doxorubicin solution (Chhikara et al., 2012). The outcomes derived from our research showed that the doxorubicin-bound nanoparticles sensitised the doxorubicin-resistant cells to the level of the sensitive cells indicating significant inhibition.

6.3.2 Human Serum Albumin (HSA) nanoparticles
In contrast to the tested doxorubicin-loaded PLGA-, PLA, and PLGA-PEG nanoparticles, doxorubicin-loaded HSA nanoparticles exerted stronger effects in ABCB1-expressing cells than doxorubicin solution. The efficacy of doxorubicin-loaded HSA nanoparticles could not be further increased by

addition of the specific ABCB1 inhibitor zosuquidar. In addition, zosuquidar and doxorubicin encapsulation into HSA nanoparticles displayed similar levels of sensitisation in ABCB1-expressing cells. Hence, HSA nanoparticle encapsulation seems to primarily increase doxorubicin efficacy by circumvention of ABCB1-mediated drug efflux in our model systems. Our findings are in agreement with other findings showing that some nano-sized drug carrier systems can bypass transporter-mediated drug transport (Bar-Zeev et al., 2017; Callaghan et al., 2014; Yuan et al., 2016).

Strategies using ABCB1 inhibitors to circumvent ABCB1-mediated drug resistance have failed in clinical trials so far. Potential reasons for this include the interaction with ABCB1 expressed at physiological barriers, which alters the systemic distribution of endogenous and exogenous ABCB1 substrates, and the presence of multiple resistance mechanisms (Szakács et al., 2006). Nanoparticles as drug carrier systems may be a way to circumvent transporter-mediated drug resistance at the cancer cell level without systemic transporter inhibition. In addition, our results indicate how multiple resistance mechanisms may limit the efficacy of therapeutic strategies focused on interference with ABCB1-mediated drug efflux. Doxorubicin-adapted cells were neither sensitised to doxorubicin to the level of parental cells by incorporation into HSA nanoparticles, nor by the ABCB1 inhibitor zosuquidar. This is likely to be the case, because adaptation to doxorubicin has been associated with the formation of multiple resistance mechanisms in addition to ABCB1 expression. In contrast, vincistine-adapted cells were sensitised to doxorubicin to the level of parental cells by both nanoparticle incorporation and zosuquidar. This suggests that cancer cell adaptation has resulted, in addition to ABCB1 expression, in vincristine-specific resistance mechanisms that (at least in this case) do not mediate cross-resistance to doxorubicin. The concentration of zosuquidar used was 1µM which is within the plasma therapeutic range according to the manufacturer's instructions; 1-16 µM. The concentration used was determined using the IC50 concentration of the parental cell line. Results from previous studies indicated that the normalised plasma concentration of doxorubicin in child cancer patients ranged between 22.6-334 ng/ml with a median of 62.8 ng/ml (Frost et al., 2002). Our results are in agreement with a range between 2.5-88.4 ng/ml in the parental, vincristine- and doxorubicin-resistant cell lines.

Hence, future therapeutic strategies using ABCB1 inhibitors may have to be based on a (more) comprehensive understanding of the factors causing resistance in a given cancer (in addition to the ABCB1 status).

7 Standardised treatment to compare resistance formation

7.1 Introduction

Drug-adapted cancer cell lines have been used to discover many clinically relevant resistance mechanisms (Juliano & Ling, 1976) (Cole et al., 1992);(S. V. Sharma et al., 2010); (Jung et al., 2016); (Joseph et al., 2013); (Nazarian et al., 2010); (Korpal et al., 2013); (Schneider et al., 2017); (M. Michaelis et al., 2011); (M. Michaelis et al., 2012). In addition, preclinical model systems such as cancer cell lines enable studies that are not feasible in patients. For example, different treatments can be compared in the same cancer cell population. This is not possible in cancer patients, who can only be treated once. Anti-cancer drugs may not only differ in their acute anti-cancer efficacy but also in their potential to induce resistance. However, differences in the potential of drugs to induce resistance have not been experimentally addressed so far. To fill this gap, we aimed to develop a standardised drug adaptation protocol that directly compared the potential of different drugs to induce resistance in a given cancer cell line.

UKF-NB-3 neuroblastoma cells were treated following a standardised protocol using the IC50 concentrations of the closely related microtubule stabilising agents cabazitaxel, docetaxel, epothilione-B and paclitaxel, and resistance formation was monitored.

This chapter will include work generated by myself and other lab members. My laboratory contribution commenced from week 50 and included the cultivation and characterisation of the sublines that had were exposed to paclitaxel.

7.2 Cell cultivation in the presence of microtubule stabilising agents following a standardised protocol

A project overview is provided in Figure 78. Five sublines were cultivated for each drug, one week in the presence, one week in the absence of the IC_{50} concentrations of the individual drugs. Originally, 1,000,000 cells/ 25 cm^2 flask were used in the weeks with and 100,000 cells/ 25 cm^2 flask in the weeks without drug. Over the course of the project the cell numbers had to be adapted to 100,000 cells/ 25 cm^2 flask also in the weeks without drug as indicated.

UKF-NB-3

UKF-NB-3-CABA$^{0.25nM}$ (sub-lines 1-5)

UKF-NB-3-EPO$^{0.10nM}$ (sub-lines 1-5)

UKF-NB-3-PAC$^{0.57nM}$ (sub-lines 1-5)

UKF-NB-3-DOCE$^{0.37nM}$ (sub-lines 1-5)

Figure 66 : **The sub-lines derived for the drug adaptation protocol.** UKF-NB-3 parental cell line was passage into five sub-lines per drug. The IC$_{50}$ concentrations of the four drugs used; docetaxel, epothilone-B, paclitaxel and cabazitaxel were determined using MTT assays. Cultivation with drug was on a bi-weekly basis.

7.3 Maintenance of the sub-lines

The MYCN-amplified human neuroblastoma cell line UKF-NB-3 was established from bone marrow metastases of INSS stage 4 neuroblastoma patient.

7.3.1 Cultivation

The cell lines were passaged weekly using 10, 000 cells per mL per $25cm^2$ flask and treated with the IC50 concentration of the drug on a bi-weekly schedule. Initially, 100, 000 cells mL per $25cm^2$ flask was passaged when the cells were cultivated in the presence of the drug and 10, 000 cells per mL per $25cm^2$ flask was passaged the week when they were cultivated in the absence of drug. However, the cells began to show signs of stress; overgrowth and non-adherence of some, resulting in the cell passaging at 10, 000 cells per mL per $25cm^2$ flask every week. This was performed on the same day every week. The cell counts were used to identify the pattern of adaptation.

MTT assays were performed every four weeks to determine the level of resistance. The protocol used was as previously described in chapter 4.4.

7.5 Results

7.5.1 Cell line cultivation in the presence of microtubule stabilising agents following a standardised protocol

The growth patterns of the sub-lines were monitored over the course of the study to observe any particular patterns of growth in the presence and absence of the drug.

The five UKF-NB-3 sub-lines cultivated in 0.10 nM of epothilone-b and the five sub-lines cultivated in 0.25 nM of cabazitaxel, was set up and monitored by other co-lab members. Results are shown in appendix 2. My participation in this project began from week 51.

7.5.2 UKF-NB-3 cell cultivation in the presence of docetaxel (0.37nM)

The growth patterns of the UKF-NB-3 sublines in the presence of docetaxel (0.37nM) are presented in figure 67-68. Subline 3 was lost in week 3 due to a lack of viable cells. From week 13 onwards, the cell number of the remaining sublines had to be reduced to 100,000 cells/ 25 cm^2 flask to avoid a loss of cell viability due to overgrowth. Despite this sign of initial adaptation, subline 5 was lost in week 25 and subline 2 in week 96. The sublines 1 and 4 were maintained until the end of the project (week 100).
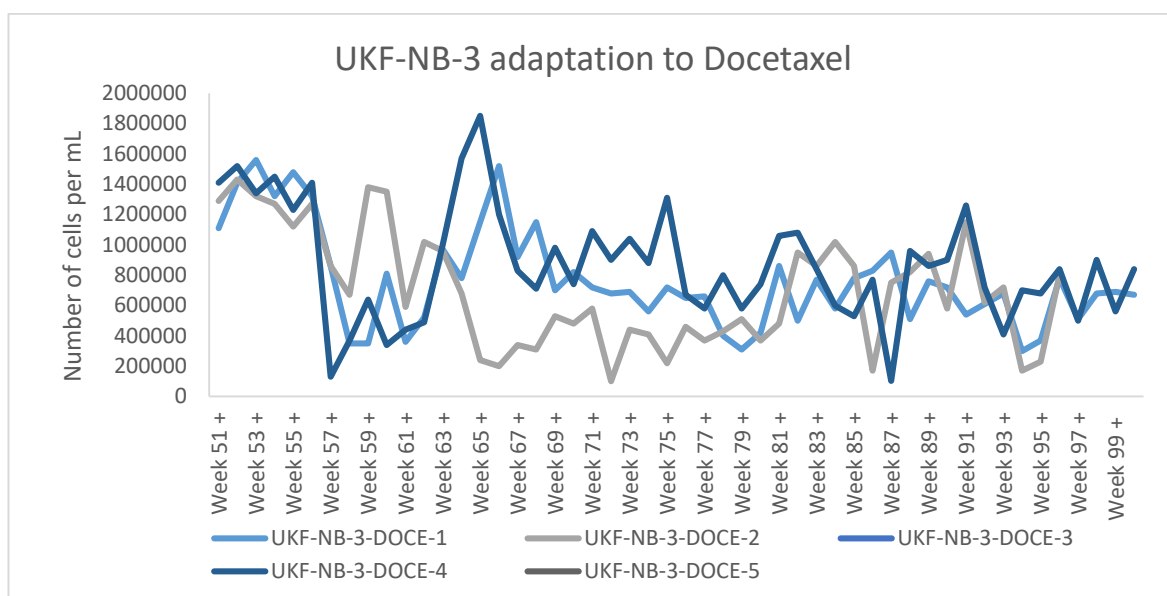
Figure 67 : **Cell numbers in the docetaxel (0.37nM)-treated sublines between week 51 and week 100**. Cell numbers were recorded in the presence (+) and absence (-) of drug to identify patterns of growth for every weekly passage. The cell number was reduced to 100,000 cells/ 25 cm^2 flask after week 19. No viable cells were detected in subline 2 at the end of week 96.
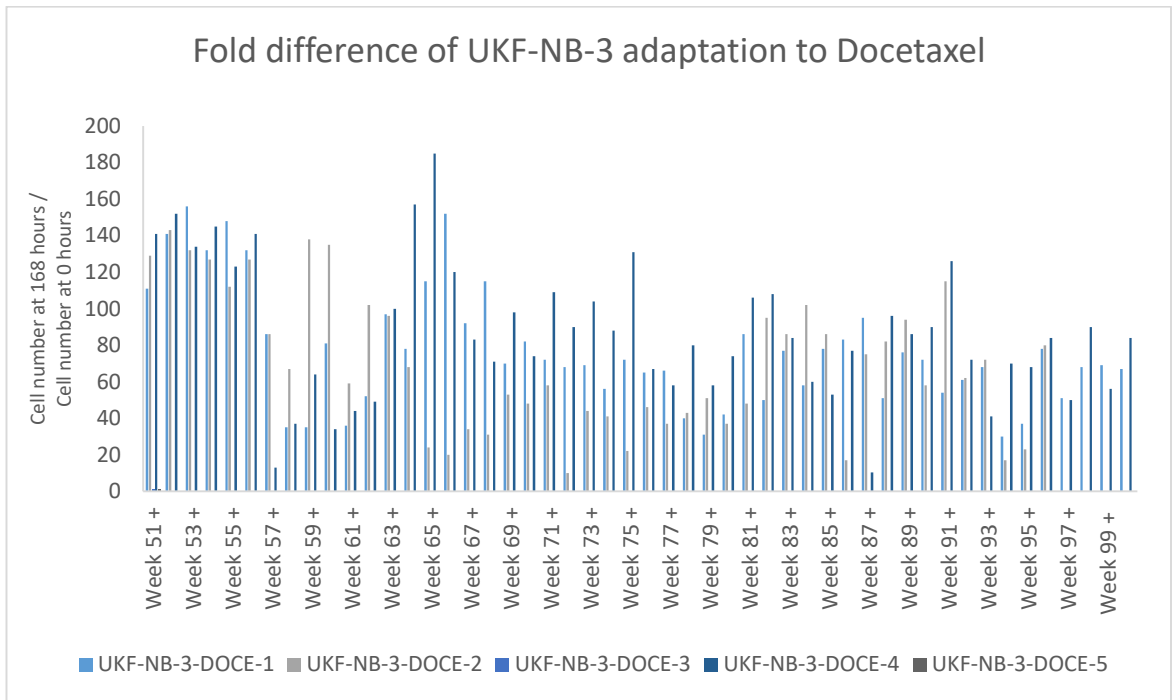
Figure 68 : Fold change in cell numbers between week 51 and week 100 in the docetaxel (0.37nM)-treated sublines. Cell numbers were recorded in the presence (+) and absence (-) of drug to identify patterns of growth for every weekly passage. The cell number was reduced after week 19. No viable cells were detected in subline 2 at the end of week 96.

7.5.3 UKF-NB-3 cell cultivation in the presence of paclitaxel (0.57nM)

The growth patterns of the UKF-NB-3 sublines in the presence of paclitaxel (0.57nM) are presented in figure 69-70. From week 17 onwards, the cell number of the remaining sublines had to be reduced to 100,000 cells/ 25 cm2 flask to avoid a loss of cell viability due to overgrowth. Despite this sign of initial adaptation, sublines 2 and 3 were lost in week 42 and subline 5 in week 74. The sublines 1 and 4 were maintained until the end of the project (week 100).
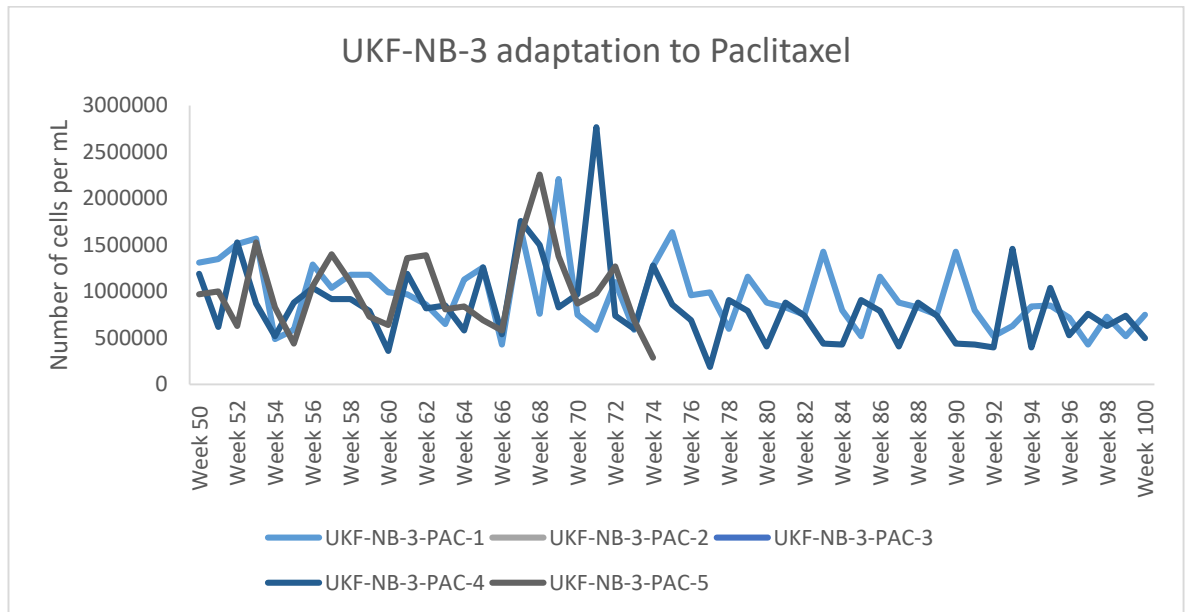
Figure 69 : **Cell numbers in the paclitaxel (0.57nM)-treated sublines between week 51 and week 100.** Cell numbers were recorded in the presence (+) and absence (-) of drug to identify patterns of growth for every weekly passage. The cell number was reduced to 100,000 cells/ 25 cm^2 flask after week 19. No viable cells were detected in subline 5 and 3 at the end of week 74.
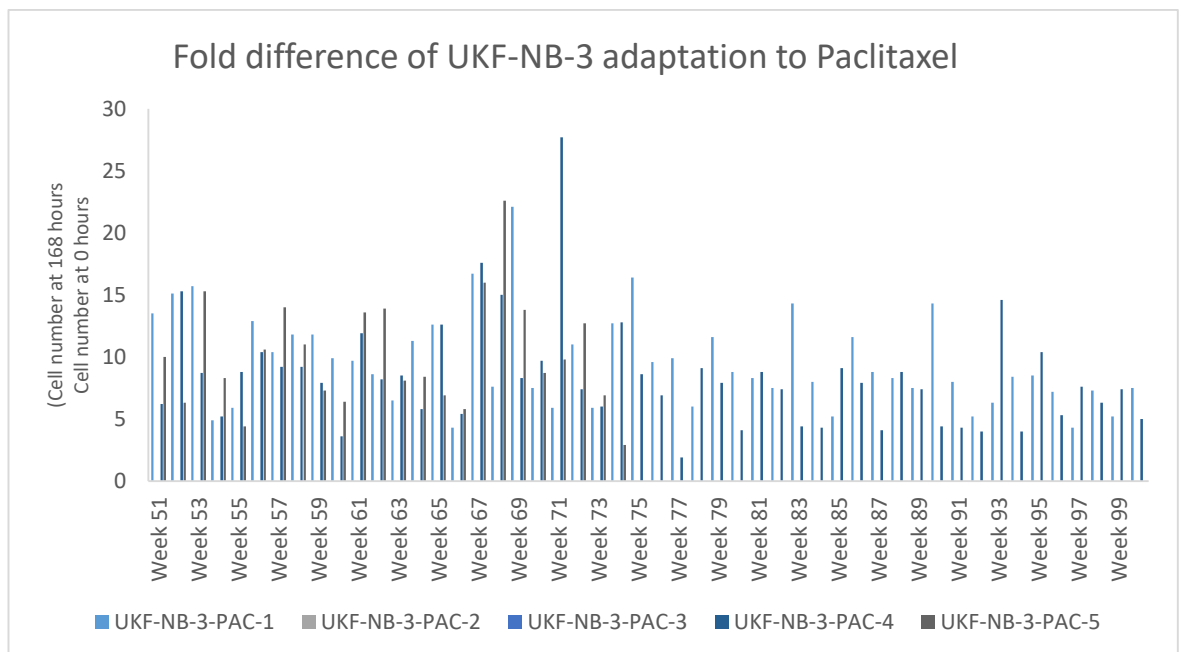
Figure 70 : **Fold change in cell numbers in the paclitaxel (0.57nM)-treated sublines between week 51 and week 100.** Cell numbers were recorded in the presence (+) and absence (-) of drug to identify patterns of growth for every weekly passage. The cell number was reduced to 100,000 cells/ 25 cm^2 flask after week 19. No viable cells were detected in subline 5 and 3 at the end of week 74.

7.5.4 Chemotherapy-induced resistance phenotype

Drug sensitivity was monitored by MTT assay (n=1) every four weeks during drug treatment. Resistance was defined by a 2-fold increase in the IC_{50} concentration of the respective drug. The sublines cultivated in the presence of epothilone-B (appendix 2) and cabazitaxel (appendix 2) showed no consistent pattern of resistance formation.

Among the sublines cultivated in the presence of docetaxel, subline 1 and 4 consistently displayed docetaxel IC_{50} values that were >2-fold higher than those determined in UKF-NB-3 cells (figure 71). The other sublines did not consistently display >2-fold changes.
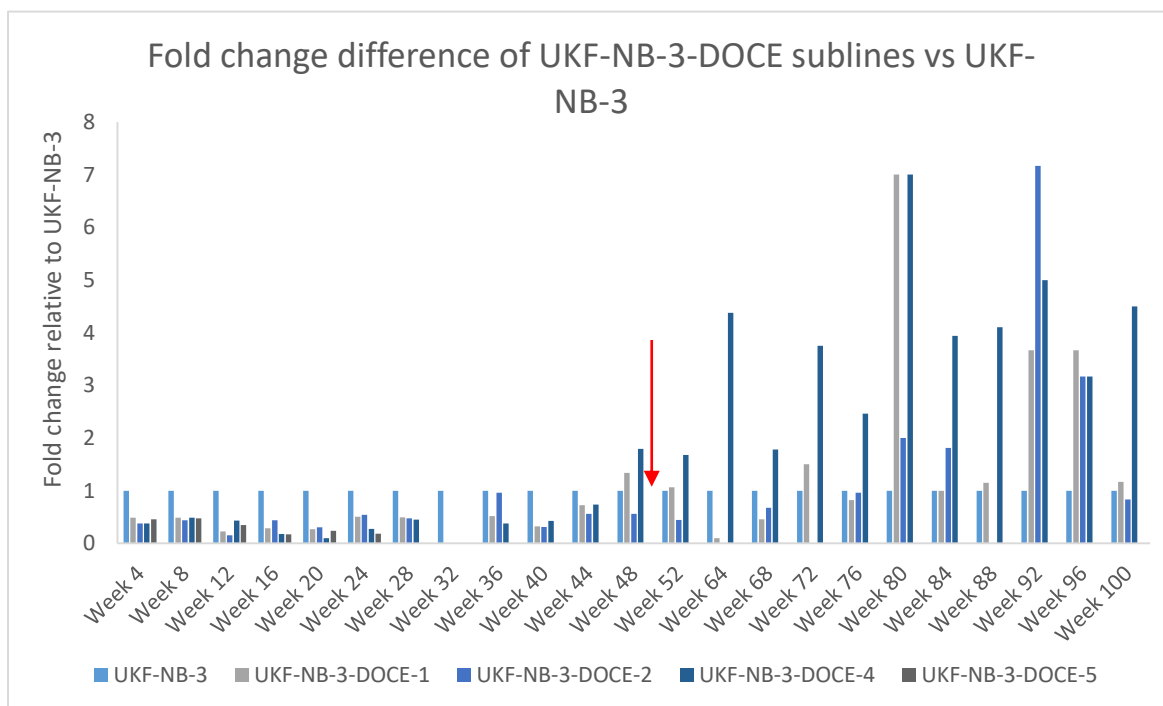
Figure 71 : IC_{50} concentrations determined from a 120-hour MTT assay for the docetaxel sub-lines in comparison to UKF-NB-3. Results show increased resistance from week 64. Each result (week 4 – 100) was derived from one MTT assay (n=1) thus no error bars or average. The red arrow indicates where I began performing the cell viability determination.

Although the sublines 1 and 4 that had been cultivated in the presence of paclitaxel were not lost during the project running time, they did not display a consistent 2-fold increase in the paclitaxel IC_{50} (figure 72).
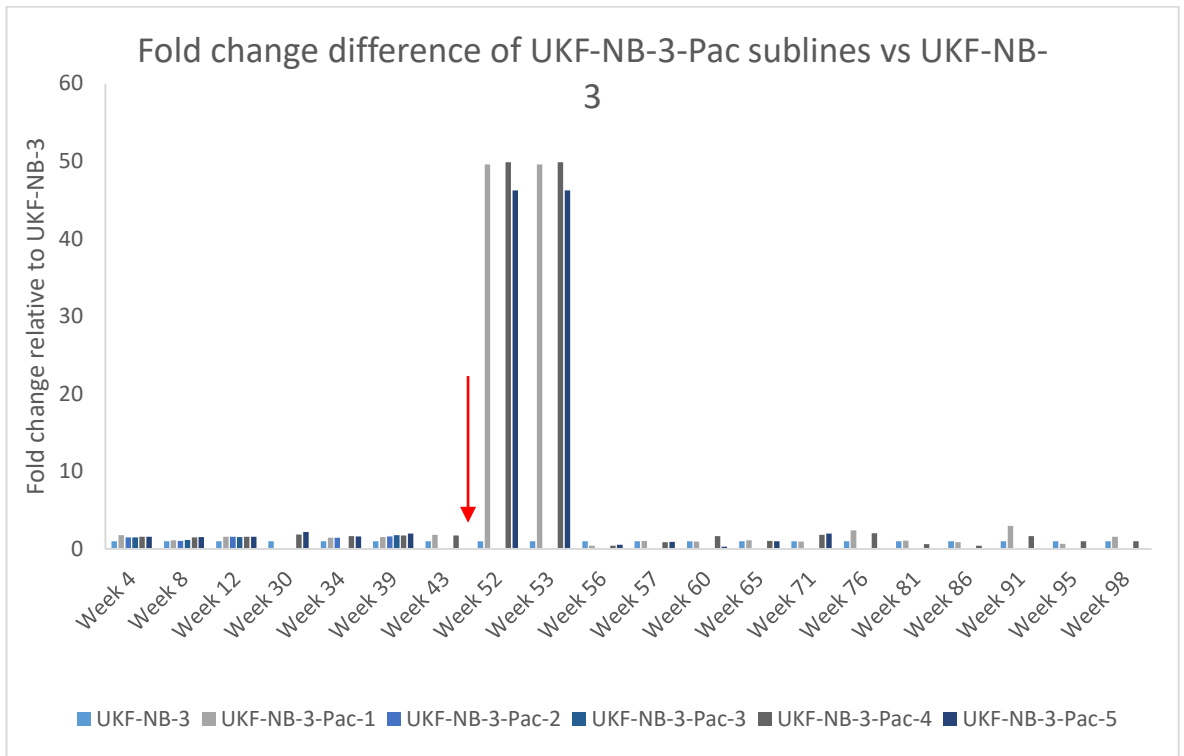
Figure 72 : **IC$_{50}$ concentrations determined from a 120-hour MTT assay for the paclitaxel sub-lines in comparison to UKF-NB-3**. Results show increased resistance during weeks 52-54. Each result (week 4 – 100) was derived from one MTT assay (n=1) thus no error bars or average. The red arrow indicates where I began performing the cell viability determination.

7.5.5 Subline characterisation at the end of the project

After the cultivation of the sublines in the presence of drug according to the standardised protocol was finished, the remaining sublines were characterised for doubling times, cell morphology, drug sensitivity profiles, and ABCB1 status.

The doubling times (Figure 73 and Table 23) and the cell morphology (Figure 74A-L) did not substantially differ between the parental UKF-NB-3 cells and the sublines that had been cultivated in the presence of docetaxel or paclitaxel except for the docetaxel-treated subline 1, which appeared to grow more in clusters than the parental cells.
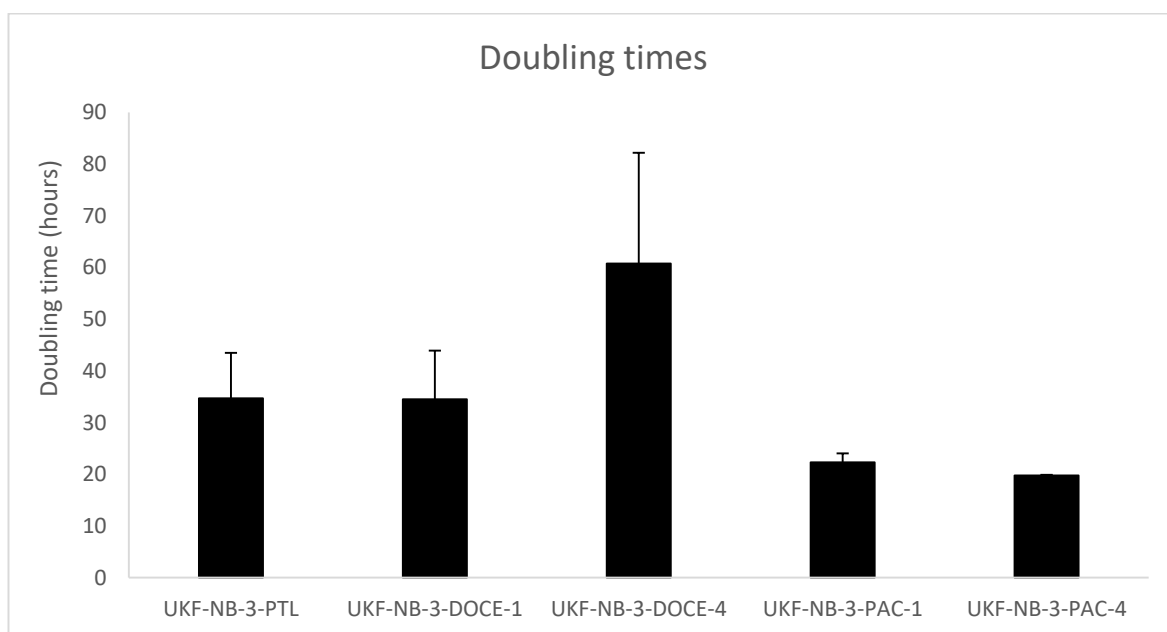
Figure 73 : **The mean doubling times of the docetacel- and paclitaxel- treated sublines in comparison to the parental cell line.** The conditions of the doubling times were performed in the absence of drug using the Roche xCELLigence real-time system. Data is expressed as a mean ± SD (n=3).

Cell line	Doubling time (hours)
UKF-NB-3-PTL	18.6 ± 1.56
UKF-NB-3-PAC-1	22.30 ± 1.77
UKF-NB-3-PAC-4	19.8 ± 0.10
UKF-NB-3-DOCE-1	34.7 ± 9.4
UKF-NB-3-DOCE-4	60.8 ± 21.4

Table 23 : The numerical data of the doubling times derived from the growth curves using the Roche xCELLigence real-time system. Data is expressed as a mean ± SD (n=3).
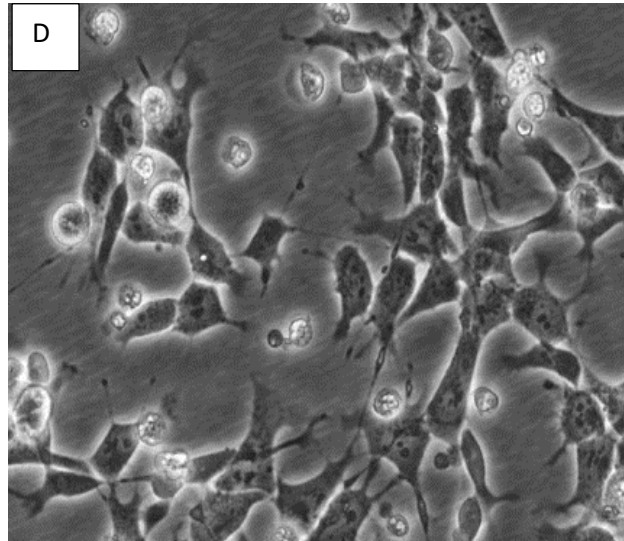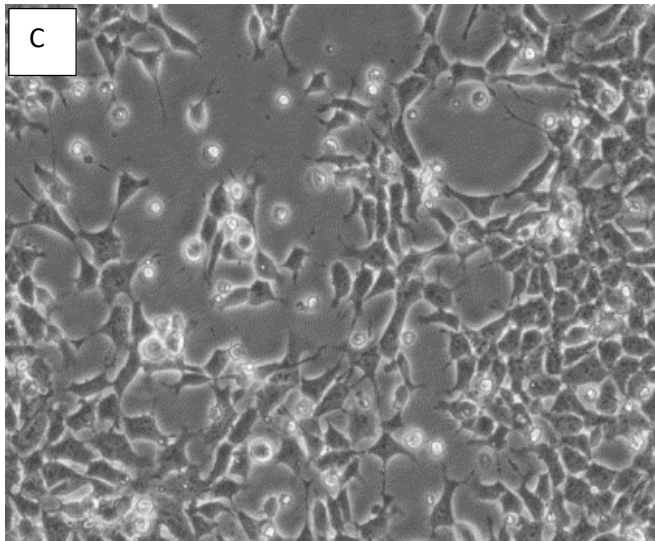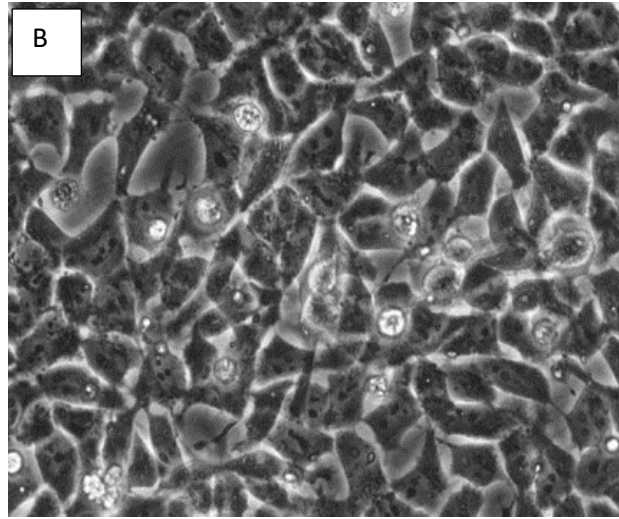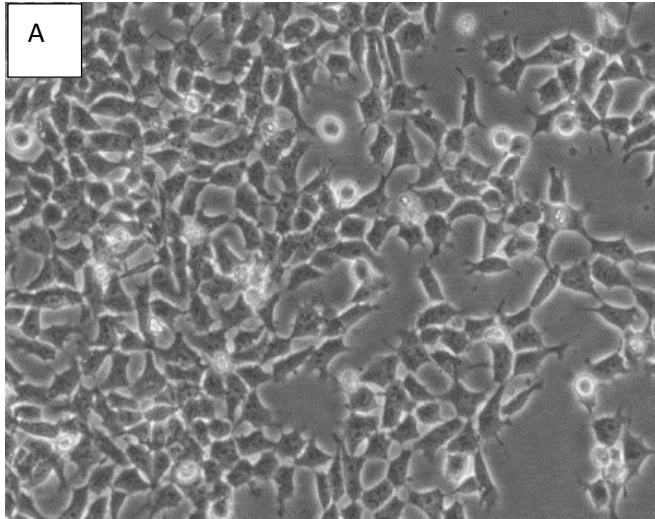
Figure 74A-D: Microscopic images of the sublines.

A) UKF-NB-3 using 1000X magnification,

B) UKF-NB-3 using 2000X magnification,

C) UKF-NB-3-PAC-1 using 1000X magnification

D) UKF-NB-3-PAC-1 using 2000X magnification
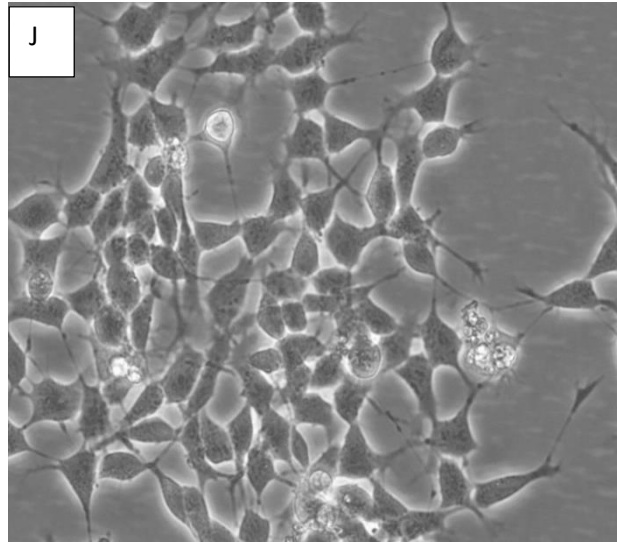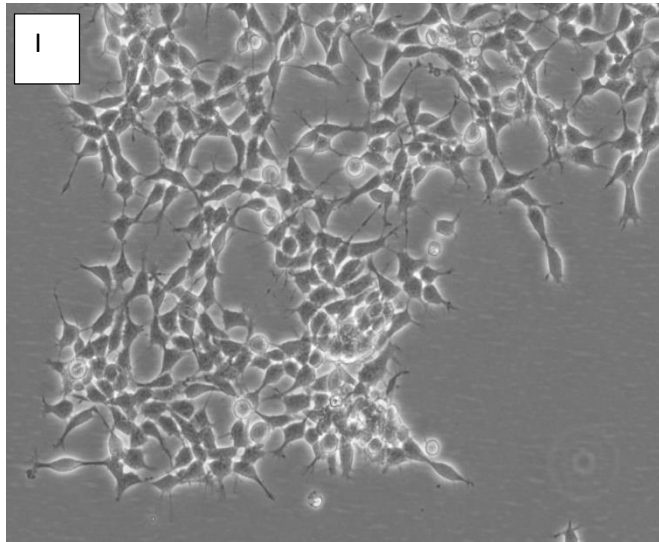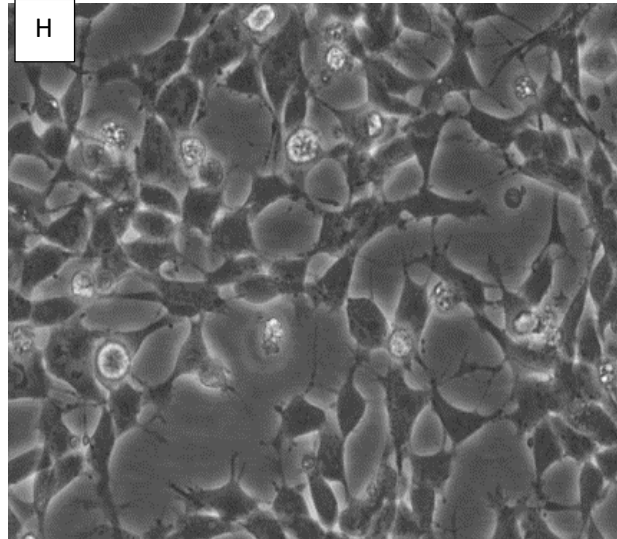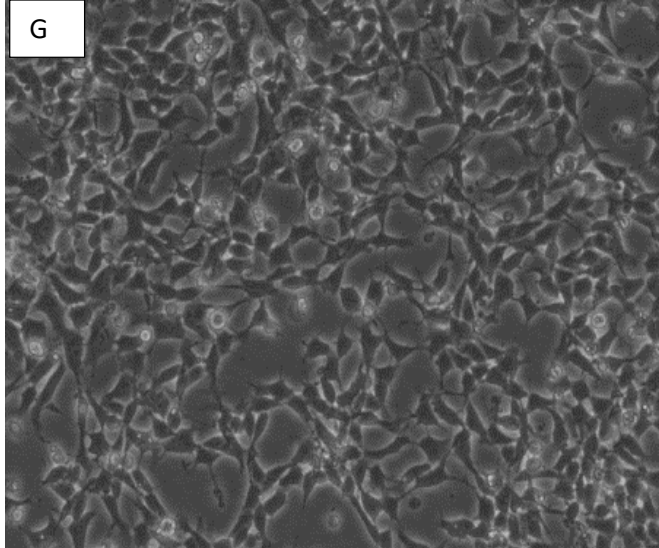
Figure 74E-H: Microscopic images of the sublines.

G) UKF-NB-3-PAC-4 using 1000X magnification,

H) UKF-NB-3-PAC-4 using 2000X magnification.

I) UKF-NB-3-DOCE-4 using 1000X magnification

J) UKF-NB-3-DOCE-4 using 2000X magnification
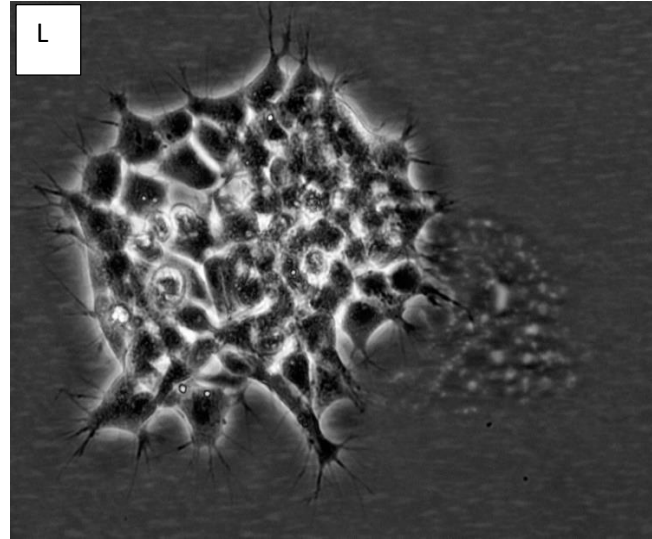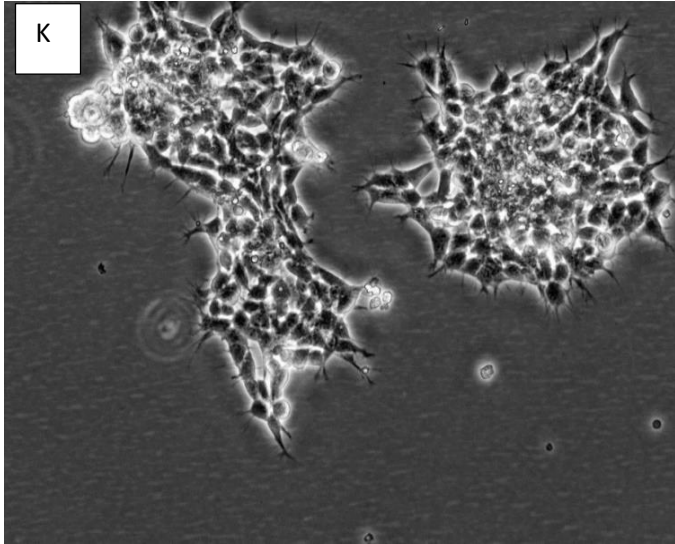
Figure 74K-L: Microscopic images of the sublines.

K) UKF-NB-3-DOCE-1 using 1000X magnification

L) UKF-NB-3-DOCE-1 using 2000X magnification

7.5.6 Drug-sensitivity profiles

Drug sensitivity profiles of the docetaxel-treated sublines were determined using the microtubule stabilising drugs docetaxel, paclitaxel, cabazitaxel, and epothilone B, the microtubule-destabilising vinca alkaloid vincristine, the ALK and Met inhibitor crizotinib, and the DNA damaging agents topotecan (topoisomerase I inhibitor) and cisplatin (DNA crosslinker) (Figure 75A-H). The results are summarised in a heatmap (Figure 76). Resistance was defined as a >2-fold change in the IC_{50} of the subline relative to parental UKF-NB-3 cells.

UKF-NB-3-DOCE-1 and UKF-NB-3-DOCE-4 cells displayed cross-resistance to paclitaxel and vincristine but not to cabazitaxel, epothilone B, crizotinib, topotecan, and cisplatin.
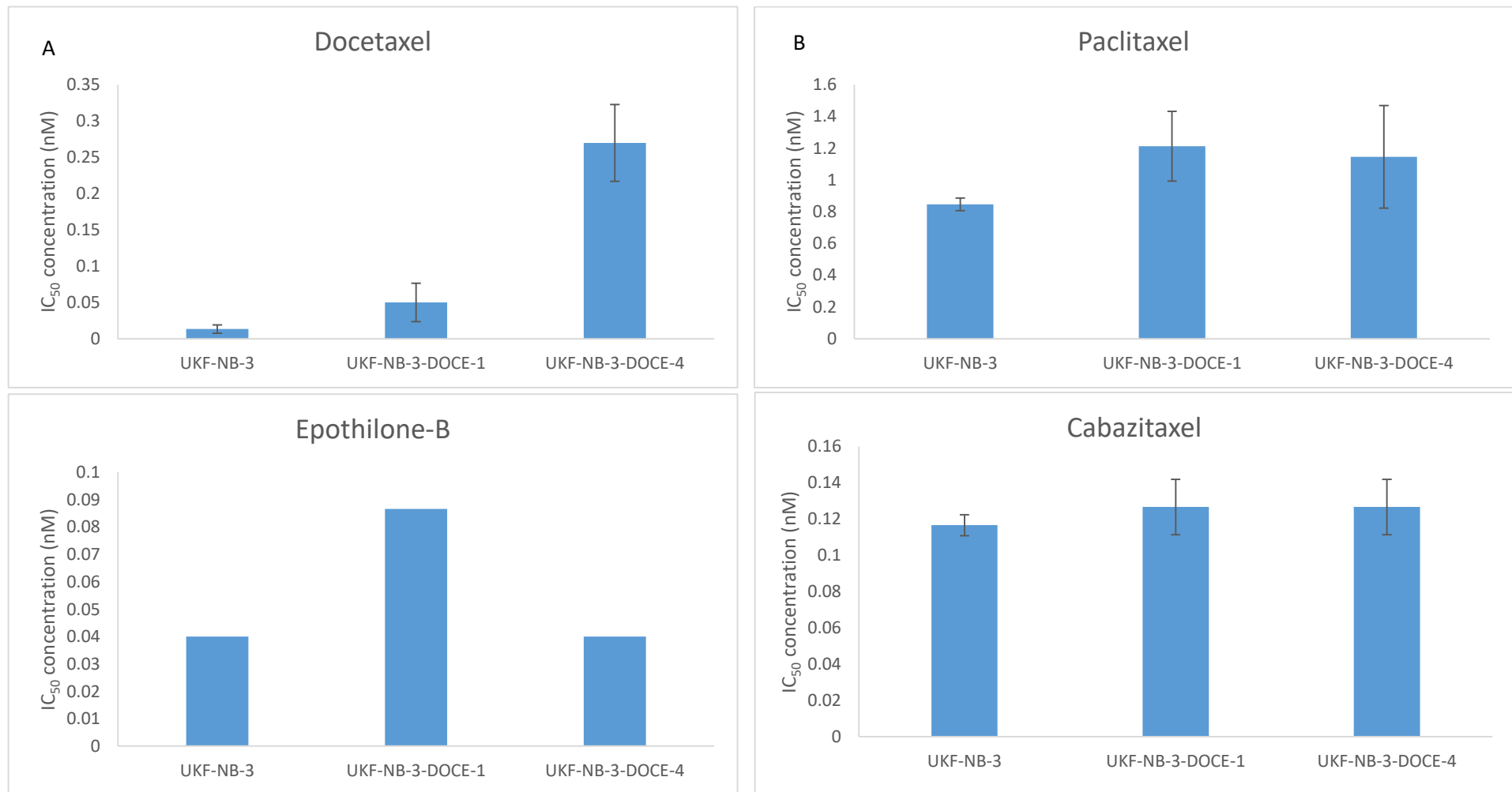
Figure 75A-D: Fold change difference of the docetaxel sub-lines relative to the sensitive cell line, UKF-NB-3. IC_{50} concentrations were derived from a 120-hour MTT assay. Results are averages of three biological repeats (n=3 ± SD).
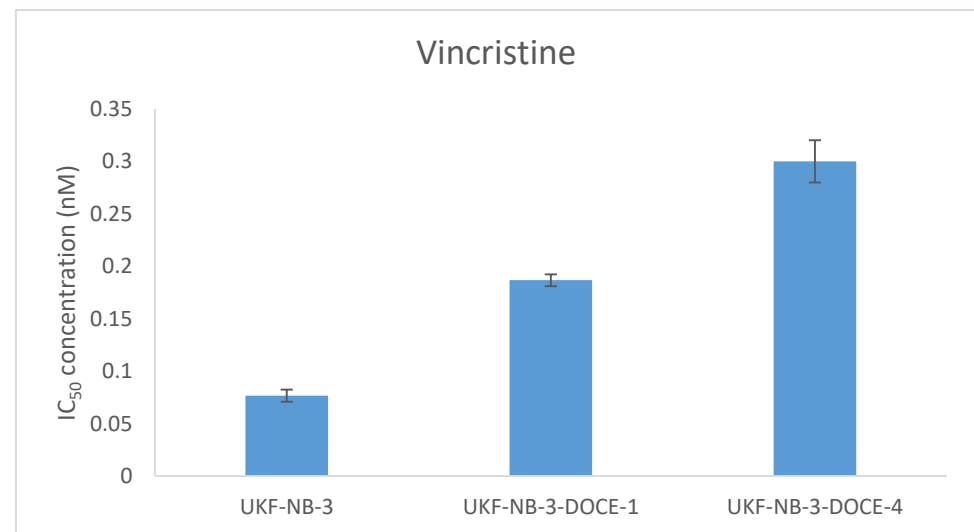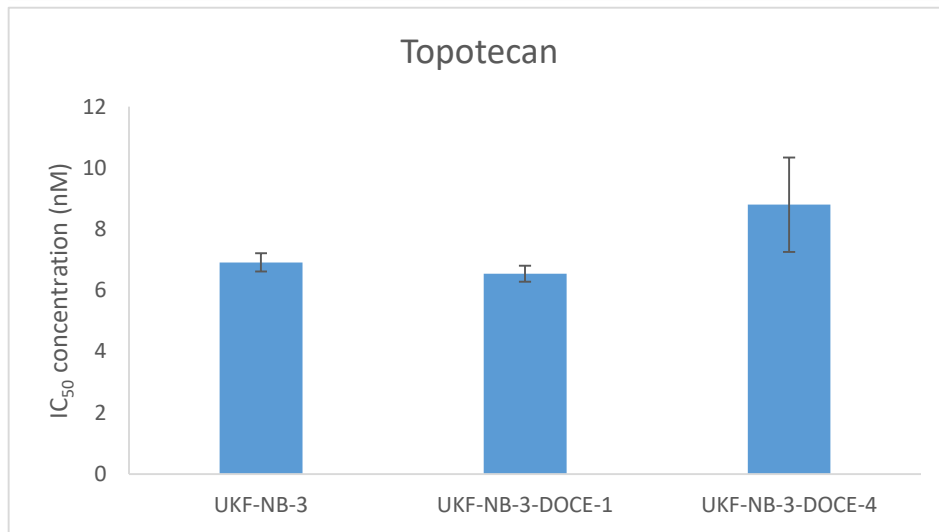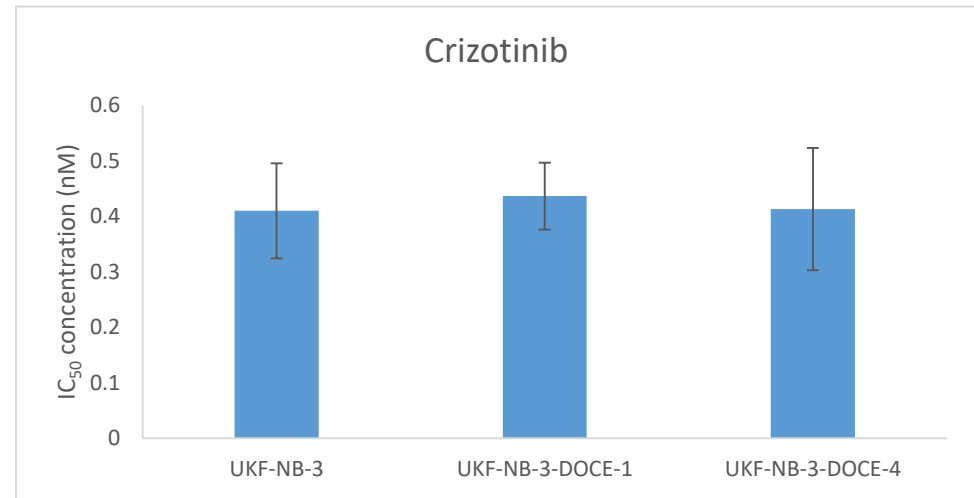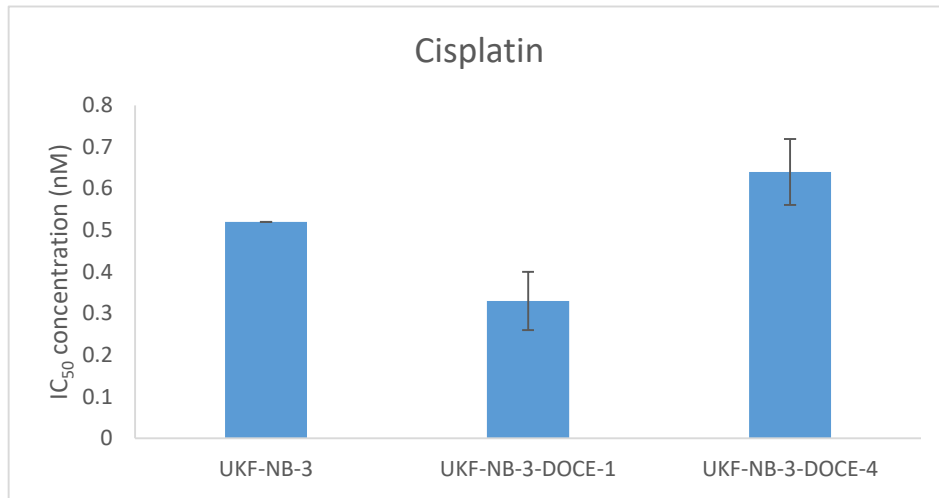
Figure 75E-H: Fold change difference of the docetaxel sublines relative to the sensitive cell line, UKF-NB-3. IC_{50} concentrations were derived from a 120-hour MTT assay. Results are averages of three biological repeats (n=3 ± SD).

Cell lines	Drugs							
	Docetaxel	Paclitaxel	Cabazitaxel	Epothilione-B	Cisplatin	Crizotinib	Vincristine	Topotecan
UKF-NB-3-DOCE-1	■ (more resistant)	(similar)	(similar)	■ (more resistant)	(similar)	(similar)	■ (more resistant)	(similar)
UKF-NB-3-DOCE-4	■ (more resistant)	(similar)	(similar)	(similar)	(similar)	(similar)	■ (more resistant)	(similar)

Legend:
- more sensitive than parental cell line
- similarly sensitive as parental cell line
- more resistant than parental cell line
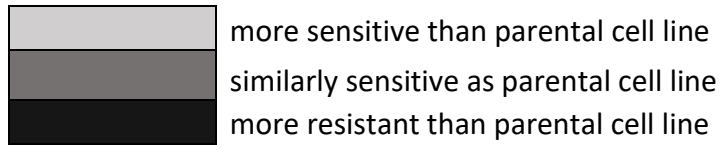
Figure 76 : **Heatmap of cross-resistance profiles of the docetaxel-treated sublines.** Heatmap image of comparative drug-resistance to the different anti-cancer drugs of the sublines cultivated in the presence of docetaxel.

7.5.7 Determination of cell sensitisation using zosuquidar and verapamil

UKF-NB-3-DOCE-4, but not UKF-NB-3-DOCE-1, was re-sensitised to docetaxel by the ABCB1 inhibitors zosuquidar and verapamil (Figure 77, Table 24). In agreement, only UKF-NB-3-DOCE-4, but not UKF-NB-3-DOCE-1, displayed increased ABCB1 protein levels (Figure 78-79) determined by immunofluorescence and western blot analysis. The antibody used had been used extensively in our lab. Immunostaining results indicated p-glycoprotein signal for all the sublines cultivated in docetaxel as well as the parental cell line. Despite the use of the secondary antibody alone used as a negative control, signal was identified which did not correlate with the western blot, which showed no p-glycoprotein expression for the parental and UKF-NB-DOCE-1. It can therefore be assumed that the immunofluorescence assay was ineffective in detecting the correct signal for the p-glycoprotein expression.
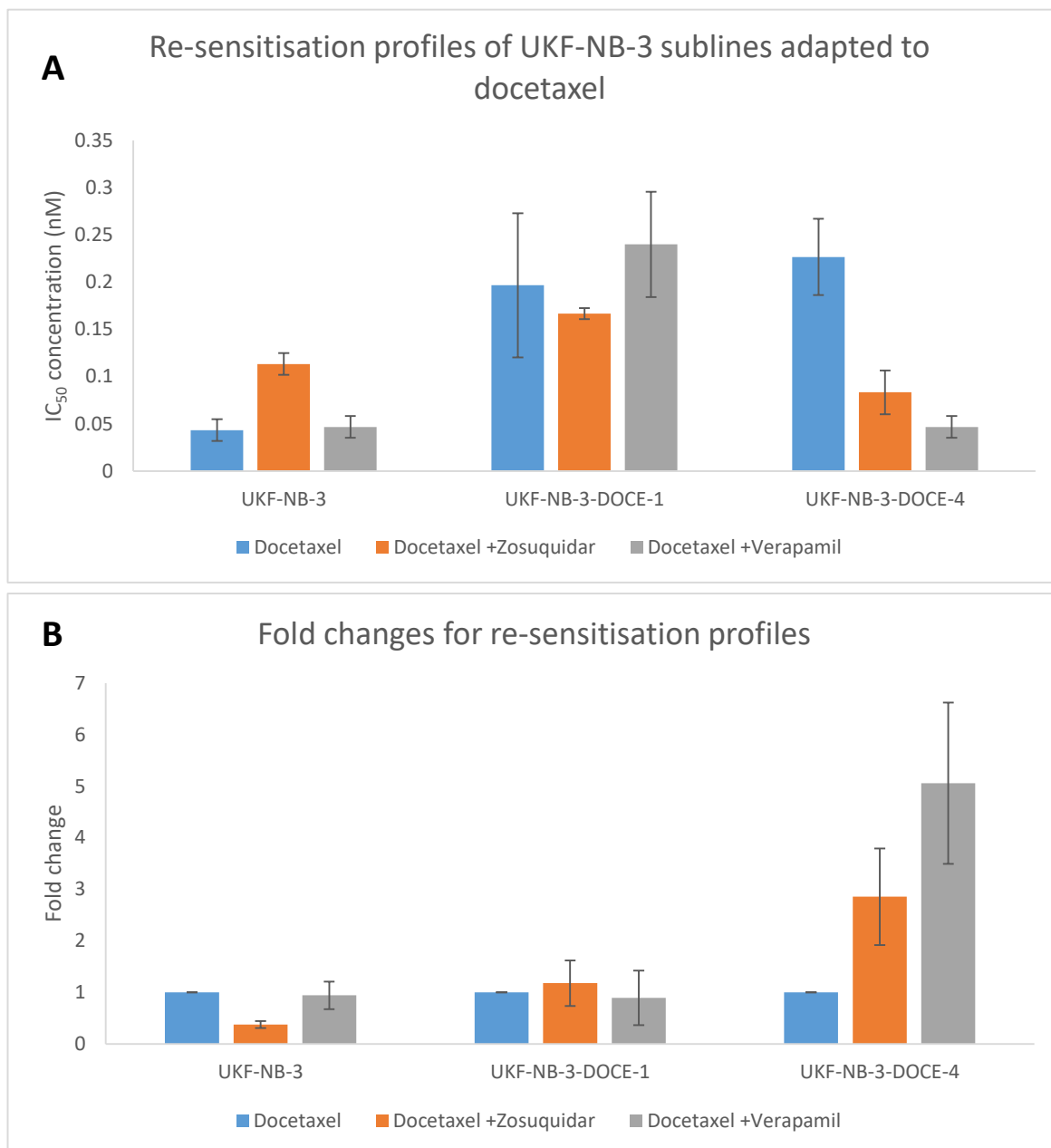
Figure 77 : A) IC$_{50}$ concentrations determined from a 120-hour MTT assay for the docetaxel sub-lines in comparison to UKF-NB-3. B) Fold change difference of docetaxel sublines treated with combinations of docetaxel with zosuquidar (1µM) and docetaxel with verapamil (10µM) in comparison to docetaxel alone. Results show increased sensitivity effects on the cells' viability when combinational therapies were used to the level of the UKF-NB-3. Each result was derived from three biological repeats of MTT assays (n=3 ± SD).

Cell line	Docetaxel IC50 (nM)[1]	Docetaxel+Zosuquidar IC50 (nM)[1]	Docetaxel+Verapamil IC50 (nM)[1]
UKF-NB-3	0.04 ± 0.01	0.11 ± 0.01	0.05 ± 0.01
UKF-NB-3-DOCE-1	0.20 ± 0.08	0.17 ± 0.01	0.24 ± 0.06
UKF-NB-3-DOCE-4	0.23 ± 0.04	0.08 ± 0.02	0.05 ± 0.01

	Fold change[2]	
Cell line	Docetaxel+Zosuquidar (nM)	Docetaxel+Verapamil (nM)
UKF-NB-3	0.38 ± 0.07	0.94 ± 0.27
UKF-NB-3-DOCE-1	1.18 ± 0.44	0.90 ± 0.53
UKF-NB-3-DOCE-4	2.86 ± 0.94	5.06 ± 1.56

Table 24 : **Effect s of docetaxel alone or in combination with zosuquidar (1µM) or verapamil (10µM) on the docetaxel-treated sublines and parental cell line in comparison.** [1] The IC50 concentrations were determined by MTT assay after 120h of incubation. Results are expressed as an average of three independent experiments (n=3 ± SD). [2] docetaxel IC50/ Docetaxel IC50 in the presence of zosuquidar or verapamil.
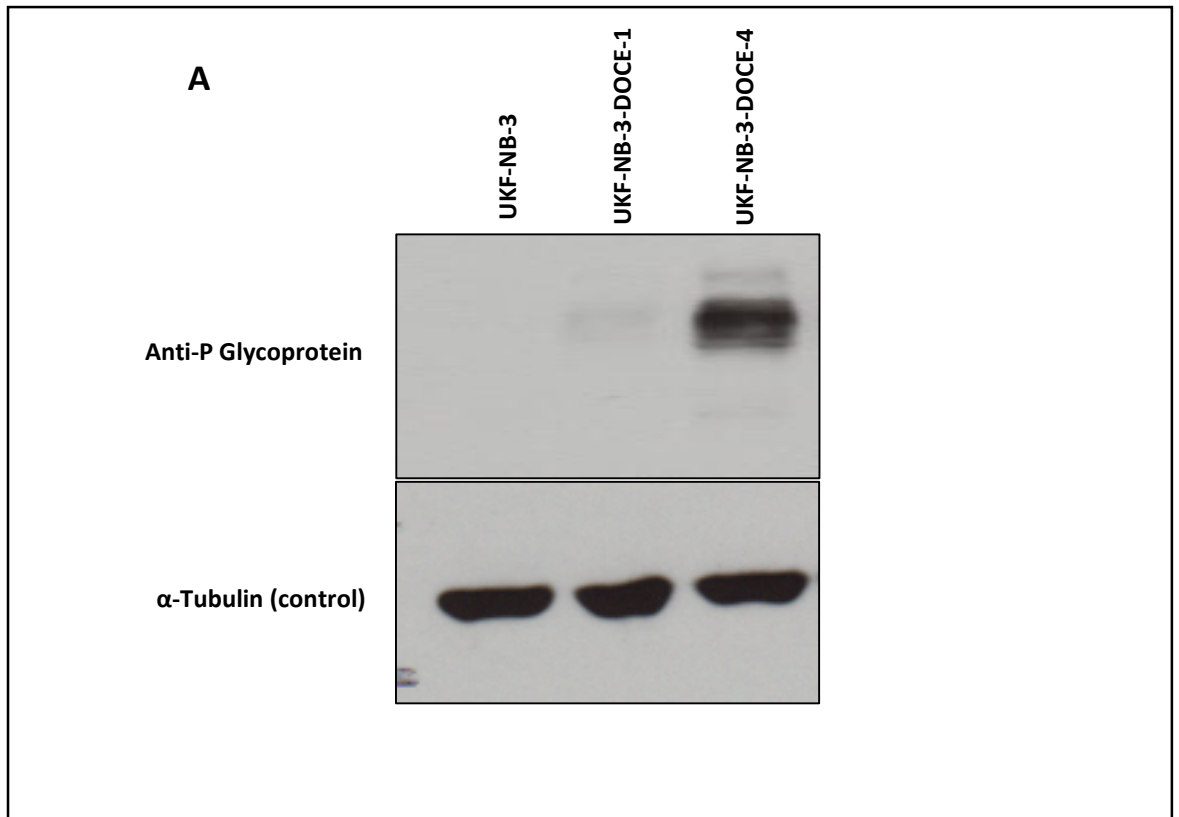
Figure 78 : ABCB1 protein levels as determined by Western blot. α-tubulin was used as a loading control. Results are representative of three independent experiments.

UKF-NB-3

| AlexFluor™488 | DAPI | Overlay |

UKF-NB-3-DOCE-1

| AlexFluor™488 | DAPI | Overlay |

UKF-NB-3-DOCE-4

| AlexFluor™488 | DAPI | Overlay |
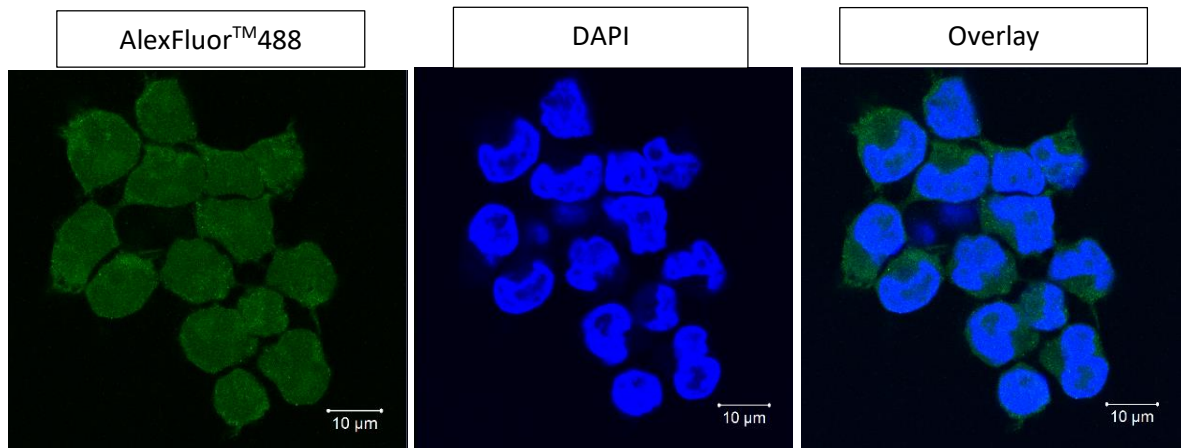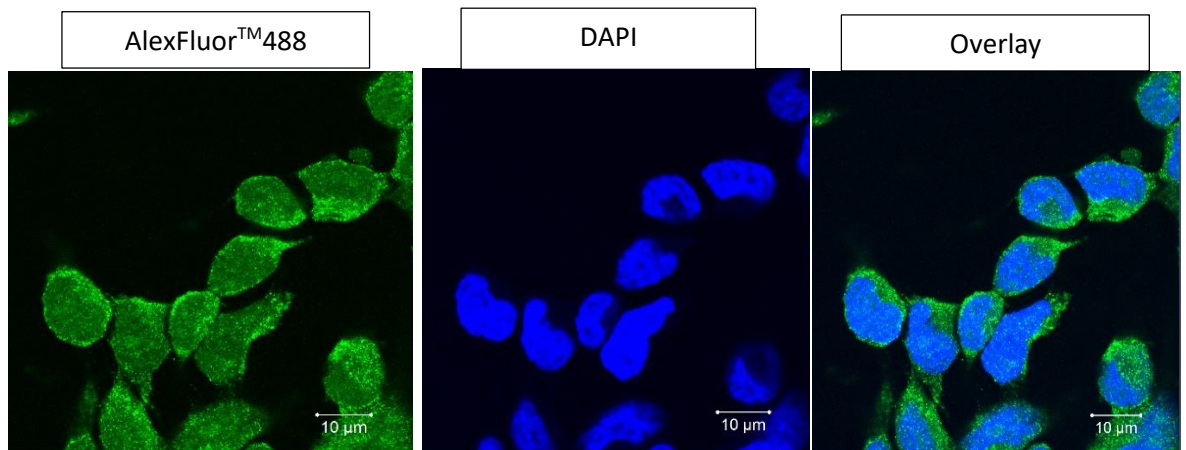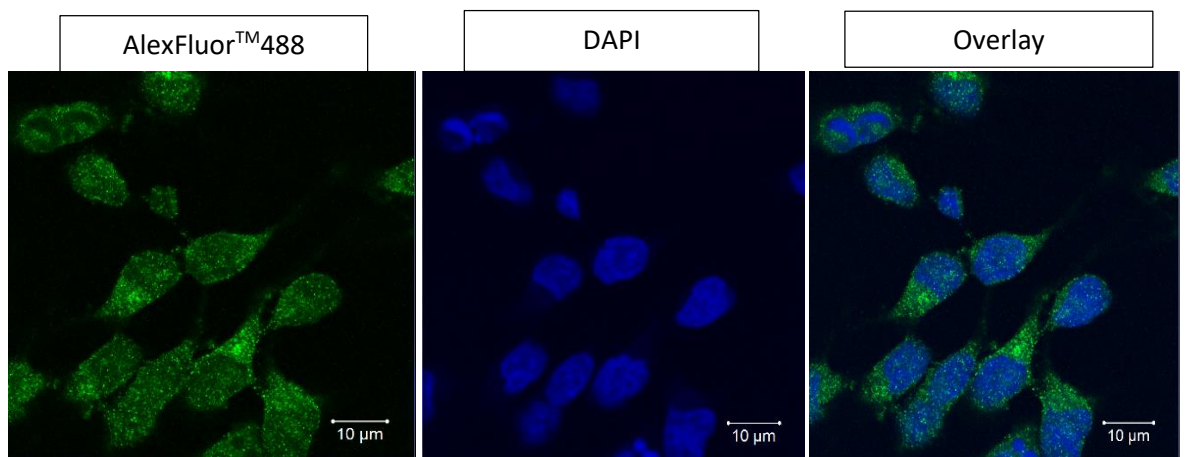
Figure 79 : **Immunofluorescent images of the docetaxel adapted sublines and sensitive cell line using anti-p glycoprotein.** Images generated using LSM 880 Elyra Airyscan (NLO) confocal microscope. Immunofluorescence results shown as DAPI (blue), Anti-P Glycoprotein (green) and merged images; all images taken at x 40 magnification (Scale bars = 10 µM.

7.6 Discussion

The development of resistance over time following exposure to a chemotherapeutic agent is known as acquired resistance, which serves as a major obstacle to therapeutic efficacy (Fojo & Menefee, 2007); (Rivera, 2010).

Within this project, we have developed the first standardised protocol to compare the capability of inducing resistance between different drugs. We used the four tubulin-binding agents; docetaxel, paclitaxel, cabazitaxel and epothilione-B as example drugs. Five sublines of the neuroblastoma cell line UKF-NB-3 were treated intermittently one week in the presence and once week in the absence of the IC_{50} concentration of the indicated drugs in the same way. Although the taxanes docetaxel, paclitaxel, and cabazitaxel are anticipated to share a common mechanism of anti-cancer action and the mechanism of epothilione-B is anticipated to be very similar (Kavallaris, 2010), the outcomes significantly differed between these drugs. The sublines treated with cabazitaxel and epothilione-B did not survive the standardised treatment protocol, while two docetaxel- and two paclitaxel-treated sublines survived until the end of the project. Notably, the two docetaxel-treated sublines had developed resistance defined as a >2-fold increased IC_{50} value relative to the parental cells, while the two paclitaxel-treated sublines did not display notable resistance. This indicates that docetaxel has an increased potential to induce resistance in UKF-NB-3 cells than the other tested compounds, in particular cabazitaxel and epothlilione-B. Interestingly, these findings are in agreement with the observation that it is more difficult to establish cabazitaxel- and epothilione-B-resistant UKF-NB-3 sublines by empirical continuous exposure to stepwise increasing drug concentrations than docetaxel- or paclitaxel-resistant UKF-NB-3 sublines. The findings also suggest that it is, in principle, possible to directly compare the potential of anti-cancer drugs to induce resistance using a standardised incubation protocol in cancer cell lines.

Although the establishment of drug adapted cancer cell lines can be strenuous and time-consuming, they have been successful in validating genetic sequences to find mutations and identifications of pathways and protein expressions to specific anticancer drugs (Xavier et al., 2016). Currently, research is still being conducted on a protocol for the development of the drug resistant cancer cell lines. So far, most methods include drug-dose escalation, whereby the cancer cells are exposed to increasing concentrations of the drug until proliferation diminishes whilst others include pulsing (on and off cultivation of cells in drug); which has noteably resulted in higher resistance levels (Breen et al., 2008). The successful generation of cisplatin, docetaxel and 5-fluorouracil (5-FU) head and neck cancer cell lines used the pulse method and provided clinics with insights on the mechanism of resistance as well as the appropriate drug use when relapse is apparent such as cross-resistance profiles to other platinum and taxol drugs and gene expressions responsible for the acquired drug resistance (Govindan,et al., 2015). Other successes include the development of acquired radio-resistant breast cancer cell lines MDA-MB-231, MCF-7 and ZR-751 which were

exposed to increasing concentrations of ionising radiotherapy and highlighted the differences in phenotypic and genotypic profiles such as EGFR signalling pathways along with MAPK and PI3K (Gray et al., 2019). Resistance models can also be developed using different cancer cell lines treated with different concentrations of an anti-cancer drug (Stordal and Davey 2007). As acquired resistance remains an impediment in effective treatment, the development of these drug-adapted cancer cell lines increases the significance of personalised medicine for clinics as they are able to understand how treatments with similarities or differences in the mechanisms of action, contribute to the disease reoccurrence and progression (Steding 2016); (Jordan et al., 2015); (Tong et al., 2015). The characterisation of the developed resistant cancer cell lines also provides a brief understanding of the duration of adaptation and resistance (Gillet et al., 2011); (Zhang et al., 2010).

The reasons for the discrepancies highlighted in our research are not entirely clear. Docetaxel and paclitaxel are both substrates of the ABC transporter ABCB1 (Vrignaud et al., 2014). The efficacy of cabazitaxel seems to be affected by ABCB1 to a lower degree than that of docetaxel and paclitaxel (Szakács et al., 2006), (George E. Duran et al., 2018), (Reynolds et al., 2015), (G. E. Duran et al., 2015). Epothlilone-B does not seem to be a subject of ABCB1-mediated resistance (Kowalski, Giannakakou, & Hamel, 1997). In this context, one of the docetaxel-treated sublines (UKF-NB-3-DOCE-4) displayed increased ABCB1 expression and was partially resensitised to docetaxel by ABCB1 inhibition whilst the other (UKF-NB-3-DOCE-1) showed the no expression and was not resensitised to docetaxel by ABCB1 inhibition. Reasons for this remains unclear as the cellular resistance to taxanes (paclitaxel and docetaxel) are mediated by the expression of ABCB1 (Galletti et al., 2007); (Hwang 2012); (Jaramillo et al., 2018). Research has demonstrated that there are up to 9 human multidrug resistance proteins (MRPs) which belong to the ABCB1 superfamily (Zhang et al., 2015); (Jiang et al., 2017). It may therefore serve as a reason why differences were observed in the sublines adapted to the same drug. Some studies have also shown that not all docetaxel resistant cells express ABCB1 suggesting that further research on other drug transporters is required (Wang et al., 2014); (Kanzaki et al., 2001).

UKF-NB-3-DOCE-4 also showed cross-resistance to the ABCB1 substrates vincristine and docetaxel but not to the tested non-ABCB1 substrate. Hence, an increased potential to induce ABCB1 may contribute to the increased potential to induce resistance observed for docetaxel. However, the processes underlying resistance formation seem to be complex, which is indicated by a lack of ABCB1 expression in UKF-NB-3-DOCE-1.

Taken together, the findings indicate that standardised treatment can, in principal, be used to compare the potential of anti-cancer drugs to induce resistance. In addition, they emphasise the complexity of the processes underlying resistance formation even if the sublines of a cell line are treated by a defined treatment protocol.

8 Conclusion

8.1 Use of drug-adapted cancer cell lines

The occurrence of resistance is a major reason for the failure of systemic anti-cancer therapies. Resistance can be intrinsic, i.e. a tumour does not show a therapy response from the beginning. However, many tumours respond initially well to the used therapies before resistant cancer cells emerge, eventually resulting in therapy failure (acquired resistance) (Holohan et al., 2013; Fenton et al., 2018).

Preclinical model systems are required to complement clinical data and clinical materials to study systematically the processes underlying resistance formation. Preclinical model systems enable the performance of systems level and functional studies that are not possible by the use of clinical material. Drug-adapted cancer cell lines have been used at least since 1960 to study acquired drug resistance in cancer (Goldstein, Slotnick, & Journey, 1960) and numerous clinically relevant drug resistance mechanisms have been identified in drug-adapted cancer cell lines (Nazarian et al., 2010); (Poulikakos et al., 2011); (Joseph et al., 2013); (Korpal et al., 2013); (Zahreddine et al., 2014); (Crystal et al., 2014); (Hata et al., 2016); (Niederst et al., 2015); (Göllner et al., 2017).

This thesis was focused on the further development and investigation of drug-adapted cancer cell lines as models. A novel set of cisplatin-adapted ovarian cancer cell lines was introduced and characterised. In addition, the potential of nanoparticle-bound doxorubicin to overcome transporter-mediated resistance was studied in doxorubicin- and vincristine-resistant cells. Finally, a standardised treatment protocol was used for the first time to directly compare the potential of different anti-cancer drugs to induce resistance.

The investigation of doxorubicin-loaded PLA, PLGA, PLGA-PEG, and HSA resulted in a number of novel and relevant findings. Studies had already demonstrated that nanoparticles can in principle circumvent transporter-mediated drug efflux (Li et al., 2016); (Niazi et al., 2016); (Yuan et al., 2016).

However, our findings added some further conceptual insights. They illustrated that the nanoparticle material is crucial. Among the nanoparticles prepared from different polymers, only HSA nanoparticles circumvented ABCB1-mediated resistance. More importantly, our results also re-emphasised the relevance of the multi-factorial and complex nature of anti-cancer drug resistance mechanisms and that this has to be considered during the design of strategies to overcome them. Although HSA nanoparticles completely circumvented ABCB1-mediated drug efflux, they did not re-sensitise doxorubicin-adapted cells to doxorubicin to the level of parental cells. This is most likely because doxorubicin-adapted cells have developed further resistance mechanisms in addition to ABCB1 expression. Given the small therapeutic window of clinical anti-cancer therapies (Wong, Barton, Acton, McLeod, & Halford, 2016); (Rivoirard et al., 2016);

(Marinello, Delcuratolo, & Capranico, 2018),), it appears likely that the remaining ABCB1-independent resistance levels may still result in therapy failure in a clinical setting.

In contrast, vincristine-adapted cells were re-sensitised to doxorubicin to the level of parental cells by encapsulation into HSA nanoparticles. This suggests that the vincristine-specific resistance mechanisms did, apart from ABCB1 expression, not mediate doxorubicin resistance. This also illustrates that an in-depth understanding of the resistance status of cancer cells is a prerequisite for the rational design of strategies to overcome them. Notably, ABCB1 inhibitors exerted similar effects like doxorubicin encapsulation into nanoparticles. Hence, the occurrence of multiple resistance mechanisms may have contributed to the failure of ABCB1 inhibitors in clinical trials (Szakács et al., 2006), and an improved understanding of the nature of resistance in individual cases may also result in strategies that more effectively use ABCB1 (and other transporter) inhibitors. This is of particular conceptual relevance, since novel anti-cancer drugs are typically tested in highly resistant patient cohorts after the failure of all available treatment options (Harrington, Hernandez-Guerrero, & Basu, 2017); (Cook, Hansen, Siu, & Abdul Razak, 2015).

The treatment of cancer cells following a defined protocol to compare the potential of anti-cancer drugs to induce resistance also yielded encouraging results. Although drugs with a very similar mechanism of action were used the assay revealed significant differences in the potential to induce resistance. Reasons for this include the differences in the substrates affinity for P-gp ATP dependent drug efflux pump (Ughachukwu and Unekwe 2012); (Orr et al., 2003).

8.2 Further approaches

Additional research will be needed to understand the development of drug resistant cancer cell lines using a standardised approach, since it seems reasonable to assume that drugs may not only differ in their acute effects on cancer cells but also (even or in particular if they induce similar acute effects) in their potential to cause resistance a better understanding of this would inform the design of more efficient therapies.

Well established approaches such as next-generation sequencing (NGS) analysis provides genome-wide genetic alterations in resistant cancer samples and their matched parental cells for the identification of mutations associated with drug resistance (Abaan et al., 2013); (Song et al., 2019). This analysis enables scanning of genomes for changes such as mutations, deletions and alterations of chromosomal copy number (Chang et al., 2011); (Behjati and Tarpey 2013).

Research has demonstrated pipelines such as exome processing, whole transcriptome (RNA-seq) processing and integrated variant analysis have successfully validated high-throughput sequencing data generated from three pancreatic cancer cell lines showing significant differences (Garnett and McDermott 2014); (Goecks et al., 2015).

Using such analysis exhibits the dynamic changes of the tumour microenvironment such as miRNA mutations which may be driving the resistance in specific anticancer drugs of specific cancer types (Beaufort et al., 2014). Evidence to support the use of whole genome sequencing of ovarian cancer cell lines, includes that from Previs et al., 2016, which revealed that there was a number of loss-of-function mutations such as BRCA1/BRCA2 and DNA repair genes such as BARD1, BRIP1, CHEK2, MRE11A, MSH6, NBN, PALB2, RAD50, RAD51C, or TP53 identified within the same six ovarian cancer cell lines which were not previously identified along with other examples (Parca et al., 2019); (Yang et al., 2013); (O'Donovan and Livingstone 2010); (Previs et al., 2016).

Another approach which can be used for further analysis is the determination of gene expression profiles to characterise cell properties and status to identify the drug-gene correlations (Fernández-Torras et al., 2019). These gene expression profiles may serve as a useful tool for gene therapy. A study which used preclinical models of breast, liver and colon cancer demonstrated the potency a specific drug, pyrvinium pamoate, in changing the cancer-associated gene expression revealing specific therapeutic targets (Chen et al., 2017). Another successful study using such method includes the use of transcriptomic and protein analysis of small-cell bladder cancer (SCBC) for the identification of the prognostic biomarkers driving resistance (Koshkin et al., 2019). Such profiles when used, increase therapeutic options, address important challenges for accurate evaluation of patient prognosis and predicts the sensitivity to specific treatments and drug combinations (Szalat et al., 2016); (Reis-Filho and Pusztai 2011); (Nasser 2009); (Van't Veer et al., 2002). In addition, researchers are able to fully exploit the genetic-therapeutic strategy by treating the resistant cancer cells with inhibitors and then identifying the targeted mutations to fully understand the advantages and limitations of the chemotherapeutic drugs for better design (Sellers 2011); (Shen et al., 2018).

Short tandem repeats (STR) analysis can be used to track genetic mutations in cancer by amplifying and analysing the loci and comparing the profiles to reference samples (Wu et al., 2018); (Promega 2012). Using this form of research could enable the comparison of the short tandem repeats of the developed drug-adapted cancer cell lines (acquired resistance) with pre-existing drug-adapted cancer cell lines (intrinsic resistance) for better understanding of the genetic mutations, tumour suppressor genes or proto-oncogenes. More specific comparisons can also be made such as the determination of the genetic changes examining the STR loci, single nucleotide polymorphisms, detection of the DNA duplications, deletions or other mutations to help identify key chromosomal regions that are altered during the course of the disease (Turajlic et al., 2012); (Walker et al., 2006); (Paulsson et al., 2003); (Costa et al., 2011).

In this context, researchers have identified genes with unstable short tandem repeats in the tumour-suppressor p53 pathway and changes associated gene expression in 35 colorectal cancers

discovering instabilities in the MAPK and Wnt signalling pathways, expressed at higher levels, playing a significant oncogenic role in the cancer (Sonay et al., 2015).

The projects discussed here involved a long-term culture which may affect the generation of drug-resistance of the cell lines. By using STR analysis, we can reveal if the same profile is maintained throughout the culturing duration to indicate the stability and heterogeneity of the cancer cells as long-term culture can lead to marked alterations in STR which serves as a useful tool in identifying possible resistance mechanism (Parson et al., 2005).

In conclusion, this project has contributed to resistance research in cancer by introducing novel models, by providing novel insights into the prospects and limitations of strategies to overcome resistance mediated by transporter-mediated drug efflux, and by developing a novel strategy to assess the potential of anti-cancer drugs to induce resistance.

8 Bibliography

Adams, G., Zekri, J., Wong, H., Walking, J., & Green, J. A. (2010). Platinum-based adjuvant chemotherapy for early-stage epithelial ovarian cancer: Single or combination chemotherapy? *BJOG: An International Journal of Obstetrics and Gynaecology*. https://doi.org/10.1111/j.1471-0528.2010.02635.x

Ai, Z., Lu, Y., Qiu, S., & Fan, Z. (2016). Overcoming cisplatin resistance of ovarian cancer cells by targeting HIF-1-regulated cancer metabolism. *Cancer Letters*. https://doi.org/10.1016/j.canlet.2016.01.009

Al-Batran, S. E., Geissler, M., Seufferlein, T., & Oettle, H. (2014). Nab-paclitaxel for metastatic pancreatic cancer: Clinical outcomes and potential mechanisms of action. *Oncology Research and Treatment*. https://doi.org/10.1159/000358890

Amable, L. (2016). Cisplatin resistance and opportunities for precision medicine. *Pharmacological Research*. https://doi.org/10.1016/j.phrs.2016.01.001

Ameller, T., Marsaud, V., Legrand, P., Gref, R., Barratt, G., & Renoir, J. M. (2003). Polyester-poly(ethylene glycol) nanoparticles loaded with the pure antiestrogen RU 58668: Physicochemical and opsonization properties. *Pharmaceutical Research*. https://doi.org/10.1023/A:1024418524688

Abaan, O. D., Polley, E. C., Davis, S. R., Zhu, Y. J., Bilke, S., Walker, R. L., Pineda, M., Gindin, Y., Jiang, Y., Reinhold, W. C., Holbeck, S. L., Simon, R. M., Doroshow, J. H., Pommier, Y., & Meltzer, P. S. (2013). The exomes of the NCI-60 panel: A genomic resource for cancer biology and systems pharmacology. *Cancer Research*. https://doi.org/10.1158/0008-5472.CAN-12-3342

Arora, A., & Scholar, E. M. (2005). Role of tyrosine kinase inhibitors in cancer therapy. In *Journal of Pharmacology and Experimental Therapeutics*. https://doi.org/10.1124/jpet.105.084145

Abal, M., Andreu, J., & Barasoain, I. (2005). Taxanes: Microtubule and Centrosome Targets, and Cell Cycle Dependent Mechanisms of Action. *Current Cancer Drug Targets*. https://doi.org/10.2174/1568009033481967

Arango, D., Wilson, A. J., Shi, Q., Corner, G. A., Arañes, M. J., Nicholas, C., Lesser, M., Mariadason, J. M., & Augenlicht, L. H. (2004). Molecular mechanisms of action and prediction of response to oxaliplatin in colorectal cancer cells. *British Journal of Cancer*. https://doi.org/10.1038/sj.bjc.6602215

Alian, O. M., Azmi, A. S., & Mohammad, R. M. (2012). Network insights on oxaliplatin anti-cancer mechanisms. *Clinical and Translational Medicine*. https://doi.org/10.1186/2001-1326-1-26

Ardizzoni, A., Boni, L., Tiseo, M., Fossella, F. V., Schiller, J. H., Paesmans, M., Radosavljevic, D., Paccagnella, A., Zatloukal, P., Mazzanti, P., Bisset, D., & Rosell, R. (2007). Cisplatin- versus carboplatin-based chemotherapy in first-line treatment of advanced non-small-cell lung cancer: an individual patient data meta-analysis. *Journal of the National Cancer Institute*. https://doi.org/10.1093/jnci/djk196.

Alcindor, T., & Beauger, N. (2011). Oxaliplatin: A review in the era of molecularly targeted therapy. *Current Oncology*. https://doi.org/10.3747/co.v18i1.708

Allison, K. H., & Sledge, G. W. (2014). Heterogeneity and cancer. In *ONCOLOGY (United States)*.

Baetke, S. C., Lammers, T., & Kiessling, F. (2015). Applications of nanoparticles for diagnosis and therapy of cancer. *British Journal of Radiology*. https://doi.org/10.1259/bjr.20150207

Bar-Zeev, M., Livney, Y. D., & Assaraf, Y. G. (2017). Targeted nanomedicine for cancer therapeutics: Towards precision medicine overcoming drug resistance. *Drug Resistance Updates*. https://doi.org/10.1016/j.drup.2017.05.002

Bilgin Sonay, T., Koletou, M., & Wagner, A. (2015). A survey of tandem repeat instabilities and associated gene expression changes in 35 colorectal cancers. *BMC Genomics*. https://doi.org/10.1186/s12864-015-1902-9

Beaufort, C. M., Helmijr, J. C. A., Piskorz, A. M., Hoogstraat, M., Ruigrok-Ritstier, K., Besselink, N., Murtaza, M., Van IJcken, W. F. J., Heine, A. A. J., Smid, M., Koudijs, M. J., Brenton, J. D., Berns, E. M. J. J., & Helleman, J. (2014). Ovarian cancer cell line panel (OCCP): Clinical importance of in vitro morphological subtypes. *PLoS ONE*. https://doi.org/10.1371/journal.pone.0103988

Behjati, S., & Tarpey, P. S. (2013). What is next generation sequencing? *Archives of Disease in Childhood: Education and Practice Edition*. https://doi.org/10.1136/archdischild-2013-304340

Breen, L., Murphy, L., Keenan, J., & Clynes, M. (2008). Development of taxane resistance in a panel of human lung cancer cell lines. *Toxicology in Vitro*. https://doi.org/10.1016/j.tiv.2008.04.005

Bethune, G., Bethune, D., Ridgway, N., & Xu, Z. (2010). Epidermal growth factor receptor (EGFR) in lung cancer: An overview and update. In *Journal of Thoracic Disease*.

Baskar, R., Lee, K. A., Yeo, R., & Yeoh, K. W. (2012). Cancer and radiation therapy: Current advances and future directions. In *International Journal of Medical Sciences*. https://doi.org/10.7150/ijms.3635

Banerji, S., & Los, M. (2006). Important Differences between Topoisomerase-I and -II Targeting Agents. In *Cancer Biology and Therapy*. https://doi.org/10.4161/cbt.5.8.3274

Bumbaca, B., & Li, W. (2018). Taxane resistance in castration-resistant prostate cancer: mechanisms and therapeutic strategies. In *Acta Pharmaceutica Sinica B*. https://doi.org/10.1016/j.apsb.2018.04.007

Barber, H. R. (1984). Ovarian cancer - diagnosis and management. *Australian Family Physician*, *150*(3), 130–133.

Burrell, R. A., McGranahan, N., Bartek, J., & Swanton, C. (2013). The causes and consequences of genetic heterogeneity in cancer evolution. *Nature*. https://doi.org/10.1038/nature12625

Borst, P., Rottenberg, S., & Jonkers, J. (2008). How do real tumors become resistant to cisplatin? In *Cell Cycle*. https://doi.org/10.4161/cc.7.10.5930

Borrell, B. (2010). How accurate are cancer cell lines? In *Nature*. https://doi.org/10.1038/463858a

Callaghan, R., Luk, F., & Bebawy, M. (2014). Inhibition of the multidrug resistance P-glycoprotein: Time for a change of strategy? *Drug Metabolism and Disposition*. https://doi.org/10.1124/dmd.113.056176

Casals, E., Gusta, M. F., Cobaleda-Siles, M., Garcia-Sanz, A., & Puntes, V. F. (2017). Cancer resistance to treatment and antiresistance tools offered by multimodal multifunctional nanoparticles. *Cancer Nanotechnology*. https://doi.org/10.1186/s12645-017-0030-4

Chen, Y., Mohanraj, V. J., & Parkin, J. E. (2003). Chitosan-dextran sulfate nanoparticles for delivery of an anti-angiogenesis peptide. *Letters in Peptide Science*. https://doi.org/10.1007/BF02442596

Chhikara, B. S., Mandal, D., & Parang, K. (2012). Synthesis, anticancer activities, and cellular uptake studies of lipophilic derivatives of doxorubicin succinate. *Journal of Medicinal Chemistry*. https://doi.org/10.1021/jm201653u

Cole, S. P. C., Bhardwaj, G., Gerlach, J. H., Mackie, J. E., Grant, C. E., Almquist, K. C., … Deeley, R. G. (1992). Overexpression of a transporter gene in a multidrug-resistant human lung cancer cell line. *Science*. https://doi.org/10.1126/science.1360704

Cook, N., Hansen, A. R., Siu, L. L., & Abdul Razak, A. R. (2015). Early phase clinical trials to identify optimal dosing and safety. *Molecular Oncology*. https://doi.org/10.1016/j.molonc.2014.07.025

Corrigan, O. I., & Li, X. (2009). Quantifying drug release from PLGA nanoparticulates. *European Journal of Pharmaceutical Sciences*. https://doi.org/10.1016/j.ejps.2009.04.004

Crystal, A. S., Shaw, A. T., Sequist, L. V., Friboulet, L., Niederst, M. J., Lockerman, E. L., … Engelman, J. A. (2014). Patient-derived models of acquired resistance can identify effective drug combinations for cancer. *Science*. https://doi.org/10.1126/science.1254721

Costa, E. O. A., Silva, D. D. M. E., Melo, A. V. De, Godoy, F. R., Nunes, H. F., Pedrosa, E. R., Flores, B. C., Rodovalho, R. G., Da Silva, C. C., & Da Cruz, A. D. (2011). The effect of low-dose exposure on germline microsatellite mutation rates in humans accidentally exposed to caesium-137 in Goiânia. *Mutagenesis*. https://doi.org/10.1093/mutage/ger028

Chen, B., Ma, L., Paik, H., Sirota, M., Wei, W., Chua, M. S., So, S., & Butte, A. J. (2017). Reversal of cancer gene expression correlates with drug efficacy and reveals therapeutic targets. *Nature Communications*. https://doi.org/10.1038/ncomms16022

Chang, H., Jackson, D. G., Kayne, P. S., Ross-Macdonald, P. B., Ryseck, R. P., & Siemers, N. O. (2011). Exome sequencing reveals comprehensive genomic alterations across eight cancer cell lines. *PLoS ONE*. https://doi.org/10.1371/journal.pone.0021097

Chen, H. H. W., & Kuo, M. T. (2013). Overcoming platinum drug resistance with copper-lowering agents. *Anticancer Research*.

Chen, H. H. W., Song, I. S., Hossain, A., Choi, M. K., Yamane, Y., Liang, Z. D., Lu, J., Wu, L. Y. H., Siddik, Z. H., Klomp, L. W. J., Savaraj, N., & Kuo, M. T. (2008). Elevated glutathione levels confer cellular sensitization to cisplatin toxicity by up-regulation of copper transporter hCtr1. *Molecular Pharmacology*. https://doi.org/10.1124/mol.108.047969

Chankova, S. G., Dimova, E., Dimitrova, M., & Bryant, P. E. (2007). Induction of DNA double-strand breaks by zeocin in Chlamydomonas reinhardtii and the role of increased DNA double-strand breaks rejoining in the formation of an adaptive response. *Radiation and Environmental Biophysics*. https://doi.org/10.1007/s00411-007-0123-2

Chiarle, R., Voena, C., Ambrogio, C., Piva, R., & Inghirami, G. (2008). The anaplastic lymphoma kinase in the pathogenesis of cancer. In *Nature Reviews Cancer*. https://doi.org/10.1038/nrc2291

Campling, B. G. (2006). The problem of platinum resistance. In *Cancer Biology and Therapy*. https://doi.org/10.4161/cbt.5.9.3368

Champoux, J. J. (2001). DNA Topoisomerases: Structure, Function, and Mechanism. *Annual Review of Biochemistry*. https://doi.org/10.1146/annurev.biochem.70.1.369

Cheung-Ong, K., Giaever, G., & Nislow, C. (2013). DNA-damaging agents in cancer chemotherapy: Serendipity and chemical biology. In *Chemistry and Biology*. https://doi.org/10.1016/j.chembiol.2013.04.007

Cheng, K. L., Bradley, T., & Budman, D. R. (2008). Novel microtubule-targeting agents - the epothilones. In *Biologics: Targets and Therapy*. https://doi.org/10.2147/btt.s3487

Crown, J., & O'Leary, M. (2000). The taxanes: An update. In *Lancet*. https://doi.org/10.1016/S0140-6736(00)02074-2

Choi, Y., & Yu, A.-M. (2014). ABC Transporters in Multidrug Resistance and Pharmacokinetics, and Strategies for Drug Development. *Current Pharmaceutical Design*. https://doi.org/10.2174/13816128200514021416512

Chang, C., Bahadduri, P. M., Polli, J. E., Swaan, P. W., & Ekins, S. (2006). Rapid identification of P-glycoprotein substrates and inhibitors. *Drug Metabolism and Disposition*. https://doi.org/10.1124/dmd.106.012351

Cook, N., Jodrell, D. I., & Tuveson, D. A. (2012). Predictive in vivo animal models and translation to clinical trials. In *Drug Discovery Today*. https://doi.org/10.1016/j.drudis.2012.02.003

Damia, G., & Broggini, M. (2019). Platinum Resistance in Ovarian Cancer: Role of DNA Repair. *Cancers*. https://doi.org/10.3390/cancers11010119

Danaei, M., Dehghankhold, M., Ataei, S., Hasanzadeh Davarani, F., Javanmard, R., Dokhani, A., … Mozafari, M. R. (2018). Impact of particle size and polydispersity index on the clinical applications of lipidic nanocarrier systems. *Pharmaceutics*. https://doi.org/10.3390/pharmaceutics10020057

Danhier, F., Ansorena, E., Silva, J. M., Coco, R., Le Breton, A., & Préat, V. (2012). PLGA-based nanoparticles: An overview of biomedical applications. *Journal of Controlled Release*. https://doi.org/10.1016/j.jconrel.2012.01.043

Dasari, S., & Bernard Tchounwou, P. (2014). Cisplatin in cancer therapy: Molecular mechanisms of action. *European Journal of Pharmacology*. https://doi.org/10.1016/j.ejphar.2014.07.025

Deshpande, P. P., Biswas, S., & Torchilin, V. P. (2013). Current trends in the use of liposomes for tumor targeting. *Nanomedicine*. https://doi.org/10.2217/nnm.13.118

Dhandapani, M., & Goldman, A. (2017). Preclinical Cancer Models and Biomarkers for Drug Development: New Technologies and Emerging Tools. *Journal of Molecular Biomarkers & Diagnosis*. https://doi.org/10.4172/2155-9929.1000356

Di Nicolantonio, F., Mercer, S. J., Knight, L. A., Gabriel, F. G., Whitehouse, P. A., Sharma, S., … Cree, I. A. (2005). Cancer cell adaptation to chemotherapy. *BMC Cancer*. https://doi.org/10.1186/1471-2407-5-78

Dilruba, S., & Kalayda, G. V. (2016). Platinum-based drugs: past, present and future. *Cancer Chemotherapy and Pharmacology*. https://doi.org/10.1007/s00280-016-2976-z

Domura, R., Sasaki, R., Ishikawa, Y., & Okamoto, M. (2017). Cellular Morphology-Mediated Proliferation and Drug Sensitivity of Breast Cancer Cells. *Journal of Functional Biomaterials*. https://doi.org/10.3390/jfb8020018

Dreis, S., Rothweiler, F., Michaelis, M., Cinatl, J., Kreuter, J., & Langer, K. (2007). Preparation, characterisation and maintenance of drug efficacy of doxorubicin-loaded human serum

albumin (HSA) nanoparticles. *International Journal of Pharmaceutics*. https://doi.org/10.1016/j.ijpharm.2007.03.036

Duran, G. E., Derdau, V., Weitz, D., Philippe, N., Blankenstein, J., Atzrodt, J., … Sikic, B. I. (2018). Cabazitaxel is more active than first-generation taxanes in ABCB1(+) cell lines due to its reduced affinity for P-glycoprotein. *Cancer Chemotherapy and Pharmacology*. https://doi.org/10.1007/s00280-018-3572-1

Duran, G. E., Wang, Y. C., Francisco, E. B., Rose, J. C., Martinez, F. J., Coller, J., … Sikic, B. I. (2015). Mechanisms of Resistance to Cabazitaxel. *Molecular Cancer Therapeutics*. https://doi.org/10.1158/1535-7163.MCT-14-0155

Da Cunha Santos, G., Shepherd, F. A., & Tsao, M. S. (2011). EGFR Mutations and Lung Cancer. *Annual Review of Pathology: Mechanisms of Disease*. https://doi.org/10.1146/annurev-pathol-011110-130206

Dezhenkova, L. G., Tsvetkov, V. B., & Shtil, A. A. (2014). Topoisomerase I and II inhibitors: chemical structure, mechanisms of action and role in cancer chemotherapy. *Russian Chemical Reviews*. https://doi.org/10.1070/rc2014v083n01abeh004363

Delgado, J. L., Hsieh, C. M., Chan, N. L., & Hiasa, H. (2018). Topoisomerases as anticancer targets. In *Biochemical Journal*. https://doi.org/10.1042/BCJ20160583

Drabløs, F., Feyzi, E., Aas, P. A., Vaagbø, C. B., Kavli, B., Bratlie, M. S., Peña-Diaz, J., Otterlei, M., Slupphaug, G., & Krokan, H. E. (2004). Alkylation damage in DNA and RNA - Repair mechanisms and medical significance. In *DNA Repair*. https://doi.org/10.1016/j.dnarep.2004.05.004

De Weger, V. A., Beijnenb, J. H., & Schellensa, J. H. M. (2014). Cellular and clinical pharmacology of the taxanes docetaxel and paclitaxel -A review. In *Anti-Cancer Drugs*. https://doi.org/10.1097/CAD.0000000000000093

Dasari, S., & Bernard Tchounwou, P. (2014). Cisplatin in cancer therapy: Molecular mechanisms of action. In *European Journal of Pharmacology*. https://doi.org/10.1016/j.ejphar.2014.07.025

de Sousa, G. F., Wlodarczyk, S. R., & Monteiro, G. (2014). Carboplatin: Molecular mechanisms of action associated with chemoresistance. In *Brazilian Journal of Pharmaceutical Sciences*. https://doi.org/10.1590/S1984-82502014000400004

Dilruba, S., & Kalayda, G. V. (2016). Platinum-based drugs: past, present and future. In *Cancer Chemotherapy and Pharmacology*. https://doi.org/10.1007/s00280-016-2976-z

Da Silva, V. A., Da Silva, K. A. E. P., Delou, J. M. A., Da Fonseca, L. M., Lopes, A. G., & Capella, M. A. M. (2014). Modulation of ABCC1 and ABCG2 proteins by ouabain in human breast cancer cells. *Anticancer Research*.

Day, C. P., Merlino, G., & Van Dyke, T. (2015). Preclinical Mouse Cancer Models: A Maze of Opportunities and Challenges. In *Cell*. https://doi.org/10.1016/j.cell.2015.08.068

Dagogo-Jack, I., & Shaw, A. T. (2018). Tumour heterogeneity and resistance to cancer therapies. In *Nature Reviews Clinical Oncology*. https://doi.org/10.1038/nrclinonc.2017.166

Eckstein, N. (2011). Platinum resistance in breast and ovarian cancer cell lines. *Journal of Experimental and Clinical Cancer Research*. https://doi.org/10.1186/1756-9966-30-91

Filipits, M. (2004). Mechanisms of cancer: Multidrug resistance. In *Drug Discovery Today: Disease Mechanisms*. https://doi.org/10.1016/j.ddmec.2004.10.001

Ferreira, D., Adega, F., & Chaves, R. (2013). The Importance of Cancer Cell Lines as in vitro Models in Cancer Methylome Analysis and Anticancer Drugs Testing. In *Oncogenomics and Cancer Proteomics - Novel Approaches in Biomarkers Discovery and Therapeutic Targets in Cancer*. https://doi.org/10.5772/53110

F. Bray, Jacques Ferlay, Isabelle Soerjomataram, Siegel;, R. L., Torre;, L. A., & Jemal, A. (2018). Global Cancer Statistics 2018: GLOBOCAN Estimates of Incidence and Mortality Worldwide for 36 Cancers in 185 Countries. *CA: A Cancer Journal for Clinicians*. https://doi.org/10.3322/caac.21492

Fojo, T., & Menefee, M. (2007). Mechanisms of multidrug resistance: The potential role of microtubule-stabilizing agents. In *Annals of Oncology*. https://doi.org/10.1093/annonc/mdm172

Fernández-Torras, A., Duran-Frigola, M., & Aloy, P. (2019). Encircling the regions of the pharmacogenomic landscape that determine drug response. *Genome Medicine*. https://doi.org/10.1186/s13073-019-0626-x

Frost, B. M., Eksborg, S., Björk, O., Abrahamsson, J., Behrendtz, M., Castor, A., Forestier, E., & Lönnerholm, G. (2002). Pharmacokinetics of doxorubicin in children with acute lymphoblastic leukemia: Multi-institutional collaborative study. *Medical and Pediatric Oncology*. https://doi.org/10.1002/mpo.10052

Fumoleau, P., Coudert, B., Isambert, N., & Ferrant, E. (2007). Novel tubulin-targeting agents: Anticancer activity and pharmacologic profile of epothilones and related analogues. *Annals of Oncology*. https://doi.org/10.1093/annonc/mdm173

Fuertes, M., Castilla, J., Alonso, C., & Pérez, J. (2012). Cisplatin Biochemical Mechanism of Action: From Cytotoxicity to Induction of Cell Death Through Interconnections Between Apoptotic and Necrotic Pathways. *Current Medicinal Chemistry*. https://doi.org/10.2174/0929867033368484

Fisher, R., Pusztai, L., & Swanton, C. (2013). Cancer heterogeneity: Implications for targeted therapeutics. In *British Journal of Cancer*. https://doi.org/10.1038/bjc.2012.581

Galluzzi, L., Senovilla, L., Vitale, I., Michels, J., Martins, I., Kepp, O., … Kroemer, G. (2012). Molecular mechanisms of cisplatin resistance. *Oncogene*. https://doi.org/10.1038/onc.2011.384

Goldstein, M. N., Slotnick, I. J., & Journey, L. J. (1960). IN VITRO STUDIES WITH HELA CELL LINES SENSITIVE AND RESISTANT TO ACTINOMYCIN D. *Annals of the New York Academy of Sciences*. https://doi.org/10.1111/j.1749-6632.1960.tb20171.x

Göllner, S., Oellerich, T., Agrawal-Singh, S., Schenk, T., Klein, H. U., Rohde, C., … Müller-Tidow, C. (2017). Loss of the histone methyltransferase EZH2 induces resistance to multiple drugs in acute myeloid leukemia. *Nature Medicine*. https://doi.org/10.1038/nm.4247

Gradinaru, V., Thompson, K. R., Zhang, F., Mogri, M., Kay, K., Schneider, M. B., & Deisseroth, K. (2007). Targeting and Readout Strategies for Fast Optical Neural Control In Vitro and In Vivo. *Journal of Neuroscience*. https://doi.org/10.1523/JNEUROSCI.3578-07.2007

Garnett, M. J., & McDermott, U. (2014). The evolving role of cancer cell line-based screens to define the impact of cancer genomes on drug response. In *Current Opinion in Genetics and Development*. https://doi.org/10.1016/j.gde.2013.12.002

Goecks, J., El-Rayes, B. F., Maithel, S. K., Khoury, H. J., Taylor, J., & Rossi, M. R. (2015). Open pipelines for integrated tumor genome profiles reveal differences between pancreatic cancer tumors and cell lines. *Cancer Medicine*. https://doi.org/10.1002/cam4.360

Gillet, J. P., Calcagno, A. M., Varma, S., Marino, M., Green, L. J., Vora, M. I., Patel, C., Orina, J. N., Eliseeva, T. A., Singal, V., Padmanabhan, R., Davidson, B., Ganapathi, R., Sood, A. K., Rueda, B. R., Ambudkar, S. V., & Gottesman, M. M. (2011). Redefining the relevance of established cancer cell lines to the study of mechanisms of clinical anti-cancer drug resistance. *Proceedings of the National Academy of Sciences of the United States of America*. https://doi.org/10.1073/pnas.1111840108

Gray, M., Turnbull, A. K., Ward, C., Meehan, J., Martínez-Pérez, C., Bonello, M., Pang, L. Y., Langdon, S. P., Kunkler, I. H., Murray, A., & Argyle, D. (2019). Development and characterisation of acquired radioresistant breast cancer cell lines. *Radiation Oncology*. https://doi.org/10.1186/s13014-019-1268-2

Govindan, S. V. aliyaveeda., Kulsum, S., Pandian, R. S. omasundar., Das, D., Seshadri, M., Hicks, W., Kuriakose, M. A. braha., & Suresh, A. (2015). Establishment and characterization of triple drug resistant head and neck squamous cell carcinoma cell lines. *Molecular Medicine Reports*. https://doi.org/10.3892/mmr.2015.3768

Galletti, E., Magnani, M., Renzulli, M. L., & Botta, M. (2007). Paclitaxel and docetaxel resistance: Molecular mechanisms and development of new generation taxanes. In *ChemMedChem*. https://doi.org/10.1002/cmdc.200600308

Galluzzi, L., Vitale, I., Michels, J., Brenner, C., Szabadkai, G., Harel-Bellan, A., Castedo, M., & Kroemer, G. (2014). Systems biology of cisplatin resistance: Past, present and future. In *Cell Death and Disease*. https://doi.org/10.1038/cddis.2013.428

Gillet, J. P., & Gottesman, M. M. (2010). Mechanisms of multidrug resistance in cancer. *Methods in Molecular Biology (Clifton, N.J.)*. https://doi.org/10.1007/978-1-60761-416-6_4

Gill, S. S., Anjum, N. A., Gill, R., Jha, M., & Tuteja, N. (2015). DNA damage and repair in plants under ultraviolet and ionizing radiations. In *Scientific World Journal*. https://doi.org/10.1155/2015/250158

Gómez-Miragaya, J., Palafox, M., Paré, L., Yoldi, G., Ferrer, I., Vila, S., Galván, P., Pellegrini, P., Pérez-Montoyo, H., Igea, A., Muñoz, P., Esteller, M., Nebreda, A. R., Urruticoechea, A., Morilla, I., Pernas, S., Climent, F., Soler-Monso, M. T., Petit, A., … González-Suárez, E. (2017). Resistance to Taxanes in Triple-Negative Breast Cancer Associates with the Dynamics of a CD49f+ Tumor-Initiating Population. *Stem Cell Reports*. https://doi.org/10.1016/j.stemcr.2017.03.026

Gradishar, W. (2009). Management of advanced breast cancer with the epothilone B analog, ixabepilone. In *Drug Design, Development and Therapy*. https://doi.org/10.2147/dddt.s3122

Galsky, M. D., Dritselis, A., Kirkpatrick, P., & Oh, W. K. (2010). Cabazitaxel. In *Nature Reviews Drug Discovery*. https://doi.org/10.1038/nrd3254

Guo, S., Jiang, X., Mao, B., & Li, Q. X. (2019). The design, analysis and application of mouse clinical trials in oncology drug development. *BMC Cancer*. https://doi.org/10.1186/s12885-019-5907-7

Gargiulo, G. (2018). Next-generation in vivo modeling of human cancers. In *Frontiers in Oncology*. https://doi.org/10.3389/fonc.2018.00429

Galuschka, C., Proynova, R., Roth, B., Augustin, H. G., & Muller-Decker, K. (2017). Models in translational oncology: A public resource database for preclinical cancer research. *Cancer Research*. https://doi.org/10.1158/0008-5472.CAN-16-3099

Gay, L., Baker, A. M., & Graham, T. A. (2016). Tumour Cell Heterogeneity. In *F1000Research*. https://doi.org/10.12688/f1000research.7210.1

Hadjesfandiari, N., & Parambath, A. (2018). Stealth coatings for nanoparticles: Polyethylene glycol alternatives. In *Engineering of Biomaterials for Drug Delivery Systems: Beyond Polyethylene Glycol*. https://doi.org/10.1016/B978-0-08-101750-0.00013-1

Harrington, J. A., Hernandez-Guerrero, T. C., & Basu, B. (2017). Early Phase Clinical Trial Designs – State of Play and Adapting for the Future. *Clinical Oncology*. https://doi.org/10.1016/j.clon.2017.10.005

Hata, A. N., Niederst, M. J., Archibald, H. L., Gomez-Caraballo, M., Siddiqui, F. M., Mulvey, H. E., … Engelman, J. A. (2016). Tumor cells can follow distinct evolutionary paths to become resistant to epidermal growth factor receptor inhibition. *Nature Medicine*. https://doi.org/10.1038/nm.4040

Holohan, C., Van Schaeybroeck, S., Longley, D. B., & Johnston, P. G. (2013). Cancer drug resistance: An evolving paradigm. *Nature Reviews Cancer*. https://doi.org/10.1038/nrc3599

Hui, R. C.-Y., Francis, R. E., Guest, S. K., Costa, J. R., Gomes, A. R., Myatt, S. S., … Lam, E. W.-F. (2008). Doxorubicin activates FOXO3a to induce the expression of multidrug resistance gene ABCB1 (MDR1) in K562 leukemic cells. *Molecular Cancer Therapeutics*. https://doi.org/10.1158/1535-7163.MCT-07-0397

Hwang, C. (2012). Overcoming docetaxel resistance in prostate cancer: A perspective review. *Therapeutic Advances in Medical Oncology*. https://doi.org/10.1177/1758834012449685

Huang, W., & Zhang, C. (2018). Tuning the Size of Poly(lactic-co-glycolic Acid) (PLGA) Nanoparticles Fabricated by Nanoprecipitation. *Biotechnology Journal*. https://doi.org/10.1002/biot.201700203

Housman, G., Byler, S., Heerboth, S., Lapinska, K., Longacre, M., Snyder, N., & Sarkar, S. (2014). Drug resistance in cancer: An overview. In *Cancers*. https://doi.org/10.3390/cancers6031769

Hecht, S. M. (2000). Bleomycin: New perspectives on the mechanism of action. In *Journal of Natural Products*. https://doi.org/10.1021/np990549f

Hao, F., Wang, S., Zhu, X., Xue, J., Li, J., Wang, L., Li, J., Lu, W., & Zhou, T. (2017). Pharmacokinetic-Pharmacodynamic Modeling of the Anti-Tumor Effect of Sunitinib Combined with Dopamine in the Human Non-Small Cell Lung Cancer Xenograft. *Pharmaceutical Research*. https://doi.org/10.1007/s11095-016-2071-5

Holmes, D. (2015). The problem with platinum. *Nature*. https://doi.org/10.1038/527s218a

Hendrikx, J. J. M. A., Beijnen, J. H., & Schinkel, A. H. (2014). P-gp and taxanes. In *Oncoscience*. https://doi.org/10.18632/oncoscience.56

Hernández-Vargas, H., Palacios, J., & Moreno-Bueno, G. (2007). Molecular profiling of docetaxel cytotoxicity in breast cancer cells: Uncoupling of aberrant mitosis and apoptosis. *Oncogene*. https://doi.org/10.1038/sj.onc.1210102

Hato, S. V., Khong, A., De Vries, I. J. M., & Lesterhuis, W. J. (2014). Molecular pathways: The immunogenic effects of platinum-based chemotherapeutics. *Clinical Cancer Research*. https://doi.org/10.1158/1078-0432.CCR-13-3141

Hodges, L. M., Markova, S. M., Chinn, L. W., Gow, J. M., Kroetz, D. L., Klein, T. E., & Altman, R. B. (2011). Very important pharmacogene summary: ABCB1 (MDR1, P-glycoprotein). *Pharmacogenetics and Genomics*. https://doi.org/10.1097/FPC.0b013e3283385a1c

Hogenesch, H., & Nikitin, A. Y. (2012). Challenges in pre-clinical testing of anti-cancer drugs in cell culture and in animal models. *Journal of Controlled Release*. https://doi.org/10.1016/j.jconrel.2012.02.031

Hsu, H. H., Chen, M. C., Baskaran, R., Lin, Y. M., Day, C. H., Lin, Y. J., Tu, C. C., Vijaya Padma, V., Kuo, W. W., & Huang, C. Y. (2018). Oxaliplatin resistance in colorectal cancer cells is mediated via activation of ABCG2 to alleviate ER stress induced apoptosis. *Journal of Cellular Physiology*. https://doi.org/10.1002/jcp.26406

Johnstone, T. C., & Lippard, S. J. (2013). The effect of ligand lipophilicity on the nanoparticle encapsulation of Pt(IV) prodrugs. *Inorganic Chemistry*. https://doi.org/10.1021/ic4010642

Joseph, J. D., Lu, N., Qian, J., Sensintaffar, J., Shao, G., Brigham, D., … Hager, J. H. (2013). A clinically relevant androgen receptor mutation confers resistance to second-generation antiandrogens enzalutamide and ARN-509. *Cancer Discovery*. https://doi.org/10.1158/2159-8290.CD-13-0226

Jordan, V. C., Curpan, R., & Maximov, P. Y. (2015). Estrogen receptor mutations found in breast cancer metastases integrated with the molecular pharmacology of selective ER modulators. *Journal of the National Cancer Institute*. https://doi.org/10.1093/jnci/djv075

Jiang, Z. S., Sun, Y. Z., Wang, S. M., & Ruan, J. S. (2017). Epithelial-mesenchymal transition: Potential regulator of ABC transporters in tumor progression. In *Journal of Cancer*. https://doi.org/10.7150/jca.19079

Jaramillo, A. C., Al Saig, F., Cloos, J., Jansen, G., & Peters, G. J. (2018). How to overcome ATP-binding cassette drug efflux transporter-mediated drug resistance? *Cancer Drug Resistance*. https://doi.org/10.20517/cdr.2018.02

Johnstone, T. C., Suntharalingam, K., & Lippard, S. J. (2016). The Next Generation of Platinum Drugs: Targeted Pt(II) Agents, Nanoparticle Delivery, and Pt(IV) Prodrugs. In *Chemical Reviews*. https://doi.org/10.1021/acs.chemrev.5b00597

Johnstone, T. C., Park, G. Y., & Lippard, S. J. (2014). Understanding and improving platinum anticancer drugs - Phenanthriplatin. *Anticancer Research*.

Ji, N., Yang, Y., Cai, C.-Y., Lei, Z.-N., Wang, J.-Q., Gupta, P., Teng, Q.-X., Chen, Z.-S., Kong, D., & Yang, D.-H. (2018). VS-4718 Antagonizes Multidrug Resistance in ABCB1- and ABCG2-

Overexpressing Cancer Cells by Inhibiting the Efflux Function of ABC Transporters. *Frontiers in Pharmacology*. https://doi.org/10.3389/fphar.2018.01236

Jackson, S. J., & Thomas, G. J. (2017). Human tissue models in cancer research: Looking beyond the mouse. In *DMM Disease Models and Mechanisms*. https://doi.org/10.1242/dmm.031260

Juliano, R. L., & Ling, V. (1976). A surface glycoprotein modulating drug permeability in Chinese hamster ovary cell mutants. *BBA - Biomembranes*. https://doi.org/10.1016/0005-2736(76)90160-7

Jung, J., Lee, J. S., Dickson, M. A., Schwartz, G. K., Le Cesne, A., Varga, A., … Watters, J. (2016). TP53 mutations emerge with HDM2 inhibitor SAR405838 treatment in de-differentiated liposarcoma. *Nature Communications*. https://doi.org/10.1038/ncomms12609

Jordan, M. A., & Wilson, L. (2004). Microtubules as a target for anticancer drugs. In *Nature Reviews Cancer*. https://doi.org/10.1038/nrc1317

Kavallaris, M. (2010). Microtubules and resistance to tubulin-binding agents. *Nature Reviews Cancer*. https://doi.org/10.1038/nrc2803

Kelderman, S., Schumacher, T. N. M., & Haanen, J. B. A. G. (2014). Acquired and intrinsic resistance in cancer immunotherapy. *Molecular Oncology*. https://doi.org/10.1016/j.molonc.2014.07.011

Kim, H. J., Yoon, A., Ryu, J. Y., Cho, Y. J., Choi, J. J., Song, S. Y., … Bae, D. S. (2016). C-MET as a Potential Therapeutic Target in Ovarian Clear Cell Carcinoma. *Scientific Reports*. https://doi.org/10.1038/srep38502

Korpal, M., Korn, J. M., Gao, X., Rakiec, D. P., Ruddy, D. A., Doshi, S., … Zhu, P. (2013). An F876l mutation in androgen receptor confers genetic and phenotypic resistance to MDV3100 (Enzalutamide). *Cancer Discovery*. https://doi.org/10.1158/2159-8290.CD-13-0142

Kotchetkov, R., Drjever, P. H., Cinatl, J., Michaelis, M., Karaskova, J., Blaheta, R., … Cinatl, J. (2005). Increased malignant behavior in neuroblastoma cells with acquired multi-drug resistance does not depend on P-gp expression. *International Journal of Oncology*. https://doi.org/10.3892/ijo.27.4.1029

Kowalski, R. J., Giannakakou, P., & Hamel, E. (1997). Activities of the microtubule-stabilizing agents epothilones A and B with purified tubulin and in cells resistant to paclitaxel (Taxol®). *Journal of Biological Chemistry*. https://doi.org/10.1074/jbc.272.4.2534

Koshkin, V. S., Garcia, J. A., Reynolds, J., Elson, P., Magi-Galluzzi, C., McKenney, J. K., Isse, K., Bishop, E., Saunders, L. R., Balyimez, A., Rashid, S., Hu, M., Stephenson, A. J., Fergany, A. F., Lee, B. H., Haber, G. P., Dowlati, A., Gilligan, T., Ornstein, M. C., … Grivas, P. (2019). Transcriptomic and protein analysis of small-cell bladder cancer (SCBC) Identifies prognostic biomarkers and DLL3 as a relevant therapeutic target. *Clinical Cancer Research*. https://doi.org/10.1158/1078-0432.CCR-18-1278

Kanzaki, A., Toi, M., Nakayama, K., Bando, H., Mutoh, M., Uchida, T., Fukumoto, M., & Takebayashi, Y. (2001). Expression of multidrug resistance-related transporters in human breast carcinoma. *Japanese Journal of Cancer Research*. https://doi.org/10.1111/j.1349-7006.2001.tb01115.x

Kuo, M. T., & Chen, H. H. W. (2010). Role of glutathione in the regulation of cisplatin resistance in cancer chemotherapy. In *Metal-Based Drugs*. https://doi.org/10.1155/2010/430939

Kawaguchi, J., Adachi, S., Yasuda, I., Yamauchi, T., Nakashima, M., Ohno, T., Shimizu, M., Yoshioka, T., Itani, M., Kozawa, O., & Moriwaki, H. (2012). Cisplatin and ultra-violet-C synergistically down-regulate receptor tyrosine kinases in human colorectal cancer cells. *Molecular Cancer*. https://doi.org/10.1186/1476-4598-11-45

Koga, Y., & Ochiai, A. (2019). Systematic Review of Patient-Derived Xenograft Models for Preclinical Studies of Anti-Cancer Drugs in Solid Tumors. *Cells*. https://doi.org/10.3390/cells8050418

Katt, M. E., Placone, A. L., Wong, A. D., Xu, Z. S., & Searson, P. C. (2016). In vitro tumor models: Advantages, disadvantages, variables, and selecting the right platform. In *Frontiers in Bioengineering and Biotechnology*. https://doi.org/10.3389/fbioe.2016.00012

Khaled, W. T., & Liu, P. (2014). Cancer mouse models: Past, present and future. In *Seminars in Cell and Developmental Biology*. https://doi.org/10.1016/j.semcdb.2014.04.003

Khalife, O., Muhammad, M., Kenj, M., & Salamoon, M. (2015). Alkylating Agents. In *Cyclophosphamide: Clinical Pharmacology, Uses and Potential Adverse Effects*. https://doi.org/10.1684/bdc.2011.1471

Kondo, N., Takahashi, A., Ono, K., & Ohnishi, T. (2010). DNA damage induced by alkylating agents and repair pathways. In *Journal of Nucleic Acids*. https://doi.org/10.4061/2010/543531

Kavallaris, M. (2010). Microtubules and resistance to tubulin-binding agents. In *Nature Reviews Cancer*. https://doi.org/10.1038/nrc2803

Kelland, L. (2007). The resurgence of platinum-based cancer chemotherapy. In *Nature Reviews Cancer*. https://doi.org/10.1038/nrc2167

Lengyel, E. (2010). Ovarian cancer development and metastasis. *American Journal of Pathology*. https://doi.org/10.2353/ajpath.2010.100105

Leonard, G. D. (2003). The Role of ABC Transporters in Clinical Practice. *The Oncologist*. https://doi.org/10.1634/theoncologist.8-5-411

Levina, V., Marrangoni, A. M., DeMarco, R., Gorelik, E., & Lokshin, A. E. (2008). Drug-selected human lung cancer stem cells: Cytokine network, tumorigenic and metastatic properties. *PLoS ONE*. https://doi.org/10.1371/journal.pone.0003077

Li, W., Zhang, H., Assaraf, Y. G., Zhao, K., Xu, X., Xie, J., … Chen, Z. S. (2016). Overcoming ABC transporter-mediated multidrug resistance: Molecular mechanisms and novel therapeutic drug strategies. *Drug Resistance Updates*. https://doi.org/10.1016/j.drup.2016.05.001

Lippert, T. H., Ruoff, H.-J., & Volm, M. (2008). Intrinsic and Acquired Drug Resistance in Malignant Tumors The main reason for therapeutic failure. *Arzneimittel-Forschung (Drug Research)*. https://doi.org/10.1055/s-0031-1296504

Lomis, N., Westfall, S., Farahdel, L., Malhotra, M., Shum-Tim, D., & Prakash, S. (2016). Human Serum Albumin Nanoparticles for Use in Cancer Drug Delivery: Process Optimization and In Vitro Characterization. *Nanomaterials*. https://doi.org/10.3390/nano6060116

Löschmann, N., Michaelis, M., Rothweiler, F., Zehner, R., Cinatl, J., Voges, Y., … Cinatl, J. (2013). Testing of SNS-032 in a Panel of Human Neuroblastoma Cell Lines with Acquired Resistance to a Broad Range of Drugs. *Translational Oncology*. https://doi.org/10.1593/tlo.13544

Luz, C. M., Boyles, M. S. P., Falagan-Lotsch, P., Pereira, M. R., Tutumi, H. R., Oliveira Santos, E., … Leite, P. E. C. (2017). Poly-lactic acid nanoparticles (PLA-NP) promote physiological modifications in lung epithelial cells and are internalized by clathrin-coated pits and lipid rafts.

Journal of Nanobiotechnology. https://doi.org/10.1186/s12951-016-0238-1

Lenz, H. J. (2006). Anti-EGFR mechanism of action: antitumor effect and underlying cause of adverse events. In *Oncology (Williston Park, N.Y.)*.

Lee, J. J., & Swain, S. M. (2008). The epothilones: Translating from the laboratory to the clinic. In *Clinical Cancer Research*. https://doi.org/10.1158/1078-0432.CCR-07-2201

Li, K., Zhan, W., Chen, Y., Jha, R. K., & Chen, X. (2019). Docetaxel and doxorubicin codelivery by nanocarriers for synergistic treatment of prostate cancer. *Frontiers in Pharmacology*. https://doi.org/10.3389/fphar.2019.01436

Liu, L., Zuo, L. F., & Guo, J. W. (2014). ABCG2 gene amplification and expression in esophageal cancer cells with acquired adriamycin resistance. *Molecular Medicine Reports*. https://doi.org/10.3892/mmr.2014.1949

Locher, K. P. (2009). Structure and mechanism of ATP-binding cassette transporters. In *Philosophical Transactions of the Royal Society B: Biological Sciences*. https://doi.org/10.1098/rstb.2008.0125

Lorger, M., Lee, H., Forsyth, J. S., & Felding-Habermann, B. (2011). Comparison of in vitro and in vivo approaches to studying brain colonization by breast cancer cells. *Journal of Neuro-Oncology*. https://doi.org/10.1007/s11060-011-0550-4

López-Lázaro, M. (2015). Two preclinical tests to evaluate anticancer activity and to help validate drug candidates for clinical trials. *Oncoscience*. https://doi.org/10.18632/oncoscience.132

Li, Q. X., Feuer, G., Ouyang, X., & An, X. (2017). Experimental animal modeling for immuno-oncology. In *Pharmacology and Therapeutics*. https://doi.org/10.1016/j.pharmthera.2017.02.002

Mansoori, B., Mohammadi, A., Davudian, S., Shirjang, S., & Baradaran, B. (2017). The different mechanisms of cancer drug resistance: A brief review. *Advanced Pharmaceutical Bulletin*. https://doi.org/10.15171/apb.2017.041

Marinello, J., Delcuratolo, M., & Capranico, G. (2018). Anthracyclines as Topoisomerase II Poisons: From Early Studies to New Perspectives. *International Journal of Molecular Sciences*. https://doi.org/10.3390/ijms19113480

McClelland, S. E. (2017). Role of chromosomal instability in cancer progression. *Endocrine-Related Cancer*. https://doi.org/10.1530/ERC-17-0187

McGowan, J. V., Chung, R., Maulik, A., Piotrowska, I., Walker, J. M., & Yellon, D. M. (2017). Anthracycline Chemotherapy and Cardiotoxicity. *Cardiovascular Drugs and Therapy*. https://doi.org/10.1007/s10557-016-6711-0

Mealey, K. L., & Fidel, J. (2015). P-Glycoprotein Mediated Drug Interactions in Animals and Humans with Cancer. *Journal of Veterinary Internal Medicine*. https://doi.org/10.1111/jvim.12525

Melo, F. D. S. E., Vermeulen, L., Fessler, E., & Medema, J. P. (2013). Cancer heterogeneity - A multifaceted view. *EMBO Reports*. https://doi.org/10.1038/embor.2013.92

Michaelis, M., Rothweiler, F., Agha, B., Barth, S., Voges, Y., Löschmann, N., … Cinatl, J. (2012). Human neuroblastoma cells with acquired resistance to the p53 activator RITA retain functional p53 and sensitivity to other p53 activating agents. *Cell Death and Disease*. https://doi.org/10.1038/cddis.2012.35

Michaelis, M., Rothweiler, F., Barth, S., Cinat, J., Van Rikxoort, M., Löschmann, N., … Cinatl, J. (2011). Adaptation of cancer cells from different entities to the MDM2 inhibitor nutlin-3 results in the emergence of p53-mutated multi-drug-resistant cancer cells. *Cell Death and Disease*. https://doi.org/10.1038/cddis.2011.129

Michaelis, M., Rothweiler, F., Klassert, D., Von Deimling, A., Weber, K., Fehse, B., … Cinatl, J. (2009). Reversal of P-glycoprotein-mediated multidrug resistance by the murine double minute 2 antagonist nutlin-3. *Cancer Research*. https://doi.org/10.1158/0008-5472.CAN-08-1856

Michaelis, M., Rothweiler, F., Löschmann, N., Sharifi, M., Ghafourian, T., & Cinatl, J. (2015). Enzastaurin inhibits ABCB1-mediated drug efflux independently of effects on protein kinase C signalling and the cellular p53 status. *Oncotarget*. https://doi.org/10.18632/oncotarget.2889

Mishra, P., Nayak, B., & Dey, R. K. (2016). PEGylation in anti-cancer therapy: An overview. *Asian Journal of Pharmaceutical Sciences*. https://doi.org/10.1016/j.ajps.2015.08.011

Mosmann, T. (1983). Rapid colorimetric assay for cellular growth and survival: Application to proliferation and cytotoxicity assays. *Journal of Immunological Methods*. https://doi.org/10.1016/0022-1759(83)90303-4

Moulder, S. (2010). Intrinsic resistance to chemotherapy in breast cancer. *Women's Health*. https://doi.org/10.2217/whe.10.60

Murphy, M., & Stordal, B. (2011). Erlotinib or gefitinib for the treatment of relapsed platinum pretreated non-small cell lung cancer and ovarian cancer: A systematic review. *Drug Resistance Updates*. https://doi.org/10.1016/j.drup.2011.02.004

Matsuo, K., Lin, Y. G., Roman, L. D., & Sood, A. K. (2010). Overcoming platinum resistance in ovarian carcinoma. In *Expert Opinion on Investigational Drugs*. https://doi.org/10.1517/13543784.2010.515585

Montagnani, F., Turrisi, G., Marinozzi, C., Aliberti, C., & Fiorentini, G. (2011). Effectiveness and safety of oxaliplatin compared to cisplatin for advanced, unresectable gastric cancer: A systematic review and meta-analysis. *Gastric Cancer*. https://doi.org/10.1007/s10120-011-0007-7

Morgillo, F., Della Corte, C. M., Fasano, M., & Ciardiello, F. (2016). Mechanisms of resistance to EGFR-targeted drugs: Lung cancer. In *ESMO Open*. https://doi.org/10.1136/esmoopen-2016-000060

Mitchison, T. J. (1988). Microtubule dynamics and kinetochore function in mitosis. In *Annual Review of Cell Biology*. https://doi.org/10.1146/annurev.cellbio.4.1.527

Mukhtar, E., Adhami, V. M., & Mukhtar, H. (2014). Targeting microtubules by natural agents for cancer therapy. In *Molecular Cancer Therapeutics*. https://doi.org/10.1158/1535-7163.MCT-13-0791

Martinez-Balibrea, E., Martínez-Cardus, A., Gines, A., Ruiz De Porras, V., Moutinho, C., Layos, L., Manzano, J. L., Buges, C., Bystrup, S., Esteller, M., & Abad, A. (2015). Tumor-related molecular mechanisms of oxaliplatin resistance. In *Molecular Cancer Therapeutics*. https://doi.org/10.1158/1535-7163.MCT-14-0636

Meegan, M. J., & O'Boyle, N. M. (2019). Special issue " anticancer drugs". *Pharmaceuticals*. https://doi.org/10.3390/ph12030134

Mao, Q. (2008). BCRP/ABCG2 in the placenta: Expression, function and regulation. In *Pharmaceutical Research*. https://doi.org/10.1007/s11095-008-9537-z

Mo, W., & Zhang, J. T. (2012). Human ABCG2: Structure, function, and its role in multidrug resistance. In *International Journal of Biochemistry and Molecular Biology*.

McIntosh, K., Balch, C., & Tiwari, A. K. (2016). Tackling multidrug resistance mediated by efflux transporters in tumor-initiating cells. In *Expert Opinion on Drug Metabolism and Toxicology*. https://doi.org/10.1080/17425255.2016.1179280

Melo, F. D. S. E., Vermeulen, L., Fessler, E., & Medema, J. P. (2013). Cancer heterogeneity - A multifaceted view. In *EMBO Reports*. https://doi.org/10.1038/embor.2013.92

Nazarian, R., Shi, H., Wang, Q., Kong, X., Koya, R. C., Lee, H., … Lo, R. S. (2010). Melanomas acquire resistance to B-RAF(V600E) inhibition by RTK or N-RAS upregulation. *Nature*. https://doi.org/10.1038/nature09626

Niazi, M., Zakeri-Milani, P., Najafi Hajivar, S., Soleymani Goloujeh, M., Ghobakhlou, N., Shahbazi Mojarrad, J., & Valizadeh, H. (2016). Nano-based strategies to overcome p-glycoprotein-mediated drug resistance. *Expert Opinion on Drug Metabolism and Toxicology*. https://doi.org/10.1080/17425255.2016.1196186

Niederst, M. J., Sequist, L. V., Poirier, J. T., Mermel, C. H., Lockerman, E. L., Garcia, A. R., … Engelman, J. A. (2015). RB loss in resistant EGFR mutant lung adenocarcinomas that transform to small-cell lung cancer. *Nature Communications*. https://doi.org/10.1038/ncomms7377

Nasser, S. M. (2009). Gene expression profiling in breast cancer. In *Journal Medical Libanais*. https://doi.org/10.1146/annurev.pathol.3.121806.151505

Norbury, C. J., & Zhivotovsky, B. (2004). DNA damage-induced apoptosis. In *Oncogene*. https://doi.org/10.1038/sj.onc.1207532

Nikolaou, M., Pavlopoulou, A., Georgakilas, A. G., & Kyrodimos, E. (2018). The challenge of drug resistance in cancer treatment: a current overview. *Clinical and Experimental Metastasis*. https://doi.org/10.1007/s10585-018-9903-0

Niu, N., & Wang, L. (2015). In vitro human cell line models to predict clinical response to anticancer drugs. In *Pharmacogenomics*. https://doi.org/10.2217/pgs.14.170

Ogino, S., Fuchs, C. S., & Giovannucci, E. (2012). How many molecular subtypes? Implications of the unique tumor principle in personalized medicine. *Expert Review of Molecular Diagnostics*. https://doi.org/10.1586/erm.12.46

O'Donovan, P. J., & Livingston, D. M. (2010). BRCA1 and BRCA2: Breast/ovarian cancer susceptibility gene products and participants in DNA double-strand break repair. In *Carcinogenesis*. https://doi.org/10.1093/carcin/bgq069

Orr, G. A., Verdier-Pinard, P., McDaid, H., & Horwitz, S. B. (2003). Mechanisms of Taxol resistance related to microtubules. In *Oncogene*. https://doi.org/10.1038/sj.onc.1206934

O'Kane, G. M., Barnes, T. A., & Leighl, N. B. (2018). Resistance to epidermal growth actor receptor tyrosine kinase inhibitors, T790M, and clinical trials. In *Current Oncology*. https://doi.org/10.3747/co.25.3796

Ohashi, K., Maruvka, Y. E., Michor, F., & Pao, W. (2013). Epidermal growth factor receptor tyrosine kinase inhibitor-resistant disease. In *Journal of Clinical Oncology*. https://doi.org/10.1200/JCO.2012.43.3912

Oehler, C., Dickinson, D., Broggini-Tenzer, A., Hofstetter, B., Hollenstein, A., Riesterer, O., Vuong, V., & Pruschy, M. (2007). Current Concepts for the Combined Treatment Modality of Ionizing Radiation with Anticancer Agents. *Current Pharmaceutical Design*. https://doi.org/10.2174/138161207780162935

Ohmichi, M., Hayakawa, J., Tasaka, K., Kurachi, H., & Murata, Y. (2005). Mechanisms of platinum drug resistance. In *Trends in Pharmacological Sciences*. https://doi.org/10.1016/j.tips.2005.01.002

Ogilvie, L. A., Kovachev, A., Wierling, C., Lange, B. M. H., & Lehrach, H. (2017). Models of models: A translational route for cancer treatment and drug development. *Frontiers in Oncology*. https://doi.org/10.3389/fonc.2017.00219

Park, H. S., Nam, S. H., Kim, J., Shin, H. S., Suh, Y. D., & Hong, K. S. (2016). Clear-cut observation of clearance of sustainable upconverting nanoparticles from lymphatic system of small living mice. *Scientific Reports*. https://doi.org/10.1038/srep27407

Pasqualato, A., Palombo, A., Cucina, A., Mariggiò, M. A., Galli, L., Passaro, D., … Bizzarri, M. (2012). Quantitative shape analysis of chemoresistant colon cancer cells: Correlation between morphotype and phenotype. *Experimental Cell Research*. https://doi.org/10.1016/j.yexcr.2012.01.022

Petrović, M., & Todorović, D. (2016). BIOCHEMICAL AND MOLECULAR MECHANISMS OF ACTION OF CISPLATIN IN CANCER CELLS. *Medicine and Biology*.

Poulikakos, P. I., Persaud, Y., Janakiraman, M., Kong, X., Ng, C., Moriceau, G., … Solit, D. B. (2011). RAF inhibitor resistance is mediated by dimerization of aberrantly spliced BRAF(V600E). *Nature*. https://doi.org/10.1038/nature10662

Prabhakaran, P., Hassiotou, F., Blancafort, P., & Filgueira, L. (2013). Cisplatin Induces Differentiation of Breast Cancer Cells. *Frontiers in Oncology*. https://doi.org/10.3389/fonc.2013.00134

Parson, W., Kirchebner, R., Mühlmann, R., Renner, K., Kofler, A., Schmidt, S., & Kofler, R. (2005). Cancer cell line identification by short tandem repeat profiling: power and limitations. *The FASEB Journal*. https://doi.org/10.1096/fj.04-3062fje

Paulsson, K., Panagopoulos, I., Knuutila, S., Jee, K. J., Garwicz, S., Fioretos, T., Mitelman, F., & Johansson, B. (2003). Formation of trisomies and their parental origin in hyperdiploid childhood acute lymphoblastic leukemia. *Blood*. https://doi.org/10.1182/blood-2003-05-1444

Promega. (2012). *Short Tandem Repeat Analysis in the Research Laboratory*. PubHub.

Parca, L., Pepe, G., Pietrosanto, M., Galvan, G., Galli, L., Palmeri, A., Sciandrone, M., Ferrè, F., Ausiello, G., & Helmer-Citterich, M. (2019). Modeling cancer drug response through drug-specific informative genes. *Scientific Reports*. https://doi.org/10.1038/s41598-019-50720-0

Previs, R. A., Sood, A. K., Mills, G. B., & Westin, S. N. (2016). The rise of genomic profiling in ovarian cancer. In *Expert Review of Molecular Diagnostics*. https://doi.org/10.1080/14737159.2016.1259069

Pellegrini, P., Serviss, J. T., Lundbäck, T., Bancaro, N., Mazurkiewicz, M., Kolosenko, I., Yu, D., Haraldsson, M., D'Arcy, P., Linder, S., & De Milito, A. (2018). A drug screening assay on cancer cells chronically adapted to acidosis. *Cancer Cell International*. https://doi.org/10.1186/s12935-018-0645-5

Paul, M. K., & Mukhopadhyay, A. K. (2012). Tyrosine kinase – Role and significance in Cancer. *International Journal of Medical Sciences*. https://doi.org/10.7150/ijms.1.101

Pauli, C., Hopkins, B. D., Prandi, D., Shaw, R., Fedrizzi, T., Sboner, A., Sailer, V., Augello, M., Puca, L., Rosati, R., McNary, T. J., Churakova, Y., Cheung, C., Triscott, J., Pisapia, D., Rao, R., Mosquera, J. M., Robinson, B., Faltas, B. M., … Rubin, M. A. (2017). Personalized in vitro and in vivo cancer models to guide precision medicine. *Cancer Discovery*. https://doi.org/10.1158/2159-8290.CD-16-1154

P.R. Xavier, C., Pesic, M., & Helena Vasconcelos, M. (2016). Understanding Cancer Drug Resistance by Developing and Studying Resistant Cell Line Models. *Current Cancer Drug Targets*. https://doi.org/10.2174/1568009616666151113120705

Reynolds, C. P., Kang, M. H., Maris, J. M., Kolb, E. A., Gorlick, R., Wu, J., … Smith, M. A. (2015). Initial testing (stage 1) of the anti-microtubule agents cabazitaxel and docetaxel, by the pediatric preclinical testing program. *Pediatric Blood and Cancer*. https://doi.org/10.1002/pbc.25611

Riss, T. L., Moravec, R. A., Niles, A. L., Duellman, S., & Benink, H. A. (2013). Cell Viability Assays. In *Assay Guidance Manual*. https://doi.org/10.1016/j.acthis.2012.01.006

Rivera, E. (2010). Implications of anthracycline-resistant and taxane-resistant metastatic breast cancer and new therapeutic options. *Breast Journal*. https://doi.org/10.1111/j.1524-4741.2009.00896.x

Rivoirard, R., Vallard, A., Langrand-Escure, J., Ben Mrad, M., Wang, G., Guy, J. B., … Magne, N. (2016). Thirty years of phase i radiochemotherapy trials: Latest development. *European Journal of Cancer*. https://doi.org/10.1016/j.ejca.2016.01.012

Rizvi, S. A. A., & Saleh, A. M. (2018). Applications of nanoparticle systems in drug delivery technology. *Saudi Pharmaceutical Journal*. https://doi.org/10.1016/j.jsps.2017.10.012

Robey, R. W., Pluchino, K. M., Hall, M. D., Fojo, A. T., Bates, S. E., & Gottesman, M. M. (2018). Revisiting the role of ABC transporters in multidrug-resistant cancer. *Nature Reviews Cancer*. https://doi.org/10.1038/s41568-018-0005-8

Rocha, C. R. R., Kajitani, G. S., Quinet, A., Fortunato, R. S., & Menck, C. F. M. (2016). NRF2 and glutathione are key resistance mediators to temozolomide in glioma and melanoma cells. *Oncotarget*. https://doi.org/10.18632/oncotarget.10129

Rodrigues de Azevedo, C., von Stosch, M., Costa, M. S., Ramos, A. M., Cardoso, M. M., Danhier, F., … Oliveira, R. (2017). Modeling of the burst release from PLGA micro- and nanoparticles as function of physicochemical parameters and formulation characteristics. *International Journal of Pharmaceutics*. https://doi.org/10.1016/j.ijpharm.2017.08.118

Ruan, G., & Feng, S. S. (2003). Preparation and characterization of poly(lactic acid)-poly(ethylene glycol)-poly(lactic acid) (PLA-PEG-PLA) microspheres for controlled release of paclitaxel. *Biomaterials*. https://doi.org/10.1016/S0142-9612(03)00419-8

Reis-Filho, J. S., & Pusztai, L. (2011). Gene expression profiling in breast cancer: Classification, prognostication, and prediction. In *The Lancet*. https://doi.org/10.1016/S0140-6736(11)61539-0

Rabik, C. A., & Dolan, M. E. (2007). Molecular mechanisms of resistance and toxicity associated with platinating agents. In *Cancer Treatment Reviews*. https://doi.org/10.1016/j.ctrv.2006.09.006

Roos, W. P., & Kaina, B. (2013). DNA damage-induced cell death: From specific DNA lesions to the DNA damage response and apoptosis. In *Cancer Letters*. https://doi.org/10.1016/j.canlet.2012.01.007

Rechache, N. S., Riggins, R. B., Shajahan, A. N., Zwart, A., & Clarke, R. (2010). *Abstract 4857: The role of autophagy in taxane resistant breast cancer models*. https://doi.org/10.1158/1538-7445.am10-4857

Raymond, E., Faivre, S., Chaney, S., Woynarowski, J., & Cvitkovic, E. (2002). Cellular and molecular pharmacology of oxaliplatin. In *Molecular Cancer Therapeutics*.

Rosenberg, B., VanCamp, L., Trosko, J. E., & Mansour, V. H. (1969). Platinum compounds: A new class of potent antitumour agents [24]. In *Nature*. https://doi.org/10.1038/222385a0

Ruicci, K. M., Meens, J., Sun, R. X., Rizzo, G., Pinto, N., Yoo, J., Fung, K., MacNeil, D., Mymryk, J. S., Barrett, J. W., Boutros, P. C., Ailles, L., & Nichols, A. C. (2019). A controlled trial of HNSCC patient-derived xenografts reveals broad efficacy of PI3Kα inhibition in controlling tumor growth. *International Journal of Cancer*. https://doi.org/10.1002/ijc.32009

Rosa, R., Monteleone, F., Zambrano, N., & Bianco, R. (2014). In Vitro and In Vivo Models for Analysis of Resistance to Anticancer Molecular Therapies. *Current Medicinal Chemistry*. https://doi.org/10.2174/09298673113209990226

Saintas, E., Abrahams, L., Ahmad, G. T., Ajakaiye, A. O. M., Alhumaidi, A. S. H. A. M., Ashmore-Harris, C., … Michaelis, M. (2017). Acquired resistance to oxaliplatin is not directly associated with increased resistance to DNA damage in SK-N-ASrOXALI4000, a newly established oxaliplatin-resistant sub-line of the neuroblastoma cell line SK-N-AS. *PLoS ONE*. https://doi.org/10.1371/journal.pone.0172140

Schneider, C., Oellerich, T., Baldauf, H. M., Schwarz, S. M., Thomas, D., Flick, R., … Cinatl, J. (2017). SAMHD1 is a biomarker for cytarabine response and a therapeutic target in acute myeloid leukemia. *Nature Medicine*. https://doi.org/10.1038/nm.4255

Shah, S., Chandra, A., Kaur, A., Sabnis, N., Lacko, A., Gryczynski, Z., … Gryczynski, I. (2017). Fluorescence properties of doxorubicin in PBS buffer and PVA films. *Journal of Photochemistry and Photobiology B: Biology*. https://doi.org/10.1016/j.jphotobiol.2017.03.024

Shaloam, D., & Tchounwou, P. B. (2014). Cisplatin in cancer therapy: Molecular mechanisms of action. *European Journal of Pharmacology*. https://doi.org/10.1016/j.ejphar.2014.07.025.Cisplatin

Sharma, P., Hu-Lieskovan, S., Wargo, J. A., & Ribas, A. (2017). Primary, Adaptive, and Acquired Resistance to Cancer Immunotherapy. *Cell*. https://doi.org/10.1016/j.cell.2017.01.017

Sharma, S. V., Lee, D. Y., Li, B., Quinlan, M. P., Takahashi, F., Maheswaran, S., … Settleman, J. (2010). A Chromatin-Mediated Reversible Drug-Tolerant State in Cancer Cell Subpopulations. *Cell*. https://doi.org/10.1016/j.cell.2010.02.027

Siddik, Z. H. (2003). Cisplatin: Mode of cytotoxic action and molecular basis of resistance. *Oncogene*. https://doi.org/10.1038/sj.onc.1206933

Singh, R., & Lillard, J. W. (2009). Nanoparticle-based targeted drug delivery. *Experimental and Molecular Pathology*. https://doi.org/10.1016/j.yexmp.2008.12.004

Stanta, G., & Bonin, S. (2018). Overview on Clinical Relevance of Intra-Tumor Heterogeneity. *Frontiers in Medicine*. https://doi.org/10.3389/fmed.2018.00085

Stordal, B., Pavlakis, N., & Davey, R. (2007). Oxaliplatin for the treatment of cisplatin-resistant cancer: A systematic review. *Cancer Treatment Reviews*. https://doi.org/10.1016/j.ctrv.2007.01.009

Suk, J. S., Xu, Q., Kim, N., Hanes, J., & Ensign, L. M. (2016). PEGylation as a strategy for improving nanoparticle-based drug and gene delivery. *Advanced Drug Delivery Reviews*. https://doi.org/10.1016/j.addr.2015.09.012

Szakács, G., Paterson, J. K., Ludwig, J. A., Booth-Genthe, C., & Gottesman, M. M. (2006). Targeting multidrug resistance in cancer. *Nature Reviews Drug Discovery*. https://doi.org/10.1038/nrd1984

Shen, Z., Song, J., Yung, B. C., Zhou, Z., Wu, A., & Chen, X. (2018). Emerging Strategies of Cancer Therapy Based on Ferroptosis. In *Advanced Materials*. https://doi.org/10.1002/adma.201704007

Sellers, W. R. (2011). A blueprint for advancing genetics-based cancer therapy. In *Cell*. https://doi.org/10.1016/j.cell.2011.09.016

Szalat, R., Avet-Loiseau, H., & Munshi, N. C. (2016). Gene expression profiles in myeloma: Ready for the real world? In *Clinical Cancer Research*. https://doi.org/10.1158/1078-0432.CCR-16-0867

Song, Y. G., Wang, S., Zhao, Y. J., Jiang, N., Qiao, G., Zhao, J., Di, Y., Wang, X., & Ren, J. (2019). Dynamic changes of circulating tumor DNA in peripheral blood predict the efficacy of TKI in the treatment of lung adenocarcinoma with EGFR mutation. *Chinese Journal of Lung Cancer*. https://doi.org/10.3779/j.issn.1009-3419.2019.09.03

Stordal, B., & Davey, M. (2007). Understanding cisplatin resistance using cellular models. In *IUBMB Life*. https://doi.org/10.1080/15216540701636287

Steding, C. E. (2016). Creating chemotherapeutic-resistant breast cancer cell lines: Advances and future perspectives. In *Future Oncology*. https://doi.org/10.2217/fon-2016-0059

Stordal, B., Pavlakis, N., & Davey, R. (2007). Oxaliplatin for the treatment of cisplatin-resistant cancer: A systematic review. In *Cancer Treatment Reviews*. https://doi.org/10.1016/j.ctrv.2007.01.009

Szakács, G., Paterson, J. K., Ludwig, J. A., Booth-Genthe, C., & Gottesman, M. M. (2006). Targeting multidrug resistance in cancer. In *Nature Reviews Drug Discovery*. https://doi.org/10.1038/nrd1984

Schettino, C., Bareschino, M. A., Ricci, V., & Ciardiello, F. (2008). Erlotinib: An EGF receptor tyrosine kinase inhibitor in non-small-cell lung cancer treatment. *Expert Review of Respiratory Medicine*. https://doi.org/10.1586/17476348.2.2.167

Shaw, A. T., Kim, D. W., Nakagawa, K., Seto, T., Crinó, L., Ahn, M. J., De Pas, T., Besse, B., Solomon, B. J., Blackhall, F., Wu, Y. L., Thomas, M., O'Byrne, K. J., Moro-Sibilot, D., Camidge, D. R., Mok,

T., Hirsh, V., Riely, G. J., Iyer, S., … Jänne, P. A. (2013). Crizotinib versus chemotherapy in advanced ALK-positive lung cancer. *New England Journal of Medicine*. https://doi.org/10.1056/NEJMoa1214886

Seltsam, A., & Müller, T. H. (2011). UVC irradiation for pathogen reduction of platelet concentrates and plasma. *Transfusion Medicine and Hemotherapy*. https://doi.org/10.1159/000323845

Sarkaria, J. N., Kitange, G. J., James, C. D., Plummer, R., Calvert, H., Weller, M., & Wick, W. (2008). Mechanisms of chemoresistance to alkylating agents in malignant glioma. In *Clinical Cancer Research*. https://doi.org/10.1158/1078-0432.CCR-07-1719

Swift, L. H., & Golsteyn, R. M. (2014). Genotoxic anti-cancer agents and their relationship to DNA damage, mitosis, and checkpoint adaptation in proliferating cancer cells. In *International Journal of Molecular Sciences*. https://doi.org/10.3390/ijms15033403

Sato, S., & Itamochi, H. (2015). DNA Repair and Chemotherapy. In *Advances in DNA Repair*. https://doi.org/10.5772/59513

Samadi, N., Ghanbari, P., Mohseni, M., Tabasinezhad, M., Sharifi, S., Nazemieh, H., & Rashidi, M. R. (2014). Combination therapy increases the efficacy of docetaxel, vinblastine and tamoxifen in cancer cells. *Journal of Cancer Research and Therapeutics*. https://doi.org/10.4103/0973-1482.139152

Seetharam, R. N., Sood, A., & Goel, S. (2009). Oxaliplatin: Preclinical perspectives on the mechanisms of action, response and resistance. In *ecancermedicalscience*. https://doi.org/10.3332/ecancer.2009.153

Stewart, D. J. (2007). Mechanisms of resistance to cisplatin and carboplatin. In *Critical Reviews in Oncology/Hematology*. https://doi.org/10.1016/j.critrevonc.2007.02.001

Siddik, Z. H. (2003). Cisplatin: Mode of cytotoxic action and molecular basis of resistance. In *Oncogene*. https://doi.org/10.1038/sj.onc.1206933

Senthebane, D. A., Rowe, A., Thomford, N. E., Shipanga, H., Munro, D., Al Mazeedi, M. A. M., Almazyadi, H. A. M., Kallmeyer, K., Dandara, C., Pepper, M. S., Parker, M. I., & Dzobo, K. (2017). The role of tumor microenvironment in chemoresistance: To survive, keep your enemies closer. In *International Journal of Molecular Sciences*. https://doi.org/10.3390/ijms18071586

Turajlic, S., Furney, S. J., Lambros, M. B., Mitsopoulos, C., Kozarewa, I., Geyer, F. C., MacKay, A., Hakas, J., Zvelebil, M., Lord, C. J., Ashworth, A., Thomas, M., Stamp, G., Larkin, J., Reis-Filho, J. S., & Marais, R. (2012). Whole genome sequencing of matched primary and metastatic acral melanomas. *Genome Research*. https://doi.org/10.1101/gr.125591.111

Towne, T. G., & Murray, A. (2014). Cisplatin. In *Encyclopedia of Toxicology: Third Edition*. https://doi.org/10.1016/B978-0-12-386454-3.00288-8

Tong, M., Zheng, W., Lu, X., Ao, L., Li, X., Guan, Q., Cai, H., Li, M., Yan, H., Guo, Y., Chi, P., & Guo, Z. (2015). Identifying clinically relevant drug resistance genes in drug-induced resistant cancer cell lines and post-chemotherapy tissues. *Oncotarget*. https://doi.org/10.18632/oncotarget.5649

Tapia, G., & Diaz-Padill, I. (2013). Molecular Mechanisms of Platinum Resistance in Ovarian Cancer. In *Ovarian Cancer - A Clinical and Translational Update*. https://doi.org/10.5772/55562

Trastoy, M. O., Defais, M., & Larminat, F. (2005). Resistance to the antibiotic Zeocin by stable expression of the Sh ble gene does not fully suppress Zeocin-induced DNA cleavage in human cells. *Mutagenesis*. https://doi.org/10.1093/mutage/gei016

Terada, N., Kamoto, T., Tsukino, H., Mukai, S., Akamatsu, S., Inoue, T., Ogawa, O., Narita, S., Habuchi, T., Yamashita, S., Mitsuzuka, K., Arai, Y., Kandori, S., Kojima, T., Nishiyama, H., Kawamura, Y., Shimizu, Y., Terachi, T., Sugi, M., … Tsuchiya, N. (2019). The efficacy and toxicity of cabazitaxel for treatment of docetaxel-resistant prostate cancer correlating with the initial doses in Japanese patients. *BMC Cancer*. https://doi.org/10.1186/s12885-019-5342-9

Townsend, D. (2007). Carboplatin. In *xPharm: The Comprehensive Pharmacology Reference*. https://doi.org/10.1016/B978-008055232-3.61386-8

Toyoda, Y., Takada, T., & Suzuki, H. (2019). Inhibitors of human ABCG2: From technical background to recent updates with clinical implications. In *Frontiers in Pharmacology*. https://doi.org/10.3389/fphar.2019.00208

Taylor, N. M. I., Manolaridis, I., Jackson, S. M., Kowal, J., Stahlberg, H., & Locher, K. P. (2017). Structure of the human multidrug transporter ABCG2. *Nature*. https://doi.org/10.1038/nature22345

Ughachukwu, P., & Unekwe, P. (2012). Efflux pump-mediated resistance in chemotherapy. *Annals of Medical and Health Sciences Research*. https://doi.org/10.4103/2141-9248.105671

Vähäkangas, K. H., Veid, J., Karttunen, V., Partanen, H., Sieppi, E., Kummu, M., Myllynen, P., & Loikkanen, J. (2011). The Significance of ABC Transporters in Human Placenta for the Exposure of the Fetus to Xenobiotics. In *Reproductive and Developmental Toxicology*. https://doi.org/10.1016/B978-0-12-382032-7.10079-7

Van Staveren, W. C. G., Solís, D. Y. W., Hébrant, A., Detours, V., Dumont, J. E., & Maenhaut, C. (2009). Human cancer cell lines: Experimental models for cancer cells in situ? For cancer stem cells? In *Biochimica et Biophysica Acta - Reviews on Cancer*. https://doi.org/10.1016/j.bbcan.2008.12.004

Van't Veer, L. J., Dai, H., Van de Vijver, M. J., He, Y. D., Hart, A. A. M., Mao, M., Peterse, H. L., Van Der Kooy, K., Marton, M. J., Witteveen, A. T., Schreiber, G. J., Kerkhoven, R. M., Roberts, C., Linsley, P. S., Bernards, R., & Friend, S. H. (2002). Gene expression profiling predicts clinical outcome of breast cancer. *Nature*. https://doi.org/10.1038/415530a

Vergote, I. B., Jimeno, A., Joly, F., Katsaros, D., Coens, C., Despierre, E., … Pujade-Lauraine, E. (2014). Randomized phase III study of erlotinib versus observation in patients with no evidence of disease progression after first-line platin-based chemotherapy for ovarian carcinoma: A European Organisation for Research and Treatment of Cancer-Gynaecological Ca. *Journal of Clinical Oncology*. https://doi.org/10.1200/JCO.2013.50.5669

Voges, Y., Michaelis, M., Rothweiler, F., Schaller, T., Schneider, C., Politt, K., … Cinatl, J. (2016). Effects of YM155 on survivin levels and viability in neuroblastoma cells with acquired drug resistance. *Cell Death & Disease*. https://doi.org/10.1038/cddis.2016.257

Vrignaud, P., Semiond, D., Benning, V., Beys, E., Bouchard, H., & Gupta, S. (2014). Preclinical profile of cabazitaxel. *Drug Design, Development and Therapy*. https://doi.org/10.2147/DDDT.S64940

Wong, H. H., Barton, C., Acton, G., McLeod, R., & Halford, S. (2016). Trends in the characteristics, dose-limiting toxicities and efficacy of phase I oncology trials: The Cancer Research UK experience. *European Journal of Cancer*. https://doi.org/10.1016/j.ejca.2016.07.004

Walker, B. A., Leone, P. E., Jenner, M. W., Li, C., Gonzalez, D., Johnson, D. C., Ross, F. M., Davies, F. E., & Morgan, G. J. (2006). Integration of global SNP-based mapping and expression arrays reveals key regions, mechanisms, and genes important in the pathogenesis of multiple myeloma. *Blood*. https://doi.org/10.1182/blood-2006-02-005496

Wang, H., Vo, T., Hajar, A., Li, S., Chen, X., Parissenti, A. M., Brindley, D. N., & Wang, Z. (2014). Multiple mechanisms underlying acquired resistance to taxanes in selected docetaxel-resistant MCF-7 breast cancer cells. *BMC Cancer*. https://doi.org/10.1186/1471-2407-14-37

Wong, A. H. H., Li, H., Jia, Y., Mak, P. I., Martins, R. P. D. S., Liu, Y., Vong, C. M., Wong, H. C., Wong, P. K., Wang, H., Sun, H., & Deng, C. X. (2017). Drug screening of cancer cell lines and human primary tumors using droplet microfluidics. *Scientific Reports*. https://doi.org/10.1038/s41598-017-08831-z

Wilding, J. L., & Bodmer, W. F. (2014). Cancer cell lines for drug discovery and development. In *Cancer Research*. https://doi.org/10.1158/0008-5472.CAN-13-2971

Wang, P., An, F., Zhuang, X., Liu, J., Zhao, L., Zhang, B., Liu, L., Lin, P., & Li, M. (2014). Chronopharmacology and mechanism of antitumor effect of erlotinib in Lewis tumor-bearing mice. *PLoS ONE*. https://doi.org/10.1371/journal.pone.0101720

Wang, J. C. (2002). Cellular roles of DNA topoisomerases: A molecular perspective. In *Nature Reviews Molecular Cell Biology*. https://doi.org/10.1038/nrm831

Wang, L., & Du, G. H. (2018). Paclitaxel. In *Natural Small Molecule Drugs from Plants*. https://doi.org/10.1007/978-981-10-8022-7_89

Wu, Q., Li, M. Y., Li, H. Q., Deng, C. H., Li, L., Zhou, T. Y., & Lu, W. (2013). Pharmacokinetic-pharmacodynamic modeling of the anticancer effect of erlotinib in a human non-small cell lung cancer xenograft mouse model. *Acta Pharmacologica Sinica*. https://doi.org/10.1038/aps.2013.101

Wu, H., Liu, Y., Kang, H., Xiao, Q., Yao, W., Zhao, H., Wang, E., & Wei, M. (2015). Genetic Variations in ABCG2 Gene Predict Breast Carcinoma Susceptibility and Clinical Outcomes after Treatment with Anthracycline-Based Chemotherapy. *BioMed Research International*. https://doi.org/10.1155/2015/279109

Wu, C. J., Hwa, H. L., Chang, W. C., Hsu, H. C., Wu, M. Z., & Sheu, B. C. (2018). Short tandem repeat analysis for confirmation of uterine non-gestational choriocarcinoma in a postmenopausal Taiwanese woman. *Medicine (United States)*. https://doi.org/10.1097/MD.0000000000009899

Xin, Y., Yin, M., Zhao, L., Meng, F., & Luo, L. (2017). Recent progress on nanoparticle-based drug delivery systems for cancer therapy. *Cancer Biology & Medicine*. https://doi.org/10.20892/j.issn.2095-3941.2017.0052

Xiong, J., Mao, D. A., & Liu, L. Q. (2015). Research Progress on the Role of ABC Transporters in the Drug Resistance Mechanism of Intractable Epilepsy. In *BioMed Research International*. https://doi.org/10.1155/2015/194541

Yardley, D. A. (2013). Nab-Paclitaxel mechanisms of action and delivery. *Journal of Controlled Release*. https://doi.org/10.1016/j.jconrel.2013.05.041

Yuan, Y., Cai, T., Xia, X., Zhang, R., Chiba, P., & Cai, Y. (2016). Nanoparticle delivery of anticancer drugs overcomes multidrug resistance in breast cancer. *Drug Delivery*. https://doi.org/10.1080/10717544.2016.1178825

Yang, W., Soares, J., Greninger, P., Edelman, E. J., Lightfoot, H., Forbes, S., Bindal, N., Beare, D., Smith, J. A., Thompson, I. R., Ramaswamy, S., Futreal, P. A., Haber, D. A., Stratton, M. R., Benes, C., McDermott, U., & Garnett, M. J. (2013). Genomics of Drug Sensitivity in Cancer (GDSC): A resource for therapeutic biomarker discovery in cancer cells. *Nucleic Acids Research*. https://doi.org/10.1093/nar/gks1111

Yeldag, G., Rice, A., & Hernández, A. del R. (2018). Chemoresistance and the self-maintaining tumor microenvironment. In *Cancers*. https://doi.org/10.3390/cancers10120471

Yuan, Y., Cai, T., Xia, X., Zhang, R., Chiba, P., & Cai, Y. (2016). Nanoparticle delivery of anticancer drugs overcomes multidrug resistance in breast cancer. In *Drug Delivery*. https://doi.org/10.1080/10717544.2016.1178825

Yang, B., Ma, Y. F., Liu, Y., Yang, C.-M., Chen, N.-C., Shen, H.-C., Chou, C.-H., Yeh, P.-S., Lin, H.-J., Chang, C.-Y., Cheng, T.-J., & Lin, K.-C. (2015). Elevated Expression of Nrf-2 and ABCG2 Involved in Multi-drug Resistance of Lung Cancer SP Cells\r[Guideline of neuropathic pain treatment and dilemma from neurological point of view]. *Drug Research*.

Yoshino, H., Nawamaki, M., Murakami, K., & Kashiwakura, I. (2019). Effects of irradiated cell conditioned medium on the response of human lung cancer cells to anticancer treatment in vitro. *World Academy of Sciences Journal*. https://doi.org/10.3892/wasj.2019.11

Zabielska-Koczywąs, K., & Lechowski, R. (2017). The use of liposomes and nanoparticles as drug delivery systems to improve cancer treatment in dogs and cats. *Molecules*. https://doi.org/10.3390/molecules22122167

Zahreddine, H. A., Culjkovic-Kraljacic, B., Assouline, S., Gendron, P., Romeo, A. A., Morris, S. J., … Borden, K. L. B. (2014). The sonic hedgehog factor GLI1 imparts drug resistance through inducible glucuronidation. *Nature*. https://doi.org/10.1038/nature13283

Zardavas, D., Maetens, M., Irrthum, A., Goulioti, T., Engelen, K., Fumagalli, D., … Piccart, M. (2014). The AURORA initiative for metastatic breast cancer. *British Journal of Cancer*. https://doi.org/10.1038/bjc.2014.341

Zhang, J., & Marksaltzman, W. (2013). Engineering biodegradable nanoparticles for drug and gene delivery. *Chemical Engineering Progress*, *109*(3), 25–30.

Zhou, Z., Badkas, A., Stevenson, M., Lee, J. Y., & Leung, Y. K. (2015). Herceptin conjugated PLGA-PHis-PEG pH sensitive nanoparticles for targeted and controlled drug delivery. *International Journal of Pharmaceutics*. https://doi.org/10.1016/j.ijpharm.2015.03.081

Zhu, Z., Du, S., Du, Y., Ren, J., Ying, G., & Yan, Z. (2018). Glutathione reductase mediates drug resistance in glioblastoma cells by regulating redox homeostasis. *Journal of Neurochemistry*. https://doi.org/10.1111/jnc.14250

Zhang, X., Yashiro, M., Qiu, H., Nishii, T., Matsuzaki, T., & Hirakawa, K. (2010). Establishment and characterization of multidrug-resistant gastric cancer cell lines. *Anticancer Research*.

Zhang, Y. K., Wang, Y. J., Gupta, P., & Chen, Z. S. (2015). Multidrug Resistance Proteins (MRPs) and Cancer Therapy. *AAPS Journal*. https://doi.org/10.1208/s12248-015-9757-1

Zhang, F., Wang, W., Long, Y., Liu, H., Cheng, J., Guo, L., Li, R., Meng, C., Yu, S., Zhao, Q., Lu, S., Wang, L., Wang, H., & Wen, D. (2018). Characterization of drug responses of mini patient-derived xenografts in mice for predicting cancer patient clinical therapeutic response. *Cancer Communications (London, England)*. https://doi.org/10.1186/s40880-018-0329-5

Zhu, L., & Chen, L. (2019). Progress in research on paclitaxel and tumor immunotherapy. *Cellular and Molecular Biology Letters*. https://doi.org/10.1186/s11658-019-0164-y

Zheng, H. C. (2017). The molecular mechanisms of chemoresistance in cancers. In *Oncotarget*. https://doi.org/10.18632/oncotarget.19048

9 Appendix

Appendix 1

1.1 Polymer nanoparticle preparation using emulsion diffusion

The reagents, PLGA (Resomer ® RG502H), PLA (Resomer ® R203H) and PLGA-PEG (Resomer ® RGP d50155) (Evonik Industries AG, Essen, Germany) were dissolved in an organic solvent (ethyl acetate for PLGA and PLGA-PEG and dichloromethane for PLA) and 200 μL of methanoic doxorubicin solution (2.5mg/mL), using the chemicals Ethyl acetate, dichloromethane and methanol (VWR International GmbH (Darmstadt, Germany). The solution was poured into a (1% m/v) PVA solution made from Poly (vinyl alcohol) (PVA, 30, 000-70, 000 Da) obtained from Sigma-Aldrich Chemie GmbH, Karlsruhe, Germany and was then homogenised using Ultra Turrax (IKA-Werje, Staufen, Germany), stirred overnight, purified by centrifugation at 21, 000 g for 15 minutes (Eppendorf Centrifuge 5430 R, Eppendorf, Hamburg, Germany) and re-dispersed in pure water. After this, a resulting pellet from centrifugation was dissolved into DMSO (dimethyl sulfoxide) obtained from Carl Roth GmbH, Karlsruhe, Germany, to then determine the volume of doxorubicin using HPLC. For PLGA nanoparticles which had an increased amount of doxorubicin entrapped using methanoic doxorubicin solution (2.5 mg/mL) (Doxorubicin was purchased from LGC standards GmbH, Wesel, Germany), corresponding volumes of total doxorubicin were used (1.0, 1.5 and 2.0 mg). For a further increase of drug load that ranged from 10.0 to 50.0 mg/mL, different aqueous doxorubicin solutions were used to achieve a varied range of total doxorubicin amounts (0.5, 2.5, 5.0, 7.5, 12.5 and 25.0 mg).

However, the polymer amount remained the same at 50 mg/mL whilst a PVA solution (1% m/v) which was phosphate buffered to pH 7 using Dulbecco's Phosphate buffered saline (PBS) purchased from Biochrom GmbH (Berlin, Germany) was used for the preparation of doxorubicin-loaded nanoparticles.

1.2 Polymer nanoparticle preparation using solvent displacement

This preparation method was achieved by dissolving a 60 mg polymer in a 2 mL acetone containing 200 μL of doxorubicin solution (2.5 mg/mL) which was inserted into 4 mL of 2% (m/v) PVA solution. This step enabled the production of PLGA and PLGA-PEG nanoparticles in a 4 mL 1% (m/v) PVA solution resulting in PLA nanoparticle production. The chemicals used for the preparation, acetone and acetonitrile were obtained from Carl Roth GmbH, Karlsruhe, Germany. The solution was stirred overnight at 550 rpm where the evaporation of the organic solvent had taken place.

The nanoparticles PLGA and PLA were purified by centrifugation and re-dispersed into pure water as performed in the emulsion diffusion process. A further purification step was used for the PLGA-PEG nanoparticles; which involved centrifugation at 30, 000 g three times for 60 mins and re-dispersion in purified water.

1.3 Particle size

The average particle size, zeta potential and polydispersity were measured using the nanoparticle suspensions which were diluted with purified water (1:1000) and was measured using the instrument, photon correlation spectroscopy (PCS) using Malvern zetasizer Nano, Malvern Instruments, Herrenberg, Germany, at temperature of 22°C using a backscattering angel of 173°C. Lazser Doppler microelectrophoresis was used to determine the zeta potential using the same diluted nanoparticle suspension.

The particle diameters presented in Figure 65 showed similarity between the PLGA nanoparticles preparation method of emulsion diffusion (173.5 ± 5.9 nm) and solvent displacement (179.4 ± 7.6 nm) method. However, PLGA-PEG nanoparticles prepared by solvent displacement 72.6 ± 3.3 nm differed to the diameter size prepared by emulsion diffusion (> 200 nm).

The PLA nanoparticles which were prepared using emulsion diffusion had the diameter of 246.2 ± 2.9 nm whilst those prepared by solvent displacement had the size of 192.1 ± 2.5 nm. A monodisperse size distribution was identified for all nanoparticle preparation. This was determined by the polydispersity indices which was <0.1.
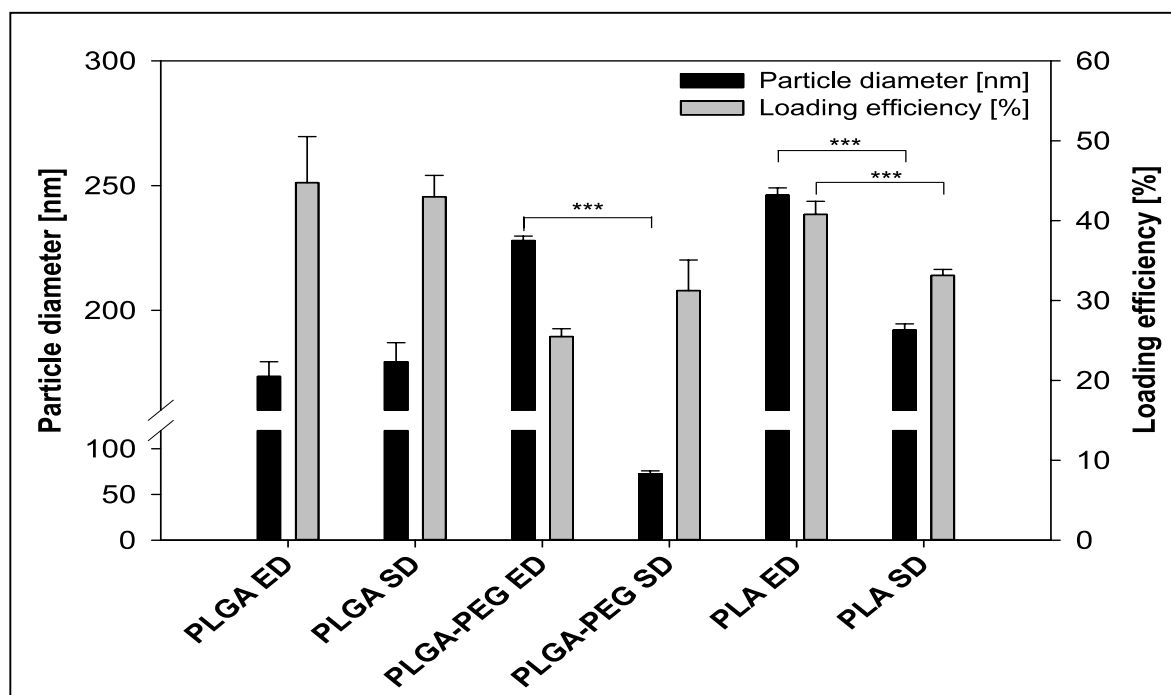
Figure 80: Particle diameters and loading efficiencies for different nanoparticles produced using emulsion diffusion (ED) and solvent displacement (SD). The data was expressed as an average of n=3 ± SD.

1.4 Scanning electron microscopy (SEM)

In order to determine the polydispersity of the nanoparticles, the nanoparticle suspensions were to 0.25 mg/ml using purified water and dropped on a filter (MF-Millipore™ membrane filter VSWP, 0.1 μm) and desiccated for 24 h. The membranes were then sputtered with gold under argon atmosphere (SCD 040, BAL-TEC, Balzers, Liechtenstein). The images as shown in figure 81, were

derived at an accelerated 10, 000 V at a working distance of 10 mm using CamScan CS4, Cambridge

Scanning Company, Cambridge, UK) to determine the particle diameters and Monodispersity.

Figure 81: Scanning electron microscopy (SEM) images taken at x10 000 magnification. (A) PLGA nanoparticles ED, (B) PLGA nanoparticles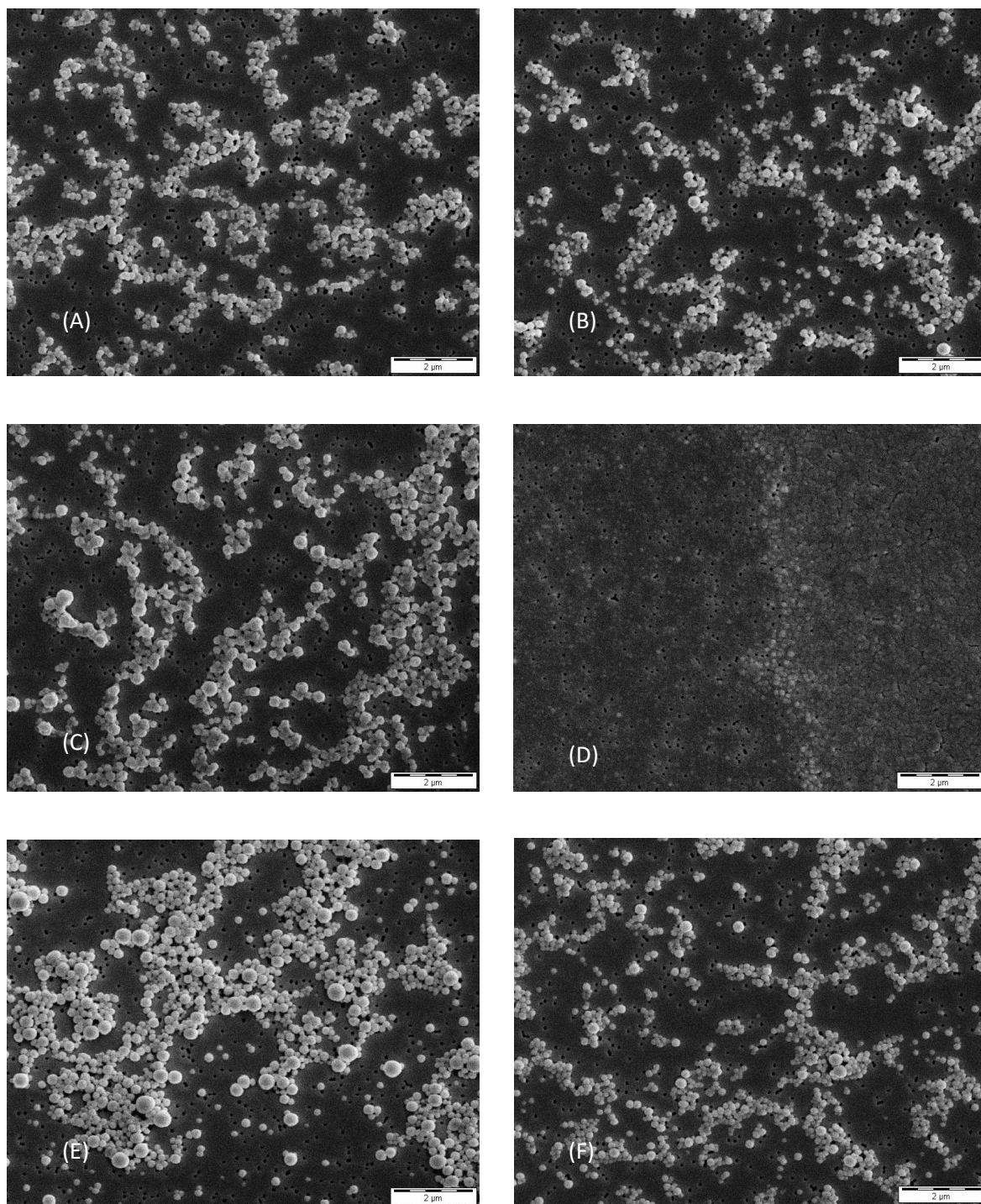 SD, (C) PLGA-PEG nanoparticles ED, (D) PLGA-PEG nanoparticles SD, (E) PLA nanoparticles ED, (F) PLA nanoparticles SD. (solvent displacement (SD) and emulsion diffusion (ED)).

1.5 Influence of the preparation technique on loading efficiency and drug release

HPLC-UV (HPLC 1200 series, Agilent Technologies GmbH, Böblingen, Germany) at a wavelength of 485 nm using a LiChroCART 250 x 4 mm LiChrosper 100 RP 18 column (Merk KGaA, Darmstadt, Germany) were used to determine the amount of doxorubicin incorporated into the nanoparticles.

The loading efficiencies ranged between 25.5 ± 1.0% to 44.8 ± 5.8% of the applied doxorubicin for the different preparation techniques of the nanoparticles as shown in Figure 80. Similar drug loads of the PLGA and PLGA-PEG nanoparticles prepared by solvent displacement and emulsion diffusion reached between 2.6 ± 0.2 µg doxorubicin/mg nanoparticle and 6.7 ± 0.3 µg doxorubicin/mg nanoparticle (figure 80).

NP system	NP yield [mg NP/mL]	NP yield [%]	Drug load [µg Dox/mg NP]
PLGA ED	3.3 ± 0.4	66.8 ± 7.2	6.7 ± 0.3
PLGA SD	8.5 ± 0.4	70.4 ± 3.0	5.1 ± 0.2
PLGA-PEG ED	4.2 ± 0.1	84.4 ± 1.8	3.0 ± 0.2
PLGA-PEG SD	7.6 ± 0.9	63.6 ± 7.4	4.1 ± 0.6
PLA ED	8.0 ± 1.0	79.6 ± 9.8	2.6 ± 0.2
PLA SD	5.3 ± 0.2	44.1 ± 1.8	6.3 ± 0.1

Table 25: Nanoparticle (NP) yield and doxorubicin (Dox) drug load results for nanoparticles prepared by emulsion diffusion (ED) or solvent displacement (SD) technique (data expressed as means ± SD, n ≥ 3).

Specifically, different preparations of PLA nanoparticles prepared had a significant difference between the preparation techniques; solvent displacement: 6.3 ± 0.1 µg/ doxorubicin/ mg nanoparticle and emulsion diffusion: 2.6 ± 0.2 µg doxorubicin/mg nanoparticle (Table 13).

PVA solution	Diameter [nm]	PDI	ZP [mV]
unmod	177.9 ± 1.0	0.039 ± 0.031	-41.6 ± 2.0
pH 7	174.1 ± 2.8	0.057 ± 0.030	-43.8 ± 3.7

Table 26: Results showing particle diameter, PDI, and zeta potential (ZP) for PLGA nanoparticles prepared by an unmodified PVA solution and a PVA solution adjusted to pH 7 (data expressed as means ± SD, n = 3).

The results as shown in figure 82, demonstrated the drug release behaviour expressed by all the nanoparticles as that of a burst release due to the drastic peak release of doxorubicin observed within the first 1 hour. Nevertheless, this release characteristic was not as definite in PLGA nanoparticles as the amount of doxorubicin decreased more after thirty minutes of the initial release This surveillance was more pronounced in the PLGA nanoparticles prepared by solvent displacement suggesting that perhaps the combination of drug to BSA solution added stimulated plasma proteins presence and slow release of doxorubicin compared to other nanoparticle systems.

The pH of the PLGA nanoparticles was increased to 7 for the loading efficiency and drug release kinetics optimisation. At this pH value, doxorubicin is of a lipophilic deprotonated manner with no influence on the characteristics of the nanoparticle (e.g particle diameter, PDI and zeta potential) (Table 26).
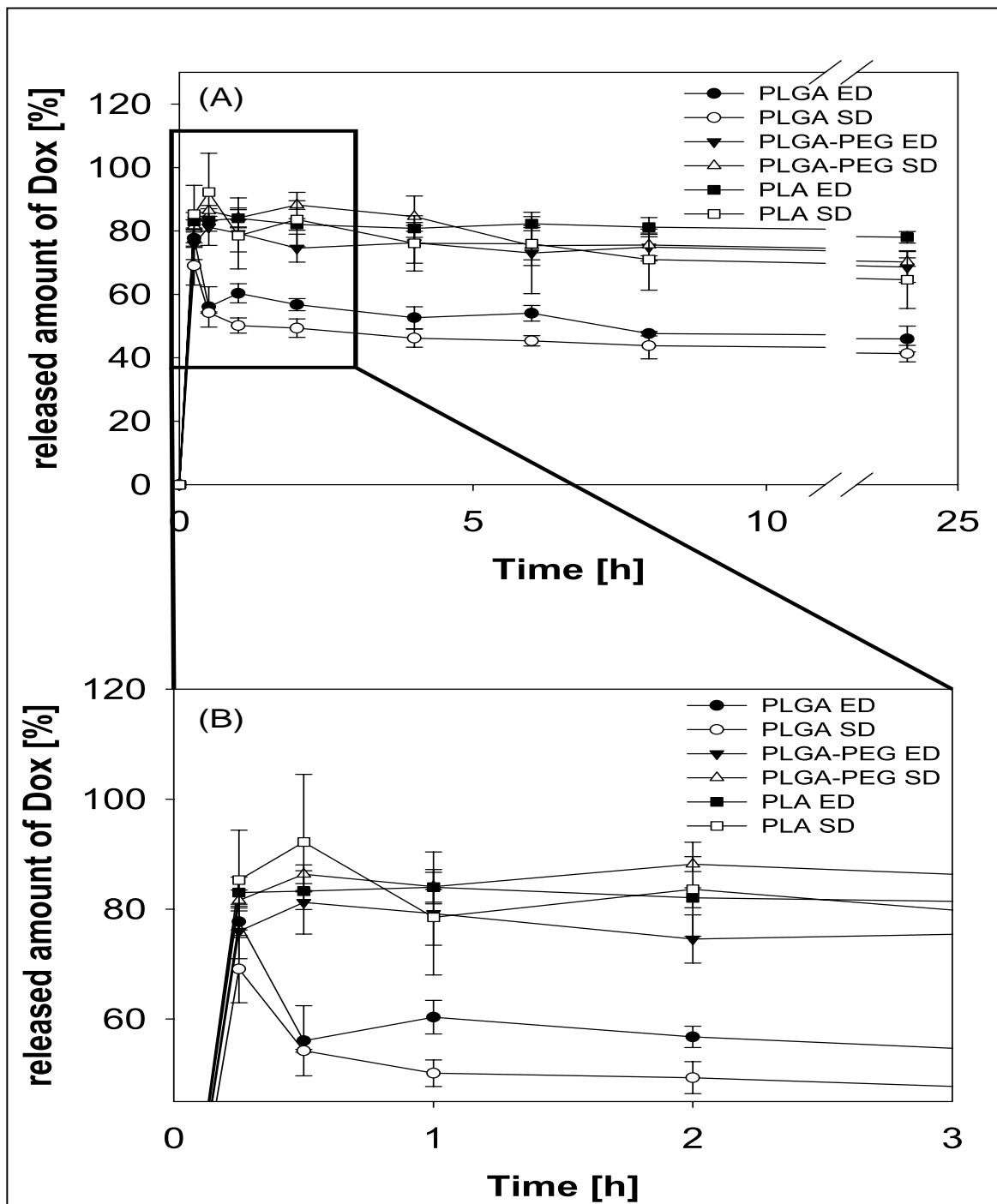
Figure 82: (A) Doxorubicin (Dox) release profiles for all nanoparticle systems using emulsion diffusion (ED) or solvent displacement (SD) preparation technique over 24 h. (B) Detailed section of the timeframe 0–3 h (data expressed as means ± SD, n = 3).

Conversely, the loading efficiency and drug load at this pH value, increased; (6.7 ± 0.3 µg doxorubicin/mg nanoparticle (44.8 ± 5.8% loading efficiency) without pH adjustment to 7.9 ± 0.8 µg doxorubicin/mg nanoparticle (60.2 ± 3.8% loading efficiency) at pH 7). The adjustment of doxorubicin amount further enhanced the drug load of PLGA nanoparticles (non-adjusted pH: 18.0 ± 3.2 µg doxorubicin/mg nanoparticle; pH7: 31.6 ± 3.1 µg doxorubicin/mg nanoparticle, respectively). The amount of doxorubicin did not change the loading efficiency at pH 7 but the aqueous solution in replacement of methanol, had an increment effect. (Figure 83).
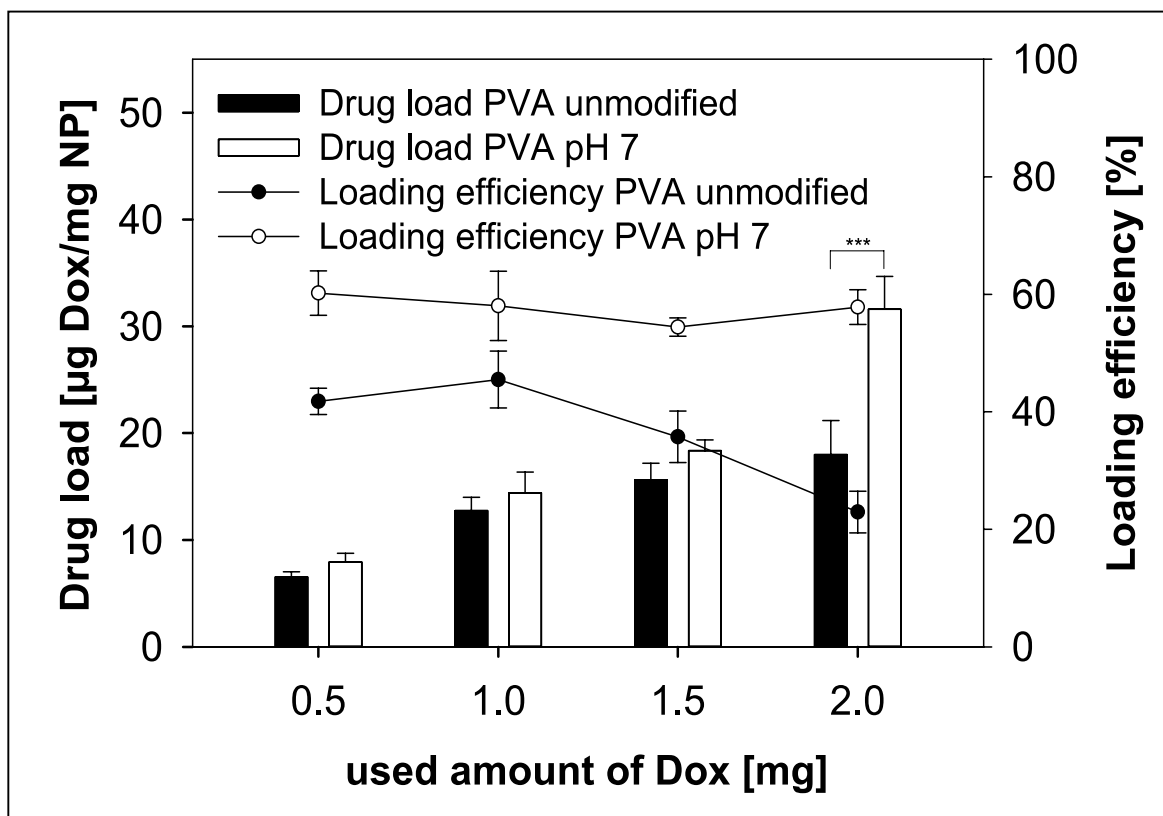

Figure 83 : Doxorubicin (Dox) load and loading efficiency for PLGA nanoparticles (NPs) prepared using an unmodified PVA solution and a PVA solution adjusted to pH 7. Data is expressed as means ± SD, n = 3).

When methanol was not used, the amount of doxorubicin was increased to 5 mg to 7.5 mg per 50 mg PLGA. There was an increase of drug load when the amount of doxorubicin increased to 5 mg (52.5 ± 0.4 µg doxorubicin/mg nanoparticle). However, there was no significant increase using 7.5 mg doxorubicin (54.4 ± 3.4 µg doxorubicin/mg nanoparticle) (Figure 84A). Increasing doxorubicin further than this, resulted in instability of the nanoparticle systems as with particle diameter and polydispersity index (Figure 84B).
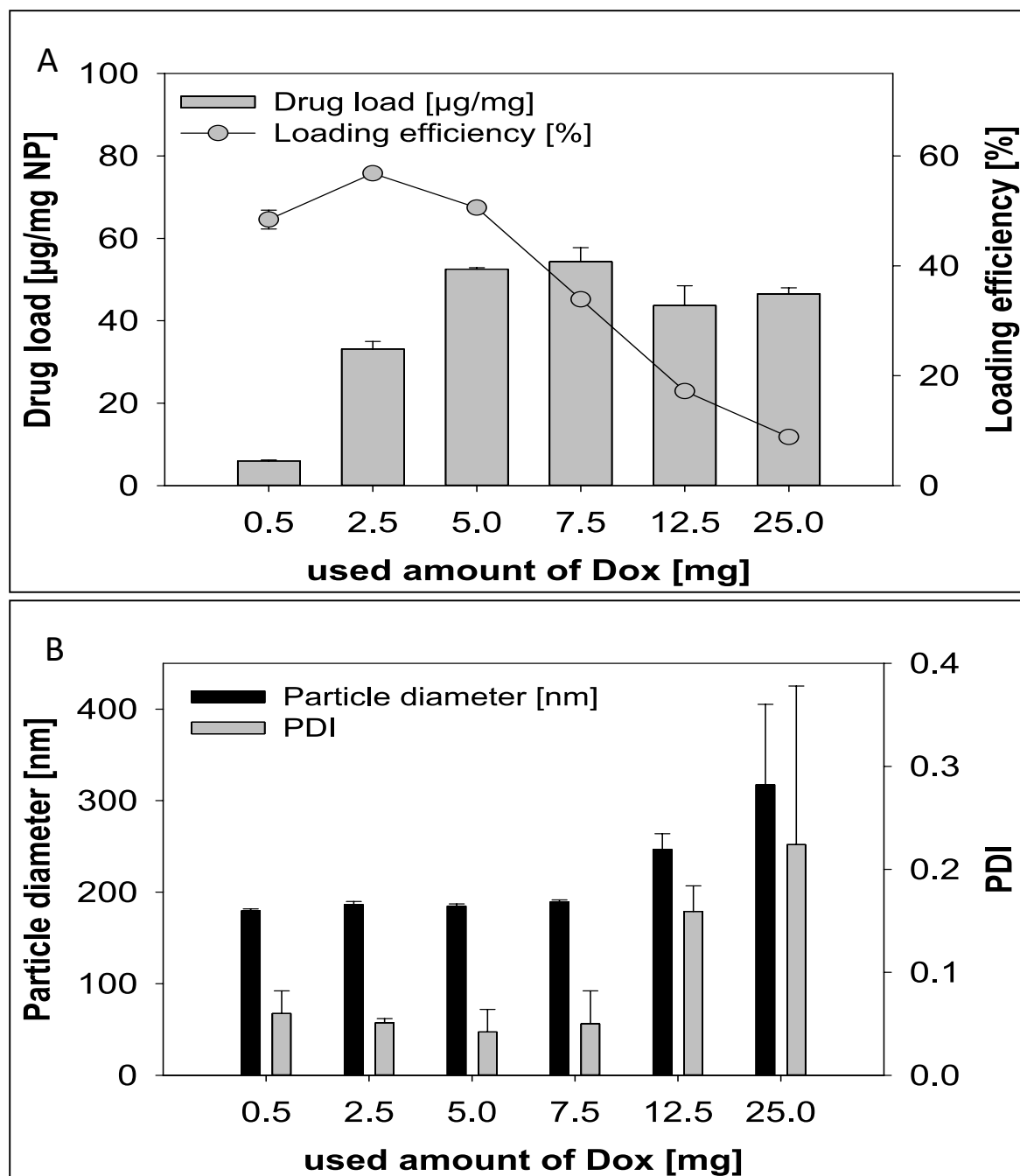

Figure 84 : (A) Drug load and loading efficiencies as well as (B) particle diameter and PDI for different amounts of doxorubicin (Dox) used for the preparation of PLGA nanoparticles by emulsion diffusion technique. Data expressed as means ± SD, n = 3).

Differences in doxorubicin loading amounts as well as preparation at specific pH of 7 resulted in an increase in loading efficiency for PLGA nanoparticles, specifically 5 mg doxorubicin and 7.5 mg doxorubicin amounts ($50.6 \pm 0.6\%$ and $33.9 \pm 0.5\%$, respectively). PLGA nanoparticles which were prepared at pH 7 with 5 mg doxorubicin were used for cell culture experiments due to the controlled and sustained doxorubicin release exerted (Figure 85).
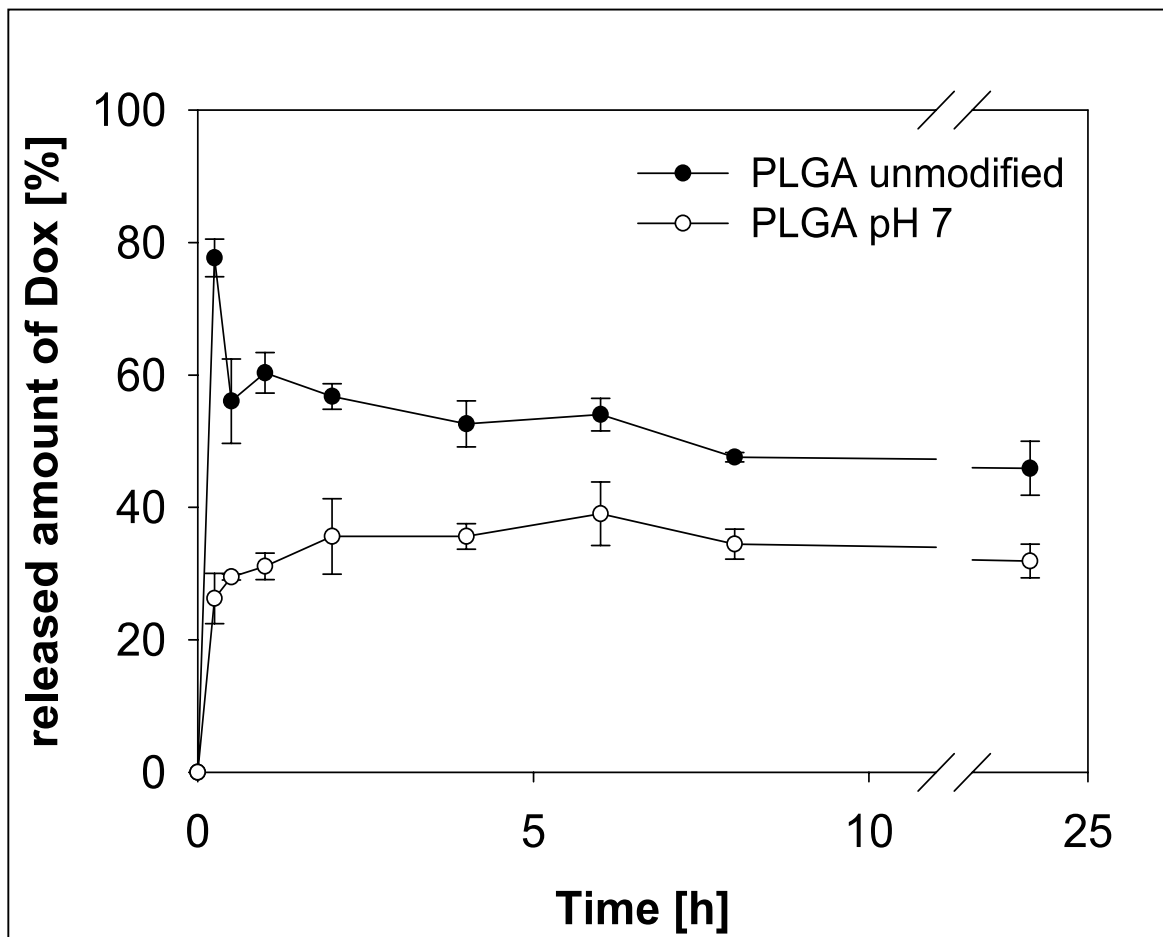

Figure 85 : **Release profiles of doxorubicin from PLGA nanoparticles prepared using an unmodified PVA solution and a PVA solution adjusted to pH 7 (data expressed as means ± SD, n = 3).**

To study the drug release of the nanoparticles, a suspension of 1 mg in 1 ml of PBS containing 5% (m/v) bovine serum albumin obtained from Sigma-Aldrich Chemie GmbH, Karlsruhe, Germany, was shaken at the speed of 500 rpm at 37° C.

The suspensions were then centrifuged at 30, 00 g for 15 min following a further dilution with 750 µL ethanol (96%, v/v) of each supernatant aliquot (250 µL) after 0, 0.5, 1, 2, 4, 7, 8 and 24 h for the precipitation of BSA. A further centrifugation step was performed at 30, 000 g for 10 min for the analysis of the amount of doxorubicin released using the supernatant. The resultant pellet was then dissolved in DMSO.

1.2 Human serum albumin (HSA) nanoparticles

1.2.1 Preparation

Doxorubicin-loaded human serum albumin (HSA) nanoparticles were prepared by the desolvation technique which involved the addition of 100 μL of a 1% (w/v) aqueous doxorubicin solution (LDC standards GmbH, Wesel, Germany) to 500 μL of a 40 mg/mL (w/v) HSA solution (Sigma-Aldrich Chemie GmbH, Karlsruhe, Germany). The mixture was then incubated at room temperature for 2 h whilst being stirred at 500 rpm using a Cimaric Multipoint stirrer (Thermo Scientific, Langenselbold, Germany). Using a peristaltic pump (Ismatec ecoline, Ismatec, Weritheim-Mondfeld, Germany), 4 mL of 96% ethanol, was added at room temperature under stirring at a flow rate of 1 mL/min.

The resulting nanoparticles were stabilised using a cross-linking process. Different amounts of glutaraldehyde (Sigma-Aldrich Chemie GmbH, Karlsruhe, Germany) was added that corresponded to different percentages necessary for the quantitative crosslinking of the 60 primary amino groups present in the HSA molecules of the particle matrix. The cross-linking percentages used were 40%, 100% and 200% with 0% which involved no stabilisation/cross-links. Theoretical cross-linking at 40% contained the addition of 4.7 μL 8% (w/v) aqueous glutaraldehyde solution, 100% crosslinking of the HSA amino groups, contained the addition of 11.8 μL 8% (w/v) aqueous glutaraldehyde solution and 200% crosslinking contained the addition of 23.6 μL 8% (w/v) aqueous glutaraldehyde solution. The nanoparticles suspension was then stirred at 550 rpm for the duration of 12 hours, purified by centrifugation at 16,000 g for 12 minutes and re-suspended in purified water. Supernatants at this stage were collected for drug content determination using HPLC and for the loading efficiency of doxorubicin. The particle size distribution and doxorubicin quantification using HPLC-UV as mentioned in section 5.2.3 and 5.2.4. The particle size and polydispersity indices of the nanoparticles are shown in Table 27.

Nanoparticles	Diameter (nm)	Polydispersity	Drug load (μg doxorubicin/ mg nanoparticle)
HSA(0%)	848.7	0.500	370.9
HSA(40%)	485.8	0.189	151.9
HSA(100%)	496.4	0.213	190.5
HSA(200%)	463.4	0.153	164.8

Table 27: **Polydispersity indices, drug load and particle size of the HSA nanoparticles.**

The cross-linked particles displayed similar polydispersity indices between 0.153 and 0.213 as well as the diameter ranging between 460 – 500 nm. The two values indicate that they were of a narrow, monodisperse size distribution. Similarities of drug load was also observed excluding HSA nanoparticle (0%) where it was much higher (just below a 2-fold increase). The increased amount indicated that this may have been due to the openness of the doxorubicin binding sites known to be on HSA molecules in solution in comparison to those available on the HSA nanoparticles.

Appendix 2

2.1 Standardised adaptation protocol

2.1.1 UKF-NB-3 cell cultivation in the presence of epothilone-b (patupilone) 0.10nM

The growth patterns of the individual UKF-NB-3 sublines in the presence of the IC_{50} concentration of epothilone B (0.10nM) are shown in Figure 86 and 87). From week 19 onwards, the cell number had to be reduced to 100,000 cells/ 25 cm^2 flask to avoid a loss of cell viability due to overgrowth. Despite this sign of initial adaptation subline 5 was lost in week 17 and the remaining sublines were lost in week 47 due to a lack of viable cells.
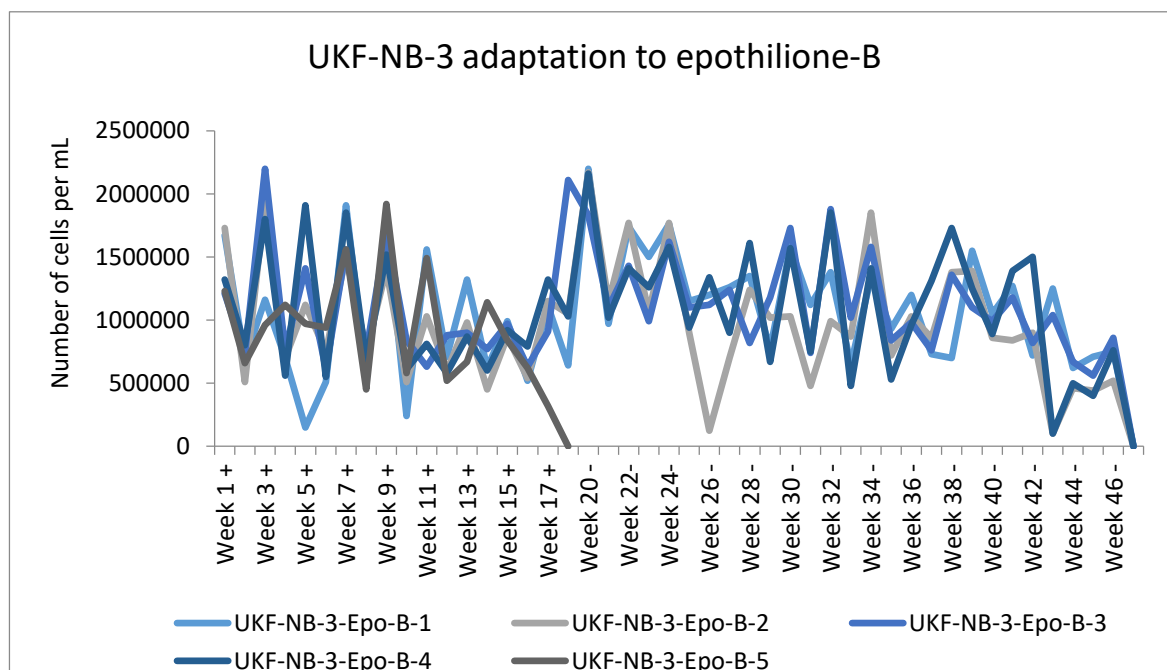

Figure 86 : **Cell numbers in the epothilone B (0.10nM)-treated sublines.** Cell numbers were recorded in the presence (+) and absence (-) of drug to identify patterns of growth for every weekly passage. Recordings for week 18-20 are not included due to no recordings made by the lab member involved. The cell number was reduced to 100,000 cells/ 25 cm^2 flask after week 19. No viable cells were detected in subline 5 at the end of week 17 and in the remaining sublines at the end of week 47.
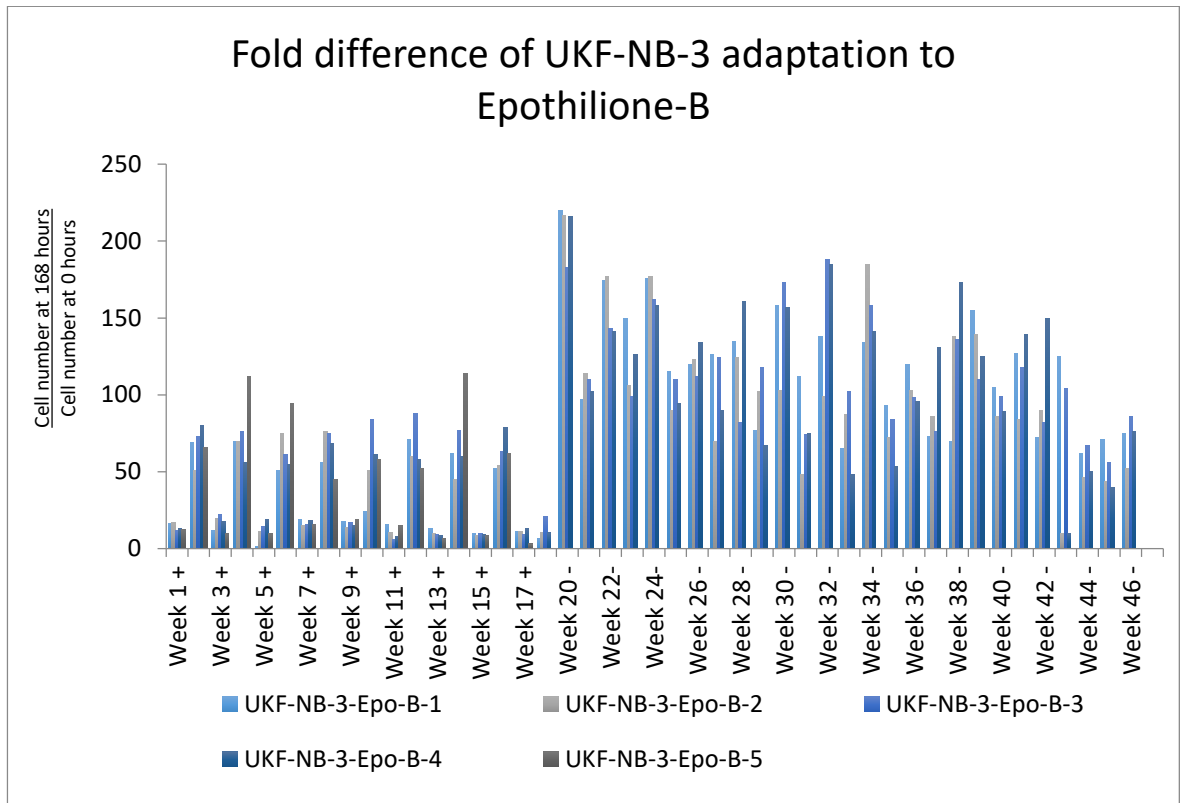
Figure 87 : **Fold change in cell numbers between week 1 and week 47 in the epothilone B (0.10nM)-treated sublines.** Cell numbers were recorded in the presence (+) and absence (-) of drug to identify patterns of growth for every weekly passage. Recordings for week 18-20 are not included due to no recordings made by the lab member involved. The cell number was reduced after week 19. No viable cells were detected in subline 5 at the end of week 17 and in the remaining sublines at the end of week 47.

2.1.2 UKF-NB-3 cell cultivation in the presence of cabazitaxel (0.25nM)

The growth patterns of the UKF-NB-3 sublines in the presence of cabazitaxel (0.25nM) are presented in Figure 88 and 89. From week 13 onwards, the cell number had to be reduced to 100,000 cells/ 25 cm^2 flask to avoid a loss of cell viability due to overgrowth. Despite this sign of initial adaptation, the sublines 1, 3, 4, and 5 were lost in week 23 due to a lack of viable cells. Subline 2 was lost in week 37.
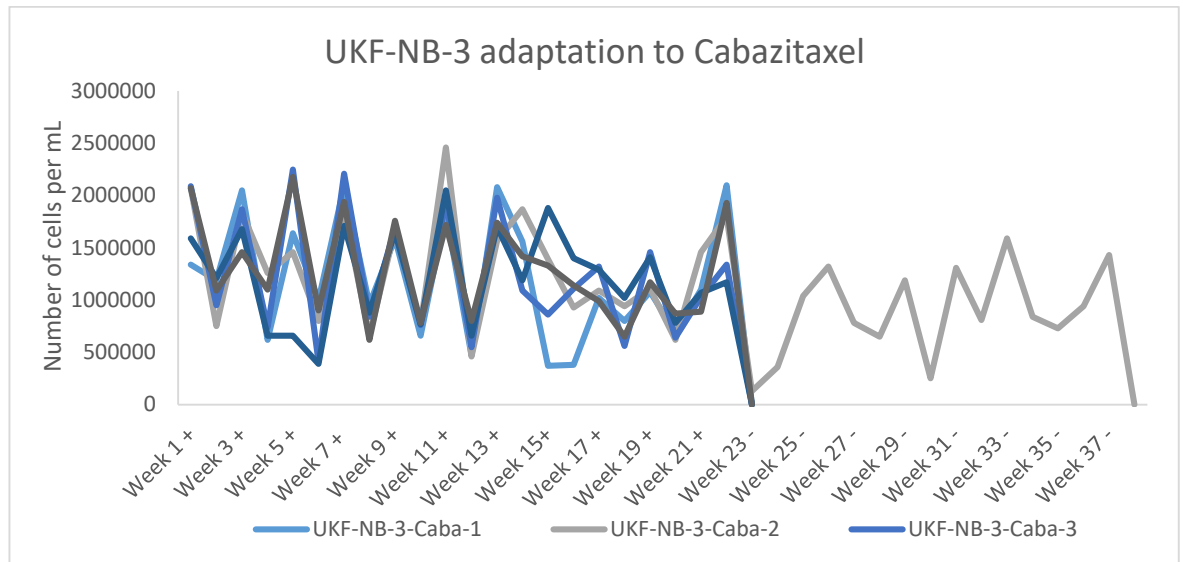

Figure 88: **Cell numbers in the cabazitaxel (0.25nM)-treated sublines.** Cell numbers were recorded in the presence (+) and absence (-) of drug to identify patterns of growth for every weekly passage. The cell number was reduced to 100,000 cells/ 25 cm^2 flask after week 19. No viable cells were detected in subline 1,3,4 and 5 at the end of week 23 and in the remaining subline at the end of week 38.
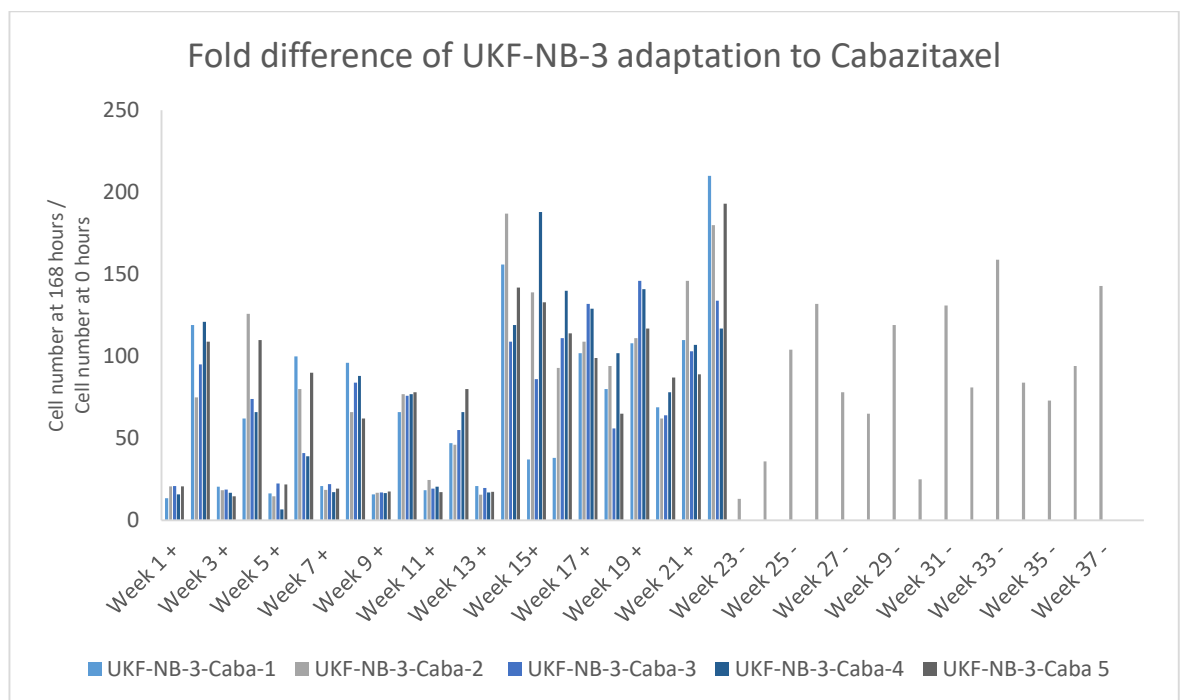

Figure 89 : **Fold change in cell numbers between week 1 and week 38 in the cabazitaxel (0.25nM)-treated sublines.** Cell numbers were recorded in the presence (+) and absence (-) of drug to identify patterns of growth for every weekly passage. The cell number was reduced after week 19. No viable cells were detected in subline 1,3,4,5 at the end of week 23 and in the remaining sublines at the end of week 38.

2.1.3 UKF-NB-3 cell cultivation in the presence of docetaxel 0.37(nM)

The growth patterns of UKF-NB-3 sublines in the presence of docetaxel (0.37nM) are presented in figure 90 and 91) from week 1 to week 50.
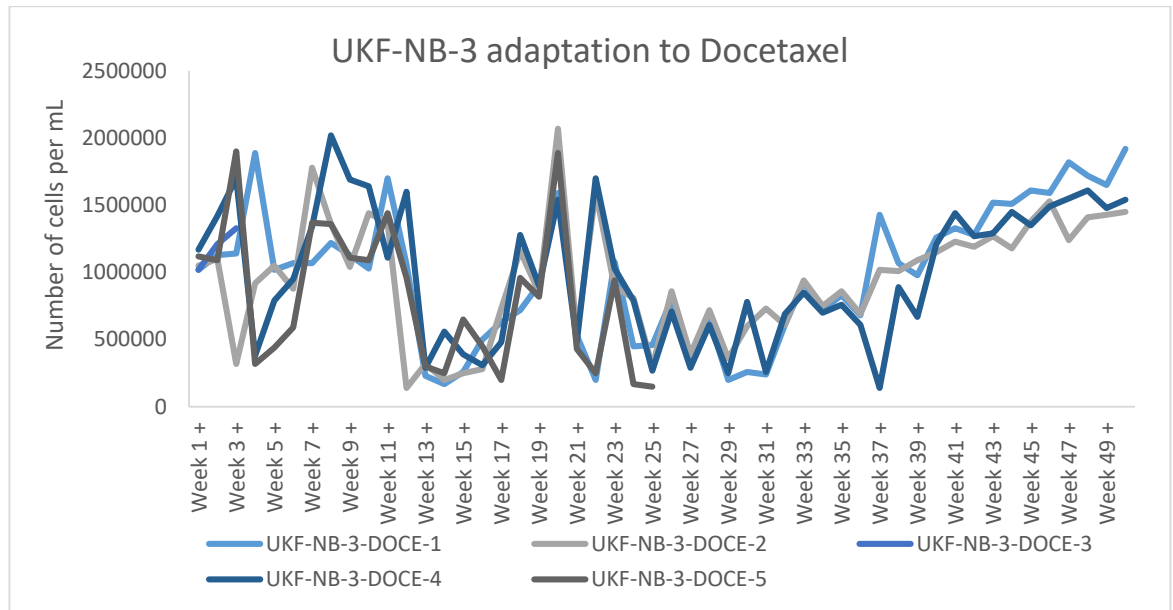

Figure 90: **Cell numbers in the docetaxel (0.37nM)-treated sublines between week 1 and week 50**. Cell numbers were recorded in the presence (+) and absence (-) of drug to identify patterns of growth for every weekly passage. The cell number was reduced to 100,000 cells/ 25 cm^2 flask after week 19. No viable cells were detected in subline 3 at the end of week 3 and in subline 5 at the end of week 25.
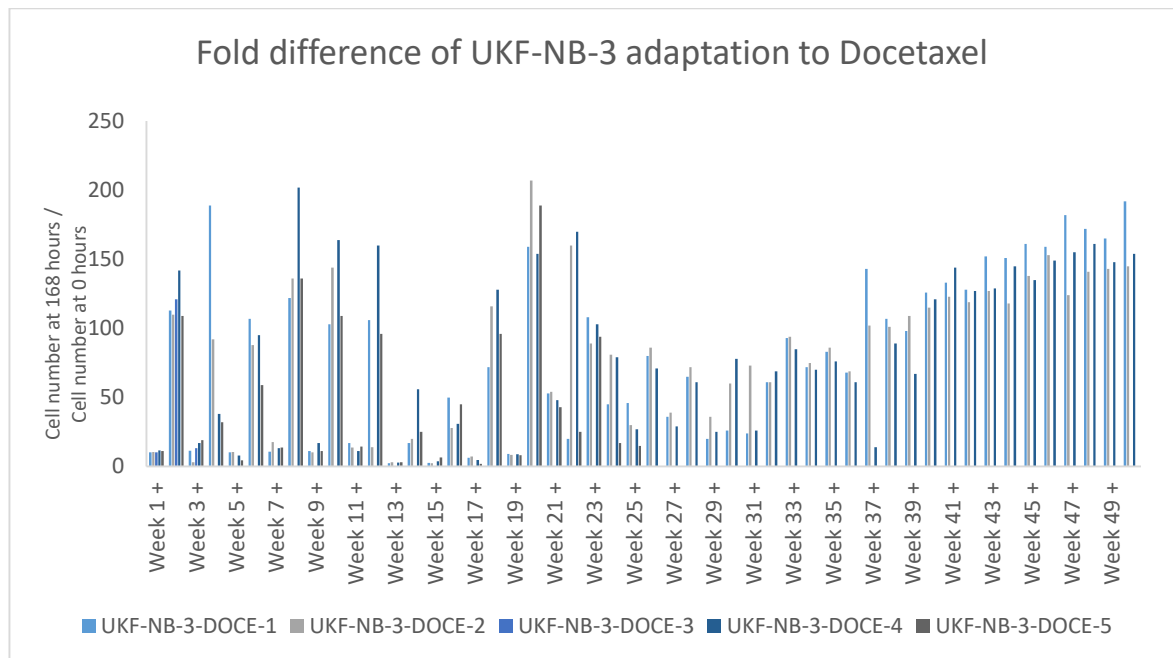

Figure 91 : Fold change in cell numbers between week 1 and week 50 in the docetaxel (0.37nM)-treated sublines. Cell numbers were recorded in the presence (+) and absence (-) of drug to identify patterns of growth for every weekly passage. The cell number was reduced after week 19. No viable cells were detected in subline 3 at the end of week 3 and in subline 5 at the end of week 25.

2.1.4 UKF-NB-3 cell cultivation in the presence of paclitaxel 0.57(nM)

The growth patterns of UKF-NB-3 sublines in the presence of paclitaxel (0.57nM) are presented in figure 92 and 93) from week 1 to week 50.
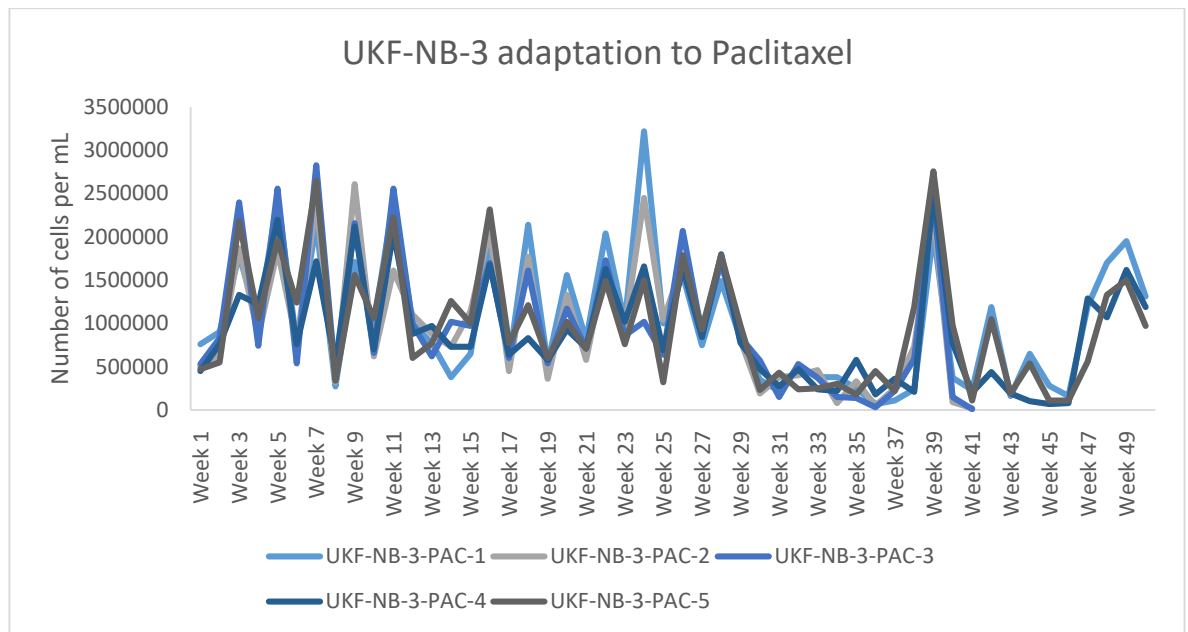

Figure 92 : **Cell numbers in the paclitaxel (0.57nM)-treated sublines between week 1 and week 50.** Cell numbers were recorded in the presence (+) and absence (-) of drug to identify patterns of growth for every weekly passage. The cell number was reduced to 100,000 cells/ 25 cm^2 flask after week 19. No viable cells were detected in subline 2 and 3 at the end of week 41.
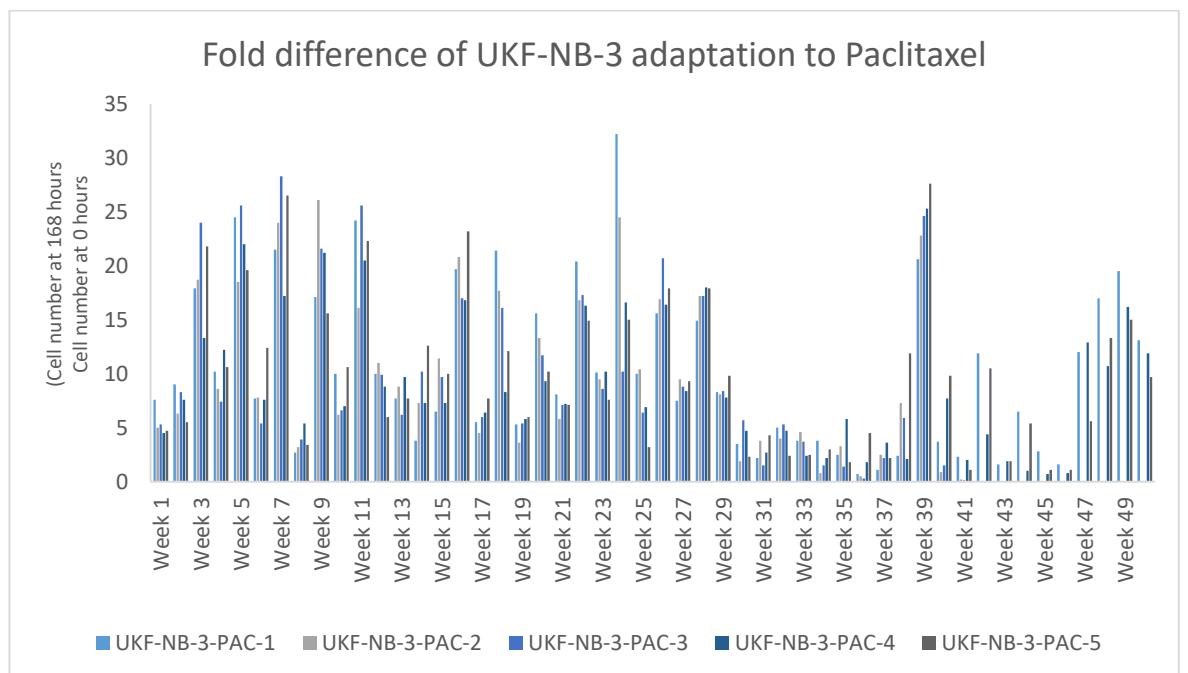

Figure 93 : **Fold change in cell numbers in the paclitaxel (0.57nM)-treated sublines between week 1 and week 50.** Cell numbers were recorded in the presence (+) and absence (-) of drug to identify patterns of growth for every weekly passage. The cell number was reduced to 100,000 cells/ 25 cm^2 flask after week 19. No viable cells were detected in subline 2 and 3 at the end of week 41.

2.2.1 Chemotherapy-induced resistance phenotype

Drug sensitivity was monitored by MTT assay (n=1) every four weeks during drug treatment. Resistance was defined by a 2-fold increase in the IC_{50} concentration of the respective drug. The sublines cultivated in the presence of epothilone-B (figure 94) and cabazitaxel (figure 95) showed no consistent pattern of resistance formation.
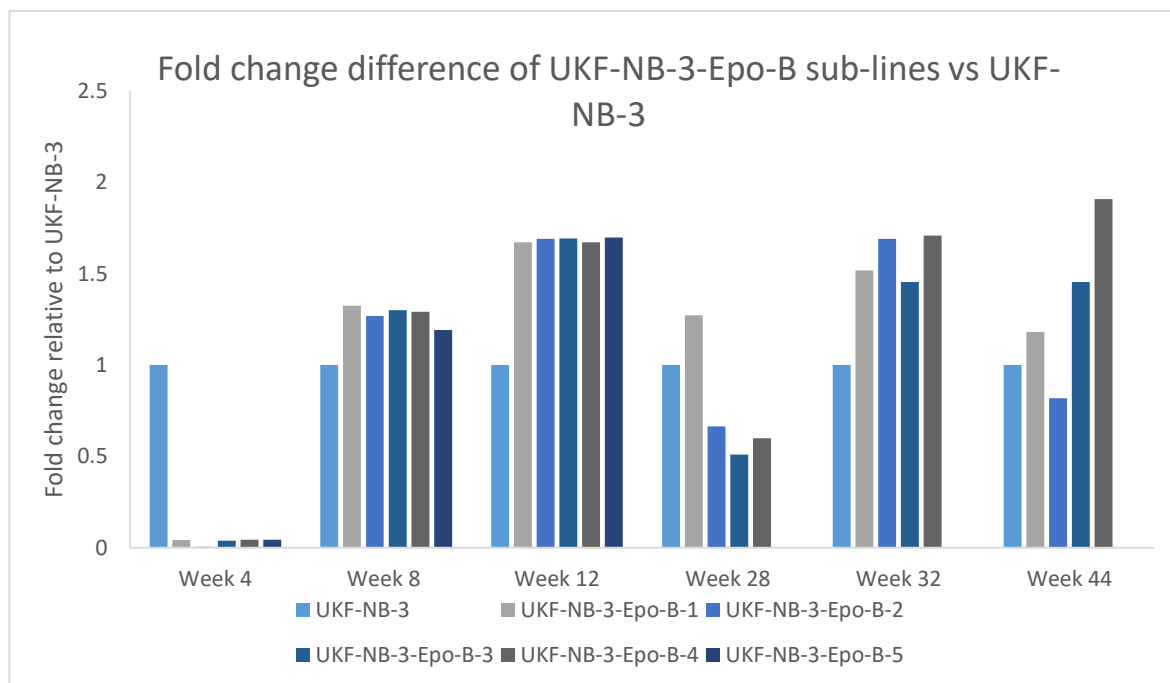

Figure 94: **IC_{50} concentrations determined from a 120-hour MTT assay for sublines cultivated in the presence of epothilione-B in comparison to UKF-NB-3.** Each result (week 4, 8, 12, 28, 32, 44) was derived from one MTT assay (n=1).
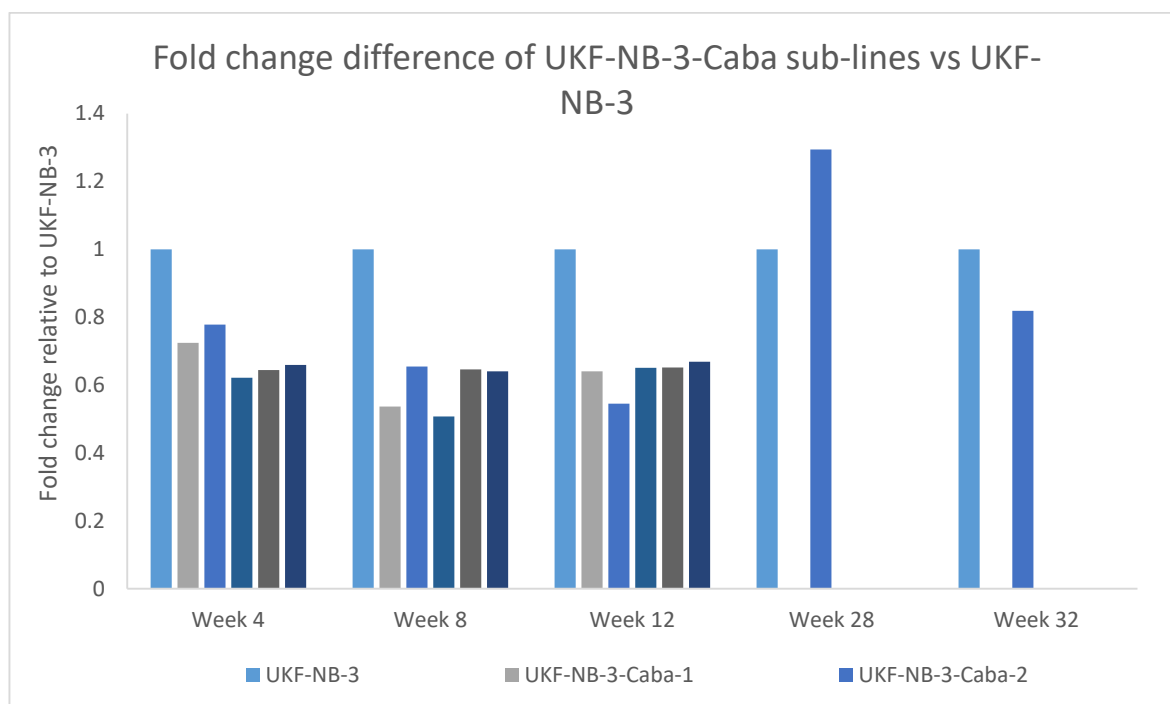

Figure 95 : IC_{50} concentrations determined from a 120-hour MTT assay for the cabazitaxel sub-lines in comparison to UKF-NB-3. Results show no level of resistance. Each result (week 4, 8, 12, 16, 28, 32) was derived from one MTT assay (n=1) thus no error bars or average.